Master Thesis in Geosciences

Vertical variation in reservoir core geochemistry

Bitumen samples from a well in the deep and hot Devonian age Embla Oil Field, Offshore Norway

Tesfamariam Berhane Abay

UNIVERSITY OF OSLO

FACULTY OF MATHEMATICS AND NATURAL SCIENCES

Blank page, for double side paper print.

Remove for digital publishing

Vertical variation in reservoir Core geochemistry

Bitumen samples from a well in the deep and hot Devonian age Embla Oil Field, Offshore Norway

Tesfamariam Berhane Abay

Master Thesis in Geosciences

Discipline: Petroleum Geology and Geophysics (PEGG)

Department of Geosciences

Faculty of Mathematics and Natural Sciences

UNIVERSITY OF OSLO

June, 2010

Tutor(s): Assoc. Prof. Dag A. Karlsen

This work is published digitally through DUO – Digitale Utgivelser ved UiO

http://www.duo.uio.no

It is also catalogued in BIBSYS (http://www.bibsys.no/english)

Abstract

A total of 21 core samples from well 2/7-26S of the Embla Field and One reference sample from Oseberg have been geochemically studied. In the studied well the Embla Field consists of two main reservoir units, the Upper and the Lower sandstones. Altered volcanic rocks found beneath the Lower sandstone unit. Migrated hydrocarbon is known to appear in the Embla Field.

The objective of this study is to carry out geochemical analysis of the samples to characterize vertically the migrated bitumen in the Embla reservoir with the purpose of understanding the process of reservoir filling and its often complex history which are the key for source rock and oil/gas characterization. For this purpose geochemical evaluation of the Paleozoic samples have been carried out in an attempt to understand the heterogeneity of the reservoir.

The geochemical analytical methods used in this study are Iatroscan TLC-FID, GC-FID and GC-MS. These techniques yielded several chromatograms and maturity and facies parameters, which are used to evaluate the geochemical heterogeneities of the reservoir vertically in terms of hydrocarbon abundance, composition, maturation, facies source and biodegradation.

The two most important sections of the reservoir, the Upper and Lower sandstone are rich in hydrocarbon. However, great variations have been observed both in abundance and composition.

The Embla samples are highly mature with vitrinite reflectance of more than 0.8%. The samples from the Upper and Lower sandstones show different maturity signatures. The Lower sandstone being more mature. The applicability of the biomarker based maturity is less useful for the highly mature Embla bitumen samples. Rather, aromatic hydrocarbon based maturity ratios reflect the maturity more reliably. The following maturity trend is concluded (high to low): **Lower sandstone→VB →Upper sandstone→NSO-1 → Rhyolites.**

The bitumen in the studied well of the Embla Field are concluded to be sourced from marine algal type 2 kerogen. The bitumen from the Lower sandstones is originated partly from a more algal, restricted anoxic environment.

Acknowledgements

I would like to thank my supervisor Dr. Dag A. Karlsen for giving me the opportunity to study what I find to be the most interesting field in the study of geosciences. I am sincerely grateful for his outstanding professional support, inspiration and courage I have received throughout the course of the thesis work. He has always been welcoming and encouraging me to ask questions and discuss on the progress of my work. I have always felt welcome to ask questions and receive guidance both concerning theoretical as well as practical issues.

I would also like to thank Kristian Backer-Owe for his help and guidance in the lab and interesting discussions.
I also, would like to thank Jan Hendrik van Koeverden and Phan Nghia for useful discussions and nice time we had.

Finally my deepest gratitude goes to all my friends and fellow students at the Department of Geosciences, we have had a lot of fun together!

Oslo, June 2010

Tesfamariam Berhane Abay

Table of Contents

1. Introduction

1.1. Introduction

The Embla field, located 5 km south of the Eldfisk Alpha platform, is the first development of a pre-Jurassic reservoir in the Norwegian sector of the Central Graben (Knight et al., 1993). The Embla field is a deep hot reservoir with reservoir temperature of about 165°C.

Petroleum geochemistry is the application of chemical principles to the study of the origin, migration, accumulation, and alteration of petroleum (oil and gas) and the use of this knowledge in exploring for and recovering petroleum (Hunt, 1996).
Biomarkers are defined as molecules with a base structure that was inherited from a living organism and deposited in sediments with no or only small changes in their structure (Tissot and Welte, 1984). They are found in oil, bitumen, rocks and sediments. Less than 1% of the organic material that is deposited in the sediments is found in the form of petroleum. These biomarker signatures are often called the “fingerprints” of the source rock and they help in understanding the origin of migrated petroleum in the samples of interest. The presence of these biomarkers in all samples of petroleum to date indicates the biological origin of the organic matter in the formation of petroleum and informs about the genetic relationship between petroleum, the amount of petroleum expelled and the quality and maturity of the source rock from which the petroleum originated.

The analytical procedures used in this study are Iatroscan TLC-FID, GC-FID and GC-MS, and the chromatograms, chemical facies and maturity parameters are used as tools to discern intra reservoir variation in the oil (facies and maturity of the source rock and "in-reservoir" processes like biodegradation) between the Upper and Lower parts of the reservoir. In this case vertical variation in bitumen in well 2/7-26S of the Embla Field tells us about the filling history and the level of vertical petroleum communication.

1.2. Objectives of the thesis

The objective of the thesis is to characterize the migrated bitumen in the Embla reservoir with the purpose of understanding the process of vertical petroleum communication and reservoir filling and its often complex history which are the key for source rock and oil/gas characterization. Detailed geochemical evaluation of the Paleozoic samples will be carried out in an attempt to understand the heterogeneity of the Palaeozoic reservoir of the Embla Field.

To achieve these goals the thesis will in particular:

- Assess the gross occurrence and compositional variations of migrated hydrocarbons, vertically down the reservoir based on the core samples obtained from the well **2/7-26S.**
- Evaluate the maturity level of the migrated hydrocarbon in the Embla Field based on samples from well **2/7- 26S**.
- Discern intra reservoir similarities and variation in the samples, facies and maturity of the source rock and "in-reservoir" processes like biodegradation.
- Look into the degree of biodegradation and the potential that some of the core samples may represent paleo-oil of different origin compared to the main live oil charge-assumed to be of Mandal (Kimmeridge) formation origin (Knight et al., 1993).
- Assess the filling history and the level of petroleum communication in the field.

2. Geological frame work

This chapter presents the summary of the geological framework and settings of the study area.

The outline of the chapter is as follows:

2.1 . Regional geological settings

2.2 . Stratigraphic settings

2.3 . Structural settings

2.4 . Reservoir rocks, traps and seals

2.1. Regional geological setting

The structural geology of the Norwegian Central Trough (also known as the Central Graben) is complex and still not fully understood (Gowers et al., 1993). The structural history of the Central Trough has been outlined and subdivided into various structural zones by (Gowers and Sæbøe, 1985) and tectonic phases (Gowers et al., 1993).

According to (Gowers et al., 1993) the structural development specific to the Central Trough area can be divided into three major stages: (1) Late Triassic to Middle Jurassic flexural uplift; (2) Late Jurassic to Early Cretaceous fragmentation; (3) Late Cretaceous to Tertiary flexural subsidence.

The Grensen Nose, one of the structural zones introduced by Gowers and Sæbøe in 1985, was part of the Mid North Sea High until subsidence in the central Graben occurred during the Late Cretaceous (Gowers and Sæbøe, 1985). Since then it is known as a structural spur protruding northwards from the Mid North Sea High. According to (Gowers et al., 1993) the Grensen Nose shows considerable internal faulting, with some old east-west trends being important, together with the NNW-SSE trend. The boundaries of the Grensen Nose are dominated by flexure (Gowers et al., 1993).

The Embla Field (see Fig. 2.1 and 3.1) is located on the west flank of the central graben of the North Sea. Because of its complicated stratigraphic and structural history, the area is geologically complex (Snow et al., 1991).

The Embla Field, an oil field, is located on the Grensen Nose in Block 2/7 to the south-west of the Eldfisk Field on the downthrown side of the Skrubbe fault (Bharati, 1997) (see Fig. 2.1).

Sears et al. (1993), based on 3D seismic data, suggested that much of the basement framework in the Central Graben was created during the Caledonian Orogeny which created the NW-SE and NE-SW trending diffuse shear zones, and that subsequent reactivation along these existing basement lineaments occurred from Late Paleozoic to Cretaceous times. Fraser et al. (1993) suggested that the mobilization of the Permian salt underlying the central

Graben has played a pivotal role in influencing patterns of structure and sedimentation, including the preservation of the coarse clastic input to the basin in an arid continental environment.

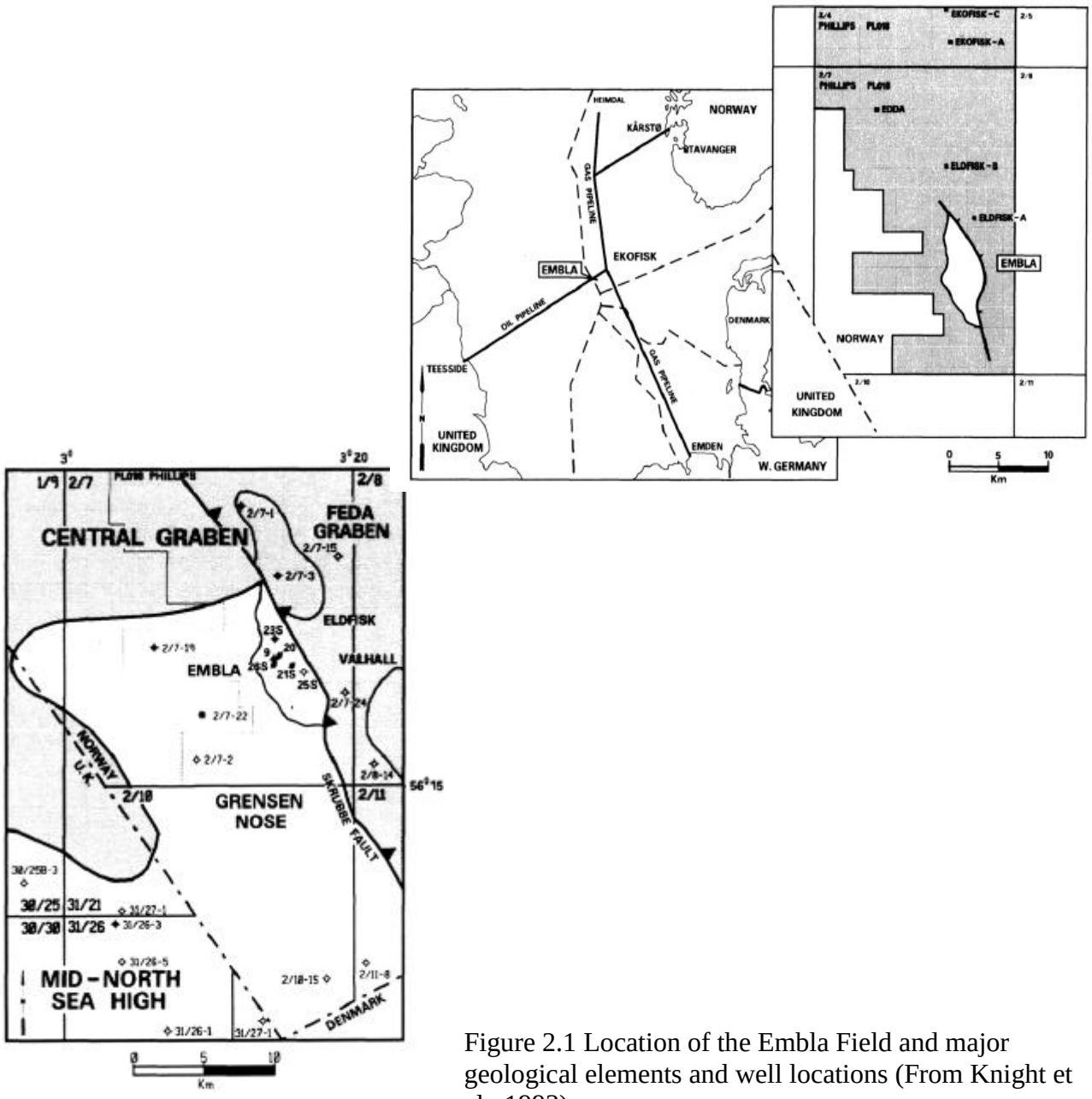

Figure 2.1 Location of the Embla Field and major geological elements and well locations (From Knight et al., 1993).

2.2. Stratigraphic setting

The Embla Field is located on the Grensen Nose, a northwest-southeast-trending structural high considered as a northeast extension of the mid North Sea high (Knight et al., 1993). The pre-Cretaceous stratigraphy varies significantly between wells in the Embla field (Knight et al., 1993). The 2/7-26S well has encountered the most complete sequence (Fig 2.2 and Fig 2.3).

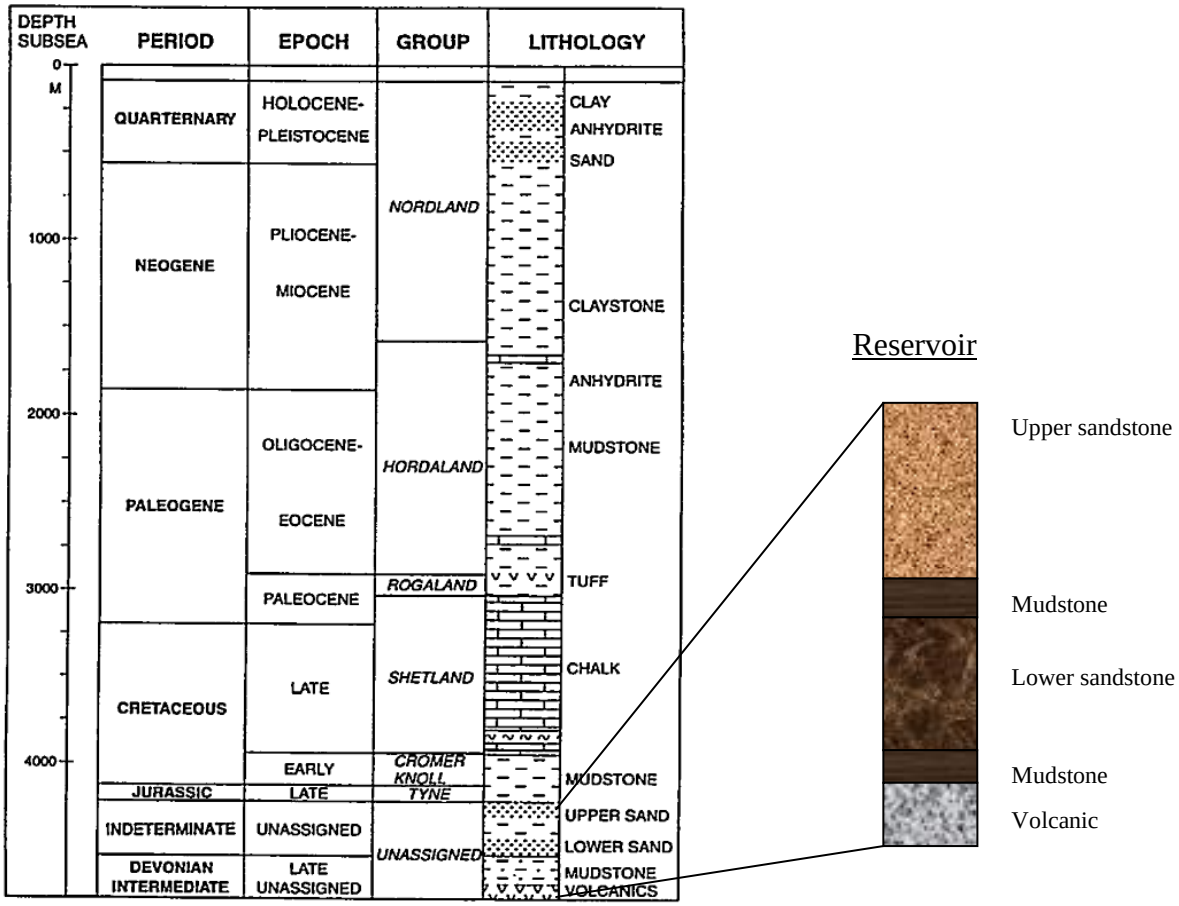

Fig. 2.2 The stratigraphy of well 2/7-26S (not to scale) (Modified after Knight et al.,1993)

The oldest unit penetrated is a red to greenish-grey, heavenly brecciaed and strongly altered rhyolitic rock identified in wells 2/7-26S and 2/7-21S. This rhyolitic unit, possibly of Devonian age, is overlain by brown to red, very fine-to fine-grained mudstones. The

reservoir section, which is moderately to well sorted micaceous sandstones and with some silty mudstones rests upon the mudstone (Knight et al., 1993). The Tyne group, an Upper Jurassic, unconformably overlies the Embla reservoir and only a very thin Mandal formation mudstone is present high on the structure (Bharati, 1997).

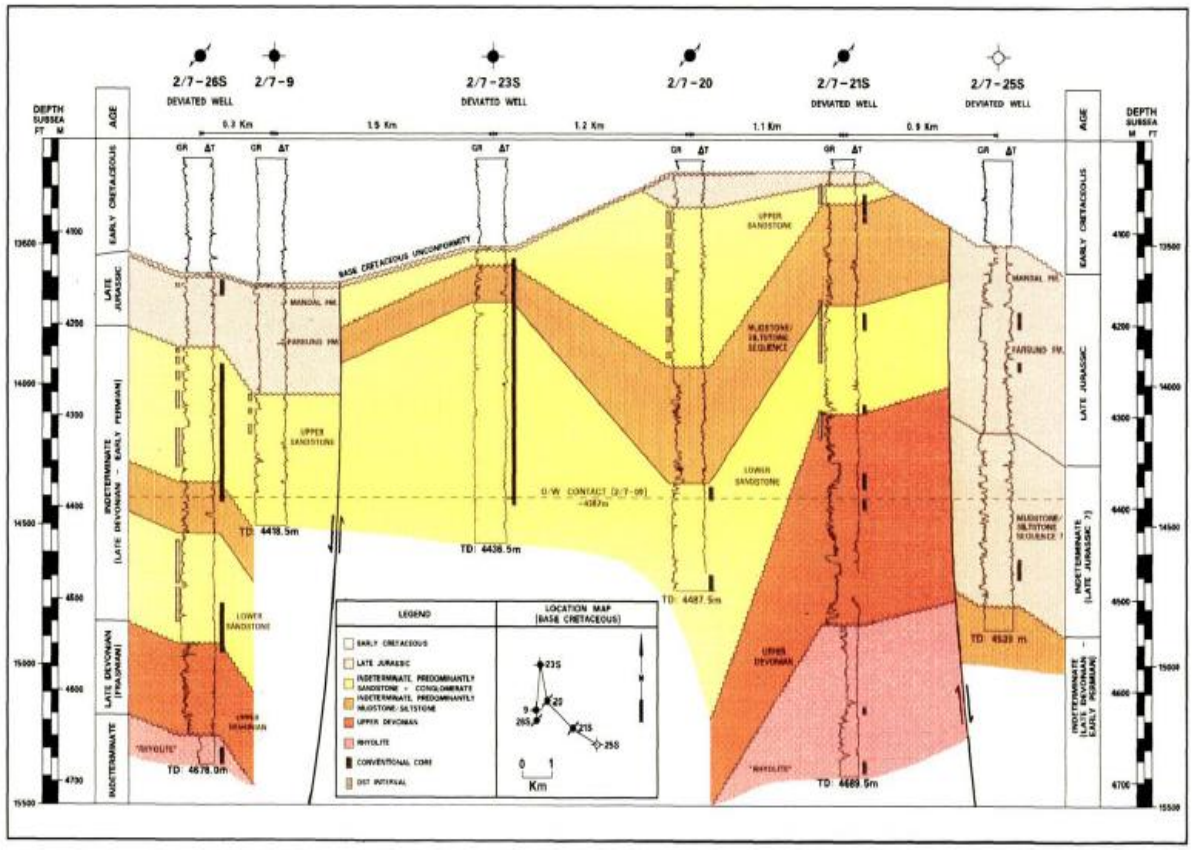

Figure 2.3 Cross section showing the stratigraphic succession and wells in the Embla Field (From Knight et al., 1993).

2.3. Structural setting

Knight et al. (1993) has interpreted the Embla Field as occurring in a westward dipping Paleozoic horst. The Embla Field structure is a faulted dome with long axis of the field

oriented northwest-southeast and bounded to the east by the Skrubbe Fault, a Late Jurassic normal fault which was reactivated in a reverse motion during late cretaceous inversion (Knight et al., 1993). The Embla Field (about 19.4 km^2) consists of a trap formed by a combination of structural and stratigraphic elements (Bharati, 1997). On the crest of the structure (4033m, well 2/7-09), the reservoir sandstones are truncated by erosion and hydrocarbons are stratigraphically trapped by the overlying mudstones of the upper Jurassic Mandal Formation and or lower Cretaceous Cromer Knoll Group. Based on both core sample information and seismic interpretations, there has been multiple tectonic events occurred in the Embla Filed (Knight et al., 1993). The cores are highly fractured and faulted and demonstrate variable fracture orientations. Observations by Knight et al. (1993) indicate that the factures have moderate to steep dips and occur as both large and smaller fracture systems. The main fracture orientations are NW-SE, NNW-SSW and NE-SW. A fault between the 2/7-09 and 2/7-20 wells, with a throw of approximately 120 m at the base of the Base cretaceous Unconformity level, divides the field into an eastern and western fault block (Knight et al., 1993). Intense faulting within the reservoir sections (based on both core samples and seismic data interpretation) indicates that there is a risk of reservoir compartmentalization (Bharati, 1997). Based on studies on production data, Knight et al. (1993), indicated the horizontal and vertical barriers to fluid flow may exist, the later may also indicating horizontal flow barriers in the form of faults or stratigraphical discontinuities. Vertical flow barriers may include caliche layers, intercalated volcanic horizons and lacustrine mudstones separating the Upper and Lower Sandstones (Knight et al, 1993).

2.4. Reservoir rocks, traps and seals

The reservoir section in the Embla field, resting directly on the Upper Devonian mudstones, consists of two major sandstone sections separated by mudstone/siltsone. The sandstone is believed to be braided fluvial and alluvial fan in origin. The intervening mudstone/siltstone sequence was deposited in a flood plain/lacustrine setting (Knight et al., 1993). The sediments consist of grey-green to red, fine- to-medium-grained, often conglomeratic sandstones with interbedded grey-green mudstones and siltstones. Intrusive and extrusive igneous rocks are found within the reservoir section. Both acid and mafic igneous rock types

are present. The igneous rocks are however severely altered by secondary processes, which have destroyed the igneous mineralogy and geochemistry. Dating of the reservoir is difficult due to the lack of microfossils. An early Permian/Carboniferous and/or Upper Devonian age has been suggested (Knight et al., 1993). The Embla field is different from all other neighboring (Cretaceous chalk) fields in that its reservoirs are pre-Cretaceous sandstones and relatively most deeply buried (Bharati, 1997). The petroleum trap is a combination of stratigraphical and structural. Residual bitumen occurs within parts of the reservoir, and this bitumen predates the mobile oil (Knight et al, 1993).

Unconformably above the reservoir section, the Upper Jurassic Tyne Group is present except near the crest where the Upper Jurassic rocks are missing. Mudstones and argillaceous limestones of the Lower Cretaceous Cromer Knoll Group overlies the Upper Jurassic. At the crest of the Embla structure the Cromer Knoll Group occurs directly upon the reservoir section, and forms the top seal of the structure (Knight et al., 1993).

3. Sample set

The samples studied in this thesis will be presented in this chapter (Table 3.2). A short description of the samples is outlined below. All the core samples are from the Embla field block 2/7 well no 26S (see Fig. 2.3 and 3.1). Samples from the different reservoir sections have been selected for analysis. This includes four sample from the Upper sandstone, nine from the Lower sandstones and four samples from the rhyolite unit. Moreovere one sample represents bitumen extracted from a vein/fractures rhyolite. The NSO-1 oil sample from the Oseberg field was included as a reference.

General history of well 2/7-26S

Well 2/7-26 S is located on the Embla Field in the Central Graben of the North Sea (see Fig. 2.1 and 3.1). It was designed to test the pre-Jurassic sandstones, which had shown commercial quantities of hydrocarbons in the 2/7-20, 2/7-21 S, and 2/7-23 S wells. The objective of the well was to confirm the presence of hydrocarbon bearing sandstones in the western fault block of the structure and to establish the productivity of this reservoir section through a program of well testing and coring. Well location and TD was chosen so that both the upper and lower sandstone members of the pre-Jurassic sequence would be penetrated. The target location was 300 m to the south of the 2/7-9 well at Base Cretaceous level. The reservoir section was expected to be highly fractured and over-pressured. Shallow gas was expected since gas had been encountered in all wells drilled from the template location over the 2/7-20 well (http://www.npd.no). Table 3.1 presents summary of information about well 26S.

UTM coordinates	515347.49E, 6243333.20N
UTM zone	31
Formation age	Devonian
Area	North Sea
Filed	Embla
Water depth	71m
Total depth (MD), m	4848m
Kelly bushing elevation (KB), m	29

Table 3.1 summary of information regarding well 26S. Note that the total depth is relative to Kelly Bushing (RKB), summarized after (www.npd.no)

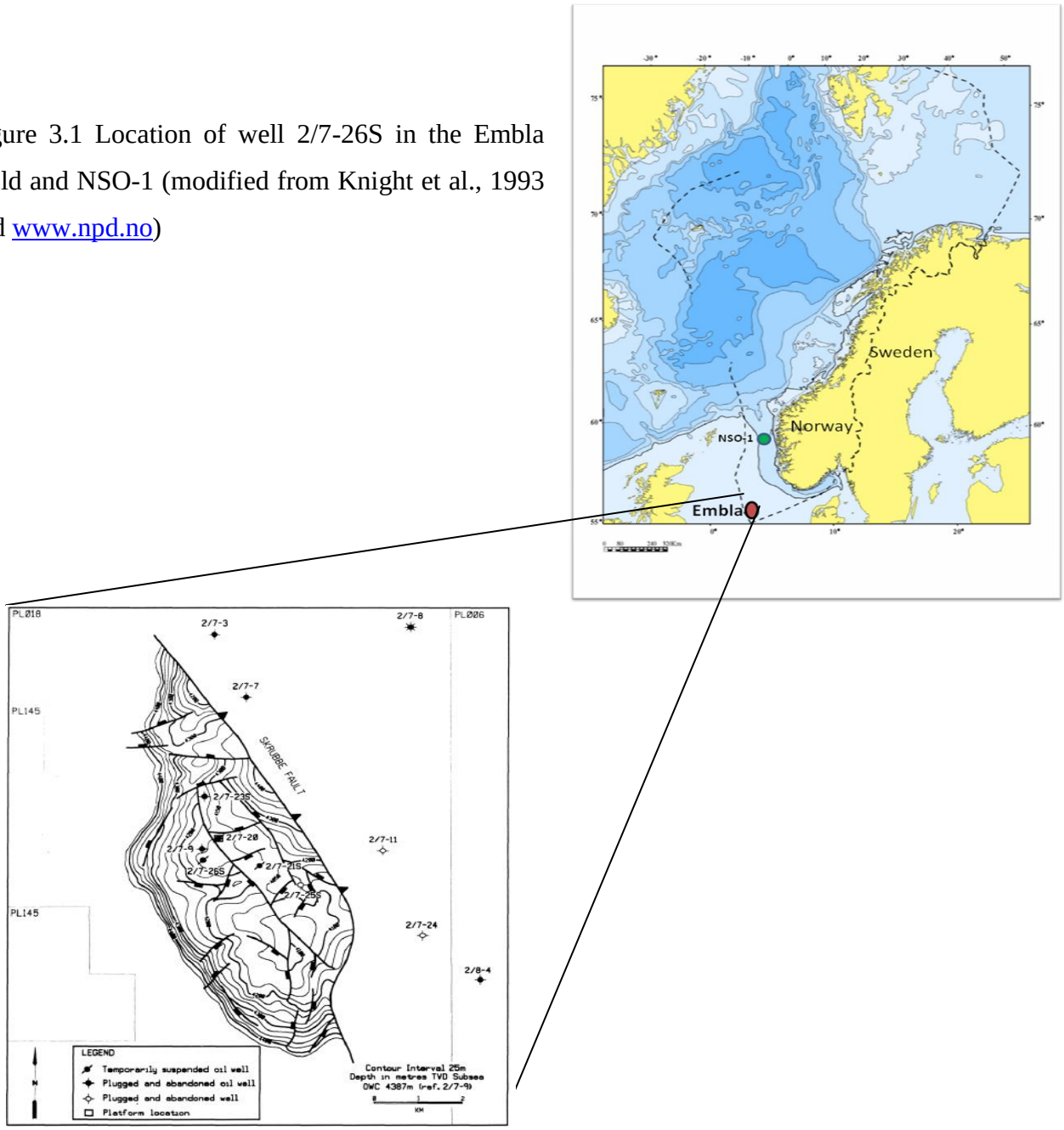

Figure 3.1 Location of well 2/7-26S in the Embla Field and NSO-1 (modified from Knight et al., 1993 and www.npd.no)

All together 21 core samples have been studied. In addition to these samples, the NSO-1 Oseberg standard oil was used as a reference point in the analytical work. Table 3.2 presents the list of the samples and their location in the stratigraphy.

no	Core name	Sample code	Depth (ft)	Depth (m)	Lithology
1	2/7-26S # 10	E1	14524	4427	Upper sandstone
2	2/7-26S # 14	E2	14570	4441	"
3	2/7-26S # 22	E3	14686	4476	"
4	2/7-26S # 30	E4	14770	4502	"
5	2/7-26S # 34	E5	14831	4520	"
6	2/7-26S # 37	M1	14873	4533	Mudstone
7	2/7-26S #38	M2	14906	4543	Mudstone
8	2/7-26S #39	E6	15323	4670	Lower sandstone
9	2/7-26S #40	E7	15343	4676	"
10	2/7-26S #41	E8	15353	4680	"
11	2/7-26S #42	E9	15372	4685	"
12	2/7-26S #44	E10	15415	4698	"
13	2/7-26S #46	E11	15427	4702	"
14	2/7-26S #47	E12	15442	4707	"
15	2/7-26S #48	E13	15451	4709	"
16	2/7-26S #49	E14	15460	4712	"
17	2/7-26S # 5,1	E15	15848.5	4831	Rhyolite
18	2/7-26S # 4,1	E16	15857.6	4833	"
19	2/7-26S # 3,1	E17	15872.5	4838	"
20	2/7-26S # 2	E18	15883.4	4841	"
21	Bitumen in vein	VB	16496	5020	Fractured rhyolite
22	NSO-1	NSO-1	Oseberg field		Kimmeridge shale oil

Table 3.2. List of samples undergone geochemical analysis. The given depths are measured depth.

The sample sets represent the Upper sandstone, Lower sandstone, rhyolites and the NSO-1. The following is a brief overview of the samples:

NSO-1

This sample is the North Sea Oil Standard, and is from the Oseberg field, on the Norwegian Continental Shelf (NOCS). It is used as astandard by the Norwegian Petroleum Directorate (NPD). It is a well known standard used to calibrate laboratory instruments before running geochemical analyzes (Weiss et al., 2000). In later chapters this sample will be referred to as NSO-1.

Upper sandstone: (2/7-26S # 10, 2/7-26S # 14, 2/7-26S # 22, 2/7-26S #30, 2/7-26S # 34)

These are core samples taken from well 2/7- 26S of the embla Field, southern part of the Norwegian Offshore Continental Shelf (NOCS) at a measured core depth between 4427 and 4520 m. The samples represent the Upper sandstone section of the reservoir. Theses samples will be assigned sample codes of **E1, E2, E3, E4** and **E5** respectively.

Mudstone: (2/7-26S # 37, 2/7-26S # 38)

These are core samples (see Fig. 3.2) taken from the Embla field, southern part of the NOCS, from well 2/7-26S at 4533 and 4543 meters core depth respectively. They represent the mudstone unit separating the Upper and Lower sandstones. The samples will be considered only in the sense of their role as representing a potential intra-reservoir vertical seal for petroleum communication between the Upper and Lower sandstone parts of the reservoir. These samples will be referred to as **M1** and **M2** respectively.

Figure 3.2. Core sample representing the mud stone unit which separates the Upper and Lower sandstones reservoir sections. It is a sample taken at a measured core depth of 4533 m. It illustrates the intra-reservoir sealing potential of the mudstone unit. The sample is named M1.

Lower sandstone: 2/7-26S # 39, 2/7-26S # 40, 2/7-26S # 41, 2/7-26S # 42, 2/7-26S # 44, 2/7-26S # 46, 2/7-26S # 47, 2/7-26S # 48, 2/7-26S # 49.

A total of nine core samples were taken from the Lower sandstone of the well 2/6-26S, Embla field at measured core depths between 4670 to 4712 m. On hand specimen the samples are darker than the Upper sandstone due to bitumen. In latter discussions the sample will be named as **E6** to **E14** respectively. See figures 3.3-3.5 for illustration of core samples from this unit.

Figure 3.3 Core sample illustrating the Lower sandstone of well 26S, Embla Field. It was taken from a measured core depth of 4676. The sample is rich in organic matter, black color. This sample will be referred to as E7.

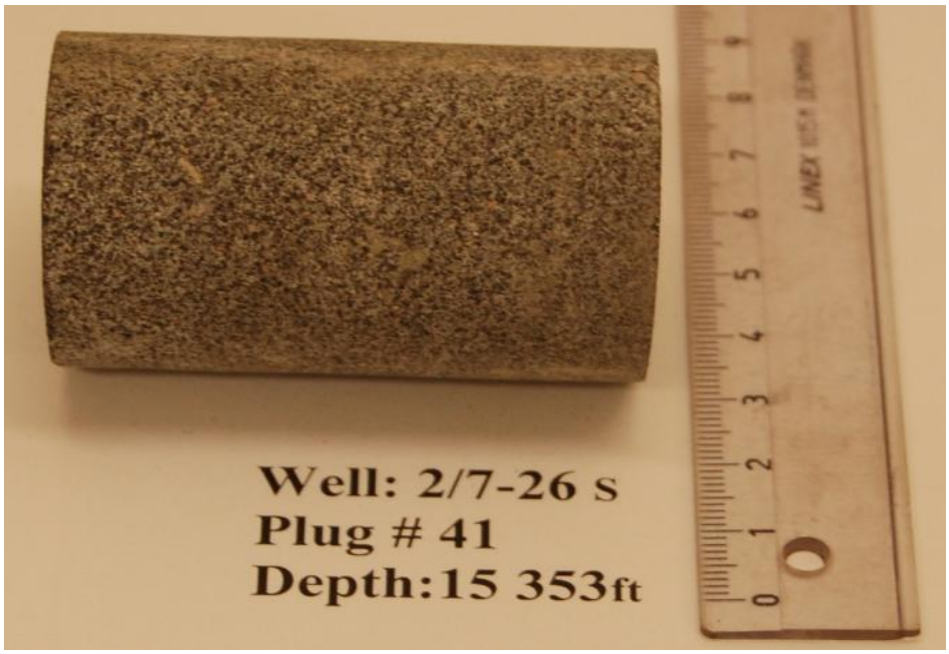

Figure 3.4 illustrating the typical sandstone in the Lower section of the Embla reservoir. It is sampled at a depth of 4680 m.

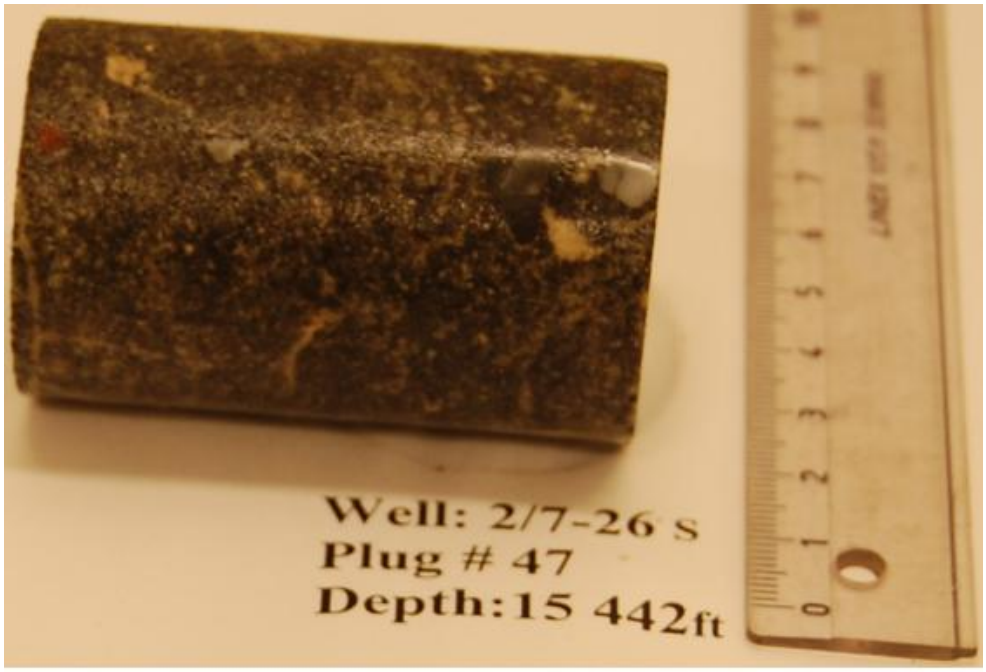

Figure 3.5. Core sample taken at a measured depth of 4707 m. It is a typical sandstone sample in the Lower sandstone with visible bitumen on it.

Rhyolites (2/7-26S # 5, 1; 2/7-26S # 4, 1; 2/7-26S # 3, 1; 2/7-26S # 2)

These core samples are taken from the rhyolite unit of the well 2/6-26S, Embla field at depths between 4831 and 4841 m. On hand specimen of the core samples and the extracted solvent were light in colour. The Samples are clean light coloured, fractured and brecciated rhyolites with dark fracture filling material. These muddy samples have been suggested to represent re-deposited rhyolite. In latter discussions the samples will be named as E15, E16, E17 and E18 respectively.

Vein bitumen (VB)

The dark material (bitumen) filled in the rhyolite fractured rock were taken out of the vein. The sample is located at a depth of 5028 m. In latter discussion the sample will be named as vein bitumen (VB). This sample is darker and more muddy than the rhyolites.

4. Analytical methods

In this chapter I present all the analytical methods used. The outline of this chapter is as follows:

4.1. Introduction

The geochemical parameters (see chapter 5) to be used for interpretation of the various aspects of the sample set based on geochemical properties can be divided into two main groups; bulk parameters and molecular parameters. The bulk parameters describe gross compositional properties of whole samples, in terms of either whole oil or total extracts, using for example percentage amount of saturate hydrocarbons, aromatic hydrocarbons and polar compounds. Thin Layer Chromatography-Flame Ionization Detection (TLC-FID) is used for this purpose.

The molecular parameters represent chemical characteristics of either specific sample fractions or whole oils, using gas chromatography with flame ionization detector (GC-FID) or gas chromatography – mass spectrometry (GC-MS). To determine the biomarkers and the relative amounts of the bulk petroleum fractions for the samples from the Devonian sandstone and rhyolites in the Embla field, samples were subjected to one or more of the following analytical procedures; Iatroscan (TLC-FID), GC-FID or GC-MS.

Gas Chromatography–Mass Spectrometry, (GC-MS) and Gas Chromatography–Flame Ionization Detector (GC-FID) are used for extraction of information about biomarkers.

During the whole analytical processes, the North Sea oil (NSO-1) from the Norwegian Petroleum Directorate (NPD) was used repeatedly as a reference oil, and has also been used in this analytical work. This reference oil is from the Oseberg Field where the source rock is the Upper Jurassic Draupne Fm. (equivalent to the Kimmeridge Clay Fm.) (Dahl and Speers, 1985).

4.2. Gas chromatography

Chromatography is a widely utilized technique which separates a complex mixture of organic compounds like gas or oil into individual molecular types. This unique way of separation was first put in use in the 1950's and makes it possible to identify compounds qualitatively and quantitatively. Chromatography is popular because it is easy to use, fast and relatively non-expensive. It enables one to separates substances on molecular level from a complex composition according to boiling point, and the results are very precise. The main principle for boiling point chromatography is that the system has two phases. These are the stationary and the mobile phases. The former is where substances are held back from further migration. The mobile phase is either gaseous or liquid. The adsorbent is the solid substance that is retained in the solid phase. Relative solubility, adsorption and volatility are three properties which control the separation.

4.2.1. The carrier gas

Soluble substances, in gas chromatography, are carried by the carrier gas through the column in the chromatograph. The carrier gas must be inert, to avoid interaction with the sample that is analyzed. Nitrogen, helium and hydrogen are commonly in use. Hydrogen needs special precautions because of its explosive nature when leaking. Helium is very pure and causes only little contamination but is very expensive, and nitrogen is inexpensive and safe to use. The carrier gas has an effect on the analysis-time and the efficiency of the column. Thus, the choice of gas can influence how quickly substances react, how they move through the

column and how fast they reach the detector. Gas is transported from the cylinder into the chromatograph by a given pressure, which can always be changed and corrected. Normally the pressure is about 2-3 kg/cm^2 (bar). A control-system/a flow-controller makes sure that the right pressure-value and speed of the gas into chromatograph is correct.

4.2.2. The injector and column

In gas chromatography, the unit where the sample is vaporized and introduced into the column is called the injector and the column is the stationary phase. Samples prepared for analysis are injected, vaporized and transported through the column. Some of the substances from the sample do not flow through the column because they absorbed in the injector. The column which looks like a spiral is usually made of quartz. There are two types of columns:

- A packed bed column that is completely packed and its stationary phase which fills the column completely are in granular form. Such type of columns is hardly in use today.
- An open tubular capillary column usually has a small diameter where a coating on the inner tube wall acts as the stationary phase. Substances flow through the hole in the center of the column.

Depending on the substance to be separated, the temperature has to adjust and must be high enough for the sample to be vaporized right away.

4.2.3. The detector

Detector measures the different substances during the separation of components which takes place in the column. Concentration-dependent-detectors and mass-flow-dependant detectors are different ways of detecting these substances. Basically the two most commonly used detectors are thermal-conductivity (TCD) and flame-ionization (FID). TCD measures the change in heat in the detectors as the analyte passes through, and does not destroy organic compounds in the process. On the other hand, this is the least precise measurement. In contrast to the TCD, the FID destroys the sample as it burns the organic compounds. However FID has order of magnitude more linear range than the TCD. Although the minor

disadvantage is that samples are destroyed in the process as the organic compounds burn in the FID, it is the most accurate detector and a choice of preference.

4.3. Sample preparation and extraction of bitumen

A total of 21 core samples from the well 2/7-26S of the Embla filed in the Norwegian sector of the North Sea were obtained. These samples were crushed into powder for geochemical analysis. To extract the bitumen from the crushed core samples a conventional Soxtec System HT 1043 Extraction Unit by Tecator was used. Approximately 3.1 g of the crushed sample was filled into pre-extracted cellulose cartridges and covered with glass wool. Approximately 40 to 50 ml of mixture of 93% dichloromethane and 7% of methanol was the solven used to dilute the samples. The solvent is then heated by the underlying stove to 90 °C. Six samples at a time boil in the solvent for two hours and lifted afterwards. Subsequently the condensing solvent rinses for one hour. To concentrate the extract, the valve, controlling the back flux of solvent into the cartridge, is closed. The concentrated extract is transferred into a 15 ml glass vial and subsequently filled up to 5 ml with dichloromethane to standardize the concentrations. The vials are sealed teflon lined plastic cork. Some samples were also extracted using a rapid "micro-extraction'' method following Karlsen and Larter (1989).

The extracted organic solvent is then concentrated and geochemically analyzed by three different methods: Iatroscan TLC-FID, GC-MS and GC-FID.

4.4. Iatroscan-Thin Layer Chromatography-Flame Ionization detection (TLC-FID)

Studying petroleum column heterogeneities in reservoirs requires a rapid method for establishing the horizontal and vertical distributions of gross petroleum composions in terms of saturated hydrocarbons, aromatic hydrocarbons and resines/asphaltenes (Karlsen and Larter, 1989). Petroleum extract from reservoir sample consists of different compound groups, i.e. hydrocarbons, a bonding between hydrogen, carbon and non-hydrocarbons i.e. resins and asphaltenes. The extracts can be separated into compound classes such as

saturated hydrocarbons, aromatic hydrocarbons and polar compounds by Iatroscan thin-layer chromatography-flame ionization detection (TLC-FID), an instrument equipped with a flame ionization detector and interfaced with an electronic integrator, was used for rod scanning and quantification (see Karlsen and Larter, 1991 for details) at the department of Geosciences, University of Oslo.

TLC-FID offers a rapid and accurate method for quantifying saturated and aromatic hydrocarbons, and resin/asphaltene fractions, in solvent extracts of petroleum source rocks, reservoir rocks and crude oils (Karlsen and Larter, 1991). The variation between these compounds can be used to characterize the petroleum populations in the reservoir (Bhullar et al., 2000) and differentiate between migrated hydrocarbons, in-situ generated hydrocarbons and also diesel drilling fluids (Karlsen and Larter, 1991). This technique is suitable to screen large sample volumes from petroleum reservoirs to obtain information for selection of samples for high-resolution analysis.

In this study, samples from the Embla Field were analyzed by an Iatroscan MK-5 model instrument coupled with a flame ionization detector (FID) connected to an electronic integrator (Perkin-Elmer LCI-100) used for rod scanning and quantification. The electronic integrator calculates the total quantity of the different compounds in the different extracts. The components were separated using silica rods, type Chromarods-S III (pore diameter 60 Å, particle size 5 μm). The chromarods are passed through the FID to remove contaminants and to obtain constant activity of the silica layer, and then all samples (3 μl) were applied onto the chromarod on a fixed point near the base of the chromarod. Eight out of 10 rods were used for the samples (2 rods pr. sample), the remaining 2 were used for test runs, one blank and the other one with the NSO-1.

To develop the Chromarods, solvents of different polarity were used to separate saturated hydrocarbons, aromatic hydrocarbons and polar compounds. The rods were placed in a solvent of normal-hexane for 36 minutes, causing the saturated hydrocarbons to rise to the uppermost part of the rods. After air drying the rods were placed in toluene for 8 minutes, causing the aromatic hydrocarbons to move to the middle of the rods. After each development the rods were then dried at 60°C (90 sec). The polar/ asphaltenes are not

mobile in these solvents and therefore remain stationary at the point of application on the lower most part of the rods. Then the Chromarods were placed in the Iatroscan instrument, the scanning speed was 30 sec/scan, and pure grade hydrogen (180 ml/min) and air (2.1 l/min) supplied by a pump were used for the detector.

As mentioned in the beginning of this chapter, a TLC-FID analysis gives you an overview of the main three fractions, i.e. saturated hydrocarbons, aromatic hydrocarbons, and polar compounds (resins and asphaltene).

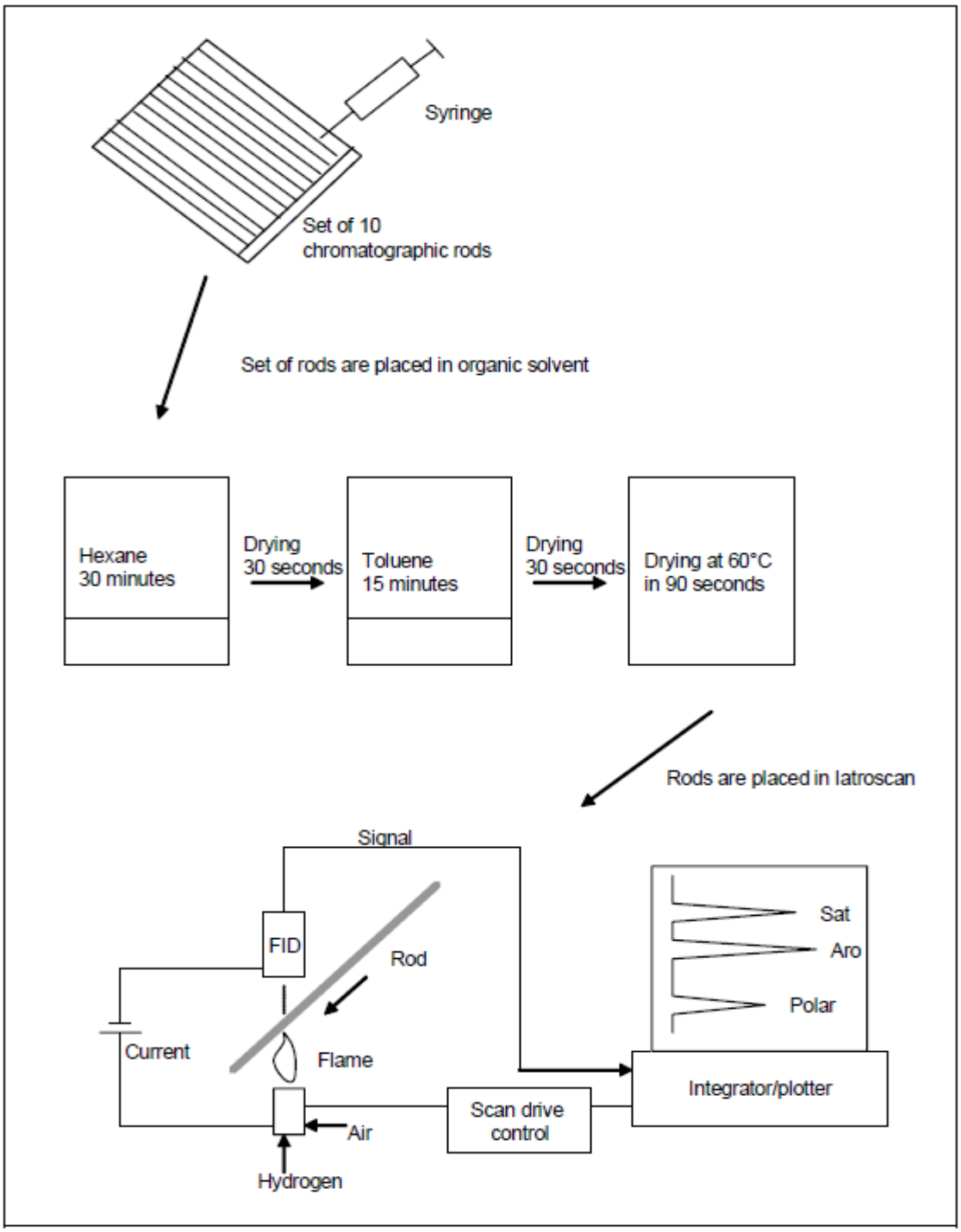

Figure 4.1. The key elements in the TLC-FID analysis for separating and quantifying saturated hydrocarbons, aromatic hydrocarbons plus resins and asphaltenes (polar compounds) (Pedersen, 2002).

4.5. Gas Chromatography–Flame Ionization Detector (GC-FID)

The GC-FID technique allows identification and quantification (relative or absolute) of individually separable major components in petroleum, such as n-alkanes, isoprenoids, toluene, hexane, xylene and so on. The sample is injected and vaporized prior to entering a chromatographic column, in which the separation of the different molecules takes place.

On the inside of the column a film layer acts as the stationary phase. The short-chained molecules, with low boiling points and high vapor pressure travel quickly through the column, while longer or more branched molecules need a longer period of time to move through the entire column. An inert gas, like nitrogen (N_2) or helium (He), is used as carrier gas, and this is the mobile phase. The column is heated according to a program from 40ºC to 325ºC in 75 minutes, and is then kept on 325ºC for 20 minutes, i.e. one run takes 95 minutes. This is to mobilize the compounds that have too low vapor pressure at ambient temperature. As the molecules exit the column they enter a flame ionization detector as described above. A computer records the signal from the FID, and the final gas chromatogram is edited and plotted using appropriate software. The X-axis in a chromatogram represents increased time and temperature, while Y-axis represents the signal intensity, i.e. in form of height of peaks equal to relative amount, of the different components.

To carry out the GC-FID analysis a Varian Capillary Gas Chromatography Model 3800, with a 25 m long Hewlett Packard Ultra II cross-linked Methyl Silicone Gum Column with a 0.2 mm inner diameter and a film thickness of 0.33 µm was used. The injector temperature was set to 330ºC with nitrogen as the carrier gas and initial column temperature of 40ºC and a hold time of 2ºC min^{-1} and a gradient of 4°C/min., which takes 75 minutes, where it was finally held for 20 min with a total run time of 95 minutes. Fig. 4.2 shows a schematic overview of a GC-FID.

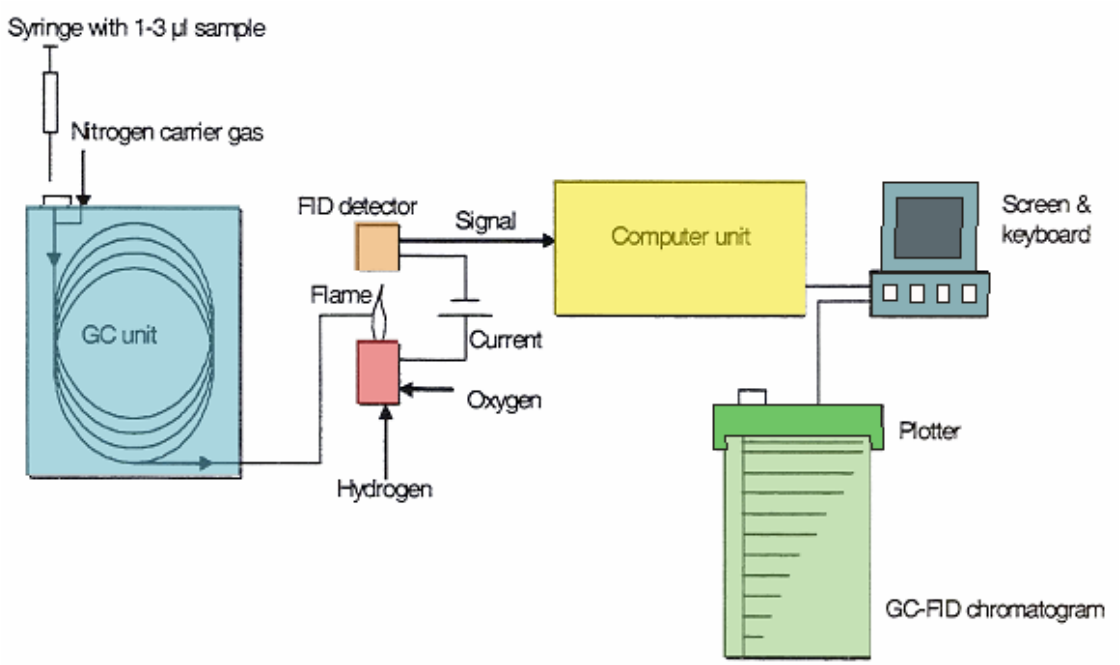

Figure 4.2. Schematic overview of the GC-FID instrument (modified from Pedersen 2002).

The GC-FID analysis was aimed at obtaining specific description of molecular compounds, and it includes the following parameter descriptions:

- Pristane/n-C17
- Phytane/n-C18
- Pristane/Phytane (Pr/Ph)

These parameters are mainly used as maturity and facies indicators, but GC-FID chromatograms may also be applied for general fingerprinting of the samples.

4.6. Molecular sieving

Before a GC-MS analysis is done, molecular sieving has to be carried out primarily to remove the n-alkanes. The n-alkanes are straight chain saturated hydrocarbons found in crude oils, and they will interfere with the signals from the biomarkers if they are present in

the sample during GC-MS analysis. Therefore, removal of the n-alkanes means that the biomarker signal will not be disturbed and the results will be more reliable. The process of molecular sieving also removes resins and asphaltenes from the samples (Pedersen et al., 2006). The function of the method is in that the molecules in the sieve have channel-like pores so that the long-chained n-alkanes will fit into this structure and be trapped. The bigger molecules will not enter these small openings and will therefore remain in the sample solution. When separating the molecular sieve from the sample the biomarkers and aromatic fractions will remain. As the result of the molecular sieving the sample will therefore be enriched in biomarkers and aromatic fractions and totally depleted in n-alkanes.

For the present study about 0.20 g of molecular sieve (5Å UOP MHS2 – 4120LC silica) was transferred into a 15 ml glass vial. About 3 ml or 3 drops of sample were then mixed with the powder-like sieve using a pipette. The sample mixture was diluted with 2-2.5 ml cyclohexane and stirred thoroughly with the pipette. Then the vial was centrifuged at 2000 rpm for 3 min in a Heraeus Sepatech Labofuge H, to settle the sieve. Subsequently, the liquid sample was poured into a new 15 ml glass vial with a pipette, and about ¾ of the solvent evaporated by a flow of nitrogen. After the sample had been concentrated the procedure was repeated. After the final evaporation of cyclohexane, the sample was transferred to vials with a pipette and sealed with a teflon-lined cap.

4.7. Gas Chromatography-Mass Spectrometry (GC-MS)

The GC-MS procedure allows identification and quantification of biomarkers. The GC-MS is a combination of a gas chromatograph (GC) for compound separation and a mass spectrometer (MS) using ionization and mass analysis for detection and identification of the components (see Figure 4.3).

The difference in the chemical properties between different molecules in the mixture will separate the molecules as the sample travels the length of the column. The molecules take different amounts of time (called the retention time) to come out of (elute from) the gas chromatograph, and this allows the mass spectrometer downstream to capture, ionize, accelerate, deflect, and detect the ionized molecules separately. The mass spectrometer does

this by breaking each molecule into ionizes fragments and detecting these fragments using their mass to charge ratio.

The different molecular fragments have different mass (m) and an electronic charge (z) equal to unit, and the ratio m/z is specific for many molecules of interest, such as biomarkers. Hopanes and triterpanes are for example found to have m/z = 191. The detector registers the m/z value and the relative abundance of the different ions. A PC program is used in recording and managing the data. The final plot shows the relative abundance of ions with the selected m/z ratio versus time elapsed (retention time). Before introducing samples to the GC-MS all n-alkanes are removed by molecular sieving. The purpose for the molecular sieving is to get a stronger biomarker signal.

In this study the GC-MS was used to analyse the bulk composition of all the samples. For this purpose a Fisons Instruments MD800 GC-MS system in SIM-mode (selected ion monitoring) with a 50 m long Chromopak CP-SIL 5CB-MS FS 50X.32 (40) WCOT fused silica-type column with an inner diameter of 0.32 mm that contained a CP-SIL5CB Low bleed/MS stationary phase was used. The initial temperature of the column was 80ºC and it was heated with 10ºC min^{-1} up to 180ºC and subsequently with 1.7ºC min^{-1} up to 310ºC, where it finally was held for 30 minutes.

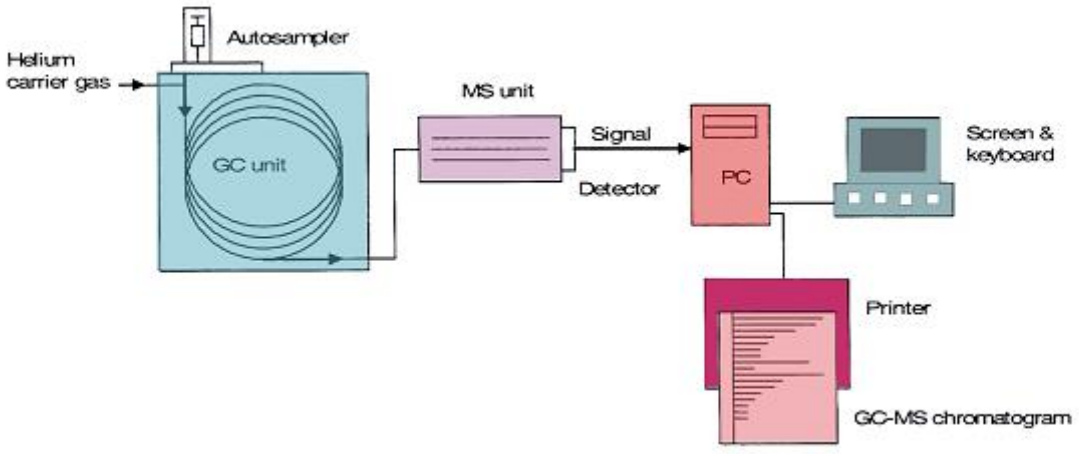

Figure 4.3. Schematic overview of the GC-MS instrument (from Pedersen, 2000).

In this study the GC-MS was used to monitor the ions with a mass/charge (m/z) ratio of 178, 191, 192, 217, 218, 231 and 253. Monitoring of these ions will give information about the n-alkane distribution and the most common biomarkers and related compounds used to establish the maturity, source and facies of the petroleum.

5. Petroleum Geochemical Interpretation parameters

The Various geochemical techniques described in chapter four resulted in different molecular parameters. These parameters are used to determine the maturity, facies and degree of biodegradation of the reservoir samples from the Embla Field. These parameters will be discussed in this chapter. The parameters are arranged by groups of related compounds in the following order:

5.1 Iatroscan TLC-FID

5.2 GC-FID

5.2.2 Pristane/Phytane

5.2.1 Pristane/n-C17 and phytane/C18

5.3 GC-MS

5.3.1 Terpanes

5.3.2 Steranes

5.3.3 Triaromatic Steroids

5.3.4 Monoaromatic Steroids

53.5 Phenanthrene and methylphenanthrene

5.3.6 Methyl-dibenzothiophene

5.1. Iatroscan TLC-FID

5.1.1. Saturated and aromatic hydrocarbons and polar compounds

Bitumen was extracted from the various samples from well 2/6-26S of the Embla Field using the procedures described in the previous chapter. The extracts were then separated into compound classes (saturated hydrocarbons, aromatic hydrocarbons and polar compounds). Iatroscan thin layer chromatography-flame ionization detection (TLC-FID) offers a rapid and exact method for quantifying the gross components of oils and extracts.

The saturated hydrocarbons/aromatic hydrocarbons (SAT/ARO) ratio mainly reflect source rock quality and maturity (Clayton and Bostick, 1986; Cornford et al., 1983). The ratio increase with increasing thermal maturity, but will also increase in the gas-phase of phase-fractionated petroleum during the migration to shallower depths (Østensen, 2005). Polar compounds in oils reflect either low maturity or biodegradation. The concentration of these compounds is low in high maturity petroleum and condensates.

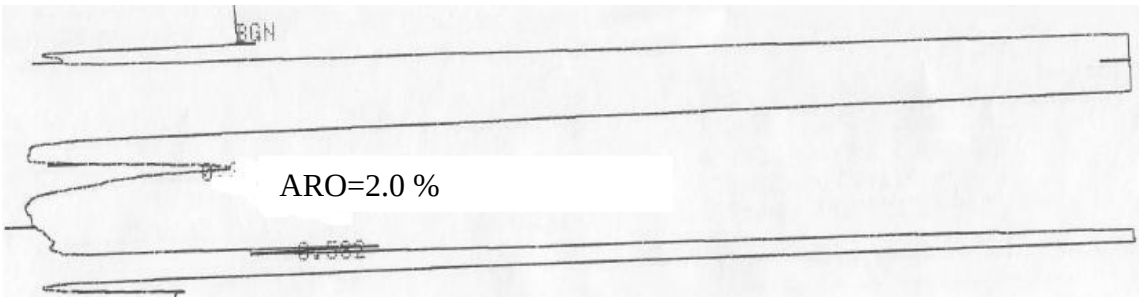

Figure 5.1. Analysis of bulk extracts in to their respective fractions by Iatroscan TLC-FID. Separation and quantification of fractions for sample E8 from Embla. SAT=saturated hydrocarbons, ARO= aromatic hydrocarbons and POL= polar compounds. Note the low concentration of aromatic compared to the saturates and polars.

Figure 5.2. Analysis of petroleum fractions by Iatroscan TLC-FID. Separation and quantification of fractions for the standard NSO-1 sample. SAT= saturated hydrocarbons, ARO= aromatic hydrocarbons and POL= polar compounds.

5.2. GC-FID

The analysis of the GC-FID of the extracts have been used to identify the n-alkanes which can be up to C_{40}, with the focus placed on the C_{15+} compounds (Figure 5.3). The n-alkane distributions together with ratio of them with isoprenoids (Pristane/n-C_{17} and Phytane/n-C_{18} ratios) can provide useful information about source and deposition facies, maturity and biodegradation of the samples.

5.2.1. n-alkane patterns

The n-alkane patterns can be used to classify chromatograms and give information about the facies and maturity of the samples (Peters and Moldowan, 1993). In normal "North Sea" petroleum the peak height decreases asymptotically with increasing carbon number. This creates a concave curve on the chromatogram. Bimodal distribution has chromatograms with two maxima groups of n-alkanes with a minimum between them. The GC-FID traces may also indicate if there is any biodegradation, in which case the unresolved complex mixture (UCM) of the compounds rises above the baseline, and the relative concentration of n-alkanes decrease compared to other compounds like isoprenoids and aromatics. Severely biodegraded samples will have reduced, or no n-alkanes, pristane or Phytane left for

detection and measurement. The UCMs in oils are amongst the most complex mixtures of organic compounds on Earth and extremely difficult to identify (Sutton et al., 2005).

5.2.2. Pristane/Phytane ratios

Pristane and Phytane are isoprenoid isoalkane biomarkers derived primarily from phytol, a side chain of the chlorophyll molecule that separates from the porphyrine structure after deposition during diagenesis and they are the most abundant source of isoprenoids (Tissot and Welte, 1978, 1984) and can be identified from GC-FID analysis. The phytol can be transformed into pristane or Phytane depending on the depositional environment. Pristane can be derived by oxidation and decarboxylation of phytol, while phytane can be derived by dehydration and reduction (Peters and Moldowan, 1993). Thus the parameter (Pristane/Phytane) provides valuable information about the depositional environment with respect to anoxic- or oxic conditions. Pr/Ph < 1 may indicate hypersaline, anoxic or carbonate or lacustrine settings. Pr/Ph > 1 indicate oxidizing or hypersaline, Pr/Ph = 1.3 – 1.7 indicate marine oil, Pr/Ph → 2.5 indicate a marine environment with considerable amount of terrestrial input, Pr/Ph > 3 – 10 indicate coal. These figures must be supported by other data in order to be conclusive. However, more recently, it has been suggested that pristane and in particular phytane also may have a bacterial origin (Peters and Moldowan, 1993). The ratio can also be used as a maturity indicator because it typically increases with increasing maturity (Alexander et al., 1981a), but because pristane and phytane during diagenesis can be derived from other sources than phytol e.g. bacterial membranes (ten Haven et al., 1987) the ratio should be used together with other parameters. Since phytane is more unstable than pristane, the Pr/Ph will increase with increased maturity. Pristane and phytane are more predominant in anoxic environments (Welte and Waples, 1973).

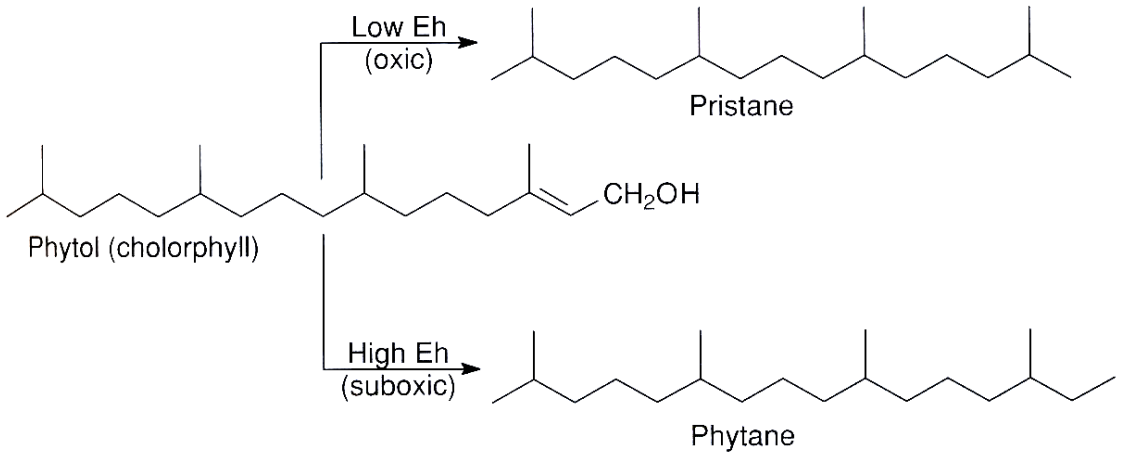

Figure 5.3. The diagentic origin of pristane and phytane *(Peters et al., 2005)*.

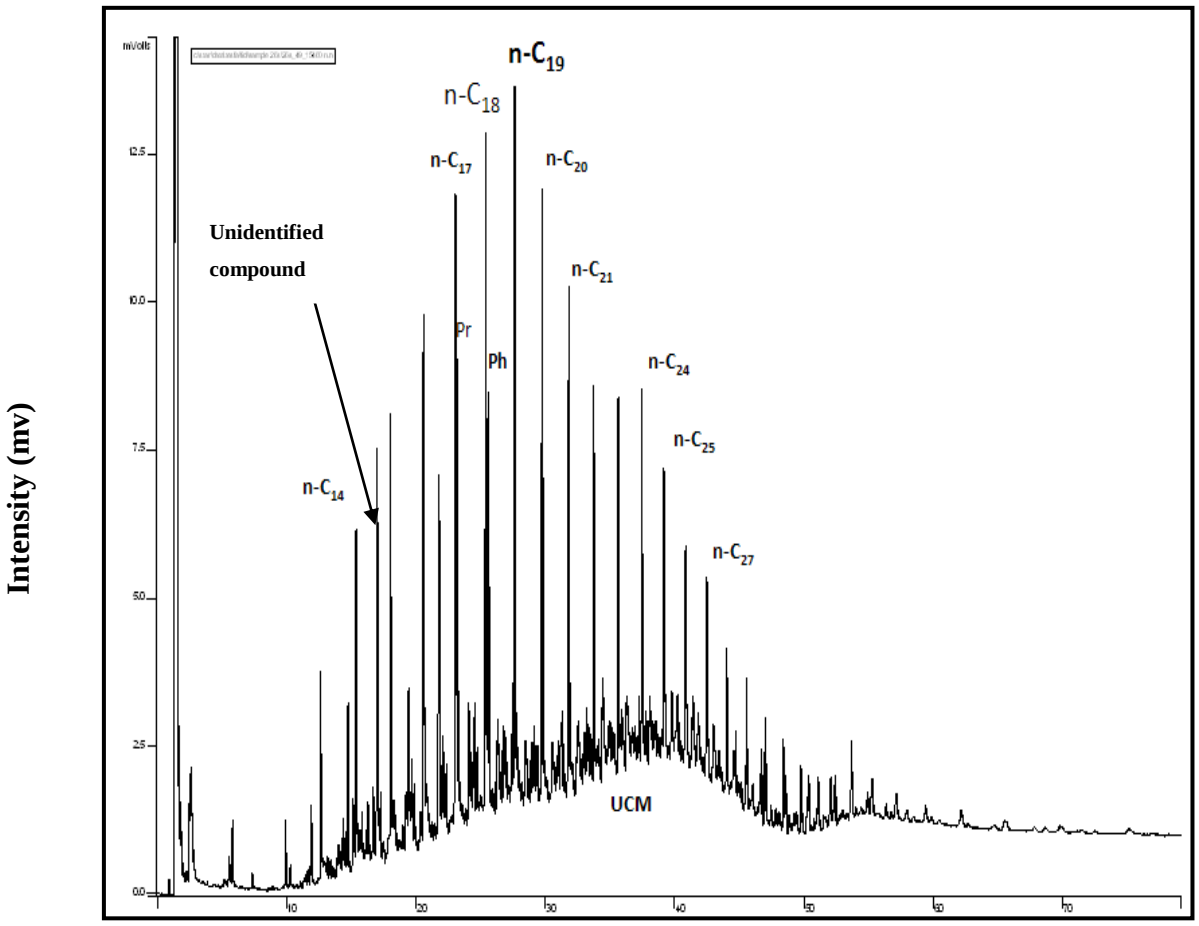

Figure 5.4. The GC-FID compounds, n-C17, pristane, n-C18 and phytane for sample E14 of the Embla samples. The lower n-alkanes (less than n-C_{12}) are not seen due to evaporation loss during storage

5.2.3. Pristane/n-C_{17} and Phytane/n-C_{18}

Pr/n-C_{17} and Ph/n-C_{18} ratios together with other parameters are used to determine source rock facies, maturity and the level of biodegradation of hydrocarbons. As source rock maturity is increased isoprenoids break down more rapidly than n-alkanes, thus low ratios indicate a more mature sample. The ratios can be used together with other parameters to rank related, non-biodegraded oils and bitumens based on thermal maturity. But care should be taken because organic input and biodegradation may affect the ratio (Peters and Moldowan, 1993).

5.2.4. Carbon Preference Index (CPI) and Odd/Even predominance (OEP)

The ratio, by weight, of odd to even molecules (Tissot and Welte, 1978) which is the predominance of molecules with an odd number of carbon atoms can be measured by the Carbon Preference Index (CPI). CPI was first introduced by Bray and Evans (1961) and can be used to indicate the thermal maturity of an oil or extract. CPI values significantly above or below 1.0 indicate that the oil or extract is thermally immature. Values close to 1.0 suggest, but do not prove an oil or extract to be thermally mature (Peters and Moldowan, 1993). Values below 1.0 indicate carbonate facies, while values higher than 1.0 indicate lacustrine environment or silisiclastic source rock.

$$CPI = 2(C_{23}+C_{25}+C_{27}+C_{29})/[C_{22}+2(C_{24}+C_{26}+C_{28})+C_{30}]$$

$$OEP = (C_{21}+6C_{23}+C_{25})/ (4C_{22}+4C_{24})$$

5.3. GC-MS

The GC-MS method was used to identify the ions with a mass/charge (m/z) ratio of 178, 191, 192, 217, 198, 217, 218, 231 and 253 (see table 5.1). Most of the peaks are then used for further evaluating the maturities and facies parameters as will be discussed in the

subsequent chapters. Figures (5.5- 5. 7) show the peaks that are identified from the chromatograms and tables 5.1-5.4) give a short description of each peak.

Ion/mass ratio	Type	
m/z = 191	Terpanes	SAT
m/z = 217	Steranes	
m/z = 218	Steranes	
m/z = 231	Triaromatic steroids	ARO
m/z = 253	Monoaromatic steroids	
m/z = 178	Phenantrene	
m/z = 192	Methylphenantrenes	
m/z = 198	Methyl-dibenzothiophenes	

Table 5.1.Ion/mass ratios used for generating the chromatograms from the GC-MS data, and the chemical compounds they belong to. SAT=Saturated hydrocarbons, ARO= aromatic hydrocarbons and SARO

5.3.1. Terpanes

Terpanes are a group of saturated hydrocarbons that can be identified on m/z=191 (Table 5.2 and Fig. 5.5).

Peak	Stereochemistry	Name	Composition
P		Tricyclic terpane	$C_{23}H_{42}$
Q		Tricyclic terpane	$C_{24}C_{44}$
R	(17R+17S)	Tricyclic terpane	$C_{25}H_{46}$
S		Tetracyclic terpane	$C_{24}H_{42}$
U		Tricyclic terpane	$C_{28}H_{48}$
V		Tricyclic terpane	$C_{29}H_{50}$
A		18α (H)-trisnorneohopane	C_{27}
B		17α (H)-trisnorhopane	C_{27}
Z		17α(H), 21β(H)-bisnorhopane	$C_{28}H_{48}$
C		17α(H), 21β(H)-norhopane	$C_{29}H_{50}$
29Ts		18α (H)–30-norneohopane	C_{29}
X		15α-methyl-17α (H)-27-diahopane	$C_{30}H_{52}$
D		17β (H), 21α (H)-30-normoretane	$C_{29}H_{50}$
E		17α (H), 21β (H)-hopane	$C_{30}H_{52}$
F		17β (H), 21α (H)-moretane	$C_{30}H_{52}$
G	22S	17α (H), 21β (H)-22-homohopane	$C_{31}H_{54}$
H	22R	17α (H), 21β (H)-22-homohopane	$C_{31}H_{54}$

Table 5.2. Triterpanes identified on the m/z= 191 chromatograms (see Figure 5.5)

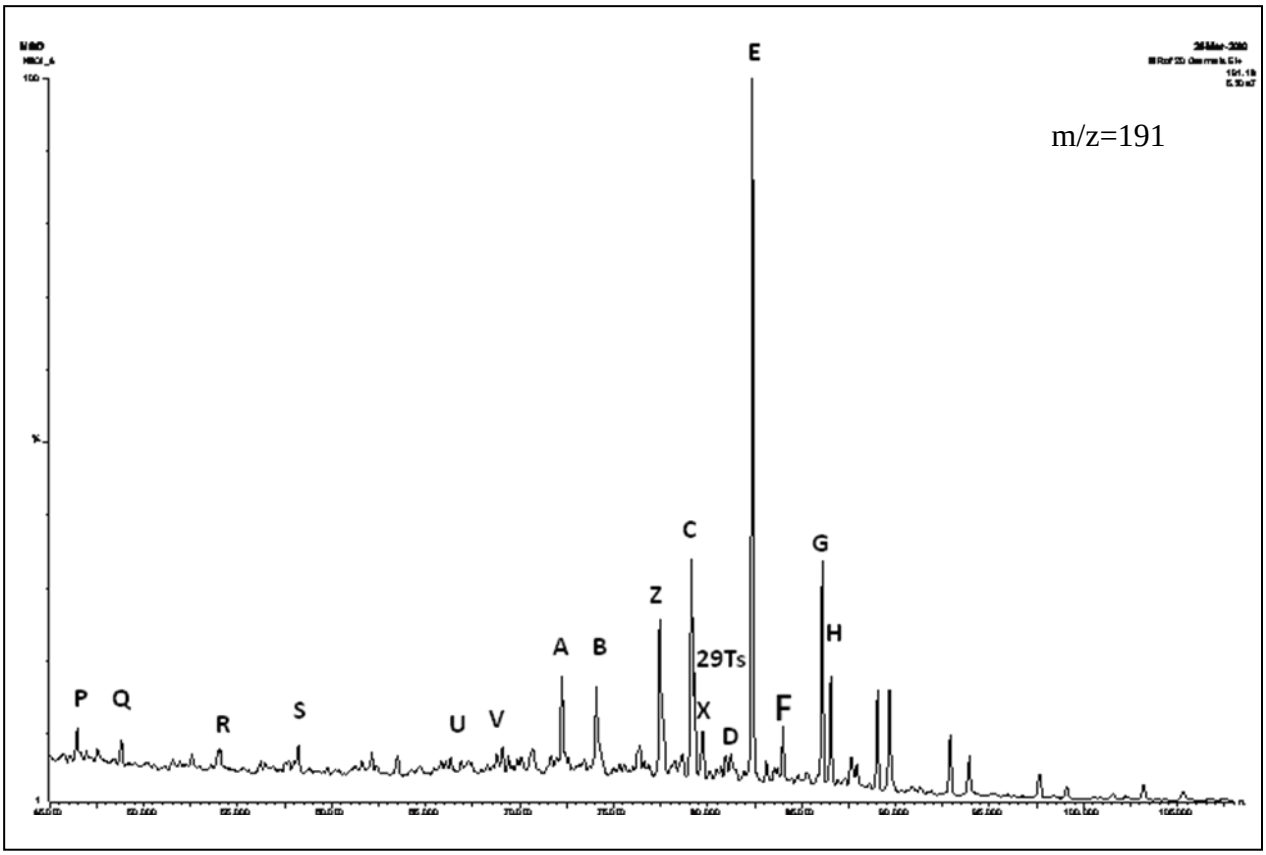

Figure 5.5 Peaks **measured on m/z= 191 GC-MS chromatograms**

5.3.2. Steranes

The Steranes are a group of tetracyclic saturated hydrocarbons (one 5-ring and three 6-rings) which can be identified on m/z = 217 (figure 5.6) and 218 (fig. 5.7). The relevant peak identification names of steranes from m/z = 217 are given in table 5.3 and from m/z = 218 in table 5.4.

Peak	Stereochemistry	Name	Composition
a	20S	13β(H), 17α(H), 20(S)-cholestane (diasterane)	$C_{27}H_{12}$
b	20R	13β(H), 17α(H), 20(R)-cholestane (diasterane)	$C_{27}H_{48}$
q	20S	24-ethyl-5α(H), 14α(H), 17α(H), 20(S)-cholestane	$C_{29}H_{52}$
r	20R	24-ethyl-5α(H), 14β(H), 17β(H), 20(R)-cholestane	$C_{29}H_{52}$
s	20S	24-ethyl-5α(H), 14β(H), 17β(H), 20(S)-cholestane	$C_{29}H_{52}$
t	20R	24-ethyl-5α(H), 14α (H), 17α(H), 20(R)-cholestane	$C_{29}H_{52}$

Table 5.3. Steranes identified on m/z = 217 chromatograms (see figure 5.6), Weiss et al. (2000).

Peak	Name
i	C_{27} regular sterane (5α(H), 14β(H), 17β(H), 20(S)-cholestane)
o	C_{28} regular sterane (24-methyl-5α(H), 14β(H), 17β(H), 20(S)-cholestane)
s	C_{29} regular sterane (24-ethyl-5α(H), 14β(H), 17β(H), 20(S)-cholestane)

Table 5.4. Steranes identified from the m/z =218 chromatograms (see figure 5.7), Weiss et al. (2000).

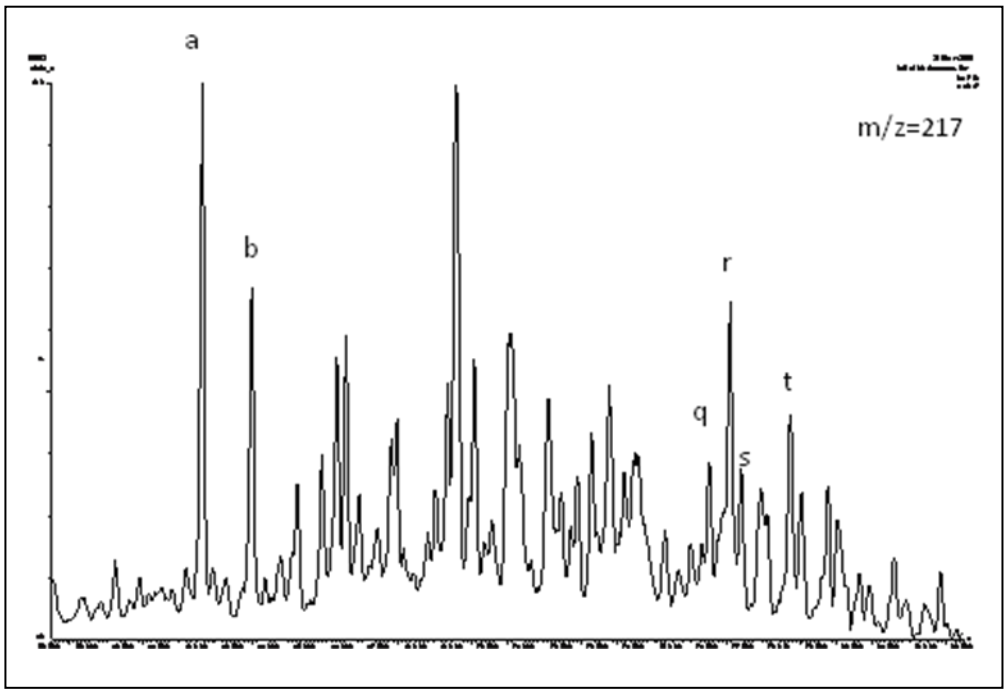

Figure 5.6. The m/z = 217 chromatogram from the T5-2 sample, showing the identified peaks of steranes (see table 4.2 for details).

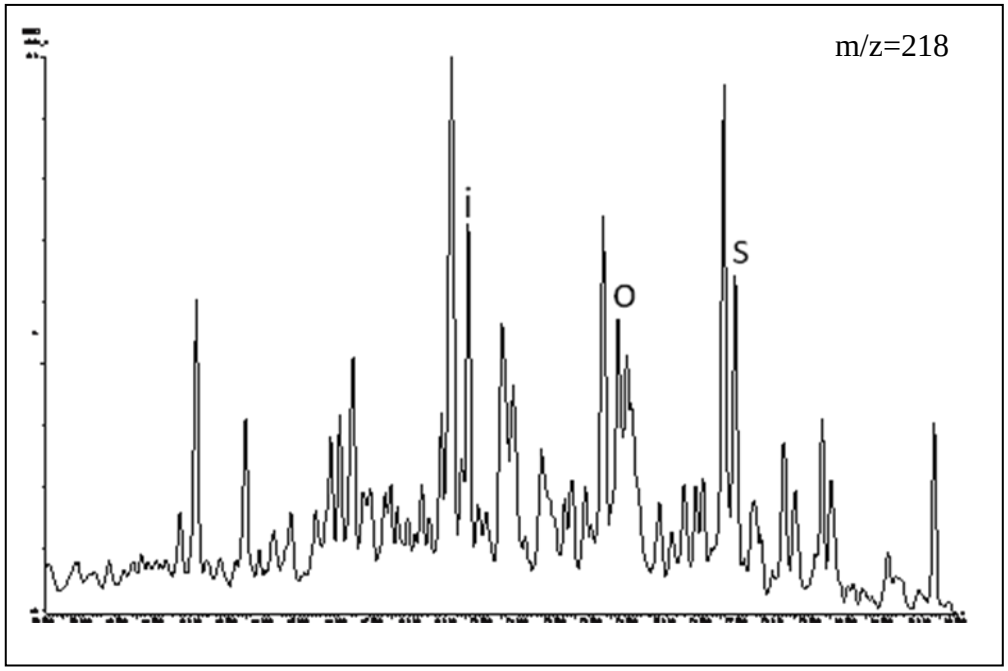

Figure 5.7. Chromatogram of m/z = 218 from the NSO-1 standard oil, mainly used to assess the % sterane compositions in terms of C27, C28, C29 steranes.

5.3.3. Triaromatic steroids

Triaromatic steroids are aromatic hydrocarbons which can be identified on m/z=231 (Fig. 5.8). They are very useful maturity assessments. Table 5.5 presents the relevant peaks of triaromatic steroids.

Peak	Name
a1	C_{20} triaromatic steroid (TA)
g1	C_{28} triaromatic steroid (TA)

Table 5.5. Triaromatic steroid hydrocarbons of m/z=231 (see figure 5.8)

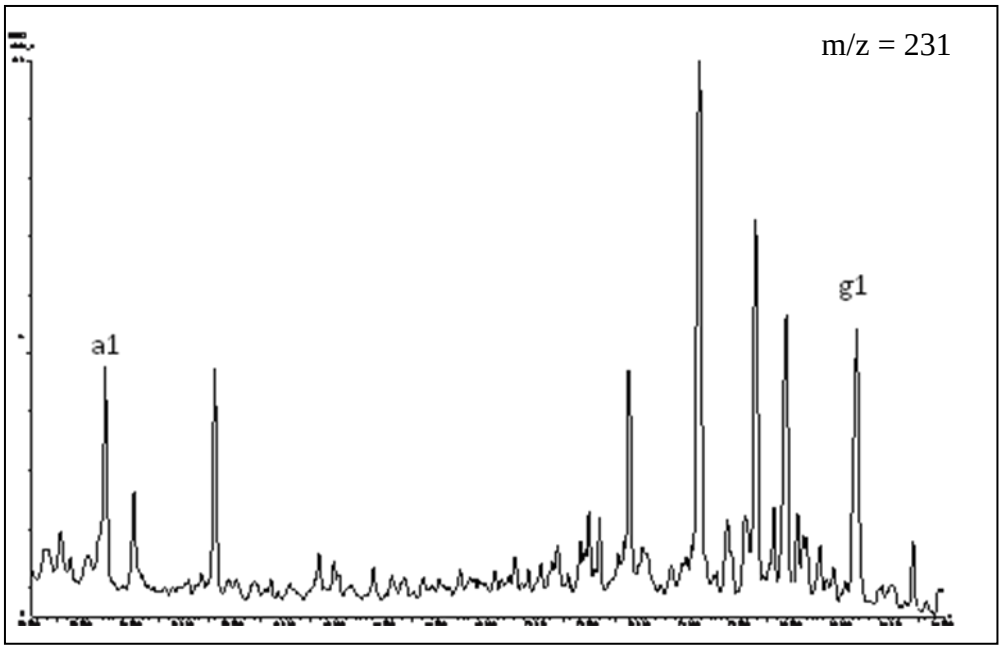

Figure 5.8. Peak measured on m/z = 231 GC-MS chromatogram (see table 5.5 for details)

5.3.4. Monoaromatic steroids

Monoaromatic steroids are aromatic hydrocarbons that can be found on m/z=253 (Fig. 5.9) and are assumed to be the precursors of the triaromatic steroids. The main use of monoaromatic steroids is for correlation (fingerprinting) and maturity assessment, comparing the ratio of triaromatic to monoaromatic steroids. The relevant peak identification names are given in table 5-6.

Peak	Name
H1	C29 monoaromatic steroid (MA)

Table 5.6 monoaromatic steroid hydrocarbon of m/z = 253 (see figure 5.9)

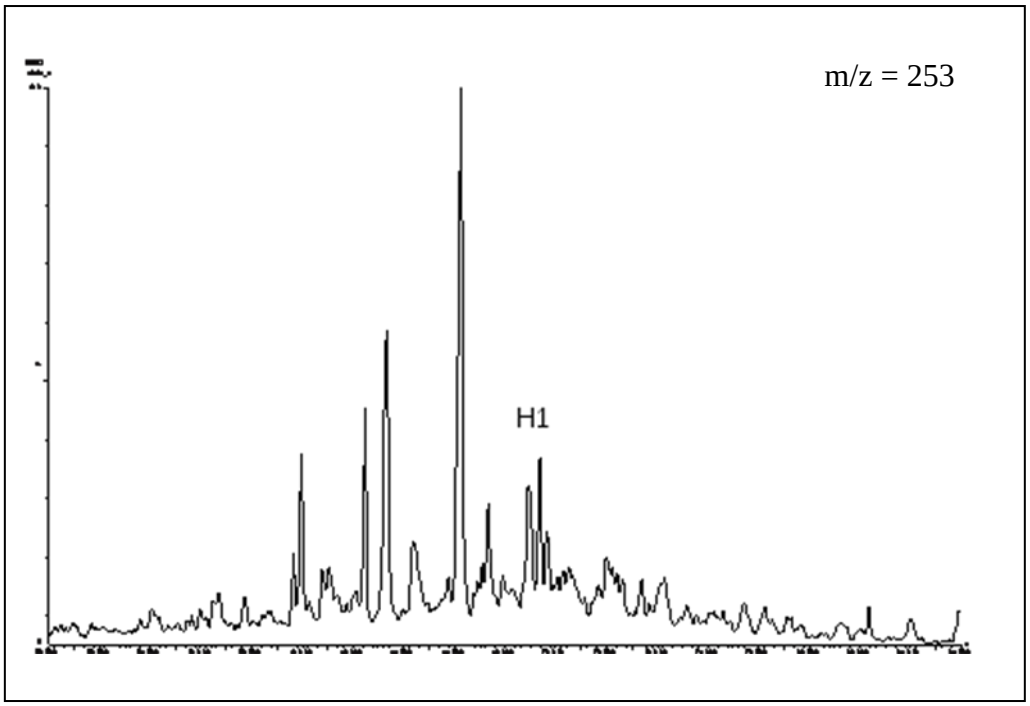

Figure 5.9. Peak measured on m/z = 253 GC-MS chromatogram (see table 5.6 for details)

5.3.5. Phenantrene and methylphenantrene

Phenantrene and methylphenantrene are aromatic hydrocarbons and their peaks can be identified on m/z=178 and 192 (Fig. 5.10). They are mainly used for maturity assessments. The peak identification names are presented in table 5-7.

Peak	Name
P	Phenanthrene
3-MP	3-methylphenanthrene
2-MP	2-methylphenanthrene
9-MP	9-methylphenanthrene
1-MP	1-methylphenanthrene

Table 5.7. Phenanthrene and methylphenanthrene identified from m/z = 178 and m/z = 192 chromatograms (see figure 5.10).

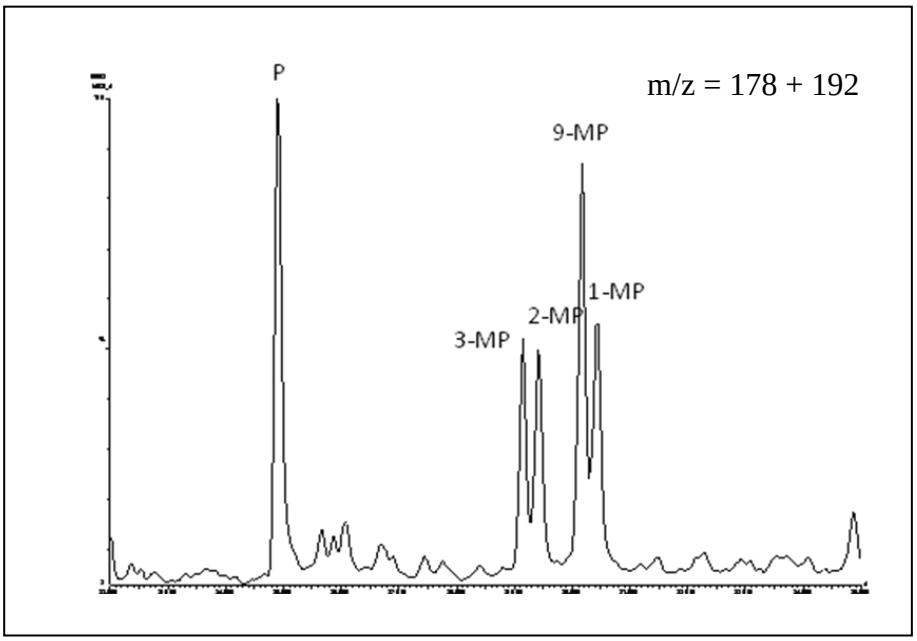

Figure 5.10. Peaks identified on m/z = 178+192 GC-MS chromatogram (see table 5.7).

5.3.6. Methyl-dibenzothiophene

Methyl-dibenzothiopenes are sulphur aromatic hydrocarbons that can be identified on m/z=198 (Fig. 5.11). The main use of these compounds is for maturity assessment and they respond better in the medium to low maturity range than do the phenanthrenes. The maturity assessment is based on measured peak heights for 4-MBDT and 1-MBDT. A big height difference for these peaks indicates high maturities *(Peters et al., 2005)*. The relevant peak identification names are given in table 5-8.

Peak	**Name**
4-MDBT	4-methyldibenzothiophene
1-MDBT	1-methyldibenzothiophene

Table 5.8. Peaks identified on m/z = 198 GC-MS chromatogram (Weiss et al., 2000).

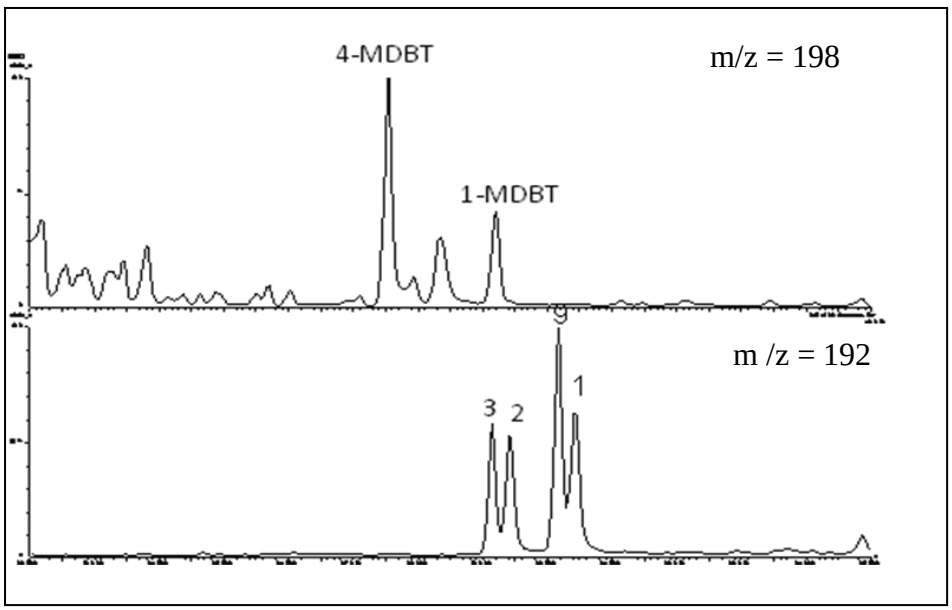

Figure 5.11. The m/z = 198 chromatogram compared with the m/z = 192 chromatogram (see table 5.8 for details).

The GC-MS techniques described in chapter four are able to detect the different molecules represented by the peaks described above. The various peaks in turn are used to calculate the parameters summarized in table 5.9. Finally the calculated parameters will be used to estimate the maturity and depositional facies of the samples from the Embla Field.

Number	Identification
1	Ts/(Ts+Tm), *(Seifert and Moldowan, 1978)*
2	Diahopane/(diahopane+normoretane), *(Cornford et al., 1986)*.
3	22S/(22S+22R) of C_{31}17α(H), 21β(H)-hopanes *(Mackenzie et al., 1980)*.
4	C_{30}-hopane/(C_{30}-hopane C_{30}-moretane) *(Mackenzie et al., 1985)*.
5	29Ts/(29Ts+norhopane) *(Moldowan et al., 1991)*.
6	Bisnorhopane/(bisnorhopane+norhopane) *(Wilhelms and Larter., 1994)*.
7	C_{23}-C_{29} tricyclic terpanes/C_{30} αβ-hopane *(modified from Mello et al., 1988)*.
8	C_{24} tetra cyclic terpanes/C_{30} αβ-hopane *(Mello et al., 1988)*.
9	Hopane/sterane from the C_{30} αβ-hopane and regular C_{29} sterane *(Mackenzie et al., 1984)*.
10	ββ/(ββ+αα) of C_{29} (20R+20S) sterane isomer *(Mackenzie et al., 1980)*.
11	20S/(20S+20R) of C_{29} 5α(H), 14α(H), 17α(H) steranes *(Mackenzie et al., 1980)*.
12	Diasterane/(diasterane + regular sterane) *(Mackenzie et al., 1985)*.
13	% C_{27} of C_{27}+C_{28}+C_{29} ββ-steranes *(Mackenzie et al., 1985)*.
14	% C_{28} of C_{27}+C_{28}+C_{29} ββ-steranes *(Mackenzie et al., 1985)*.
15	% C_{29} of C_{27}+C_{28}+C_{29} ββ-steranes *(Mackenzie et al., 1985)*.
16	C_{20}/ (C_{20}+C_{28}) triaromatic steroids (TA) *(Mackenzie et al., 1985)*.
17	C_{28} TA/(C_{28}TA+C_{29}MA) *(Peters and Moldowan., 1993)*.
18	Methylphenanthrene ratio, MPR *(Radke et al., 1982b)*.
19	Methylphenanthrene index 1, MPI 1 *(Radke et al., 1982a)*.
20	Methylphenanthrene distribution factor (F1 or MPDF) *(Kvalheim et al., 1987)*.
21	Methyldibenzothiophene ratio, MDR *(Radke., 1988)*.
22	Calculated vitrinite reflectivity, $R_{m(1)}$=1.1*log10 MPR+0.95 *(Radke., 1988)*.
23	Calculated vitrinite reflectivity, %R_c=0.6*MPI 1+0.4 *(Radke and Welte., 1983)*.
24	Calculated vitrinite reflectivity, %R_o=2.242*MPDF-0.166 *(Kvalheim et al., 1987)*.
25	Calculated vitrinite reflectivity, $R_{m(2)}$= 0.073*MDR+0.51 *(Radke., 1988)*.
26	3-methylphenanthrene/4-methyldibenzotiophene *(Radke et al., 2001)*.
27	MDBTs/MPs *(Radke et al., 2001)*.

Table 5.9 Different parameters calculated from the various peaks.

5.3.7. Explanation of parameters

In this section the different parameters which can be calculated from the different mass ion ratio will be presented. All the parameters are listed in table 5.9.

5.3.7.1 Parameters from m/z=191

From chromatogram m/z = 191 it is possible to calculate the following parameters from the identification of terpanes and triterpanes.

Parameter 1: Ts/(Ts+Tm), (maturity parameter, peaks A and B)

The amount of Ts (C27 18α (H) - trisnorneohopane) will increase compared to Tm (C_{27} 17α (H)-trisnorhopane) during maturation. Tm is believed to represent the biologically produced structure. The Ts/Tm ratio begins to decrease quite late during maturation (>0.9% Ro) (Waples and Machihara, 1991), but may be used through the entire oil window. This parameter may be influenced by the depositional environment, but it is useful non-quantitative indicator of relative maturity when used on oils of uniform or common organic facies. This maturity parameter was defined by Seifert and Moldowan (1978) and it is best fit for immature, mature and over-mature oils with maximum ratio of 1.0 (Peters and Moldowan, 1993).

Parameter 2: Diahopane/ (diahopane + normoretane), maturity parameter (peaks X and D). There is probably a relationship between maturity and this ratio. High ratios indicate high maturities (Peters and Moldowan, 1993). Peak X may also indicate terrestrial input (Peters and Moldowan, 1993).

Parameter 3: 22S/ (22S+22R) of C_{31} 17α (H), 21β (H)–hopanes (maturity parameter, peak G and H). The S and R isomers of C_{31} 17α (H), 21β (H) - hopanes behave differently during maturation. The 22S isomer is the most stable, and the ratio will therefore increase during maturation of the source rock. The equilibrium is reached fast, so the parameter is often used

for immature to early mature petroleums of an early stage in the oil window. The maximum equilibrium ratio is 0.6 (Peters and Moldowan, 1993).

Parameter 4: C30- hopane/(C30-hopane + C30-moretane) (maturity parameters peaks E and F). C30-hopane is thermally more stable than C30-moretane and the ratio will increase with increasing maturation. The range of this ratio is limited to immature samples and extracts, because the loss of C30-moretane occurs at relatively low maturity.

Parameter 5: 29Ts/(29Ts+norhopane) (maturity parameter, peaks 29Ts and C)

This parameter was introduced by Moldowan et al., (1991) and is used for maturity indication. 29Ts have higher stability than norhopane and thus this ratio will increase with increased thermal maturity (Hughes et al., 1985).

Parameter 6: Bisnorhopane/(bisnorhopane+norhopane), facies parameter (peaks Z and C). Bisnorhopane is assumed to indicate anoxic conditions (Peters and Moldowan, 1993) and it is also affected by maturity. The amount of bisorhopane is reduced through the oil window, while the norhopane peak rises relative to bisnorhopane with increased maturation. Immature samples may therefore give a more anoxic impression than more mature samples. As bisorhopane breaks down more easily than norhopane, the ratio of the two will decrease with increased thermal maturity.

Parameter 7: C23-C29 tricyclic terpanes/C30 αβ-hopane, maturity parameter (peaks P, Q, R, T, U, V and E). The amount of C23-C29 tricyclic terpanes will increase relative to the C30 αβ-hopane with increasing maturity. The parameter is valid through the entire oil window, but is strongly influenced by evaporative fractionation and phase fractionation (Karlsen et al., 1995).

Parameter 8: C24 tetracyclic terpanes/ C30 αβ-hopane, maturity parameter (peaks S and E). The amount of C24 tetracyclic terpanes will increase relative to C30 αβ-hopane with thermal maturity (Peters and Moldowan, 1993).

Parameter 9: hopane/sterane (calculated from chromatograms m/z = 191 and m/z = 217 and it is facies parameter, peaks E, q, r, s and t). Hopanes are derived mainly from bacteria, while steranes are derived from algae and higher plants. A high hopane/sterane ratio indicate

bacteria rich facies, bacterially reworked organic matter (Peters and Moldowan, 1993). Hopanes are less thermally stable than steranes, so in a sample set with uniform organic facies, the hopane/sterane parameter will somewhat more influenced by maturity in addition to the effect of facies.

5.3.7.2 Parameters from m/z=217

From the m/z = 217 chromatogram it is possible to calculate the following parameters from identification of six isomers of diacholestanes and ethyl-cholestanes.

Parameter 10*: ββ/ (ββ+αα) of the C_{29} (20R+20S) sterane isomers, maturity parameter (peaks q, r, s and t).* The ββ-isomer increases with maturity compared to the αα-isomer. The parameter is valid up till peak oil generation, but it may be affected by the mineralogy in the rock. Maximum equilibrium ratio is 0.7 (Peters and Moldowan, 1993).

Parameter 11*: 20S/ (20S+20R) of the C29 5α (H), 14α (H), 17α (H) sterane isomers, maturity parameters (peaks q, r, s, and t).* The 20R isomer converts to the 20S isomer during maturation and equilibrium is reached in the middle of the oil window, at about 0.52– 0.55 *(Seifert and Moldowan, 1986)*. This parameter can also be affected by facies, biodegradation and weathering. Maximum equilibrium ratio is 0.55 (Peters and Moldowan, 1993).

Parameter 12: Diasteranes/ (diasteranes+regular steranes) is both facies and maturity parameter (peaks a, b, q, r, s and t). The amount of diasteranes will increase with thermal maturity relative to the regular steranes. The parameter is valid through the entire oil window. Maximum ratio is 1.0. Oils from carbonate source rocks may have lower ratios than oils from clastic source rocks (Peters and Moldowan, 1993). Presence of diasteranes indicates a silisiclastic source rock.

5.3.7.3 Parameters from m/z=218

Parameters 13, **14** and **15** respectively corresponding to peaks i, o and s and they are the relative percentages of the C_{27}, C_{28} and C_{29} ββ-steranes. Percentage of these three peaks is

calculated and up on plotted in a ternary diagram they indicate organic facies (Huang and Meinschein, 1979; Moldowan et al., 1985).

5.3.7.4. Parameters from m/z=231 & 253

From the m/z = 231 and m/z = 253 chromatograms it is possible to calculate the following parameters:

Parameter 16: C_{20}/ (C_{20}+C_{28}) triaromatic steroids (TA), maturity parameter (peaks a1 and g1). During maturation the amount of C_{20} increases relative to $C_{28.}$ The parameter is valid through the entire oil window, but is very susceptible to phase fractionation (Karlsen et al., 1995). Maximum ratio is 1.0 (Peters and Moldowan, 1993).

Parameter 17: C_{28} TA/(C_{28}TA + C_{29}MA), maturity parameter (peaks g1 and H1). During the course of thermal maturation monoaromatics (MA) are rearranged to triaromatics (TA). The ratio between the two molecules is used to estimate maturity and possibly phase fractionation. The parameter is valid to peak oil generation. Maximum ratio is 1.0 (Peters and Moldowan, 1993).

5.3.7.5 Parameters from m/z=198 and 192

Tricyclic aromatic hydrocarbons are identified from the m/z = 178+192 and m/z = 198 & 192 chromatograms, and utilized in the following parameters. They are calculated from the amount of phenanthrene and the four isomers of methylphenanthrene (peaks 3, 2, 9 and 1). The number assigns the location of the methyl group (-CH_3). 3-MP and 2-MP are the most thermally stable isomers, and the 1-MP and 9-MP isomers will be more rapidly depleted during maturation.

Parameter 18: Methyl phenanthrene ratio (MPR), maturity parameter (peaks 1 and 2).
MPR = 2-MP/1-MP

Parameter 19: Methyl phenanthrene index 1 (MPI 1), maturity parameter (peaks P, 1, 2, 3 and 9).

MPI 1 = 1, 5(3-MP + 2-MP)/ (P + 9-MP + 1-MP)

Parameter 20: Methyl phenanthrene distribution factor (F1 or MPDF), maturity parameter (peaks 1, 2, 3 and9).

MPDF = (3-MP + 2-MP)/ (3-MP + 2-MP + 1-MP + 9-MP)

Parameter 21: Methyldibenzothiophene ratio, MDR, this is maturity and facies parameter (peaks 4 and 1) where MDR represents both peak 4-MDBT and 1-MDBT in m/z=198.

MDR = 4-MDBT /1-MDBT *(Radke, 1988).*

This parameter is based on the relationship between the two isomers of methyl dibenzothiophene, 4-MDBT and 1-MDBT. The 4-MDBT is the most thermally stable isomer. The thiophene structure contains a sulphur atom, so the amount of MDBT in oils may indicate the sulphur contents in the oil/ source rock.

Vitrinite reflectance has been calculated based on measurements of phenanthrene, methyl phenanthrenes and methyl dibenzothiophene:

Parameter 22: Calculated vitrinite reflection, maturity parameter, calculated from parameter 18. $R_{m\,(1)}$ = 1.1*log10MPR + 0.95

Parameter 23: Calculated vitrinite reflection, maturity parameter, calculated from parameter 19. $\%R_c$ = 0.6*MPI 1 + 0.4

Parameter 24*:* Calculated vitrinite reflection, maturity parameter, calculated from parameter 20. $\%R_o$ = 2.242*MPDF – 0.166

Parameter 25 Calculated vitrinite reflection calculated from parameter 21.

$R_{m(2)}$ = 0.073*MDR + 0.51

Parameter 26: 3-methyl phenanthrene/ 4-methyl dibenzothiophene, facies parameter (peaks 3 and 4). This parameter can be used with a parameter like Pr/Ph to indicate different types of organic facies, e.g. carbonate and shale facies (Hughes et al., 1995; Radke, 1988) and the relative amount of sulfur in the source rock (Radke, 1988).

Parameter 27: MDBTs/ MPs, facies parameter. The parameter is calculated from peak 1, 2, 3, 4 and 9 from chromatogram m/z = 178 + 192 and peak 1, 2+3 and 4 from the m/z = 192 chromatogram. Values above 1 indicate carbonate facies and values below 1 indicate shale facies.

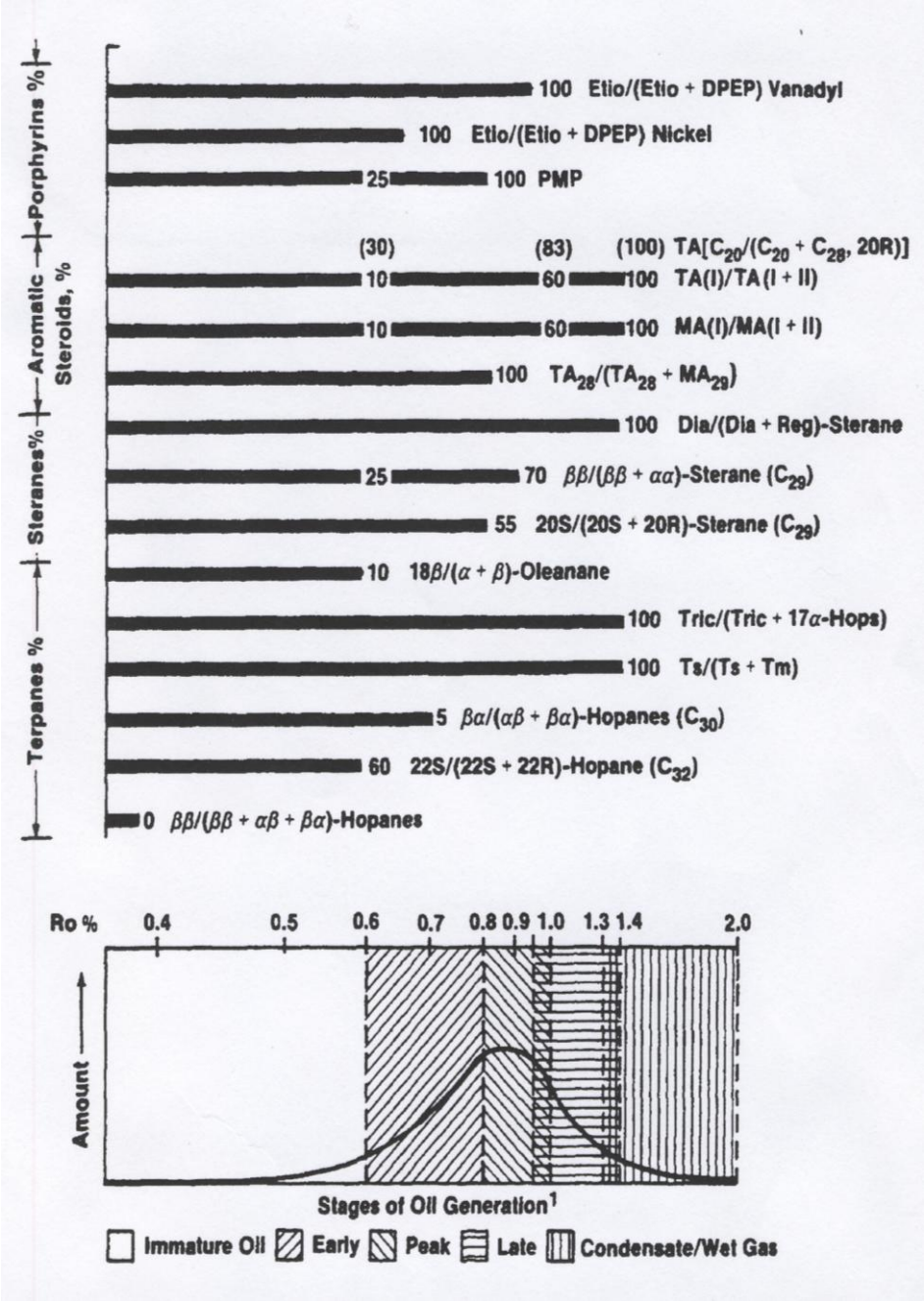

Figure 5.12. Different biomarker maturity parameters, and their corresponding range on the oil window considered to be valid From (Peters and Moldowan, 1993).

6. Results

This chapter presents the results of the analyses performed in the laboratory. Scaled-down chromatograms for each sample are also included (Fig. 6.3-6.17). See the following presentations for the number of results for each sample and various tables that give a summary of the numerical values from the petroleum geochemical laboratory analysis. The complete sets of full-scale chromatograms are found in the Appendix. The chapter has the following outline:

6.1. Iatroscan TLC-FID

Karlsen and Larter (1989, 1991) have shown that using Iatroscan TLC-FID, the petroleum populations in a reservoir can be characterized in terms of varying proportions of saturated and aromatic hydrocarbons and polar compounds. Iatroscan TLC-FID has the ability to classify reservoir bitumen in terms of composition.

The results obtained from the Iatroscan of the extracts are given in this section. Table 6.1 and Fig. 6.1 and 6.2 presents the relative percentages of the petroleum fractions such as saturated hydrocarbons, aromatic hydrocarbons and polar compounds, plus the ratio of saturated to aromatic hydrocarbons. The numbers given in the table represent the averages of two Iatroscan runs. Following is presentation of results for the sample set.

E1 (2/7-26S #10, 4427 m): From the Iatroscan TLC-FID analysis, the bulk composition of this sample was found to be 84.4% saturated hydrocarbons, 3.8% aromatic hydrocarbons and 11.8% polar compounds. The SAT/ARO ratio is 22.0. The sample produced a total extract of

56.2 mg/g rock, which is the highest amount in the sample set (see Table 6.1 and figure 6.1, 6.2 and 7.1).

E2 (2/7-26S #14, 4441 m): The bulk composition of **E2** is made up of 87.7% saturated hydrocarbons, 1.0% aromatic hydrocarbons and 11.3% polar compounds. The SAT/ARO ratio was found to be 87.7%. This sample contains a total extract of 50.3 mg/g rock (see Table 6.1 and figure 6.1, 6.2 and 7.1).

E3 (2/7-26S #22, 4476 m): The estimation of the petroleum fractions by Iatroscan TLC-FID shows that the bulk composition of this sample is made up 86.8% saturated hydrocarbons, 2.1% aromatic hydrocarbons and 11.1% polar compounds. The SAT/ARO ratio is 41.3. The sample has a total extract of 37.1 mg/g rock (see Table 6.1 and figure 6.1, 6.2 and 7.1).

E4 (2/7-26S #30, 4502 m): The Iatroscan TLC analysis showed the gross composition of sample **E4** contains 87.2% saturated hydrocarbons, 1.9% aromatic hydrocarbons and 10.9% polar compounds. The SAT/ARO ratio is 45.8. The total extractable organic matter is estimated to be 36.8 mg/g rock (see Table 6.1 and figure 6.1, 6.2 and 7.1).

E5 (2/7-26S #34, 4521 m): The bulk composition of the sample **E5** determined by Iatroscan TLC-FID was found to be 93.0% saturated hydrocarbons (the highest in the sample set), 2.7% aromatic hydrocarbons and 4.3% polar compounds (the lowest in the sample set). The SAT/ARO ratio is 34.2. The total organic matter extracted is 32.4 mg/g rock (see Table 6.1 and figure 6.1, 6.2 and 7.1).

E6 (2/7-26S #39, 4670 m): The Iatroscan TLC-FID analysis gave a bulk composition of 72.1% saturated hydrocarbons, 2.8% aromatic hydrocarbons and 25.1% polar compounds. The SAT/ARO ratio is 25.7. The sample contains 21.8 mg/g rock extractable organic matter (see Table 6.1 and figure 6.1, 6.2 and 7.1).

E7 (2/7-26S #40, 4676 m): The analysis of the core extract determined by the Iatroscan TLC-FID revealed that the bulk composition contains 76.5% saturated hydrocarbons, 1.8% aromatic hydrocarbons and 21.7% polar compounds. The SAT/ARO ratio is 42.8. The sample gave a total extract of 17.1 mg/g rock (see Table 6.1 and figure 6.1, 6.2 and 7.1).

E8 (2/7-26S #41, 4680 m): The bulk composition of the sample determined by Iatroscan TLC-FID is 71.7% saturated hydrocarbons, 2.0% aromatic hydrocarbons and 26.3% polar compounds. The SAT/ARO ratio is found to be 36.1. The sample has total extractable organic matter of 18.5 mg/g rock (see Table 6.1 and figure 6.1, 6.2 and 7.1).

E9 (2/7-26S #42, 4685 m): The gross composition of Sample **E9** determined by Iatroscan TLC-FID is 77.6% saturated hydrocarbons, 0.9% aromatic hydrocarbons and 21.5% polar compounds. The SAT/ARO is 86.8. The sample contains 20.8 mg/g rock extractable organic matter (see Table 6.1 and figure 6.1, 6.2 and 7.1).

E10 (2/7-26S #44, 4698 m): The result from the Iatroscan TLC-FID analysis, shows that the sample is composed of 70.1% saturated hydrocarbons, 0.9% aromatic hydrocarbons and 29.1% polar compounds. The SAT/ARO ratio is 80.2. The total extractable organic matter was 13.6 mg/g rock (see Table 6.1 and figure 6.1, 6.2 and 7.1).

E11 (2/7-26S #46, 4702 m): The bulk composition of the sample determined by Iatroscan TLC-FID was found to be 77.3% saturated hydrocarbons, 0.5% aromatics (the lowest in the sample set) and 22.3% polar compounds. The SAT/ARO ratio is 167.6% (the highest in the sample set). The total extractable organic matter is 6.8 mg/g rock (see Table 6.1 and figure 6.1, 6.2 and 7.1).

E12 (2/7-26S #47; 4707 m): The Iatroscan TLC-FID technique gave a bulk composition of 81.0% saturated hydrocarbons, 3.4% aromatic hydrocarbons and 15.6% polar compounds. The SAT/ARO ratio is 24.0. This sample yielded 24.1 mg/g rock extractable organic matter.

E13 (2/7-26S #48; 4710): The bulk composition of sample **E13**, determined by Iatroscan TLC-FID, is made up of 76.2% saturated hydrocarbons, 1.5% aromatic hydrocarbons and 22.3% polar compounds. The SAT/ARO ratio is 50.4. The sample produced 5.9 mg/g rock extractable organic matter (see Table 6.1 and figure 6.1, 6.2 and 7.1).

E14 (2/7-26S #49; 4712 m): The Iatroscan TLC-FID revealed that the sample **E14** is composed of 74.2% saturated hydrocarbons, 1.2% aromatic hydrocarbons and 24.6% polar

compounds. The SAT/ARO ratio was found to be 60.2. The sample produced 2.3 mg/g rock extract (see Table 6.1 and figure 6.1, 6.2 and 7.1).

E15 (2/7-26S #5,1; 4831 m): The bulk composition of the sample **E15** was estimated by Iatroscan TLC-FID to be 10.4% saturated hydrocarbons (the lowest of the sample set), 20.4% aromatic hydrocarbons and 69.2 polar compounds (the highest of the sample set). The sample also showed the lowest SAT/ARO ratio, which is 0.5. The estimated extractable organic matter was found to be 0.34 mg/g of rock (the second lowest of the sample set).

E16 (2/7-26S #4,1; 4833 m): From the Iatroscan TLC-FID analysis it was found that the bulk composition of the sample is made up of 42.3% saturated hydrocarbons, 1.7% aromatic hydrocarbons and 56.0% polar compounds. The SAT/ARO ratio is 24.2. The sample gave a total extractable organic matter of 0.42 mg/g of rock (see Table 6.1 and figure 6.1, 6.2 and 7.1).

E17 (2/7-26S #3,1; 4838 m): The bulk composition of the sample was estimated by the Iatroscan TLC-FID to be composed of 38.5% saturated hydrocarbons, 2.0% aromatic hydrocarbons and 59.5% polar compounds. The SAT/ARO ratio is 19.2. The extracted organic matter was 0.42 mg/g of rock (see Table 6.1 and figure 6.1, 6.2 and 7.1).

E18 (2/7-26S #2R, 4841m MD): The Iatroscan analysis for the bulk composition of the sample **E18** resulted in 13.7% saturated hydrocarbons, 17.2 aromatic hydrocarbons and 69.1% polar compounds. Both the aromatic hydrocarbons and polar compounds of the sample E18 present the second highest in the sample set. The SAT/ARO is 0.8, second lowest of the sample set. The total extractable organic matter constituted 0.28 mg/g rock, which is the lowest of the sample set (see Table 6.1 and figure 6.1, 6.2 and 7.1).

VB (Vein Bitumen, 5028 m): The bulk composition of the bitumen extracted from a core sample of fractured rhyolites was determined by Iatroscan TLC-FID and found to contain 57.2% saturated hydrocarbons, 4.1% aromatic hydrocarbons and 38.7% polar compounds. The SAT/ARO ratio is 14.0. The extractable organic matter from this sample was be 2.24 mg/g of rock (see Table 6.1 and figure 6.1, 6.2 and 7.1).

NSO-1: The NSO-1 sample contains 53.1% saturated hydrocarbons, 31.1% aromatic hydrocarbons and 15.8% polar compounds. The SAT/ARO ratio is 1.7.

6.2. GC-FID

The extracts from the core samples were analyzed on the GC-FID instrument as described in chapter 4. This gives information about the n-alkane and isoprenoid distribution, and can give further information about the maturity and source rock facies of the samples (Peters and Moldowan, 1993). The traces from the GC-FID may indicate the presence and degree of biodegradation, in which case the unresolved complex mixture (UCM) of compounds will be large relative to concentration of n-alkanes. In normal North Sea oils, the peak height decreases asymptotically with increasing carbon number. This creates a concave and asymptotic curve on the chromatogram. Table 6-2 presents the results from the GC-FID analysis and the chromatograms are shown in figures 6.3-6.17.

E1 (2/7-26S #10, 4427 m): The GC-FID chromatograms from the analysis of the bitumen extracted from sample **E1** gives a Pr/Ph ratio of 1.03 and Pr/n-C_{17} and Ph/n-C_{18} ratios of 0.45 and 0.38 respectively. The sample contains n-alkanes in the range of C_{13} to C_{22}. There are no n-alkanes identified below C_{13}. The peaks representing, the isoprenoids, pristane (Pr) and phytane (Ph), are smaller compared to the associated n-alkanes n-C_{17} and n-C_{18} respectively. The Unresolved complex mixture (UCM) is present in the chromatogram. The UCM hump is higher in the C_{20} to C_{30} n-alkane range. An unidentified peak which probably is contamination is seen at about the retention time of 38 minutes (see table 6.2 and Appendix A).

E2 (2/7-26S #14, 4441 m): On the GC-GID chromatogram for sample **E2** (see Table 6.2 and Fig.6.4 and Appendix A), the Pr/Ph ratio is 1.05. The Pr/n-C_{17} and Ph/n-C_{18} ratios were computed respectively, to be 0.43 and 0.37. The sample contains n-alkanes in the range of C_{12} to C_{23}. There are no n-alkanes below C_{12}. The isoprenoids Pr and Ph are smaller peaks compared to the n-alkanes n-C_{17} and n-C_{18}. Peak n-C_{19} predominates the chromatogram. The

signature of the chromatograms is masked by the unidentified higher concentration peak at about run time of 38 minutes. This is probably contamination. The UCM of this sample is significant.

E3 (2/7-26S #22, 4476 m): The GC-FID chromatogram produced for sample **E3** (see Table 6.2 and Appendix A) contains n-alkanes in the range of C_{13} to C_{21}. No n-alkanes are observed below C_{12}. The Pr/Ph ratio is 1.08. The Pr/n-C_{17} and Ph/n-C_{18} ratios, which are the lowest in the sample set, were computed to be 0.40 and 0.33, respectively. Peak n-C_{19} predominates the chromatogram. The signature of the chromatograms is masked by the unidentified higher concentration peak at about run time of 38 minutes. This is probably contamination. The UCM of this sample is moderate.

E4 (2/7-26S #30, 4502 m): From the GC-FID chromatogram (see Table 6.2, Fig. 6.5 and Appendix A) one can see n-alkanes in the range of C_{12} to C_{22}. The content of long chained n-alkanes (C_{20}+) is highly reduced compared to the shorter n-alkanes. The Pr/Ph, Pr/n-C_{17}, and Ph/n-C_{18} ratios were found to be 1.11, 0.43 and 0.35 respectively. This chromatogram also shows an unimodal n-alkane distribution maximized at n-C_{19}.The sample is contaminated, which creates an uncommon peak at about run time of 38 minutes. The UCM is moderate.

E5 (2/7-26S #34, 4520 m): The GC-FID chromatogram (see Table 6.2, Fig 6.6 and Appendix A) gave a Pr/Ph ratio of 1.11, and Pr/n-C_{17} and Ph/n-C_{18} ratios of 0.42 and 0.33 respectively. The two latter ratios are the lowest in the sample set. The sample has significant UCM.

E6 (2/7-26S #39; 4670 m): The Pr/Ph, Pr/n-C_{17}, and Ph/n-C_{18} values are respectively 1.1, 0.58 and 0.51. The sample contains n-alkanes in the range of C_{12} to C_{36}. The n-C_{19} compound dominates the chromatogram of this sample. Pristane and Phytane represent the two major peaks of the isoprenoids. A Huge UCM is shown by the rise of the base line (see table 6.2, Fig. 6.7 and Appendix A).

E7 (2/7-26S #40; 4676 m): On the GC-FID chromatogram for sample **E7** (see Table 6.2, Fig 6.8 and Appendix A), n-alkanes in the range C_{13} to C_{24} are the dominant peaks. The GC-FID chromatogram shows higher content of n-alkanes relative to the aromatic hydrocarbons, which is the case for most of the samples. The UCM hump is seen with an apex approximately at n-C_{25}. Pristane and Phytane represent the two major peaks. From the chromatogram, a Pr/Ph ratio of 1.07 and Pr/n-C_{17} and Ph/n-C_{18} ratios of 0.64 and 0.54, respectively, were calculated. The sample is contaminated as shown by the unusual high peak at the retention time of 38 minutes.

E8 (2/7-26S #41; 4680 m): The GC-FID chromatogram for sample **E8** shows n-alkane ranging from n-C_{13} to n-C_{26}. The n-alkanes show a unimodal nature distribution with maximum at n-C_{19}. The UCM hump is moderate. Pristane and Phytane represent the two major isoprenoid peaks. The Pr/Ph ratio was calculated to be 1.11. The Pr/n-C17 and Ph/n-C18 ratios are respectively 0.61 and 0.53 (see Table 6.2, Fig. 6.9 and Appendix A).

E9 (2/7-26S #42; 4685 m): The GC-FID chromatogram resulting from the analysis of this extract (see Table 6.10, Fig 6.10 and Appendix A) gives a Pr/Ph ratio of 1.02 while the Pr/n-C_{17} and Ph/n-C_{18} ratios are 0.55 and 0.48 respectively. N-alkanes ranging from C_{13} to C_{28} are identified on the chromatograms. The n-alkanes become progressively less dominant from n-C_{19} and above. The UCM hump which indicates the degree of biodegradation is present.

E10 (2/7-26S #44; 4698 m): The GC-FID chromatogram resulting from the analysis of this extract (see Table 6.2, Fig 6.11 and Appendix A) gives a Pr/Ph ratio of 1.05. The Pr/n-C_{17} and Ph/n-C_{18} ratios are 0.63 and 0.53 respectively. The chromatogram shows n-alkanes ranging from C_{13} to C_{26}. The chromatogram shows a unimodal distribution of n-alkanes with a maximum at n-C_{19}. The Pr and Ph are the major isoprenoid peaks. This sample contains a UCM hump reaching its apex at about n-C_{25}.

E11 (2/7-26S #46; 4702 m): The GC-FID chromatogram for the sample **E11** (see Table 6.2, Fig 6.12 and Appendix A) shows a Pr/Ph ratio of 0.96, which is the lowest of the sample set. The Pr/n-C17 and Ph/n-C18 ratios are 0.73 and 0.60 respectively. The chromatogram

displays n-alkanes from C_{13} to C_{22}. It shows a unimodal distribution of n-alkanes with a maximum at n-C_{19}. Relatively lower Pr and Ph peaks are observed in this chromatogram. Several unidentified compounds become dominant compared to the larger n-alkane chains. This sample contains a huge UCM hump reaching its apex at about n-C_{25}. The contamination present at a retention time of 38 minutes hides the pronounced appearance of the UCM.

E12 (2/7-26S #47; 4707 m): The GC-FID chromatogram for the sample **E12** (see Table 6.2, Fig 6.13 and Appendix A) shows a Pr/Ph ratio of 1.13. The Pr/n-C17 and Ph/n-C18 ratios are 0.60 and 0.49 respectively. The chromatogram shows n-alkanes ranging from n-C_{13} to n-C_{27}. It shows a unimodal distribution of n-alkanes with a maximum at n-C_{19}. Relatively lower Pr and Ph peaks are observed in this chromatogram. This sample contains relatively a less pronounced UCM hump.

E13 (2/7-26S #48; 4710 m): From the GC-FID chromatogram of the sample **E12** (see Table 6.2, Fig 6.14 and Appendix A) the Pr/Ph, Pr/n-C17 and Ph/n-C18 ratios, respectively, are 1.07, 0.62 and 0.54. The chromatogram shows n-alkanes ranging from C_{13} to C_{34}. It shows a unimodal distribution of n-alkanes with its maxima at n-C_{19}. Pr and Ph are the major isoprenoid peaks of the chromatogram. There are also other an identified compounds between n-C_{13} and n-C_{17} with significant concentrations. The pronounced peak which was the dominant signature and interpreted as a contamination in the previous samples is absent in this sample. This sample contains a relatively moderate UCM hump rising as an irregular baseline.

E14 (2/7-26S #49; 4712 m): The GC-FID chromatogram resulting from the analysis of the extracted bitumen of sample **E14** (see Table 6.2, Fig 6.15 and Appendix A) shows a Pr/Ph ratio of 1.10 and Pr/n-C17 and Ph/n-C18 ratios of 0.74 and 0.63 respectively. The Pr/n-C17 ratio is the highest in the sample set. From this chromatogram n-alkanes ranging from C_{12} to C_{35} are identified. This chromatogram shows a unimodal distribution of n-alkanes with maximum at n-C_{19}. The Pr and Ph are the major isoprenoid peaks of the chromatogram. Other unidentified compounds with significant concentration are available between n-C_{13} and n-C_{17}. This sample contains a moderate UCM hump.

E16 (2/7-26S #4,1; 4833 m): The GC-FID chromatogram gave a Pr/Ph ratio of 1.58, Pr/n-C_{17} and Ph/n-C_{18} ratios of 0.59 and 0.43 respectively. The n-alkanes ranging from C13 to C25 are identified in the chromatogram.

VB (Vein Bitumen, 5028 m): This sample is bitumen extracted from a rhyolite core sample which was fractured and filled with bitumen. The bitumen was taken and extracted from the core vein sample. The trace in the chromatogram shows the highest pr/ph ratio in the sample set. The Pr/Ph ratio was calculated to be 1.94. The Pr/n-C_{17} and Ph/n-C_{18} ratios are 0.56 and 0.45 respectively. This chromatogram slightly resembles the chromatogram obtained from the NSO-1, in that the peak heights of the n-alkanes decrease with increased carbon number which is typically observed from n-C13 and above. This sample, unlike the others, has its maximum n-alkane at n-C_{13} The sample is contaminated which is shown by the pronounced peak at the retention time of 38 minutes (see Table 6.2, Fig 6.16 and Appendix A)

NSO-1*:* The chromatogram for the NSO-1 sample illustrates nicely that the peak heights decrease with increasing carbon number, creating a concave curve (see Table 6.2, Fig 6.3 and Appendix A)). The Pr/Ph ratio is 1.65, the Pr/n-C_{17} is 0.60 and the Ph/n-C_{18} is 0.49.

6.3. GC-MS

The compounds of main interest called biomarkers were analyzed on the GC-MS instrument as described in chapter 4.7. The GC-MS technique makes it possible to study compounds present in only small concentrations in the complex matrix that make up the petroleum. Methyl dibenzothiophenes and phenanthrene compounds, which are not biomarkers, were also studied by GC-MS.

Based on measurements on selected peaks, several maturity and facies parameters have been calculated. See chapter 5.3 for description of the parameters and identification and description of the peaks. Table 6.3 and Fig. 6.2-6.17 present the calculated parameter values and the chromatograms respectively.

E1 (2/7-26S #10; 4427 m): From GC-MS chromatogram of biomarker data (see Table 6.3 and Appendix B) a Ts/(Ts + Tm) ratio of 0.64 for sample **E1** is calculated. The

diahopane/(diahopane + normoretan) ratio is 0.50 which is the second highest in the sample set. The 29Ts/(29Ts + norhopane) ratio is 0.21, and the bisnorhopane/(bisnorhopane + norhopane) ratio is 0.08. The hopane/sterane and the diasteranes/(diasteranes + regular steranes) ratios are 1.59 and 0.80 respectively. The hopane/sterane ratio is the second highest in the sample set. The maturity parameter C_{20}/ (C_{20} + C_{28}) ratio for the sample **E1** is 0.78, the second lowest in the sample set. The sample has the lowest, in the sample set, methyl phenanthrene index 1 (MPI1) with a calculated value of 0.36. The calculated vitrinite reflection, $\%R_c$=2.242*F1-0.166 (Kvalheim et al., 1987) was calculated to be 0.93.

E2 (2/7-26S #14; 4441 m): From the GC-MS, m/z 191 chromatogram for sample **E2** (see Table 6.3, Fig. 6.4 and Appendix B) a Ts/(Ts+Tm) value of 0.63 and diahopane/(diahopane + norhopane) ratio of 0.33 were calculated. The 29Ts/(29Ts + norhopane) and the hopane/sterane ratios are 0.15 and 1.09 respectively, the former being the second lowest in the sample set. The bisnorhopane/(bisnorhopane + norhopane) ratio which is the lowest in the sample set was found to be 0.04. The diasteranes/(diasteranes + regular steranes) ratio was calculated to be 0.96 and it is the second highest value in the sample set. The vitrinite reflection (R_m), calculated from methyl dibenzothiophene ratio (Radke, 1988) is 0.65 and this value is the second lowest in the sample set. This sample shows the highest C_{24} tetracyclic terpane/C30αβ-hopane with value of 16.13. Sample **E2** is also characterized by the highest C_{23}-C_{29} tricyclic terpanes /C30 αβ-hopane ratio, which is 47.75.

E3 (2/7-26S #22; 4476 m): From the GC-MS biomarker data (see Table 6.3 and Appendix B), the (Ts/Ts + Tm) value for sample **E3** is found to be 0.63 which is the same value as for sample E2. The 29Ts/(29Ts + norhopane), hopane/sterane, bisnorhopane/(bisnorhopane + norhopane) and the diasteranes/(diasteranes + regular steranes) ratios are 0.18, 1.12, 0.07 and 0.87 respectively. The vitrinite reflectance calculated from methyl phenanthrene index 1 (Radke, 1988) is 0.75. The sample **E3** also shows the lowest vitrinite reflectance (0.62) calculated from methyl dibenzothiophene ratio (MDR) (Radke, 1988).

E4 (2/7-26S #30; 4502): The GC-MS chromatogram for the **E4** sample (see Table 6.3, Fig. 6.5 and Appendix B) shows a Ts/(Ts + Tm) ratio of 0.67, while the 29Ts/(29Ts + norhopane) ratio is 0.24. The hopane/sterane, and diasteranes/(diasteranes + regular steranes) ratios are

1.23 and 0.88 respectively. The vitrinite reflectance calculated from methyl phenanthrene ratio (MPR) (Radke, 1988) is 0.92. See table 6.3 for comparison with the rest of the data set.

E5 (2/7-26S #34; 4521 m): From the analysis of the GC-MS biomarker data for the extract from sample **E5**, the Ts/(Ts + Tm) value was found to be 0.62, while the hopane/sterane and 29Ts/(29Ts + norhopane) ratios are 0.52 and 0.18 respectively. The ββ/(ββ + αα) sterane and C_{30}-hopane/(C_{30}- hopane + C_{30}-morethane) ratios, with values of 0.46 and 0.18 respectively, are the lowest in the sample set. The vitrinite reflection, R_c% (Radke, 1988) calculated from MPI 1, is found to be 0.64 and the %C_{29} of (C_{27} + C_{28} + C_{29}) with value of 6.40% represent the second lowest values in the sample set. The maturity parameter, 22S/(22S + 22R) of C31 17α(H), 21β(H)-hopanes with value of 0.60 is one of the highest value in the sample set. For details (see Table 6.3, Fig. 6.6 and Appendix B).

E6 (2/7-26S #39; 4670 m): From the GC-MS biomarker data (see Table 6.3, Fig. 6.7 and Appendix B), the maturity parameter Ts/(Ts + Tm) value for sample **E6** if found to be 0.61, slightly lower value than that of E5. The 29Ts/(29Ts + norhopane) and hopane/sterane ratios are 0.19 and 0.44 respectively. The diasteranes/(diasteranes + regular steranes) ratio is 0.90. The 3-methyl phenanthrene/4-methyl dibenzothiophene ratio is3.10 and it is the lowest in the sample set. The diahopane/(diahopane + normoretan) and C_{30}-hopane/(C_{30}-hopane+C_{30}-morethane) ratios with values, respectively, of 0.13 and 0.52 represent the second lowest values in the sample set. Moreover, the maturity/facies parameter methyl dibenzothiophene ratio, MDR (Radke, 1988) and its calculated vitrinite reflection R_m (Radke, 1988) reveal values of 15.20 and 1.62 respectively and both represent among the second highest values in the sample set.

E7 (2/7-26S #40; 4685 m): From the GC-MS analysis of the biomarkers of sample **E7** (see Table 6.3, Fig. 6.8 and Appendix B), the Ts/(Ts + Tm) and diasteranes/(diasteranes + regular steranes) ratios are 0.62 (same as E5) and 0.91 (slightly higher than E5) respectively. The methyl phenanthrene index 1, MPI1 (Radke et al., 1982a), methyl phenanthrene distribution fraction 1, MPDF (F1) (Kvalheim et al., 1987) and the calculated vitrinite reflection %Rc (Kvalheim et al., 1987) with values of 1.57, 0.63 and 1.25 respectively, all represent the highest values of the sample set. The 29Ts/(29Ts + norhopane), hopane/sterane and the

C_{28}TA/(C_{28} TA+C_{29} MA) ratios were calculated to be 0.14, 0.32 and 0.05 respectively. These three parameters represent the lowest values in the sample set.

E8 (2/7-26S #41; 4680 m): The GC-MS biomarker data for the E8 sample (see Table 6.3, Fig. 6.9 and Appendix B) gave a Ts/(Ts + Tm) value of 0.68, while the hopane/sterane and diasteranes/(diasteranes + regular steranes) ratios are 0.59 and 0.85 respectively. The vitrinite reflectance calculated from methyl phenanthrenes ratio (Radke, 1988) is 1.28. The methyl phenanthrene index 1, MPI1 (Radke et al., 1982a) and the corresponding calculated vitrinite reflectance %Rc (Radke, 1988) were found to be 1.50 and 1.30 respectively and they represent the second highest in the sample set.

E9 (2/7-26S #42; 4685 m): The ratio of the Ts/(Ts + Tm) value for sample **E9** is 0.71, while the 29Ts/(29Ts + norhopane) ratio is 0.22. The diasteranes/(diasteranes + regular steranes) and hopane/sterane ratios are 0.83 and 0.94 respectively. The vitrinite reflectance calculated from methyl phenanthrene ratio (Radke, 1988) is 1.13. The C_{30}-hopane/(C_{30}-hopane + C_{30}-morethane) ratio has value of 0.91 and represent the highest values next to that of NSO-1. For details (see Table 6.3, Fig. 6.10 and Appendix B)

E10 (2/7-26S #44; 4698 m): From the GC-MS chromatograms of sample **E10** (see Table 6.3, Fig. 6.11 and Appendix B), the ratio of Ts/(Ts + Tm), hopane/sterane, (29Ts/29Ts + norhopane) and diasteranes/(diasteranes + regular steranes) was found to be 0.64, 0.70, 0.16 and 0.88 respectively. The methyl dibenzothiophene ratio, MDR (Radke, 1988) and the vitrinite reflectance calculated from the MDR (Radke, 1988) show values of 38.00 and 3.28 respectively. Both values are extremely high compared to the rest of the sample set (see Table 6.3 for comparison with values of other samples). The sample also represent the highest 22S/(22S + 22R) of C_{31} 17α(H), 21β(H)-hopane with a value of 0.69. Methyl phenanthrene ratio, methyl phenanthrene distribution fraction 1 with values of 1.84 and 0.62 respectively, represent among the highest values in the sample set

E11 (2/7-26S #46; 4702 m): From the analysis of biomarkers on GC-MS, the (Ts/Ts + Tm), 29Ts/(29Ts + norhopane), hopane/sterane and diasteranes/(diasteranes + regular steranes) respectively show values of 0.73, 0.21, 0.81 and 0.85. The value for Ts/(Ts + Tm) ratio

represent the second highest in the sample set. The sample has got the highest 20S/(20S + 20R) of C_{29} 5α(H), 14α(H). 17α(H) sterane isomer ratio with a value of 0.56. Details can be seen on Table 6.3, Fig. 6.12 and Appendix B.

E12 (2/7-26S #47; 4707 m): The GC-MS chromatograms for this sample reveal a Ts/(Ts + Tm) ratio of 0.61, while the hopane/sterane and diasteranes/(diasteranes + regular steranes) ratios are 0.48 and 0.89 respectively. The ββ/(ββ + αα) of C_{29} (20S+20R) sterane isomers ratio, with a value of 0.50, is the second lowest of the sample set. Sample E12 also shows one of the lowest C_{28} TA/(C_{28} TA + C_{29} MA) ratio. For comparison with other samples refer to (Table 6.3, Fig. 6.13 and Appendix B).

E13 (2/7-26S #48; 4710): The Ts/(Ts + Tm) and diasteranes/(diasteranes + regular steranes) ratios for sample **E13** are 0.58 and 0.93 respectively. The %C_{29} of the (C_{27}+C_{28}+C_{29}) ββ-steranes for sample E13 is 5.13% which represents the lowest value in the sample set next to that of E5 (6.40%), while the percentage of C_{27} compared to C_{28} and C_{29} is 81.20%. This latter value represents the highest in the sample set. The 3-methyl phenanthrene/4-methyl dibenzothiophene ratio is 3.37, which is the second lowest in the sample set. The C_{23}-C_{29} tricyclic terpanes/C_{30} αβ-hopane and C_{28} TA/(C_{28} TA + C_{29} MA) ratios are 44 and 0.67 respectively, both ratios represent second highest in the sample set. For details refer to Table 6.3, Fig. 6.14 and Appendix B.

E14 (2/7-26S #49; 4712): From the GC-MS biomarker data (see Table 6.3, Fig. 6.15 and Appendix B), the Ts/(Ts + Tm) and diasteranes/(diasteranes + regular steranes) values for sample **E14** are 0.70 and 0.83 respectively. The hopane/sterane ratio is 1.11. The vitrinite reflectance calculated from methylphenanthrenes ratio (Radke, 1988) is 1.16. The diahopane/(diahopane + normoretan) ratio (0.10), is one of the lowest value in the sample set.

E15 (2/7-26S #5,1; 4831 m): The Ts/(Ts + Tm) and diasteranes/(diasteranes + regular steranes) ratios from the GC-MS biomarker analysis for the rhyolite sample **E15** are 0.74 and 0.97 respectively The two ratios represent the highest values in the sample set. The C_{20}/(C_{20} +C_{28}) TA steroid ratio is 0.97 (second highest in the sample set) next to that of E18,

which is also sample from the rhyolite. The percentage of C_{28} of the (C_{27}+C_{28}+C_{29}) ββ-steranes is one of the lowest in the sample set. The C_{23}-C_{29} tricyclic terpanes/C30 αβ-hopane and C_{24} tetracyclic terpane/C30 αβ-hopane ratios, with values of 45.86 and 15.14 respectively, represent the second highest in the sample set. The C_{20}/(C_{20} + C_{28}) triaromatic steroids ratio (0.97) is the second highest in the sample set, next to that of E18, also a sample from the rhyolites. For details refer to table 6.3 and Appendix B)

E16 (2/7-26S #4,1; 4833 m): From the GC-MS biomarker data (Table 6.3 and Appendix B), the Ts/(Ts + Tm) value for sample **E16** is found to be 0.70, while the 29Ts/(29Ts + norhopane) and hopane/sterane ratios are 0.22 and 1.19 respectively. The methyl dibenzothiophenes/methyl phenanthrenes ratio (parameter 27) with value of 0.03 is extremely low in the sample set. The C_{24} tetracyclic terpane/C30 αβ-hopane ratio is 1.27 and represents the second lowest in the Embla samples. The vitrinite reflectance calculated from methylphenanthrenes ratio (Radke, 1988) is 0.81, which is one of the lowest values in the studied samples. The 3-methyl phenanthrene/4-methyl dibenzothiophene ratio for sample **E16** 21.80. This value is relatively very high in the sample set (see table 6.3 for comparison of this parameter with other samples).

E17 (2/7-26S #3,1; 4838 m): The Ts/(Ts + Tm) ratio for sample **E17** was found to be 0.68. The diasteranes/(diasteranes + regular steranes) ratio for the sample is 0.80. The C_{28} TA/(C_{28}TA + C_{29}MA) ratio with value of 1.00 is among the highest values in the sample set. The vitrinite reflectance calculated from methylphenanthrene ratio (Radke, 1988) is 0.70 (second lowest in the sample set next to that of sample E18). This value is intermediate between the vitrinite reflectance calculated, using the same method, for samples E18 (0.58) and E16 (0.81). The calculated vitrinite reflectance **%Rc= 2.242*F1-0.166** (Kvalheim et al., 1987) for sample **E17** is 0.56, which is also intermediate between the values for E18 (0.49) and E16 (0.64) calculated using the same method. The vitrinite reflectance calculated for the rhyolite samples show the lowest values in the sample set (see Table 6.3 and Appendix B).

E18 (2/7-26S #2R, 4841 m): From the GC-MS biomarker data analysis, it was calculated that the Ts/(Ts + Tm) ratio has value of 0.47. This is the second lowest in the sample set. The 29Ts/(29Ts + norhopane) ratio (0.25) was found to be the second highest in the sample

set next to that of NSO-1 (0.31). The parameters such as Methyl phenanthrene ratio MPR (Radke et al., 1982b), methyl phenanthrene distribution fraction 1, MPDF (Kvalheim et al., 1987) the calculated vitrinite reflection, **Rm=1.1*log10MPR+0.95** (Radke, 1988) and **%Rc =2.24*F1-0.166** (Kvalheim et al.,1987) with values of 0.46, 0.29, 0.58 and 0.49 respectively, all represent the lowest in the sample set. The $C_{20}/(C_{20} + C_{28})$ TA ratio (0.98) for sample **E18** represents the highest in the sample set.

VB (2/7-26S, Vein bitumen): From the GC-MS biomarker data analysis (see Table 6.3, Fig. 6.16 and Appendix B), the Ts/(Ts + Tm) maturity parameter for sample **VB** was found to be the lowest in the sample set with a value of 0.42. Together with sample E14, the VB sample shows the lowest diahopane/(diahopane + normoretan) ratio (0.10) in the sample set. The diasteranes/(diasteranes + regular steranes), 20S/(20S+20R), and 22S/(22S+22R) ratios are 0.29, 0.23 and 0.44 respectively, all representing the lowest value in the sample set. Sample VB has the lowest C_{29} sterane (18.82%) compared to C_{28} (49.50%) and C_{27} (31.68%). Comparing with the whole sample set the VB sample also contains the lowest C_{27} (31.68 %) and the highest C28 (49.50%) steranes in the sample set.

NSO-1: The Ts/(Ts + Tm) ratio for the North Sea standard oil (NS0-1), which was used here as a reference sample, is found to be 0.51. The diasteranes/(diasteranes + regular steranes) ratio is 0.51. The C_{24} tetracyclic terpane/C30 αβ-hopane and the $C_{20}/(C_{20}+C_{28})$ triaromatic steroids are 0.04 and 0.45 respectively and, compared to the rest of the sample from the well **2/7-26S** of the Embla Field, they represent the lowest. The diahopane/(diahopane + normoretan), C_{30}-hopane/(C_{30}-hopane+ C_{30}-morethane), 29Ts/(29Ts+norhopane) were found to be 0.63, 0.92, and 0.31 respectively, all representing the highest value of the corresponding parameter in the sample set. Moreover, the value for hopane/sterane ratio (3.24) is by far the highest in the sample set.

6.4. Summary of results

Looking at the fractions of the bulk extracted organic matter, such as saturated, aromatic hydrocarbons and polar compounds, the studied samples show variations in abundance and

composition of the compounds vertically through depth. In the well 26S which is the complete sequence in the Embla Field great variations both in the amount of extracts and composition in the migrated petroleum is observed. The Upper sandstone contains higher extracts (average is 42.6 mg/g rock) compared to that of Lower sandstone (average is 14.5mg/g rock)

Upper sandstone

Results from the Iatroscan show, a decreasing trend in the content of total extractable organic matter (EOM) down depth. The total EOM varies from about 32.4-56.2 mg/g rock. The free hydrocarbon comprises 88-95.7% of the total EOM, the rest being non hydrocarbon compounds (NHC). Majority of the hydrocarbon portion is composed of saturates, while only 1-3.8% aromatic. The SAT/ARO ratio is very high(22.0 -86.7). The distribution of the non hydrocarbon (polar) compounds in the upper sandstone samples is quite uniform (10.9 to 11.8%) except sample E5 which showed polar content of 4.3% (see table 6.1 and Fig. 6.1, 6.2 and7.1).

Lower sandstone

The overall EOM abundance in the Lower sandstone layer is less rich than the one observed on the overlying unit and varies from about 2.3-24.1 mg/g rock. There are alternatives of rich and less rich samples (which represent zones within the layer) in terms of EOM in the lower sandstone. The less rich or lower abundance could be attributed to a relatively thin and tight units which are found intercalated with the major unit (For example compare samples **E12** and **E13,** EOM of 24.1 and 5.9 mg/g rock respectively), both from the Lower Sandstone. The free hydrocarbon content (saturated plus aromatic) in this part of the reservoir generally is also high (about 72-84% of the EOM). The content of aromatic varies between 0.5% to 3.4%. The SAT/ARO ratio ranges from 24-86.8, with the exception of one sample (**E11)**. The anomalous SAT/ARO (167.6) of sample **E11** is due to less amount of aromatic content in this unit compared to the saturates. The non hydrocarbon content (Polar) is about (15.6-29.1%). The polar content in the lower sandstone is dramatically increased and are heterogeneous in richness down depth compared to the one observed from the Upper

sandstone. The relative increase in the polar amount is compensated by the relative decrease in the saturated hydrocarbons (see table 6.1 and Fig 6.1,6.2 and 7.1) at the cost of aromatic counterparts.

Closer look at the available core samples reveals the presence of noticeable thin zones in the entire analyzed interval which contains polar rich layers. This are siltstone/mudstone interval (sample **M1** and **M2**), anomalously enriched in polar compounds compared to both sandstones. These intervals are also the poorest in the total abundance of extractable organic matter compared to the sandstones, perhaps due to lower porosity.

Rhyolite

The samples from the rhyolite unit basically contain very low EOM. The total extractable organic matter is in the range between 0.28 to 0.42 mg/g rock. However, these samples are very rich in aromatic hydrocarbons and polar compounds. The aromatic hydrocarbon are very heterogeneous within the sample group and ranges from 1.7 to 20.4%. The average aromatic fraction being 10.3% compared to that of Upper sandstone (2.3%) and Lower sandstone (1.7%). These sample groups are extremely rich in polar compounds compared to any of the samples in the studied set. The polar compound ranges from 56.0% to 69.2%.

The VB sample contains low extractable organic matter compared to the sandstones but about eight times higher than the extracts from the rhyolite.

The NSO-1 sample has a very different compositional properties than the Embla samples. The SAT/ARO ratio is extremely low, 1.7. See table 6.1 for comparison of the NSO-1 sample with the Embla samples.

The GC-FID chromatograms of the samples from the sandstones are fairly similar and show similar distribution pattern with depth. The chromatograms from the sandstones show a comparable and unimodal distribution of n-alkanes in the extracts with maximum at n-C_{19}. The slight difference in the height of the peaks mat be related to porosity or permeability differences (e.g higher porosity leading to greater loss of low molecular weight hydrocarbons) and the variations in the degree of biodegradation.

The rhyolite in the well 26S is poor in migrated hydrocarbon and dominantly consisting of non-hydrocarbon, it is not surprising not to see hydrocarbon signatures in the GC-FID.

The VB sample show GF-FID which is slightly similar to that of NSO and has the maximum peak at n-C_{13} (Fig.6.16).

From the results presented in the previous sections it is evident that most of the samples have differences in terms of the parameters from the GC-MS, which clearly indicate the different histories of oils in the sections of the reservoir.

Core Sample NR.	CODE	CORE DEPTH (ft)	CORE DEPTH (m)	Saturates	Aromatics	Polars	SAT+ARO	TOT		SAT	ARO	POL	
				mg/g rock	mg/g rock	mg/g rock	mg/g	mg/g		%	%	%	sat/aro
2/7-26S#10	E1	14524	4427	47.47	2.16	6.62	49.62	56.24		84.4	3.8	11.8	22.0
2/7-26S#14	E2	14570	4441	44.14	0.51	5.68	44.65	50.33		87.7	1.0	11.3	87.7
2/7-26S#22	E3	14686	4476	32.20	0.76	4.14	32.96	37.11		86.8	2.1	11.1	41.3
2/7-26S#30	E4	14770	4502	32.05	0.70	4.01	32.75	36.77		87.2	1.9	10.9	45.8
2/7-26S#34	E5	14831	4520	30.16	0.88	1.39	31.04	32.43		93.0	2.7	4.3	34.2
Average				37.20	1.00	4.37	38.21	42.57		87.8	2.3	9.9	46.2
2/7-26S#37	M1	14873	4533	0.92	0.05	0.60	0.97	1.57		58.7	2.9	38.3	20.1
2/7-26S#38	M2	14906	4543	0.64	0.01	0.42	0.66	1.07		60.0	1.3	38.7	46.2
Average				0.78	0.03	0.51	0.81	1.32		59.4	2.1	38.5	33.1
2/7-26S#39	E6	15323	4670	15.69	0.61	5.45	16.30	21.75		72.1	2.8	25.1	25.7
2/7-26S#40	E7	15341	4676	13.07	0.31	3.70	13.37	17.08		76.5	1.8	21.7	42.8
2/7-26S#41	E8	15353	4680	13.25	0.37	4.85	13.62	18.47		71.7	2.0	26.3	36.1
2/7-26S#42	E9	15372	4685	16.10	0.19	4.47	16.29	20.76		77.6	0.9	21.5	86.8
2/7-26S#44	E10	15415	4698	9.54	0.12	3.96	9.66	13.62		70.1	0.9	29.1	80.2
2/7-26S#46	E11	15427	4702	5.26	0.03	1.52	5.29	6.81		77.3	0.5	22.3	167.6
2/7-26S#47	E12	15442	4707	19.52	0.81	3.76	20.33	24.09		81.0	3.4	15.6	24.0
2/7-26S#48	E13	15451	4709	4.46	0.09	1.30	4.55	5.85		76.2	1.5	22.3	50.3
2/7-26S#49	E14	15460	4712	1.69	0.03	0.56	1.72	2.28		74.2	1.2	24.6	60.2
Average				10.95	0.28	3.29	11.24	14.52		75.2	1.7	23.2	63.8
2/7-26S#5,1R	E15	15848.5	4831	0.04	0.07	0.23	0.10	0.34		10.4	20.4	69.2	0.5
2/7-26S#4,1R	E16	15857.6	4833	0.18	0.01	0.24	0.19	0.42		42.3	1.7	56.0	24.2
2/7-26S#3,1	E17	15872.5	4838	0.16	0.01	0.25	0.17	0.42		38.5	2.0	59.5	19.2
2/7-26S#2R	E18	15883.4	4841	0.04	0.05	0.19	0.09	0.28		13.7	17.2	69.1	0.8
Average				0.10	0.03	0.23	0.14	0.37		26.2	10.3	63.5	11.2
Bitumen in vein	VB	16496	5028	1.32	0.09	0.84	1.41	2.24		57.2	4.1	38.7	14.0
NSO-1	NSO-1	NSO-1	NSO							53.1	31.1	15.8	1.7

Table 6.1. Results of Iatroscan TLC-FID analysis. The extracted organic matter was separated in two petroleum (SAT and ARO) and non petroleum (POL) fractions

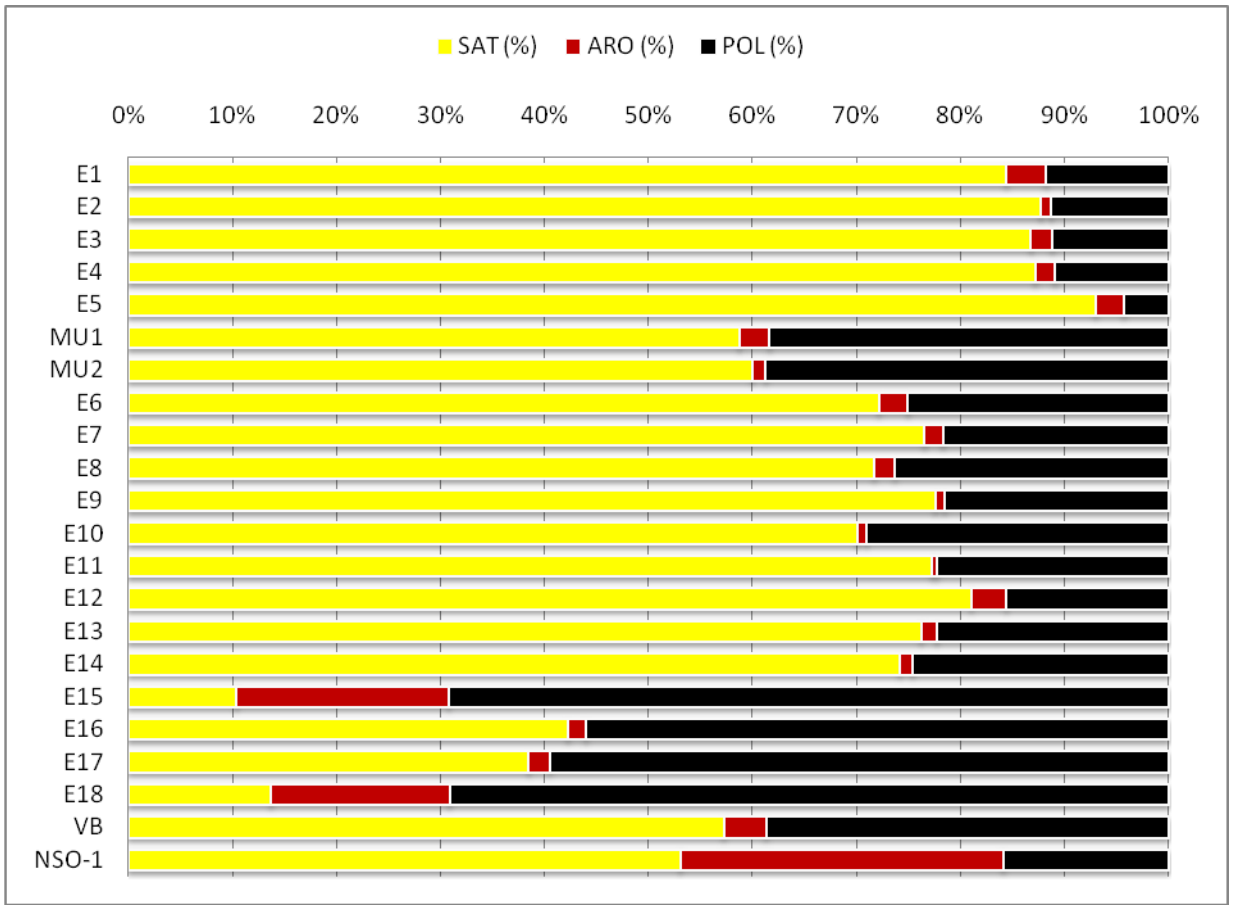

Figure 6.1 Bar chart showing the various compositions of the extracts. The extracted organic matter is broken down into three main fractions: saturates aromatics and polars. Note the increase in the contents of polar compounds and reduction of saturated hydrocarbons in the samples E15, E16, E17 and E18. NSO-1 is added for comparison. Also note that the NSO -1 has a different composition than the others.

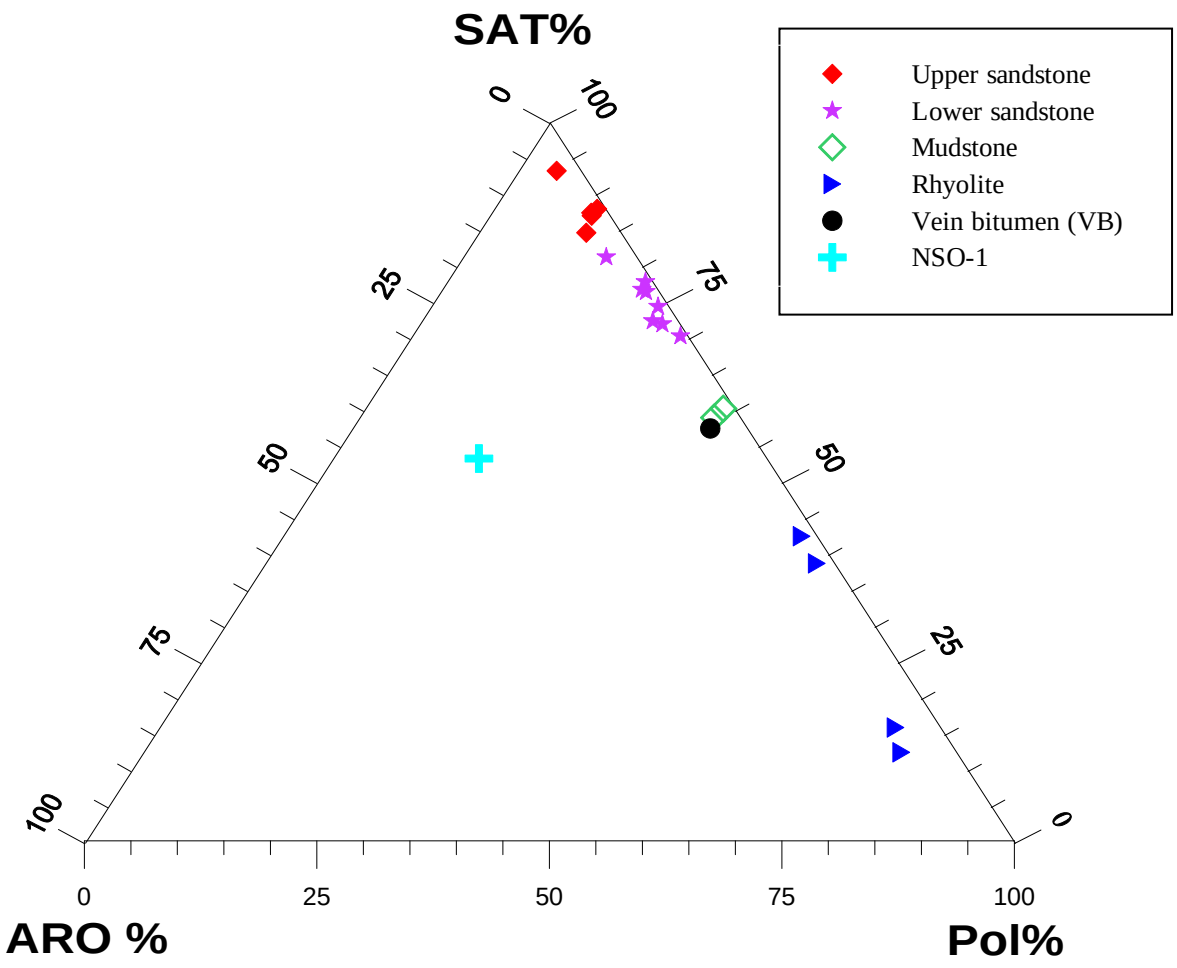

Fig 6.2. Ternary plot showing the petroleum and non petroleum fractions. The figure represents the same data as Fig 6.1

Sample	Pr/Ph	Pr/n-C17	Ph/n-C18
E1	1.03	0.45	0.38
E2	1.05	0.43	0.37
E3	1.08	0.40	0.33
E4	1.11	0.43	0.35
E5	1.11	0.42	0.33
E6	1.10	0.58	0.51
E7	1.07	0.64	0.54
E8	1.11	0.61	0.53
E9	1.02	0.55	0.48
E10	1.05	0.63	0.53
E11	0.96	0.73	0.60
E12	1.13	0.60	0.49
E13	1.07	0.62	0.54
E14	1.10	0.74	0.63
E15	ND	ND	ND
E16	1.58	0.59	0.43
E17	ND	ND	Nd
E18	ND	ND	nd
VB	1.94	0.56	0.45
NSO	1.65	0.60	0.49

Table 6.2. Data from the GC-FID analysis. ND = no data due to lack of peaks.

Sample	1	2	3	4	5	6	7	8	9	10	11	12	13
E1	0.64	0.50	0.57	0.89	0.21	0.08	17.13	2.88	1.57	0.52	0.45	0.80	49.18
E2	0.63	0.33	0.55	0.84	0.15	0.04	47.75	16.13	1.09	0.58	0.47	0.96	76.00
E3	0.63	0.33	0.60	0.88	0.18	0.07	20.67	6.43	1.12	0.56	0.47	0.87	64.29
E4	0.67	0.40	0.56	0.85	0.24	0.10	19.64	5.91	1.23	0.56	0.47	0.88	59.09
E5	0.62	0.38	0.60	0.18	0.18	0.10	36.70	9.20	0.52	0.46	0.46	0.90	72.80
E6	0.61	0.13	0.58	0.52	0.19	0.19	35.27	8.91	0.44	0.52	0.50	0.90	75.38
E7	0.62	0.33	0.60	0.67	0.14	0.08	43.75	12.25	0.32	0.52	0.55	0.91	76.26
E8	0.68	0.38	0.60	0.88	0.20	0.13	17.27	4.50	0.59	0.56	0.50	0.85	65.03
E9	0.71	0.40	0.55	0.91	0.22	0.09	9.98	2.90	0.94	0.55	0.52	0.83	58.24
E10	0.64	0.17	0.69	0.74	0.16	0.10	20.94	5.29	0.70	0.56	0.50	0.88	68.18
E11	0.73	0.29	0.56	0.91	0.21	0.08	13.34	3.97	0.81	0.57	0.56	0.85	61.15
E12	0.61	0.14	0.60	0.79	0.18	0.18	33.09	8.82	0.48	0.50	0.50	0.89	76.92
E13	0.58	0.50	0.59	0.62	0.20	0.08	44.00	11.88	0.52	0.50	0.50	0.93	81.20
E14	0.70	0.10	0.59	0.78	0.21	0.23	13.84	2.88	1.11	0.52	0.41	0.83	60.23
E15	0.74	0.46	0.60	0.78	0.21	0.15	45.86	15.14	0.98	0.57	0.33	0.97	74.00
E16	0.70	0.38	0.59	0.90	0.22	0.08	4.80	1.27	1.19	0.53	0.37	0.74	52.91
E17	0.68	0.29	0.58	0.91	0.19	0.07	9.94	2.58	0.76	0.53	0.43	0.80	61.54
E18	0.47	0.33	0.50	0.83	0.25	0.10	32.20	4.20	1.01	0.56	0.38	0.94	64.21
VB	0.42	0.10	0.44	0.74	0.17	0.71	5.60	0.70	0.40	0.80	0.23	0.29	31.68
NSO-1	0.51	0.63	0.59	0.92	0.31	0.41	0.25	0.04	3.24	0.57	0.43	0.51	38.28
*Average	0.63	0.31	0.58	0.77	0.20	0.14	24.83	6.62	0.83	0.55	0.45	0.84	64.65

Sample	14	15	16	17	18	19	20	21	22	23	24	25	26	27

Table 6.3. Parameters (1-13) calculated from the GC-MS chromatogram peaks. See chapter 5.3.7 and Table 5.9 for description of parameters.

(*Average indicates the average of the values of the parameters for the samples from Embla, it does not include NSO-1.)

E1	24.59	26.23	0.78	0.19	1.00	0.36	0.49	2.57	0.95	0.62	0.93	0.70	4.34	0.27
E2	12.00	12.00	0.91	0.07	1.48	0.66	0.58	1.94	1.14	0.79	1.13	0.65	12.15	0.11
E3	20.00	15.71	0.86	0.13	1.19	0.58	0.52	1.46	1.03	0.75	1.01	0.62	9.66	0.14
E4	20.45	20.45	0.94	0.11	0.94	0.53	0.51	3.38	0.92	0.72	0.97	0.76	7.63	0.13
E5	20.80	6.40	0.91	0.13	1.09	0.40	0.42	3.70	0.99	0.64	0.77	0.78	7.27	0.09
E6	16.15	8.46	0.94	0.14	1.74	1.30	0.60	15.20	1.21	1.18	1.17	1.62	3.10	0.28
E7	16.55	7.19	0.93	0.05	1.80	1.57	0.63	12.67	1.23	1.34	1.25	1.43	3.65	0.25
E8	18.18	16.78	0.91	0.16	2.00	1.50	0.62	12.67	1.28	1.30	1.22	1.43	3.82	0.25
E9	21.18	20.59	0.85	0.21	1.45	1.34	0.55	7.60	1.13	1.20	1.06	1.06	3.56	0.24
E10	15.91	15.91	0.88	0.12	1.84	1.39	0.62	38.00	1.24	1.23	1.22	3.28	3.42	0.26
E11	20.38	18.47	0.80	0.19	1.05	1.06	0.47	6.33	0.97	1.03	0.88	0.97	3.44	0.23
E12	15.38	7.69	0.91	0.08	1.82	1.30	0.59	12.67	1.24	1.18	1.16	1.43	3.63	0.24
E13	13.68	5.13	0.86	0.67	1.78	1.26	0.59	15.20	1.22	1.15	1.17	1.62	3.37	0.25
E14	20.47	19.30	0.81	0.33	1.55	1.31	0.58	10.86	1.16	1.19	1.13	1.30	4.49	0.19
E15	14.00	12.00	0.97	0.15	1.79	0.85	0.58	2.63	1.23	0.91	1.13	0.70	3.68	0.26
E16	22.33	24.76	0.92	0.23	0.74	0.72	0.36	2.91	0.81	0.83	0.64	0.72	21.80	0.03
E17	18.68	19.78	0.78	1.00	0.60	0.49	0.33	2.18	0.70	0.69	0.56	0.67	6.29	0.11
E18	15.79	20.00	0.98	0.12	0.46	0.47	0.29	6.91	0.58	0.68	0.49	1.01	7.58	0.05
VB	49.50	18.82	0.74	1.00	1.62	1.44	0.58	7.60	1.18	1.26	1.14	1.06	11.83	0.07
NSO-1	28.52	33.20	0.45	1.00	0.91	0.61	0.41	2.38	0.90	0.77	0.76	0.68	4.16	0.19
*Average	20.24	16.48	0.86	0.31	1.35	0.98	0.52	8.81	1.06	0.99	0.99	1.15	6.28	0.18

Table 6.3. continued... Parameters (14-27) calculated from the GC-MS chromatogram peaks. See chapter 5.3.7 and Table 5.9 for description of parameters. (*Average indicates the mean values of the parameters for the samples from Embla, for comparison with the NSO-1.)

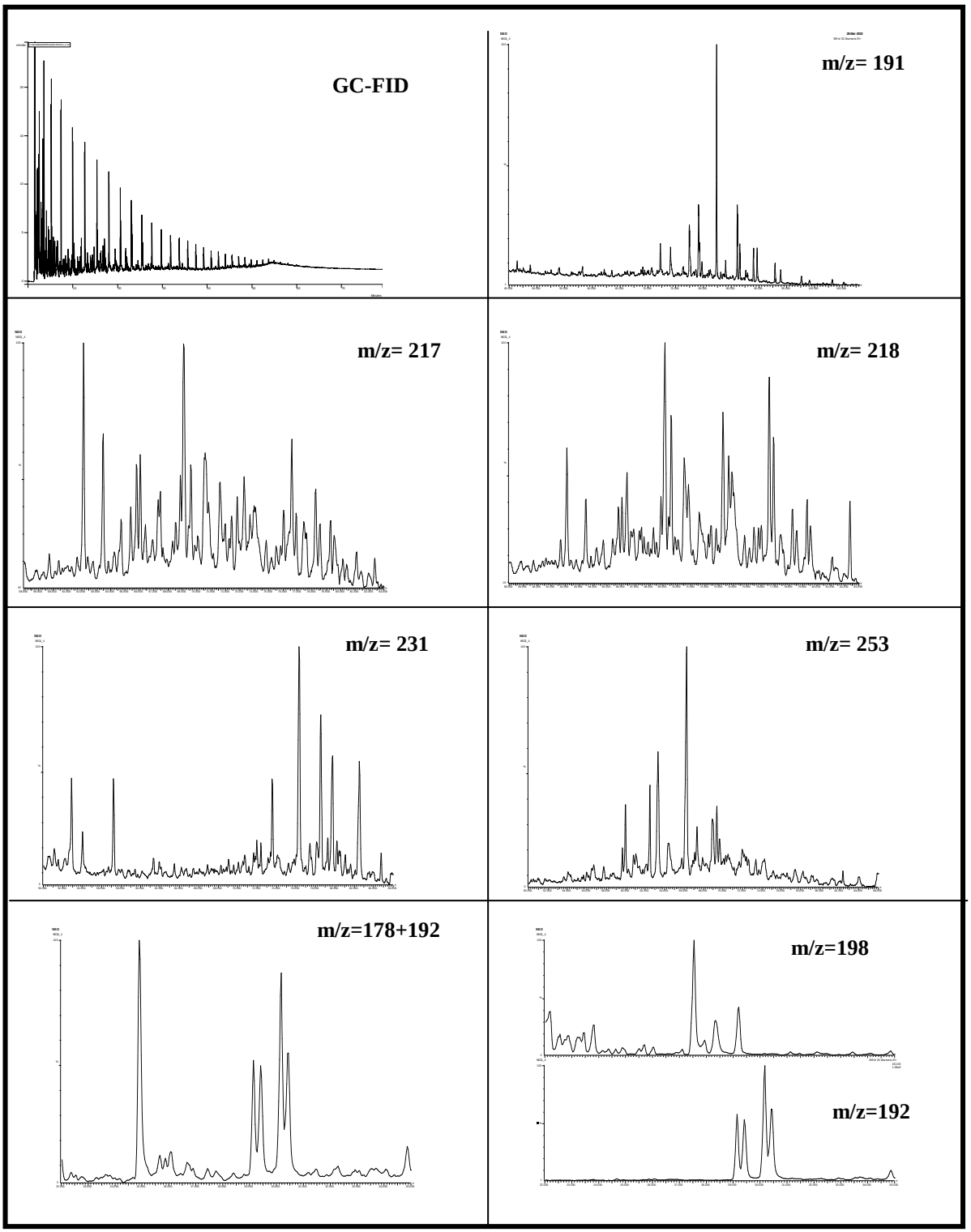

Figure 6.3. The chromatograms for the NSO-1 sample

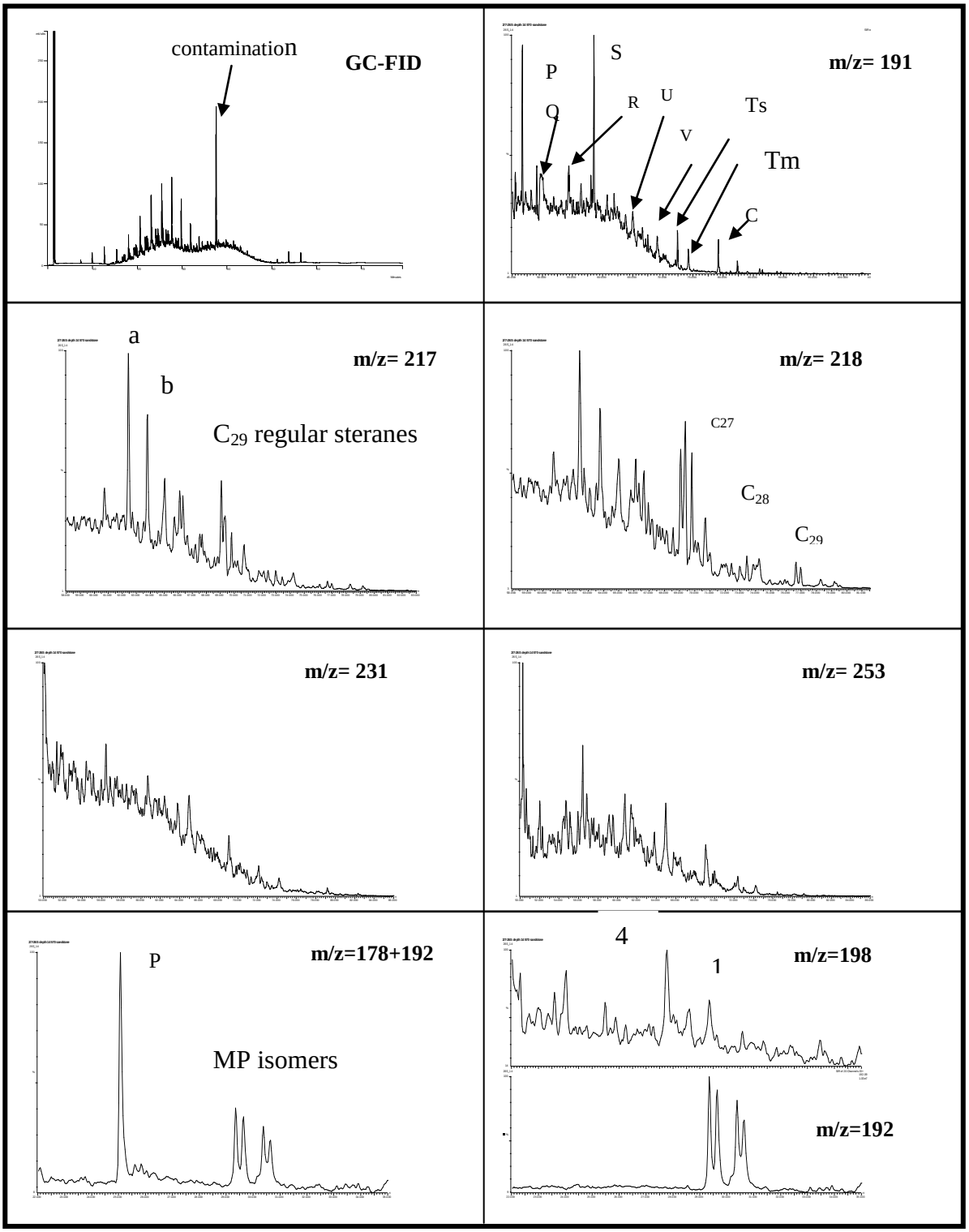

Figure 6.4. The chromatograms for the E2 sample

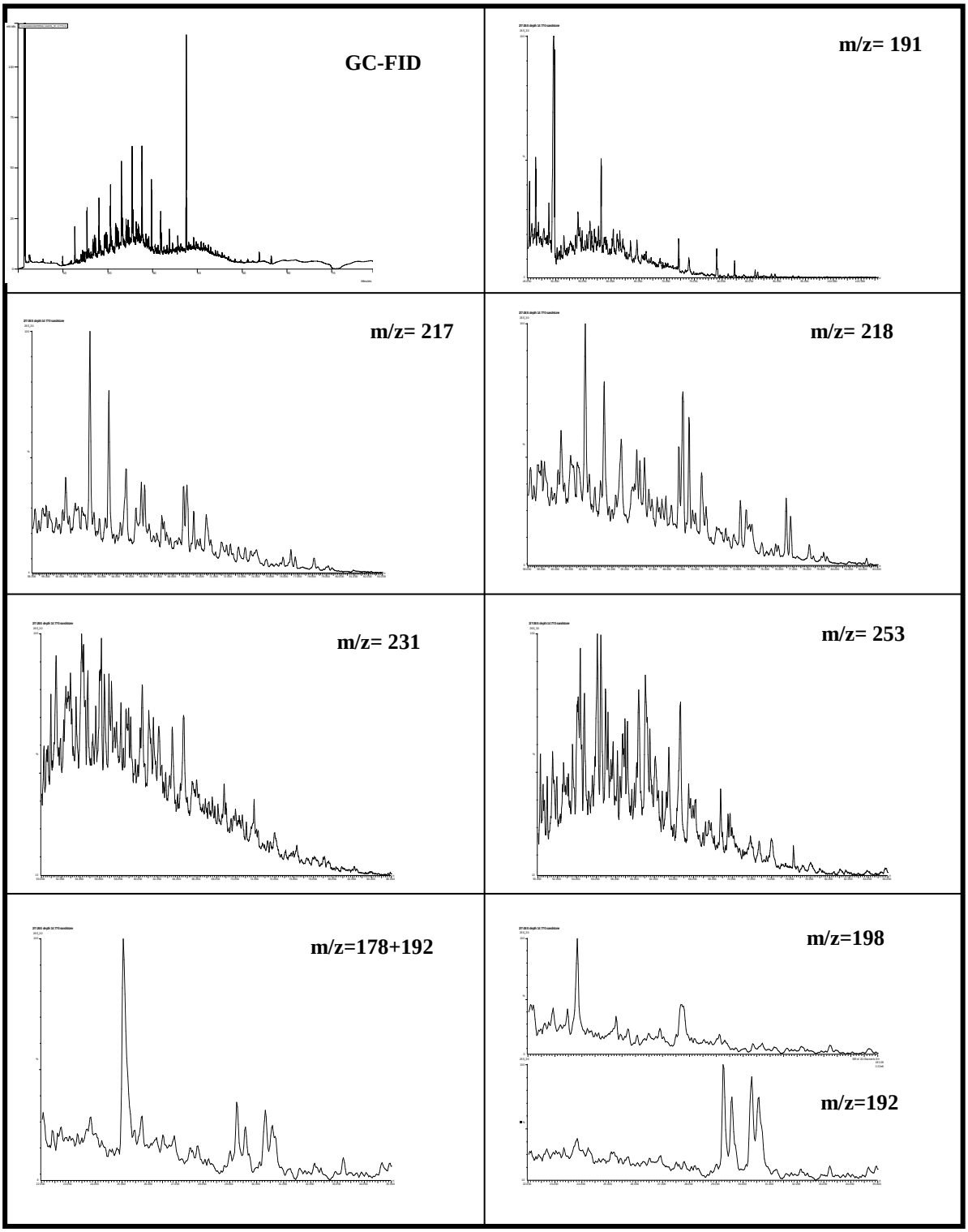

Figure 6.5. The chromatograms for the E4 sample

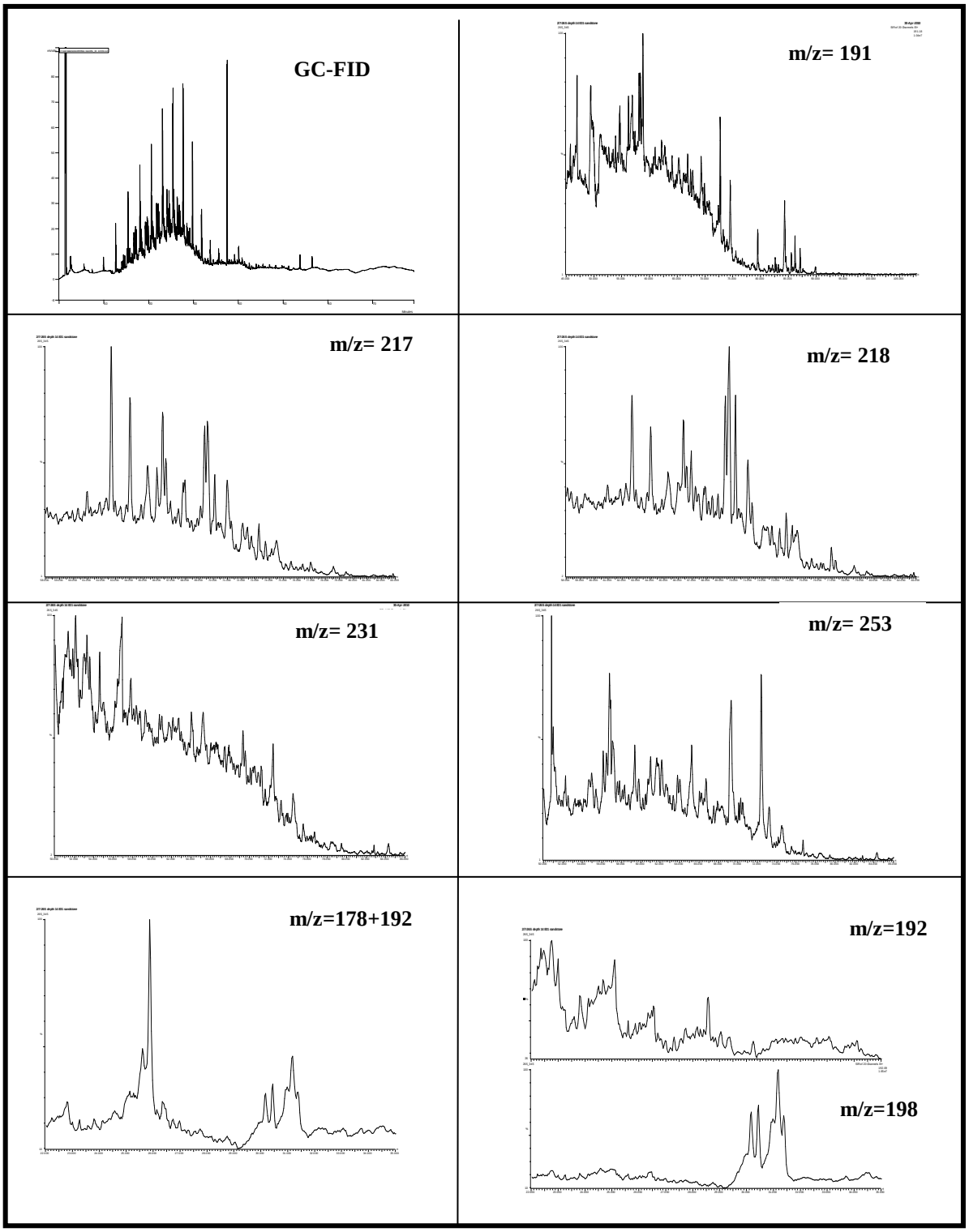

Figure 6.6. The chromatograms for the E5 sample

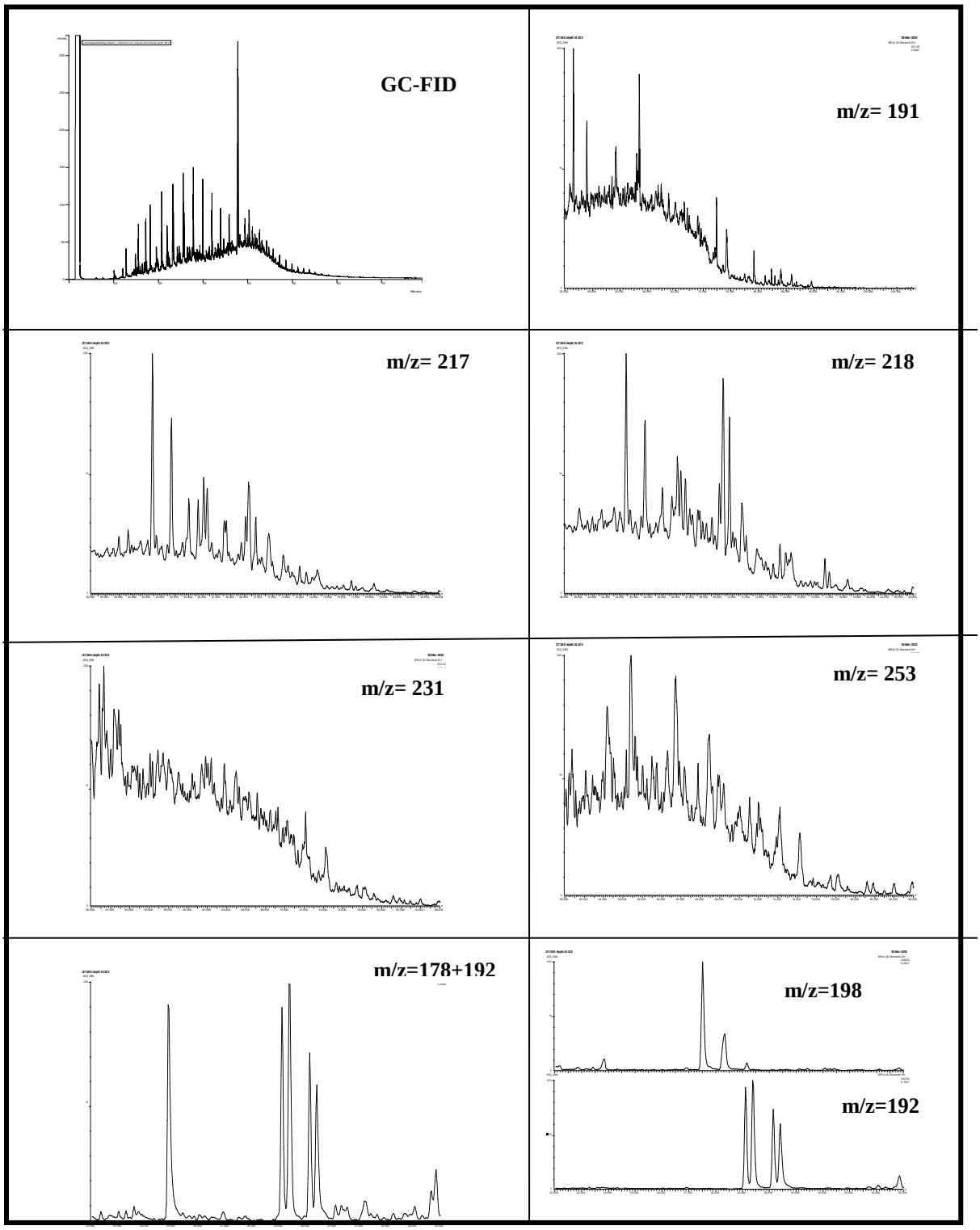

Figure 6.7. The chromatograms for the E6 sample

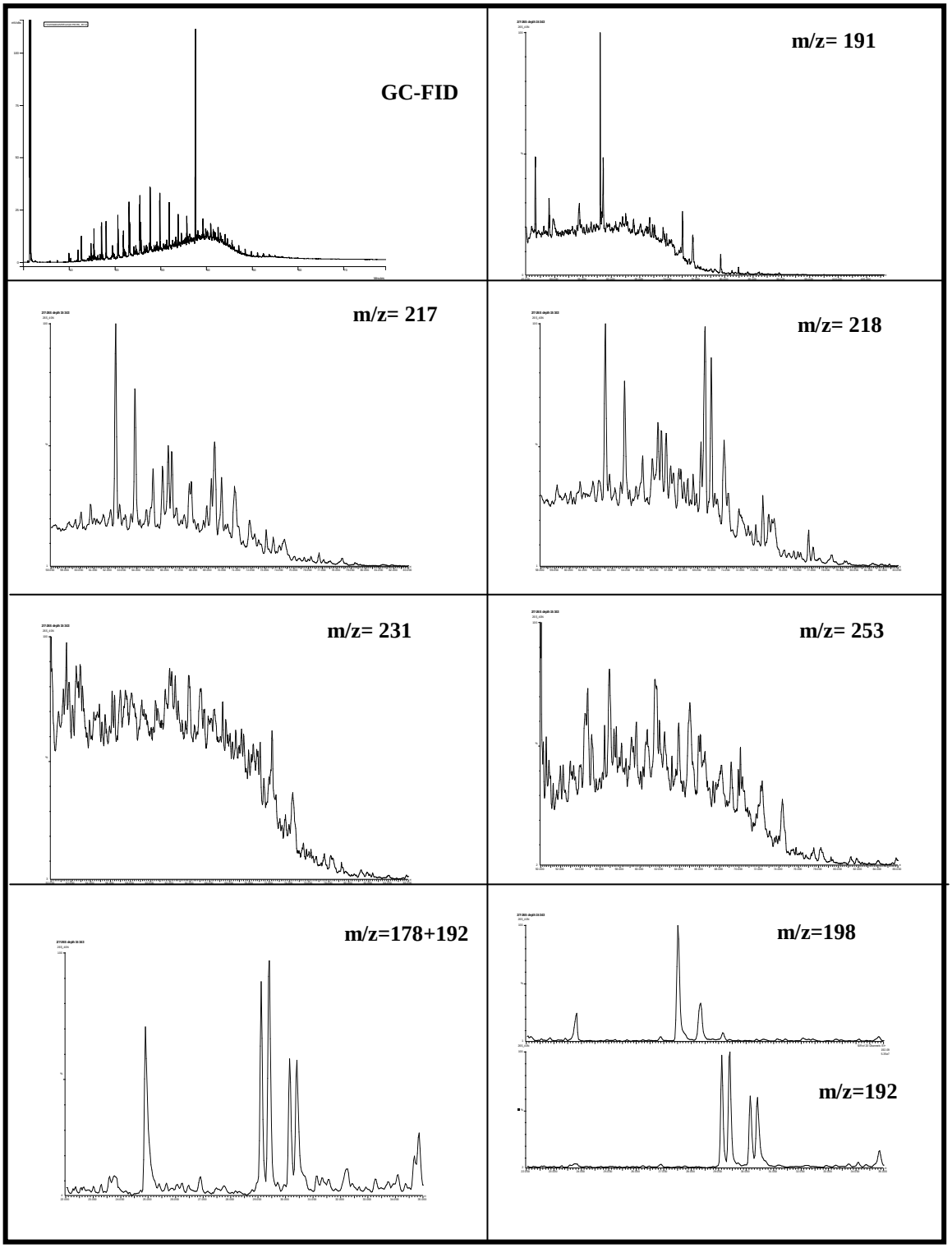

Figure 6.8. The chromatograms for the E7 sample

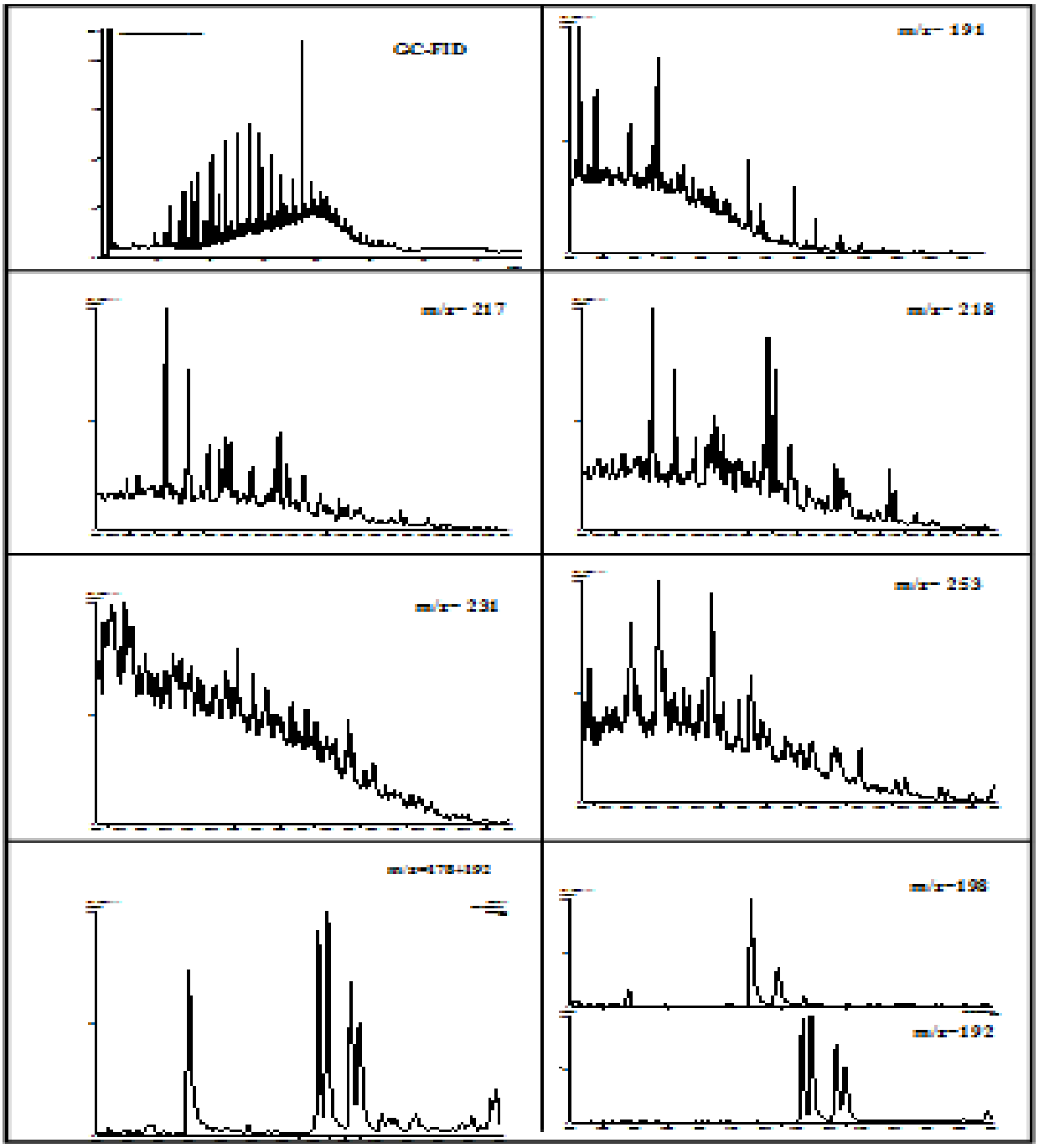

Figure 6.9. The chromatograms for the ES sample

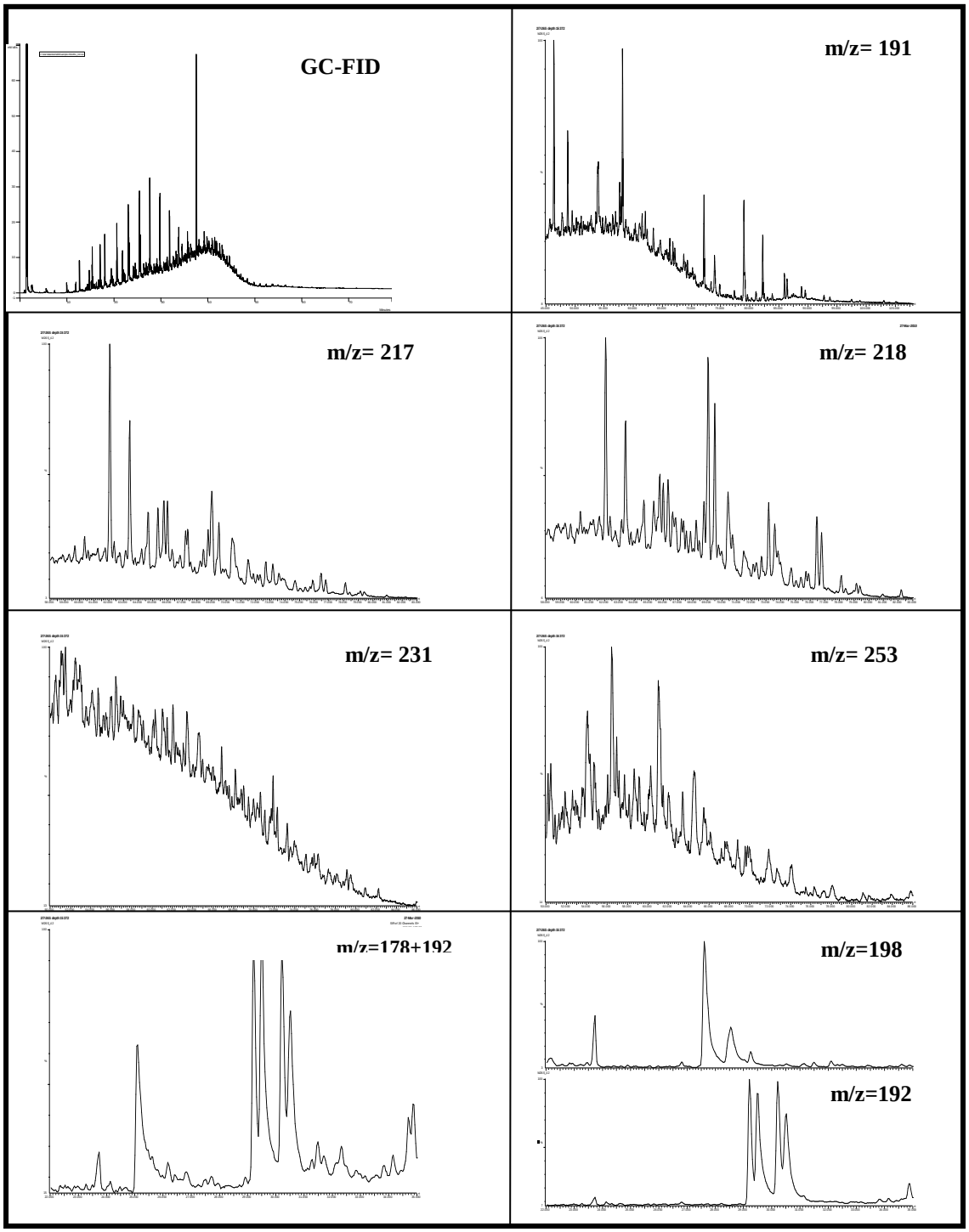

Figure 6.10. The chromatograms for the E9 sample

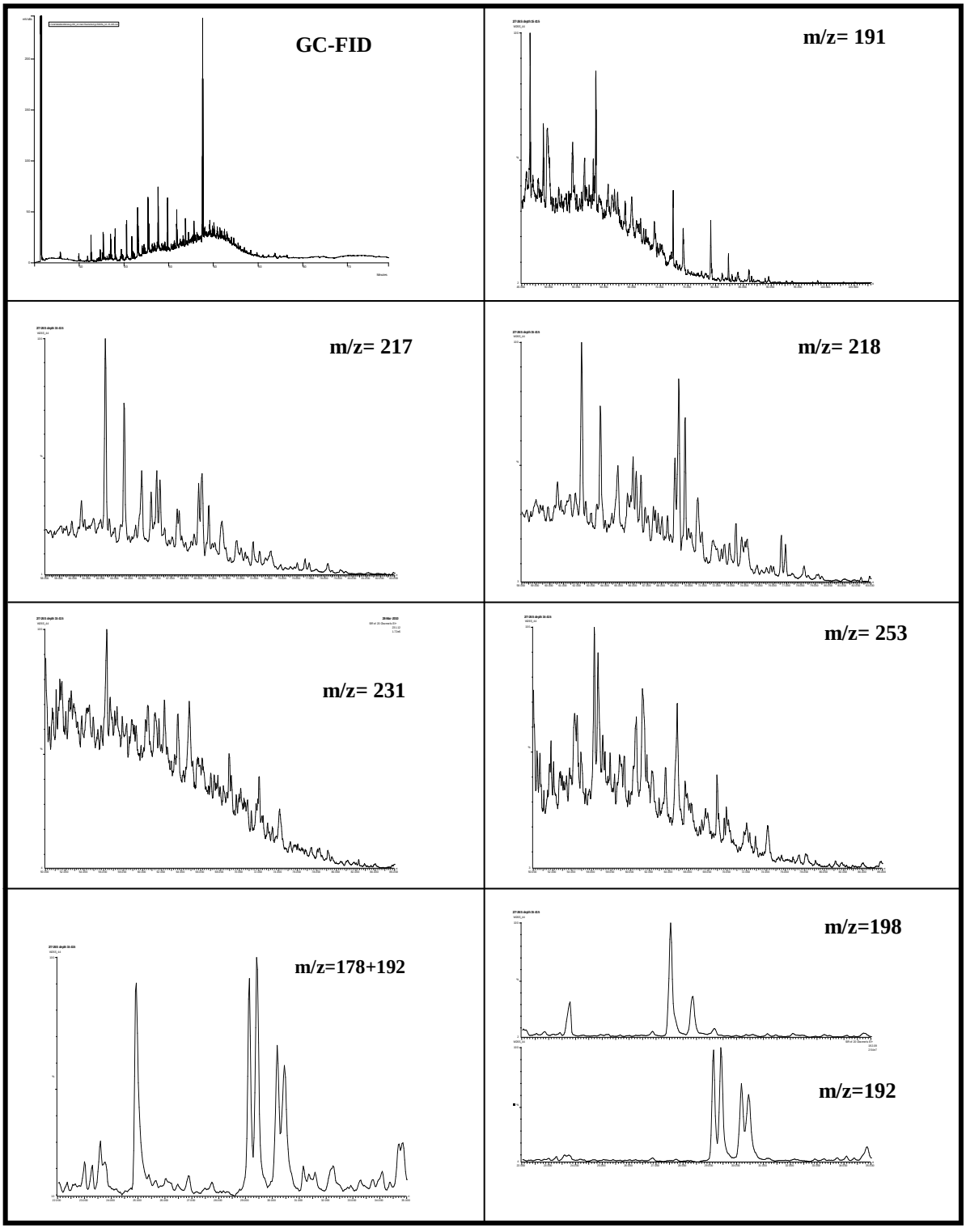

Figure 6.11. The chromatograms for the E10 sample

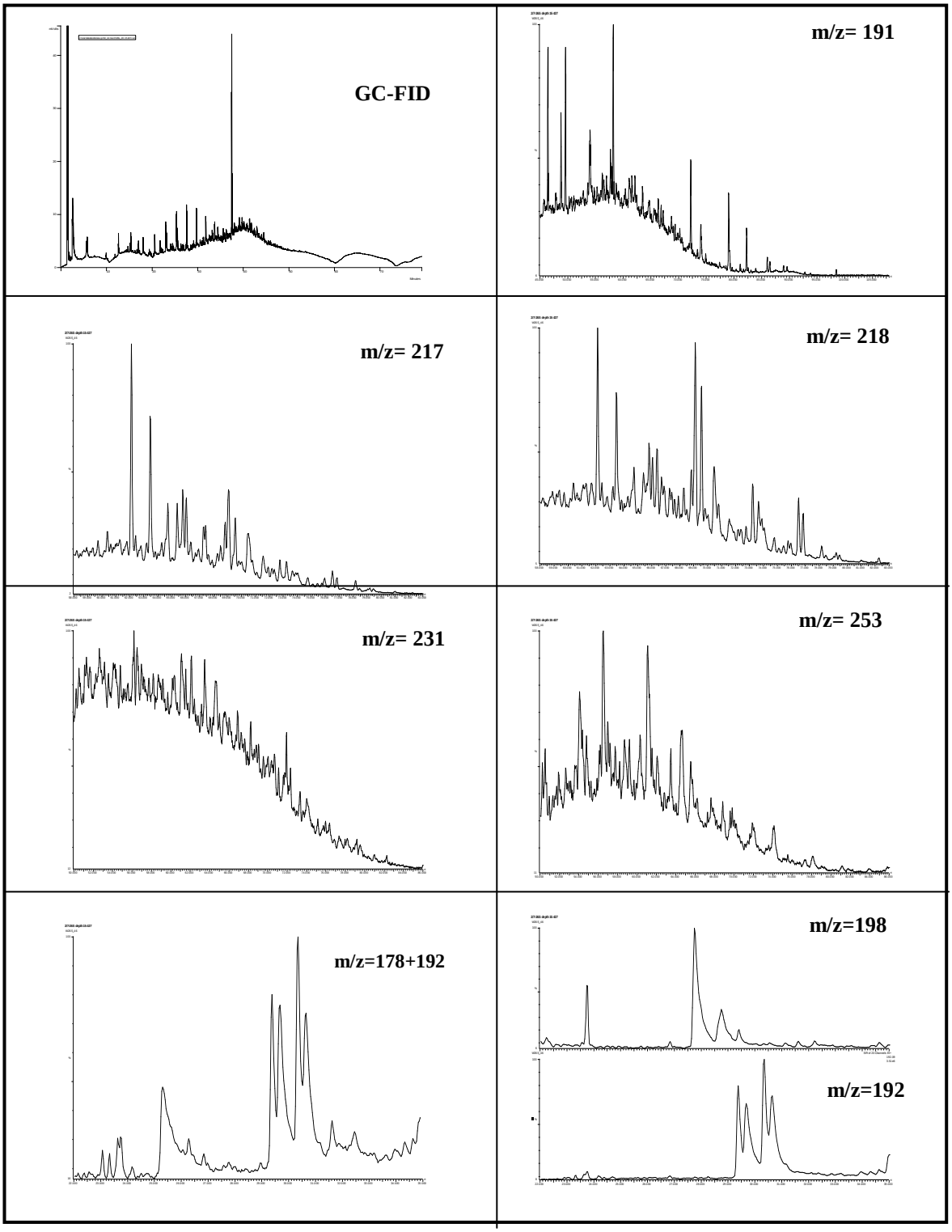

Figure 6.12. The chromatograms for the E11 sample

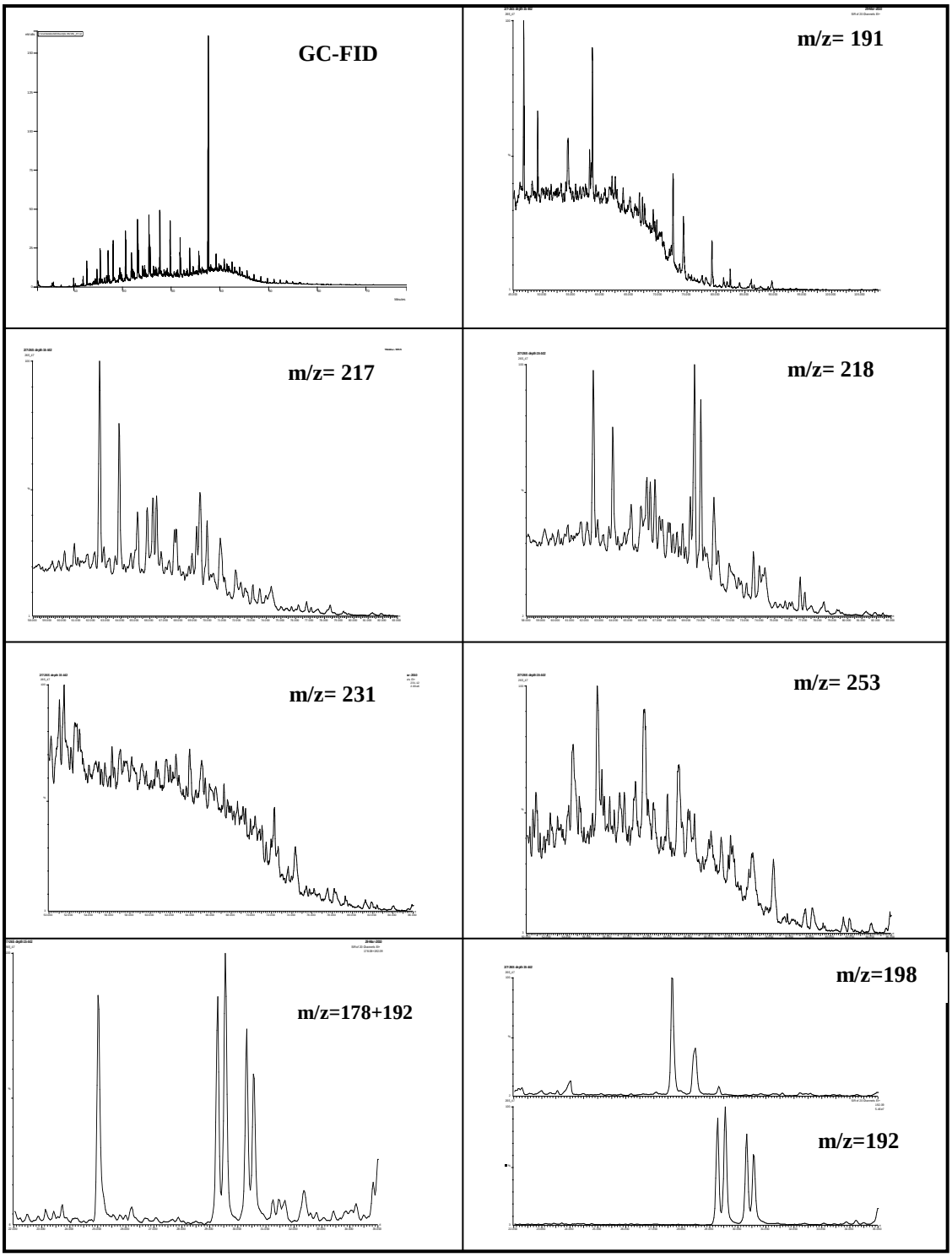

Figure 6.13. The chromatograms for the E12 sample

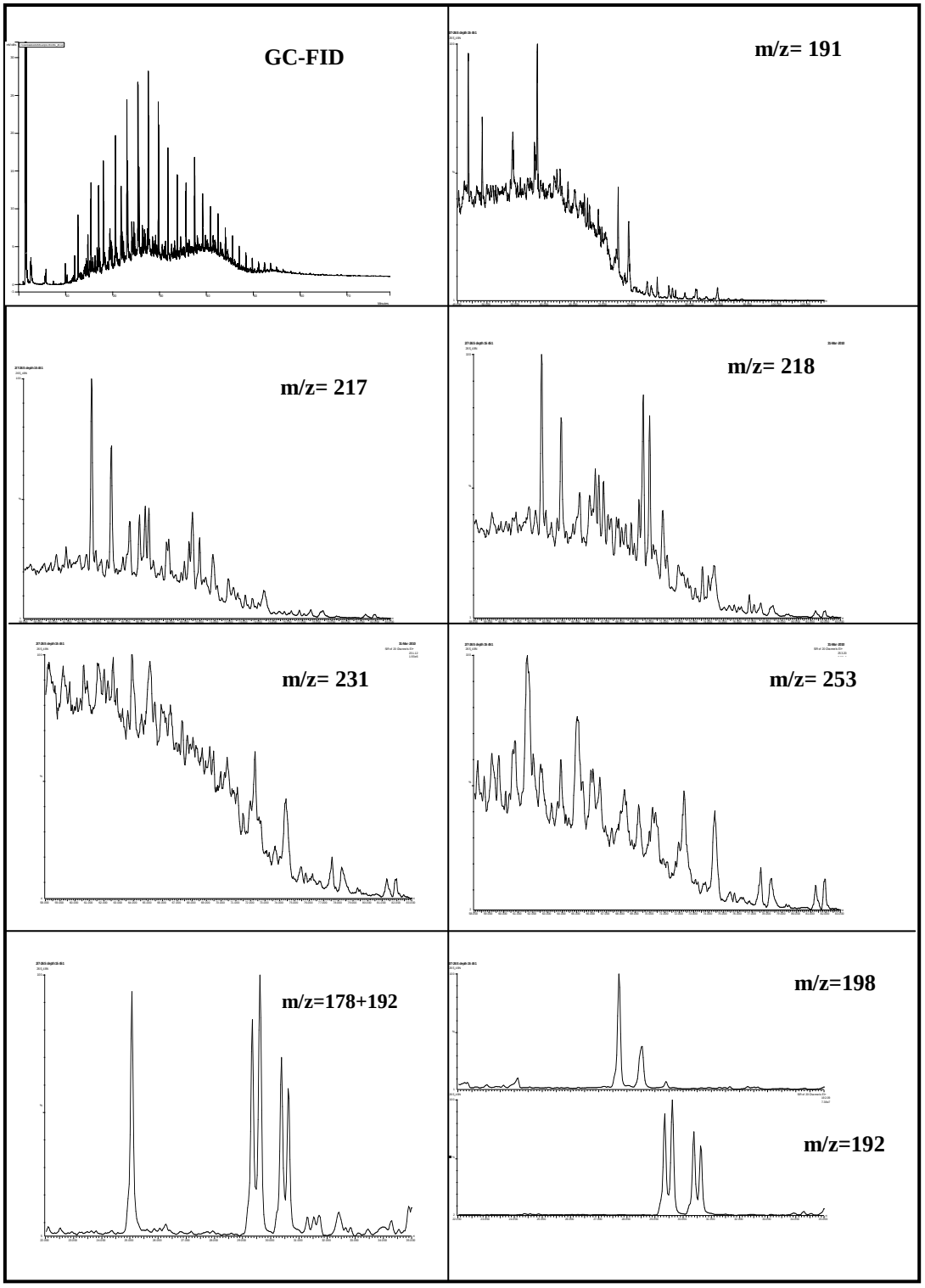

Figure 6.14. The chromatograms for the E13 sample

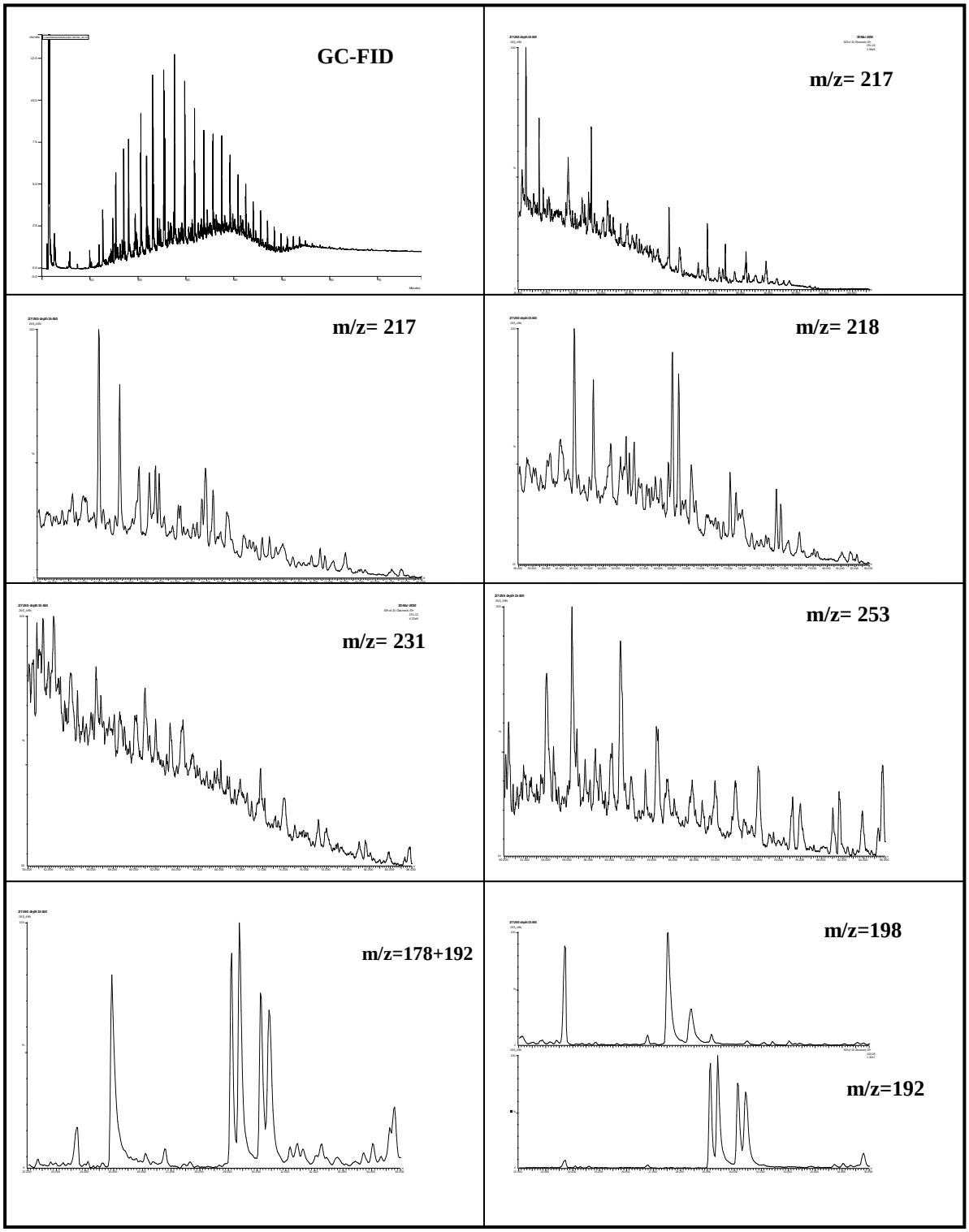

Figure 6.15. The chromatograms for the E14 sample

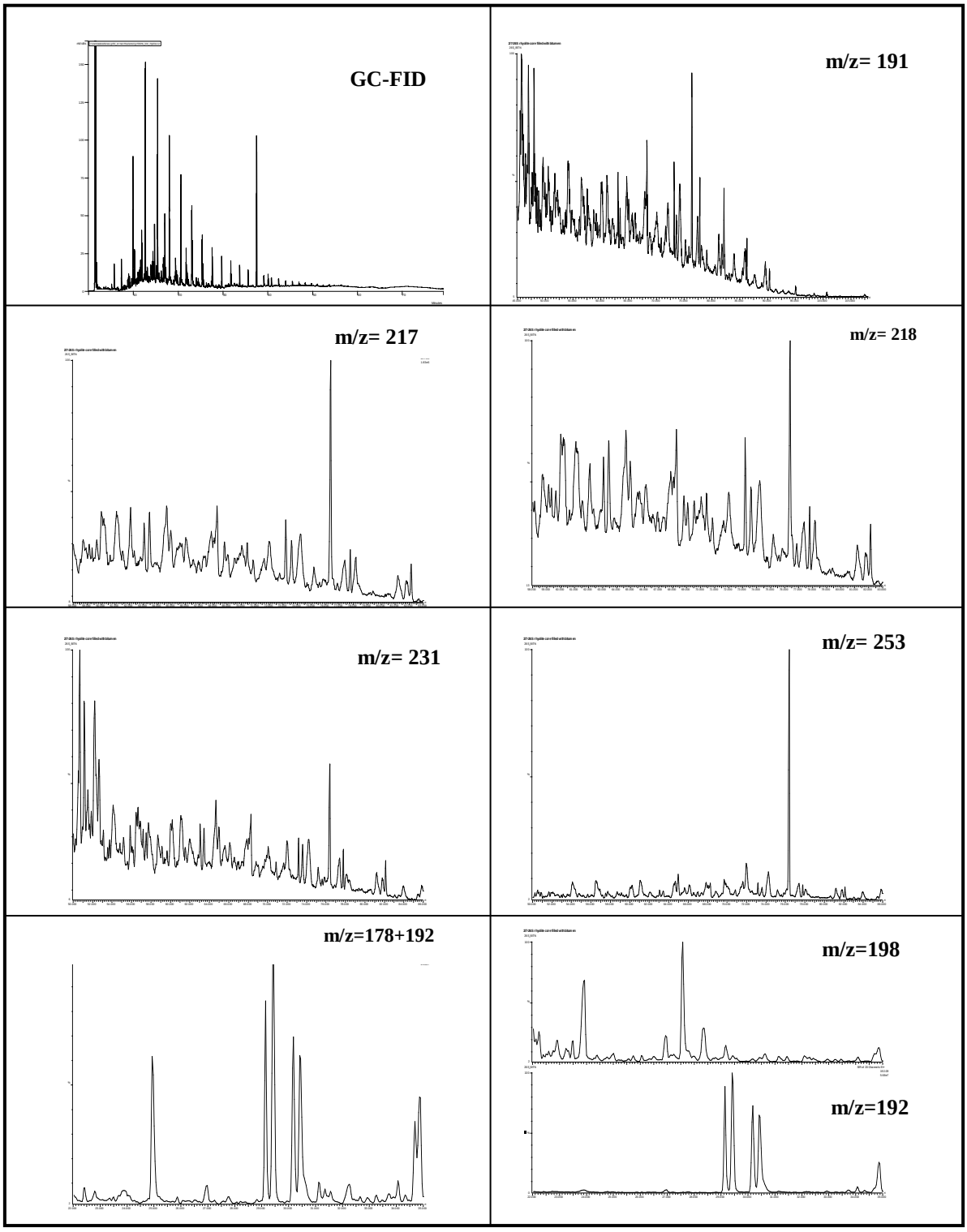

Figure 6.16. The chromatograms for the VB sample

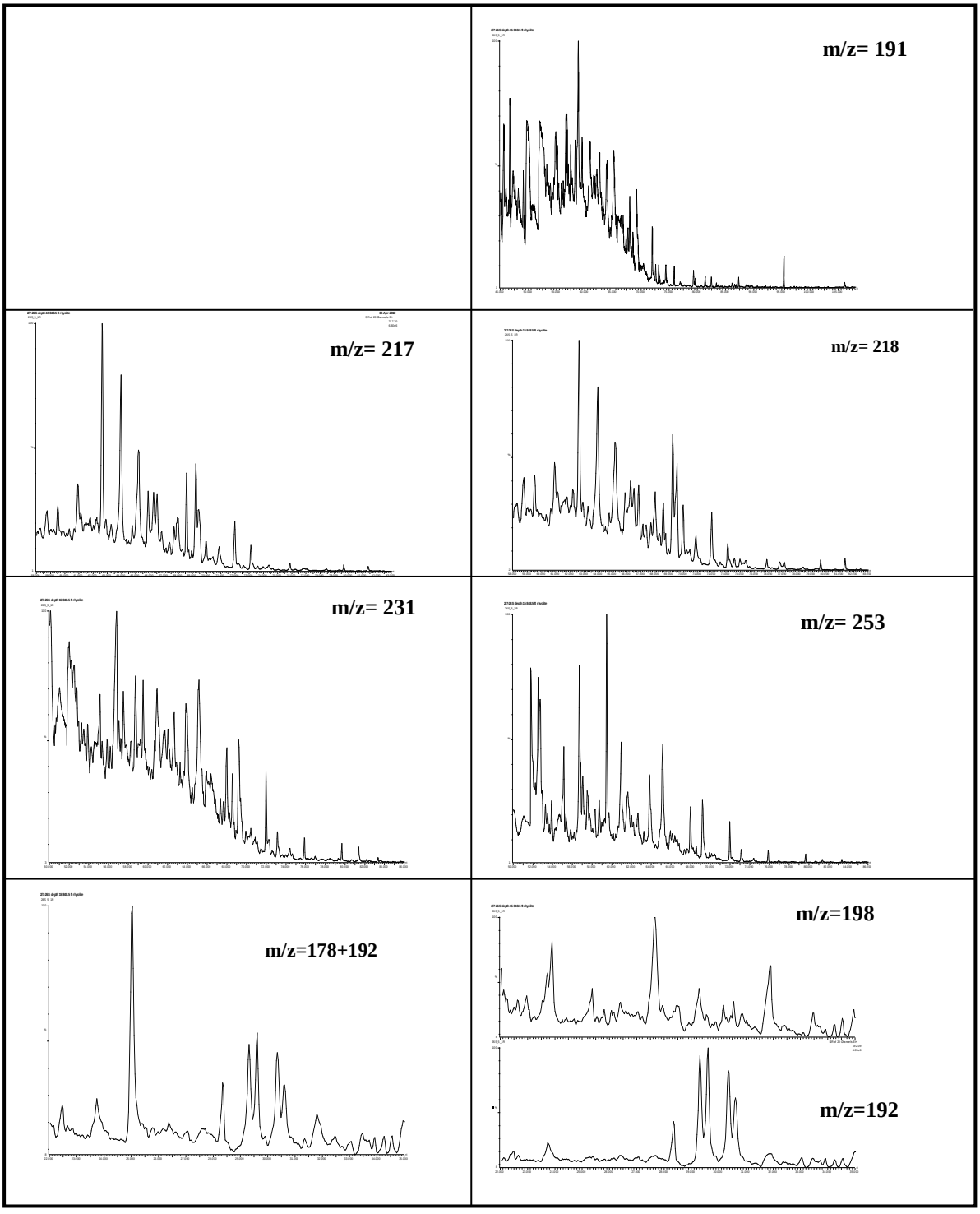

Figure 6.17. The chromatograms for the E15 sample, rhyolite at depth 4831 m. No GC-FID data is detected

7. Discussion

The results presented in the previous chapter will be discussed here. To illustrate compositional heterogeneities, maturity, organic facies and biodegradation, several plots have been generated. These plots represent the results from the different analytical techniques applied in the laboratory. Finally the chapter will give a summary of the main issues. The chapter will follow the following outline:

7. 1 Abundance of migrated bitumen
7. 2 Variations in bitumen composition
7. 3 Maturity of the Embla bitumen
7. 4 Organic facies
7. 5 Biodegradation
7. 6 Summary

7.1. Abundance of migrated bitumen

Quantitative changes in extractable saturated and aromatic hydrocarbon and polar compounds have been observed for the samples studied. As mentioned earlier in this thesis the results are based on well **2/7-26S** which penetrates through the Upper and Lower sandstone and down to the volcanic basement rocks. Of all the wells in the Embla Field, the well 26S has the most complete stratigraphic succession (Knight et al., 1993).

Base on the Iatroscan analysis, samples from the upper sandstone gave a higher amount of extractable organic matter (Table 6.1 and Figure 7.1). This part of the reservoir is the richest in terms of hydrocarbon extracts. With average free (saturated plus aromatic) hydrocarbon extracts of 38.21mg/g rock. The porosity of the Upper sandstone ranges from 10-15% (Bharati, 1997) with rhythmic distributions that would be responsible for the variations in abundance of the extracts from one sample to the other.

The amount of extract in samples from the Lower sandstone unit is approximately 30% of that in samples from the overlying unit (Upper sandstone). The average extract in this part of the reservoir is 11.24mg/g rock. For detail variations of hydrocarbon richness of the samples refer to (Table 6.1 and Figure and 7.1).

A mudstone unit (Figure 2.1), separating the Upper and the Lower sandstones, is part of the stratigraphic succession in the Embla Field. Iatroscan analysis of two (M1 and M2) samples from this unit shows that, the mudstone unit is very poor in generating hydrocarbon (see Table 6.1 and Figures 6.1, 6.2 and 7.1. Sample M1 and M2 have free hydrocarbon extracts amounting to 1.07 and 1.32 mg/g rock respectively. These samples are not discussed further, since they only can represent an impermeable unit hindering communication between the two sandstones which are highly rich in hydrocarbon.

The free hydrocarbon extracts obtained from the samples representing the rhyolite unit are really low. As it was presented in the previous chapter the free hydrocarbon extracts from the samples of this unit range from 0.09 to 0.19 mg/g rock, the average being 0.14 mg/g rock. These samples were whitish in color when examined by the naked eye except disseminated black solid bitumen. This was further confirmed from the color of the extracted solvent, which was almost as water in color.

The free hydrocarbon extract from the sample (VB) represents rhyolite vein/fracture which was filled with black bitumen was found to be 1.41 mg/g rock. This value is very low compared to the average free hydro carbon extracted from the Upper and Lower sandstones.

To sum up, referring vertically to the well 26S of the Embla Field, the Upper sandstone is the richest part of the reservoir in terms of free hydrocarbon extracts. The Lower sandstone gave free hydrocarbon extract of about 30% of that observed in the Upper sandstone. Bharati (1997) and Knight (1993) has explained the presence of significant amount of solid bitumen in the Lower sandstone, which I believe is responsible for the reduction of the porosity in the Lower sandstone and thus lower amount of saturated and aromatic hydrocarbon fraction..

The Mudstone unit represented by the two samples here is located between the two sandstones. The low amount of extract observed from this unit is attributed to the almost

impermeable property of the unit. The lithified volcanic rocks (both rhyolites and VB) are normally devoid of primary porosity, but are highly fractured (Knight et al., 1993). Because of this they are able to host the disseminated and observed vein bitumen. However, the Iatroscan result confirmed that this bitumen is not free to be extracted anymore in ample amount.

7.2. Variations in hydrocarbon composition

Extracted organic matter differentiated into hydrocarbon and non-hydrocarbon fractions using the Iatroscan TLC-FID technique reveals that the migrated hydrocarbon in the Embla Field shows great differences with respect to composition in addition to the variation in richness.

As it is shown in (Table 6.1 and Figures 6.1, 6.2 and 7.1) there is a general decrease in the amount of total extract with depth. It is also evident to see how the saturated and aromatic hydrocarbons decrease with depth while the non hydrocarbon (polar) compounds are highly enriched. The trend is more visible in the Upper sandstone than in the other units.

Comparing the two sandstones, the samples from the Upper sandstone shows relatively uniform distribution in both saturated and aromatic hydrocarbons down through the well 26S. The lower sandstone was found to host more polar compounds.

The rhyolite unit is dominated by polar compounds which accounts for an average of 63.5% of the total extractable organic matter (EOM). The Vein bitumen (VB), which represents the deepest sample from the set, shows 38.7% polar compound. This value is still very high, though lower compared to the samples from the rhyolites, which were from relatively shallower depth (4831-4841 m) compared to the depth location of VB (5028 m). For comparison of the different compositions average values of the samples from each category (Upper, Lower sandstones, Rhyolites and VB and NSO) is summarized in table 7.1.

Unit	SAT(%) (%)	ARO(%) (%)	POL(%) (%)	SAT/ARO(%)
Upper sandstone	87.8	2.3	9.9	46.2
Lower sandstone	75.2	1.7	23.2	63.8
Rhyolites	26.2	10.3	63.5	11.2
Vein Bitumen	57.2	4.1	38.7	14.0
NSO-1	53.1	31.1	15.9	1.7

Table 7.1 Summary of hydrocarbon compositional variations for the averages EOM (%) of the samples from the well 26S of the Embla Field. These values represent averages of the samples in each unit. For details, see table 6.1 **Note**: It is important to bear in mind that the Embla reservoir is highly complex and contains a lot of solid bitumen from a prior filling-event (Knight et al., 1993). This bitumen is very rich in polar compounds and has probably contributed to a higher polar fraction of the extracts. For this reason, it is difficult to correlate these extracts with oils based on the polar fraction, for example comparing with the NSO-1.

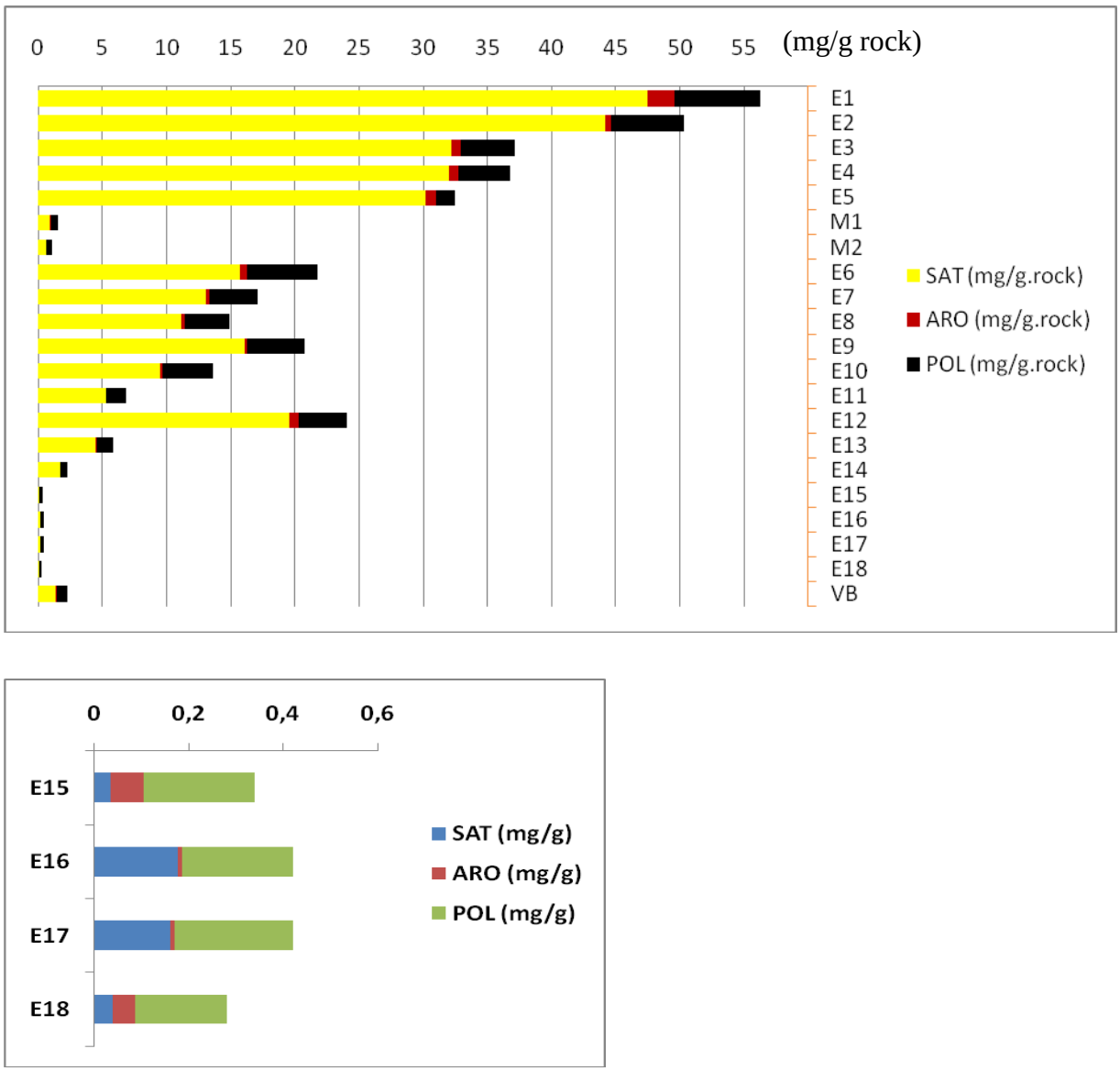

Figure 7.1: Abundance of hydrocarbon and non-hydrocarbon fractions extracted (based on Iatroscan results) in the Upper, Lower sandstone and Rhyolites of well 26S of the Embla Field. Lower figure shows a 'blow-up' plot for the extracts from the rhyolite unit (E15, E16, E17 and E18). SAT=Saturated hydrocarbons, ARO=Aromatic hydrocarbons and POL=Polar compounds.

7.3. Maturity of the Embla Bitumen

Introduction: The maturity of a petroleum sample usually refers to the degree of heat experienced by the source rock until the petroleum became expelled. The maturity normally increases with burial depth. The oil window is the depth interval in which a petroleum source rock generates and expels most of its oil. The oil window occurs in the temperature range from 60°C to 160°C (Hunt, 1996), which typically corresponds to a depth interval of 2-5 km, given geothermal gradients in the range of 30-35°C. In this subsurface the hydrocarbon generation is thought to take place from the beginning in the shallowest part (early mature), through oil peak generation about half ways (mid mature), to the generation of late mature oil or gas in the bottom of the window (late mature/thermal gas) (see Fig 5.12 for oil window range and validity of parameters within the window).

The geothermal gradient, the burial rate and the kinetic properties of kerogens also affect the relationship between temperature history, maturity and expulsion of gas and oil. The depth for onset of oil generation in the North Sea may vary as much as 500 m between the grabens and their flanking highs, due to different geothermal gradients. The most mature source rocks, are however, situated along the deeply buried Graben axis. Expulsion seems generally to take place at about 4-5 km.

In general terms, organic matter can be described as immature, mature, or post mature, depending on its relation to the oil-generative window (Tissot and Welte, 1984). Immature organic matter has been affected by diagenesis, including biological, physical, and chemical alteration, but without a pronounced effect of temperature. Mature organic matter has been affected by catagenesis, the thermal process covering the temperature range between diagenesis and metagenesis. Post mature organic matter has been heated to such high temperatures that it has been reduced to a hydrogen-poor residue capable of generating only small amounts of hydrocarbon gases.

The maturity of the samples from the Embla Field is estimated using a variety of parameters, from Iatroscan, GC-FID and from GC-MS (biomarkers). The different parameters generally show agreement for the respective sample. However, some parameters may respond in a

varying degree due to the influence of different source rock facies, migration histories, fractionation and degree of intra-reservoir mixing, biodegradation, gas stripping or water washing (Karlsen et al., 1993). Thermal maturity of organic matter typically requires integrating both biomarker and non-biomarker maturity data (Peters and Moldowan, 1993).

7.4. Maturity based on Iatroscan

Thermal alteration cause organic matter to increase its amount of low molecular weight hydrocarbons (below C_{15}). The amount of aromatic compounds in crude oils tends to decrease with increasing maturity and do therefore reflect the maturity of the oils (Tissot and Welte, 1984). Maturity of oils based on comparison between saturated fractions is difficult since this fraction tends to change less with increasing thermal maturation (Tissot and Welte, 1984). Therefore, with respect to the maturity discussion based on Iatroscan data, the relative proportion of aromatic hydrocarbons gains the most attention. The main purpose of using the Iatroscan data as maturity parameter here is to compare the maturity of the Embla samples from the common Upper Jurassic oils in the Norwegian Offshore Continental Shelf (NOCS). For this reason, examples from the Haltenbanken oils, typical normal oils on the Norwegian Offshore Continental Shelf (NOCS) presented by (Pedersen et al., 2006) are considered in addition to the NSO-1. The Haltenbanken area represents typical oils of Jurassic age, in contrast to the oil in the Embla Field.

The extracted gross composition of the Embla field and NSO-1 are presented in Table 6.1, and Figures 6.1 & 6.2. The average percentage composition for each of the Upper sandstone, Lower sandstone, Rhyolite, VB and NSO-1 samples is presented in table 7.1. The average aromatic fraction for the Upper sandstone samples and Lower sandstone respectively are 2.3 and 1.7%. The average aromatic composition for the VB sample is 4.1%. The rhyolite samples have got an average aromatic composition of 10.3%. The average aromatic fraction for the NSO-1 was found to be 31.1%.

Pedersen et al., 2006 have presented the bulk composition data for 33 oils from the Haltenbanken area and they have found an average saturated fraction of 69.4%, an aromatic fraction of 20.2% and a polar fraction of 4.08%.

From these observations we suggest that within the Embla Field the samples from the Lower sandstone have gain the highest maturity level as indicated by their lowest aromatic content and they are followed by the samples from the Upper sandstone.

All the Embla samples contain less percentage of aromatic fractions than both the NSO-1 and data presented by Pedersen et al., 2006. Therefore, the higher aromatic fraction of these oils (NOCS) could indicate that the Embla bitumen is more mature. The Haltenbanken oils show typical oil characteristics and are suggested to derive from the well known Upper Jurassic Spekk Formation (Karlsen et al., 1995).

It must be emphasized that the gross compositional data such as provided by Iatroscan TLC-FID is only a help for defining the maturity differences, as phase fractionation and water washing also affect the SAT/ARO ratio, and more reliable maturity interpretations are based on biomarker data.

7.5. Medium range maturity parameters

N-C_{17}-n-C_{19} alkanes distribution pattern

The n-alkane distribution changes as a result of the maturity of the source rock and is in particular useful for low to medium maturity oils. Hydrocarbon composition as measured by gas chromatography is sensitive to organic matter input, biodegradation, thermal maturity and evaporative loss or weathering (Figure 7.11). Peters et al. (2005) have shown the appearance of GC-FID signatures of three oils of different maturity level. Signatures from the least mature oil show bi modal n-alkane distribution, which is absent in a more mature oil. Lack of a bimodal n-alkane distribution in the more mature oil is due to largely to thermal maturation. None of the chromatograms (see Figures 6.4-6.17 and Appendix A) from the Embla Field have bimodal appearance. From the above statements we can conclude

that the bitumen extracted from the Embla Field samples are highly matured and they have been affected by evaporative loss i.e. the extracted bitumen from Embla reservoir are depleted in compounds below approximately n-C_{13}, (see Figures 6.4-6.17 and Appendix A).

Pristane/n-C17 and **Phytane/n-C18** ratios decrease with increasing thermal maturity as more n-alkanes are generated from kerogen by cracking and because the resulting carbon in the isoprenoids result in lower bond strength. The ratios can be used to assist in ranking the thermal maturity of related, non-biodegraded oils and bitumen. However, organic matter input (Alexander et al., 1981b) and secondary processes such as biodegradation, can affect these ratios. Based on the Pr/n-C17 and Ph/n-C18 ratios, which are cross-plotted in figure 7.11, the samples from the Upper sandstone of the well 26S (Embla Field) are more mature while samples from the Lower sandstone are less mature in this sample set. However, these parameters as maturity indicator might not be useful for Embla case as the bitumen samples all show evidences of biodegradation.

The **pristane/Phytan** (Pr/Ph) ratio can also be used as a maturity parameter; the ratio will increase with increasing thermal maturity (Alexander et al., 1981b). However, this ratio should be used with caution, because it can be affected both by digenetic processes and it is predominantly determined by organic facies. Regarding the samples from the Embla Field, the Pr/Ph ratio is highest for the extract from the vein bitumen (**VB**) followed by the samples from the rhyolites (see Table 6.2). The Upper and Lower sandstone show about similar values of n-alkane/isoprenoid and Pr/Ph ratios, hence no distinction on the degree of maturity can be made based on this parameter, and this suggests both units to contain oil of the same organic facies.

7.6. Biomarker maturity parameters

Long chained biomarkers constitute the heavier part of the petroleum, and it is possible that these maturity indicators in some cases show contrasting maturities compared to the medium range parameters (Karlsen et al., 2004). Reduced biomarker concentrations of all types indicate increased maturity (Mackenzie et al., 1985) or phase fractionation (Karlsen and

Skeie, 2006). Ratios of certain saturated and aromatic biomarker compounds are some of the most commonly applied thermal maturity indicators. These indicators result from two types of reactions: cracking reactions (including aromatization) and isomerizations at certain asymmetric carbon atoms. Figure (5.12) shows the approximate ranges of various biomarker thermal maturity parameters relative to the oil-generative window.

Assessment of the maturity of the migrated bitumen in the Embla Field is given below based on the different biomarker maturity parameters.

Figure 7.1 is a cross plot of the maturity parameters 20S/ (20S+20R) and ββ/ (ββ+αα) of the C_{29} steranes. The sterane parameter 20S/(20S+20R) reaches its maximum value of approximately 0.53-0.55 around maturity of Ro=0.90%. The ββ/(ββ+αα) ratio has a value of approximately 0.25 at the onset of the oil window, and reaches its maximum of about 0.68 to 0.71 around maturities of Ro=0.90 (Peters and Moldowan, 1993, and Peters et al., 2005). The 20S/(20S+20R) ratio works best for petroleum from marine, siliciclastic source rocks (Peters et al., 2005).

The sterane maturity parameters 20S/(20S+20R) and ββ/(ββ+αα) for the whole sample set show values of 0.23 to 0.56 and 0.46 to 0.58 respectively (Figure 7.1 and Table 6.3). The 20S/ (20S+20R) ratio for sample E11 is 0.56, slightly higher than the range proposed by (Peters and Moldowan, 1993, and Peters et al., 2005). Partial biodegradation of C_{29} ααα*R*-steranes can cause the 20S/(20S+20R)-value to rise above 0.5 (Hunt, 1996; Peters et al., 2005), which is the most likely explanation for the slight deviation of the maturity observed for sample E11. Moreover, sample **VB** with ββ/(ββ+αα) ratio value of 0.80 is an outlier from the range given by the authors. Such variations can reflect samples that have experienced different heating rates in the subsurface (Mackenzie et al., 1990) and high ratios as observed here can also result due to overall low biomarker content and ill-defined peaks i.e. a slight chromatographic problem. The ββ/ (ββ+αα) ratio is in general very useful in maturity determinations for most oils and bitumens (Peters and Moldowan, 1993). The high ratios of this parameter can also result from in-situ maturation on cracking as the ββ isomers remain more resistant in a deep hot reservoir.

The samples from the lower sandstone of the Embla Field show the highest maturity degree in the sample set. All samples, except one, from this part of the reservoir show maturities higher than any of the other samples in the studied sample set (Figure 7.1).

All the samples representing the Upper sandstone of the Embla Field show slightly lower maturity than those of the samples from the Lower sandstones. The VB sample seems to be the most mature sample if emphasis is placed only on the ββ/ (ββ+αα) maturity parameter, which has greater dynamic range than the 20S/(20S+20R). The typical North Sea oil (NSO-1) has maturity lower than the sandstones from the Embla Field, but higher than those samples representing the rhyolite unit. On average the rhyolite samples show the lowest maturity and this could reflect that the oil entrapped in the rhyolites represent an early filling event.

To sum up the maturity assessment based on Figure 7.1, from most mature to least mature, the samples show the following trend: **Lower sandstone→ Upper sandstone→NSO-1→ VB→ Rhyolites.** The VB sample could be even more matured than it is shown in figure 7.1.

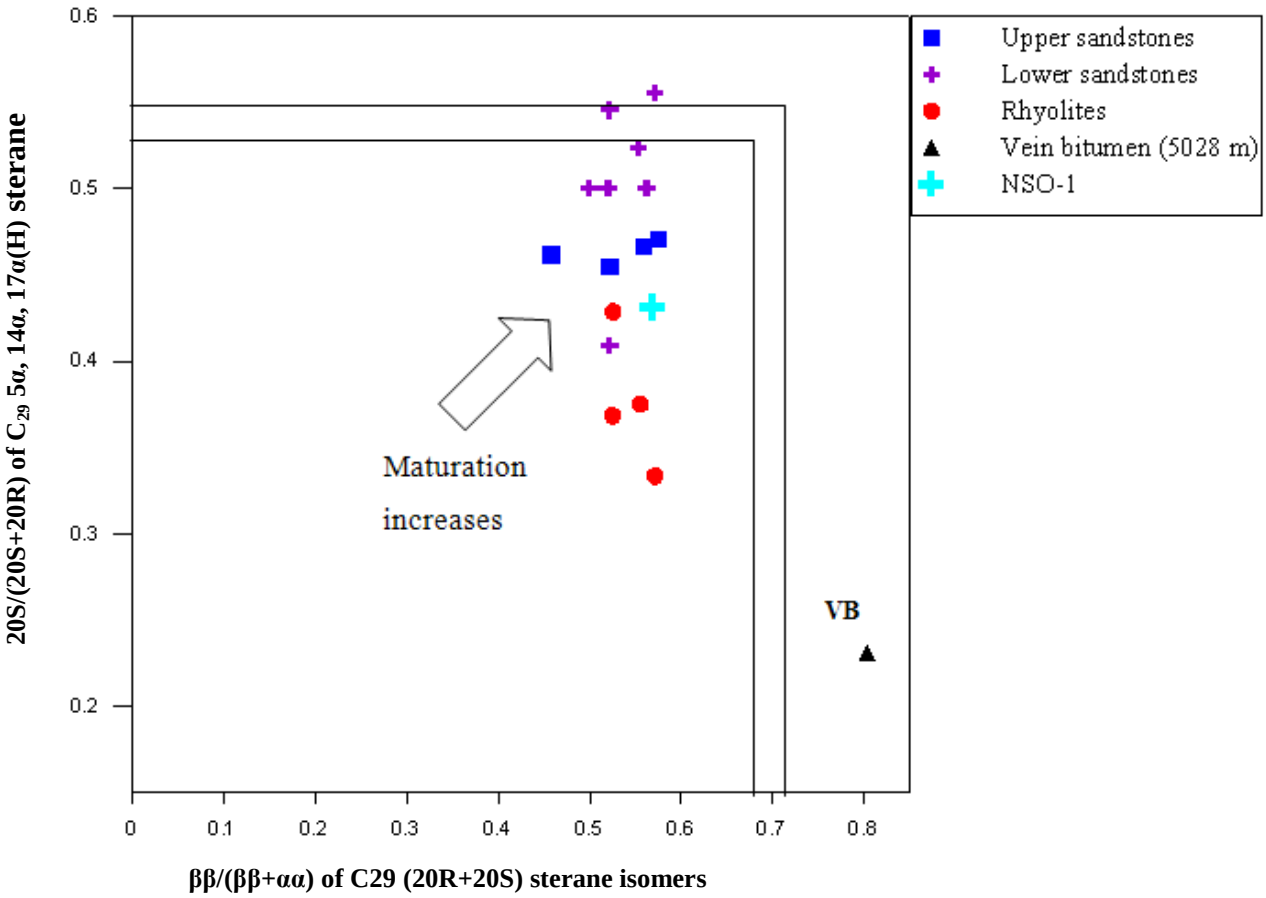

Figure 7.1. Cross plot of the maturity parameters 20S/(20S+20R) (parameter 11) and ββ/(ββ+αα) for C29 steranes (parameter 10), Modified after Seifert and Moldowan, (1986).

Figure 7.2 illustrates the maturity differences for the examined samples based on the two biomarker maturity parameters, Ts/(Ts + Tm) and the diasteranes/(diasteranes + regular steranes) ratios (see Figure 7.2 and Table 6.3). The maturity trend for the extracts indicates that the samples from the sandstones and the rhyolites lie within the peak oil window (Figure 7.2). The NSO-1 falls within the early oil window. The VB was found to be the least mature according to these parameters.

The diasteranes/(diasteranes + regular steranes) ratio may be affected by siliciclastic or carbonate facies. Oils from carbonate source rock will generally have lower ratios than oils

from clastic source rocks (Peters and Moldowan, 1993). Note the relatively low ratio for the VB sample, which might have originated from a mixed carbonate source rock facies.

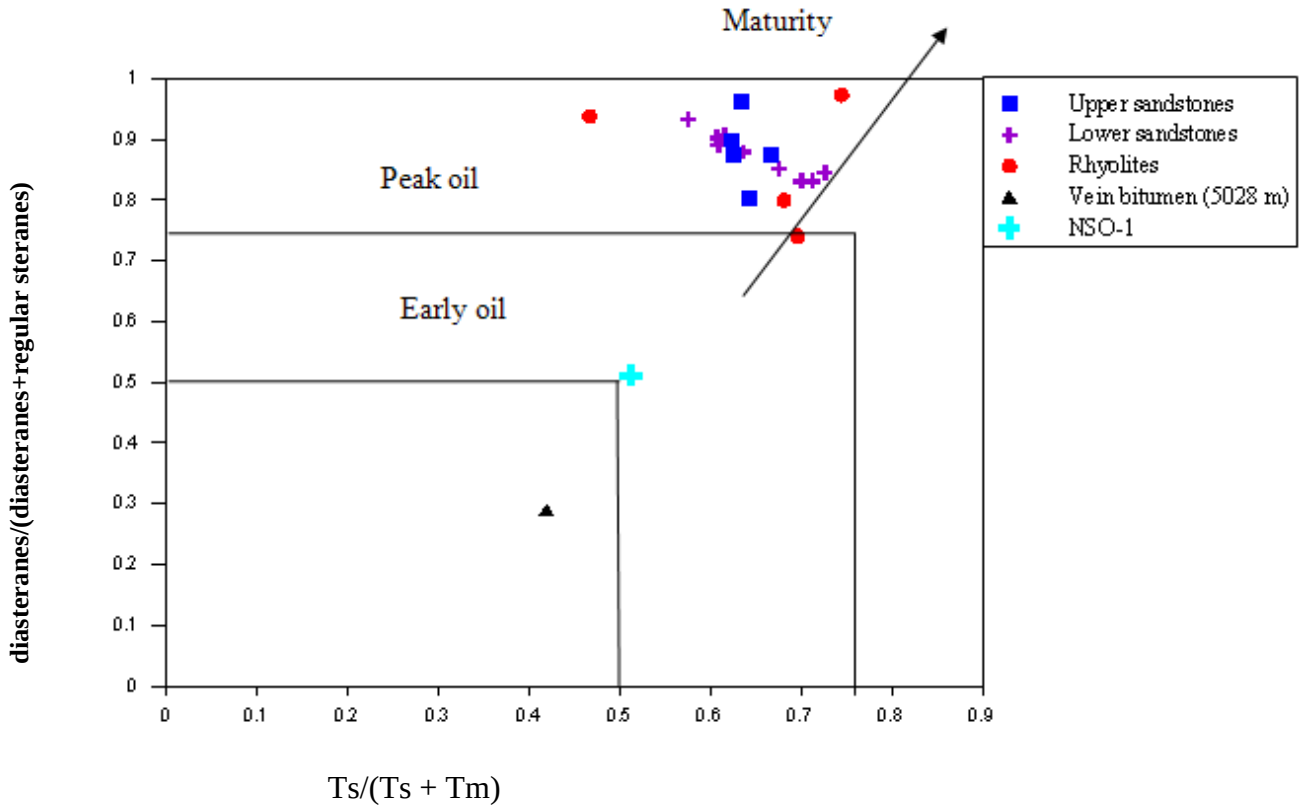

Figure 7.2 A cross plot of the parameters Ts/(Ts + Tm) and diasteranes/(diasteranes + regular steranes) indicating maturity. Both parameters can be influenced by the organic source rock facies. The values increase with maturity, and are valid for the whole oil window.

Figure 7.3 shows a plot of 22S/(22S+22R) against 20S/(20S+20R). The 20S/ (20S+20R) ratio of steranes reaches equilibrium at 0.55 (Seifert and Moldowan, 1986), corresponding to a vitrinite reflectance of 0.8%. The value for the studied samples from the Embla Field ranges between 0.23 to 0.56 for the 20S/ (20S+20R) parameter (see table 6.3 and Figure 7.3). With respect to this parameter the samples from the Lower sandstone have higher

ration followed by the samples from Upper sandstone. The NSO-1, the Rhyolites and the VB in decreasing order have values below the Upper sandstone.

The 22S/ (22S+22R) ratio of hopanes reaches equilibrium between 0.57 to 0.62 (Seifert and Moldowan, 1986) corresponding to a vitrinite reflectance of 0.6%. This value reflects that the oils are migrated and not in-situ generated. The values of the studied samples from the Embla Field show a range between 0.44 and 0.60 (except sample **E10** from the Lower sandstone which has value of 0.69) (Table 6.3 and Figure7.3). The samples from the Lower sandstone have got relatively larger values of 22S/(22S+22R) ratio followed by the NSO-1 and the Upper sandstone. The VB sample shows the lowest value.

The majority of the samples in the sample set are in the peak oil area, which indicates that most of the samples from the Embla reservoir have reached or surpassed oil generation. However, some samples especially sample VB and one sample from the rhyolite (E18) lies within the early oil generation, considering in particular the 22S/(22S+22R) parameter.

To sum up, with respect to the maturity plot shown in Figure 7.3, the following maturity trend from most mature to least mature is probable: **Lower sandstone→ Upper sandstone NSO-1 → Rhyolites → VB.** The maturity of the bitumen extracted from the vein or fracture (i.e. sample VB) has the lowest value in terms of these parameters. One possible explanation for values of less than 0.5 in terms of the 22S/(22S+22R) parameter is the following: It is the case that the 22S and 22R peaks will become rather small and disappear in to the baseline in incase of in-reservoir cracking. This is because the homo-hopanes and large molecules with an abundance of tertiary carbon atoms. As a result, at increasing reservoir temperature (today 165°C) both isomers will experience thermal stress and crack. At some stage in this process, the peak identification suffers due to co-elution with other components and deviating (both high and low) ratios may occur (karlsen et al., 1995).

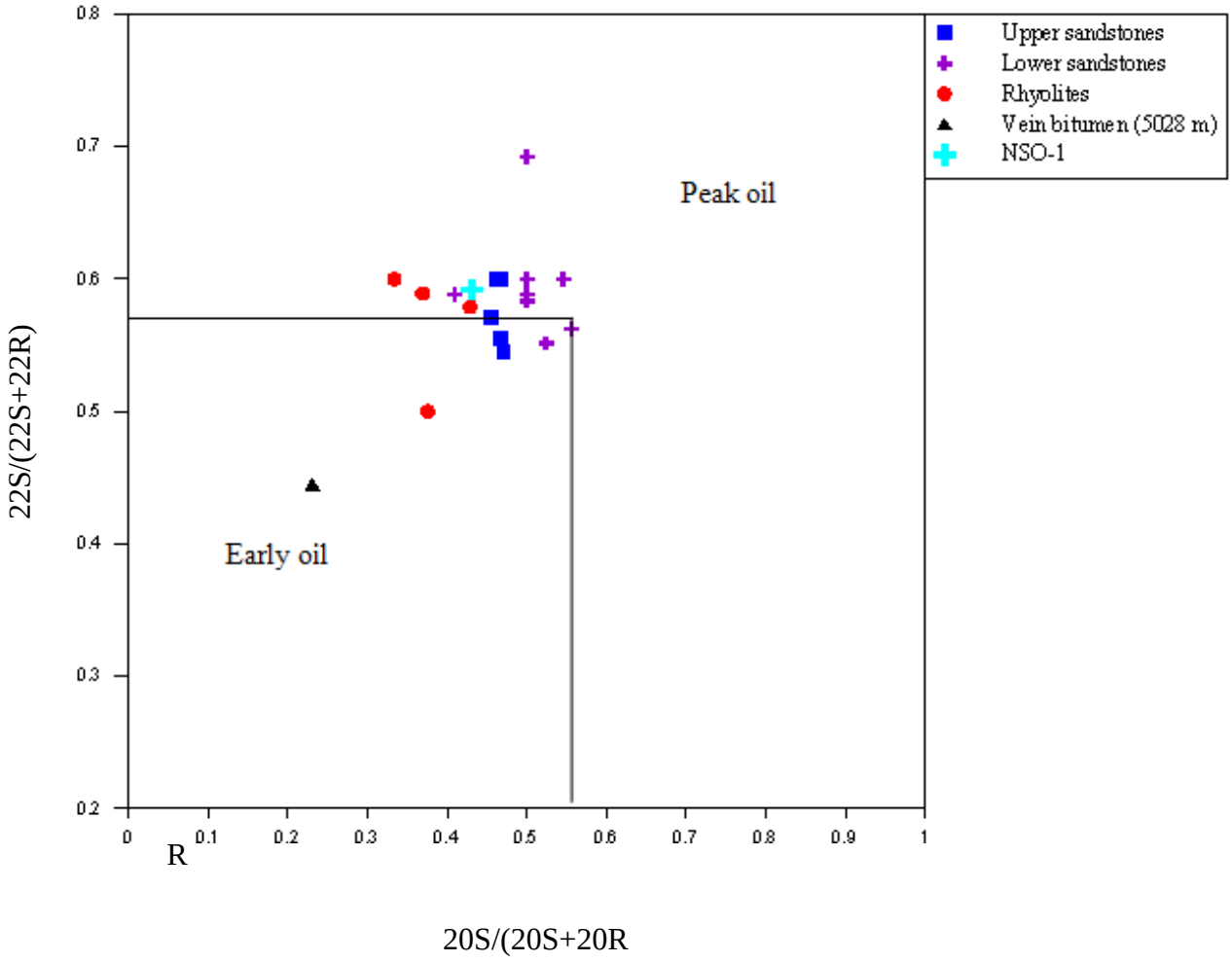

Figure 7.3. Cross plot of 20S/(20S+20R) parameter and the 22S/(22S+22R) parameter, illustrating the vertical distribution of maturity in the well 26S of the Embla Field. This shows that most of the samples from the sample set have reached peak oil generation, with only a few samples occurring in the early, to peak state of oil generation.

Figure 7.4 shows a cross plot of two maturity parameters i.e. the 22S/ (22S+22R) of the C_{31} hopane (parameter 3) and the MPDF (F1) (parameter 20). The MPDF (F1) stands for methylphenanthrene distribution fraction 1. It is an aromatic maturity parameter which is calculated from methylphenanthrene isomers. As mentioned earlier in this chapter, the 22S/

(22S+22R) rises from 0 to about (0.57 to 0.62=equilibrium) and this indicates that the main phase of oil generation has been reached or surpassed in case of the Embla Field. All samples apart from one sample from the lower sandstone (i.e. sample E10) were generated from inside the oil window in terms of maturity, indicated by the 22S/ (22S+22R) of the C_{31} hopane and only differ slightly (Fig 7.3 and Fig 7.4). Sample E10 evolved beyond this equilibrium. However, the methyl phenanthrene distribution fraction 1, MPDF (F1) (Kvalheim et al., 1987), which is calculated from the 4 isomers of methylphenantherene (3, 2, 9 and 1-MP) display a larger range (0.29 to 0.63). The MPDF values in figure 7.4 illustrate the vertical distribution of maturity. This shows that the sample set covers the oil window from early, to peak and the late state of oil generation. The samples from the rhyolite (E18, E17 and E16) and the VB sample contain the four lowest MPDF values (see Figure 7.4 and Table 6.3).

On average the samples can be placed in the following maturity trend from the most to the least mature: **Lower sandstone→ VB →Upper sandstone → NSO-1 → Rhyolites**.

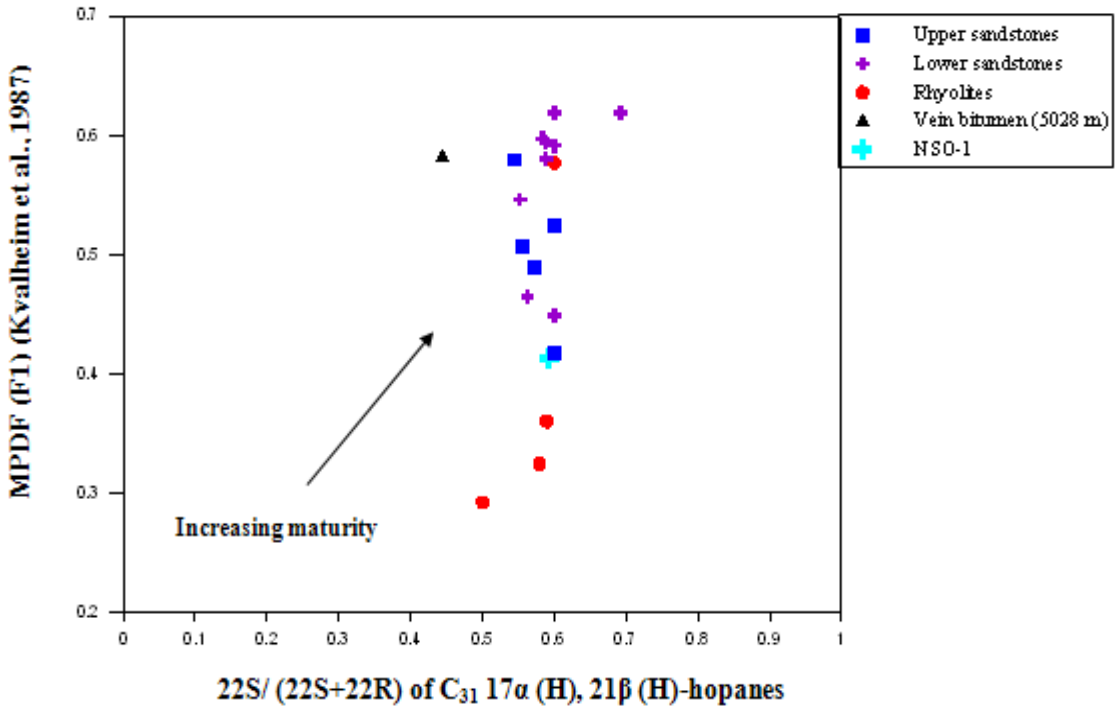

Figure 7.4. Cross plot of MPDF (F1) (parameter 20) versus 22S/ (22S+22R) of C31 17α (H), 21β (H)-hopanes (parameter 3).

Figure 7.5 is a cross plot of diasteranes/(diasteranes + regular steranes) against the maturity parameter Ro=2.242*F1-0.166. It indicates that the samples from the Lower sandstone unit of the Embla Field are the most mature, followed by samples from the Upper sandstone and samples from the rhyolites. The VB sample displays the lowest diasteranes/ (diasteranes + regular steranes) ratio (see Table 6.3 and Fig. 7.5). The low diasteranes/ (diasteranes + regular steranes) ratio for the VB sample may indicate a different source compared to the other samples. Carbonates generally contain less diasteranes than silisiclastic source rocks (Waples and Machihara, 1991).

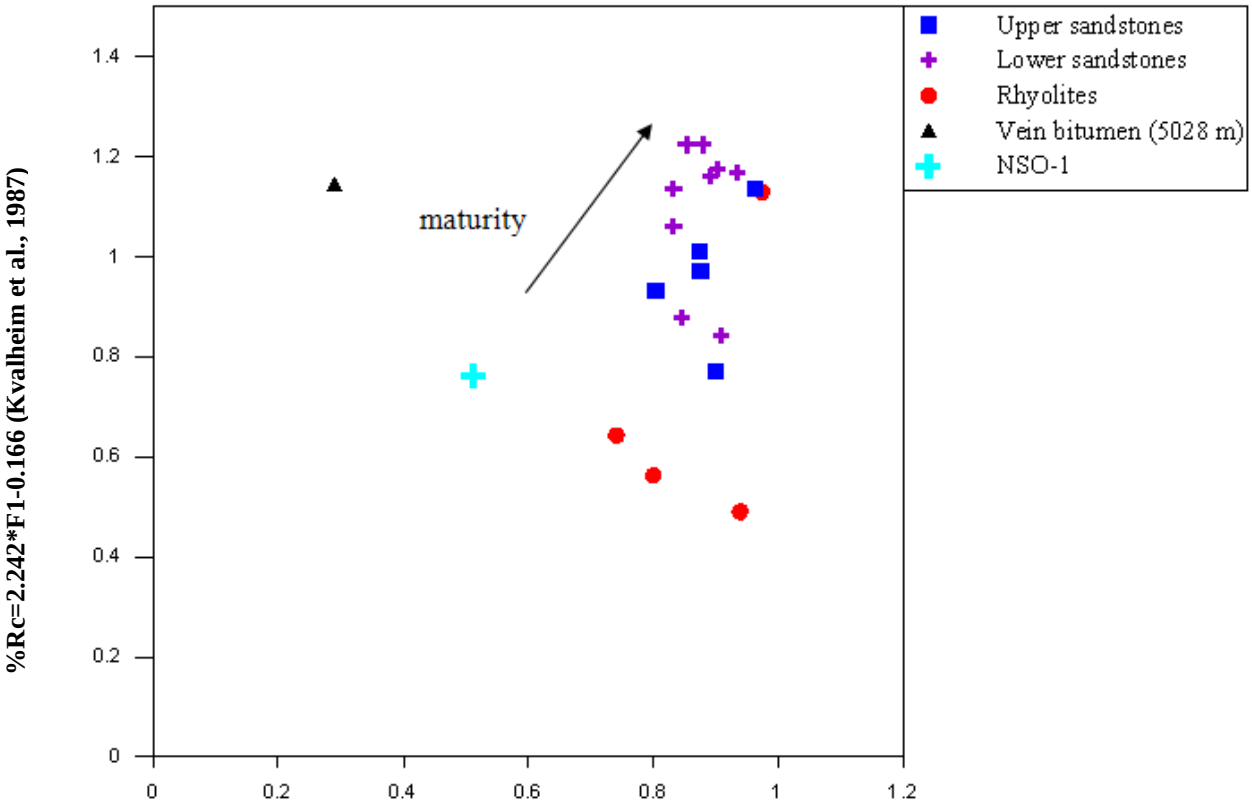

Figure 7.5. The maturity parameter diasteranes/(diasteranes + regular steranes), parameter 12, plotted against the maturity parameter Rc=2.242*F1-0.166 (parameter 24). The maturity trend observed is mainly due to the calculated vitrinite reflectance. The samples show quite uniform diasteranes/(diasteranes + regular steranes) ratios. Hence we only see evidences of weak maturity preferences in the samples from the different parts of the reservoir, concerning the steranes, but a pronounced trend for the aromatic medium range methylphenanthrenes.

7.7 Aromatic maturity parameters for the Embla Samples

Among the saturated hydrocarbons, concentration ratios based on steranes and triterpanes of the hopane type have attracted much attention as maturity indicators although the dynamic range of the **Diasteranes/(diasteranes+regular steranes)** maturation levels (Mackenzie and Maxwell, 1981). Furthermore, a drastic decrease in concentration of such biomarker molecules occurs with thermal maturity rock samples (Rullkotter et al., 1984) and the organic facies may also affect the applicability of those parameters in organic maturation studies (ten Haven et al., 1986).

The distribution of aromatic compounds in crude oils and the organic extracts of sedimentary rocks are commonly applied to problems of thermal maturation (Tissot, 1984 and Tissot and Welte, 1984). These compounds occur in oils and reservoir bitumens in concentrations which are 10-100 times higher than that of the biomarkers.

Ample evidence has been presented that in the oil-generation window concentration ratios of dibenzothiophenes (Ho et al., 1974, Hughes, 1984), phenanthrenes (Radke et al., 1982a, Radke and Welte, 1983) do change in a regular fashion with increasing maturity (Radke et al, 1986; Radke, 1987).

The samples from the lower sandstone of the Embla Field show the highest values of MPR, MPDF 1 (F1), MPI 1 and MDR (see Tables 6.3&7.2 and Figure 7.6). These values were to some extent confirmed by the biomarker parameters to be the most mature samples. The VB sample is found to have the second highest values for these parameters followed by the Upper sandstone and the NSO-1, while the samples from the rhyolites resulted in the lowest values. Thus from the highest to the lowest maturity:

Lower sandstone→VB→Upper sandstone→NSO-1 → Rhyolites.

SAMPLE	MPR	Rc MPR	MpI1	Rc MPI1	MPDF (F1)	Rc MPDF (F1)	MDR	Rc MDR
Rhyolites	0,90	0.83	0.63	0.78	0.39	0.71	3.66	0.78
NSO-1	0,91	0.90	0.61	0.77	0.41	0/76	2.38	0.68
Upper sandstone	1.14	1.0	0.51	0.70	0.50	0.96	2.61	0.70
VB	1.62	1.18	1.44	1.26	0.58	1.14	7.60	1.06
Lower sandstone	1.67	1.19	1.34	1.20	0.58	1.14	14.58	1.57

Increasing maturity ↓

Table 7.2. Average values of the aromatic compound parameters as calculated from the GC-MS. And the corresponding vitrinite reflectance calculated from the aromatic compound parameters. Both are useful biomarker parameters for highly matured samples, as the concentration of the aromatic compounds i.e. phenanthrene, methyl-phenanthrenes and methyl-dibenzothiophenes occur in much higher concentrations in mature bitumens and oils. The table shows increased aromatic parameter values and hence increases in calculated vitrinite reflectance with increasing maturity. The maturity from high to low maturity is: **Lower sandstone→VB→Upper sandstone→NSO-1 → Rhyolites**.

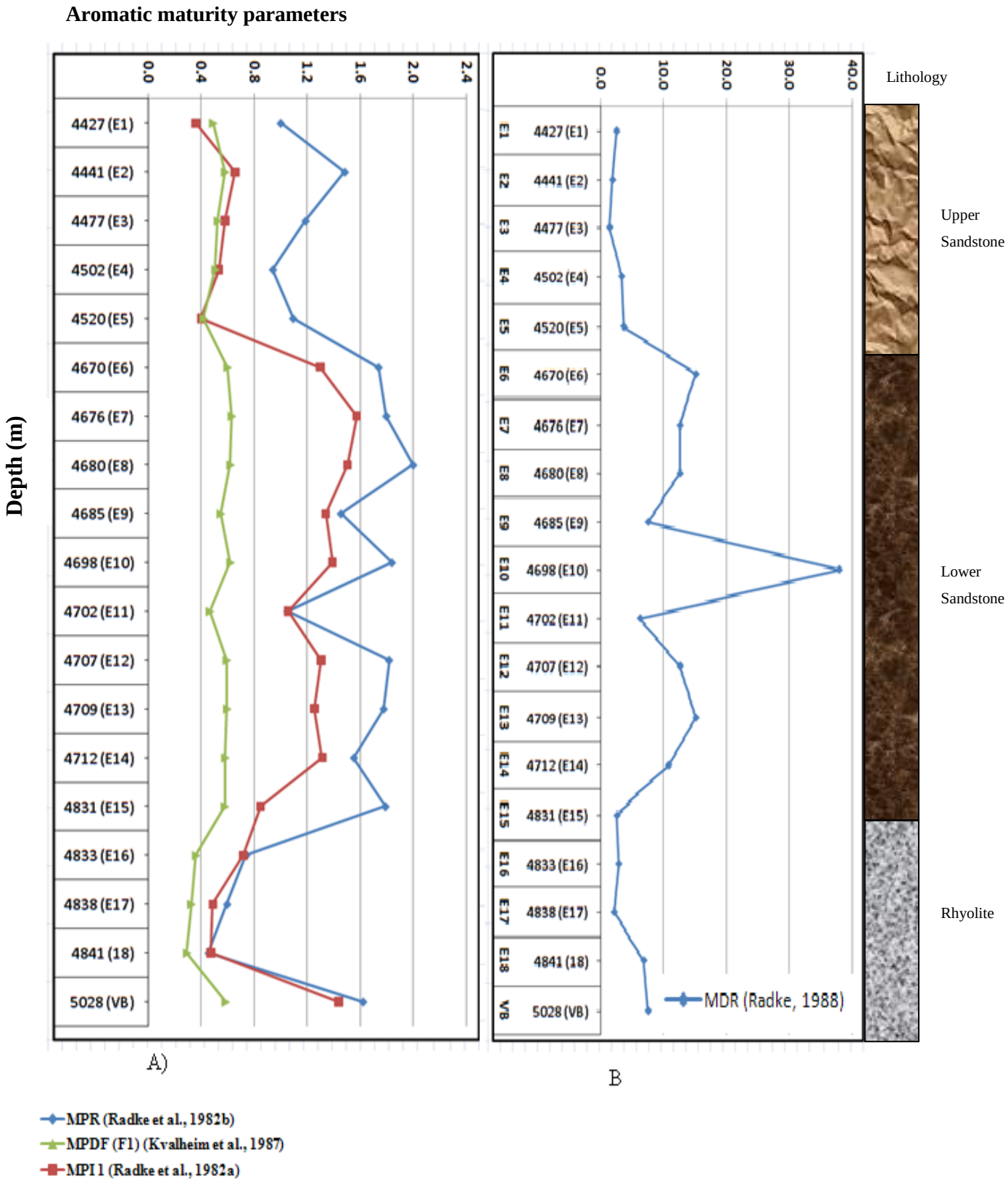

Figure 7.6: Variation in four maturity parameter with depth for the studied samples of the Embla Field. The samples from the lower sandstone were found to have the highest maturity, followed by the VB sample and the Upper sandstone. The samples from the rhyolites are the least mature, while the NSO-1 has a slightly higher maturity than the samples from the rhyolites. A pronounced increase in the MDR is observed for the **E10** sample, which is one of the samples representing the Lower sandstone. Remember E10 sample was also an outlier in the biomarker maturity parameters based on steranes and terpanes (see Fig.7.3)

Vitrinite reflectances (Table 6.3) have been calculated based on measurements of the methyl phenanthrenes and the methyl dibenzothiophenes. These are used as maturity parameters. Figure 7.7 is a cross plot of calculated vitrinite reflectance (Rc) values based on the isomers of methyldibenzothiophene (MDBT) (Rc=0.073xMDR+0.51; MDR [methyldibenzothiophene ratio] = 4-MDBT/1-MDBT; Radke, 1988] and the vitrinite reflectance calculated from the relative abundance of phenanthrene (P) and isomers of methylphenanthrenes (MP) [Rc = 0.60 x MPI + 0.40, where MPI1 [methylphenanthrenes index 1] = 1.5 x [3MP + 2MP]/[P + 9MP + 1MP], Radke, 1988). The average Rc values calculated from these parameters for the Upper, Lower sandstones, VB, rhyolites and the NSO-1 are given in table 7.2.

The maturities agree with most of the maturity assessments suggested based on the biomarkers. One sample (E10) from the Lower sandstone with a value of MDR equal to 38, the highest in the sample set, resulted in extremely high (3,28%Rc based on MDR) calculated vitrinite reflectance and plotted far off from the trend. This value (3.8%Rc) is outside the oil window. The sample (E10) also showed atypical values of the saturated hydrocarbon maturity biomarkers as well (for example see Figure 7.3). Karlsen et al., 1993 has found a vitrinite reflectance of 2.5% for C_1-C_{25} condensate extracted from hydrothermal quartz from Modum, south of Ringerike in the Oslo graben. Based on the observations, the sample set follows the following maturity trend from the most mature to the least mature: **Lower sandstone → VB → Upper sandstones→NSO-1→Rhyolites.**

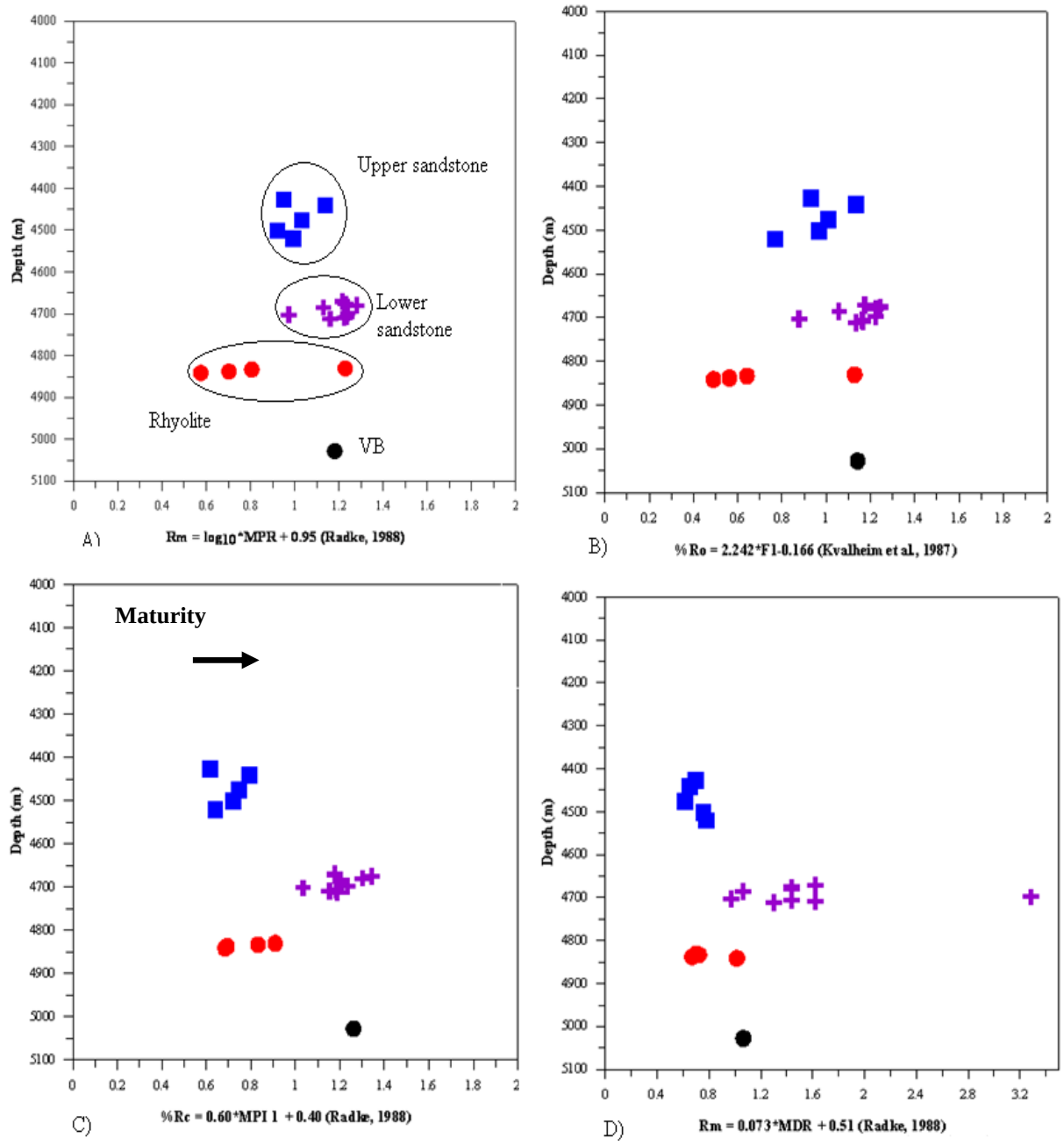

Figure 7.7: Cross plots of vitrinite reflectances calculated based on measurements of phenanthrene, methyl phenanthrenes and methyldibenzothiophene. These parameters are used as maturity indicators. The vitrinite reflectance (Rc) values are calculated from A) **$Rm=log_{10}MPR+0.95$ (**Radke, 1988), B**) %Ro=2.242*F1.0.166** (Kvelheim et al., 1987), C**) %Rc=0.60*MPI 1+0.40** (Radke, 1988) and D) **Rm=0.073*MDR+0.51** (Radke, 1988).

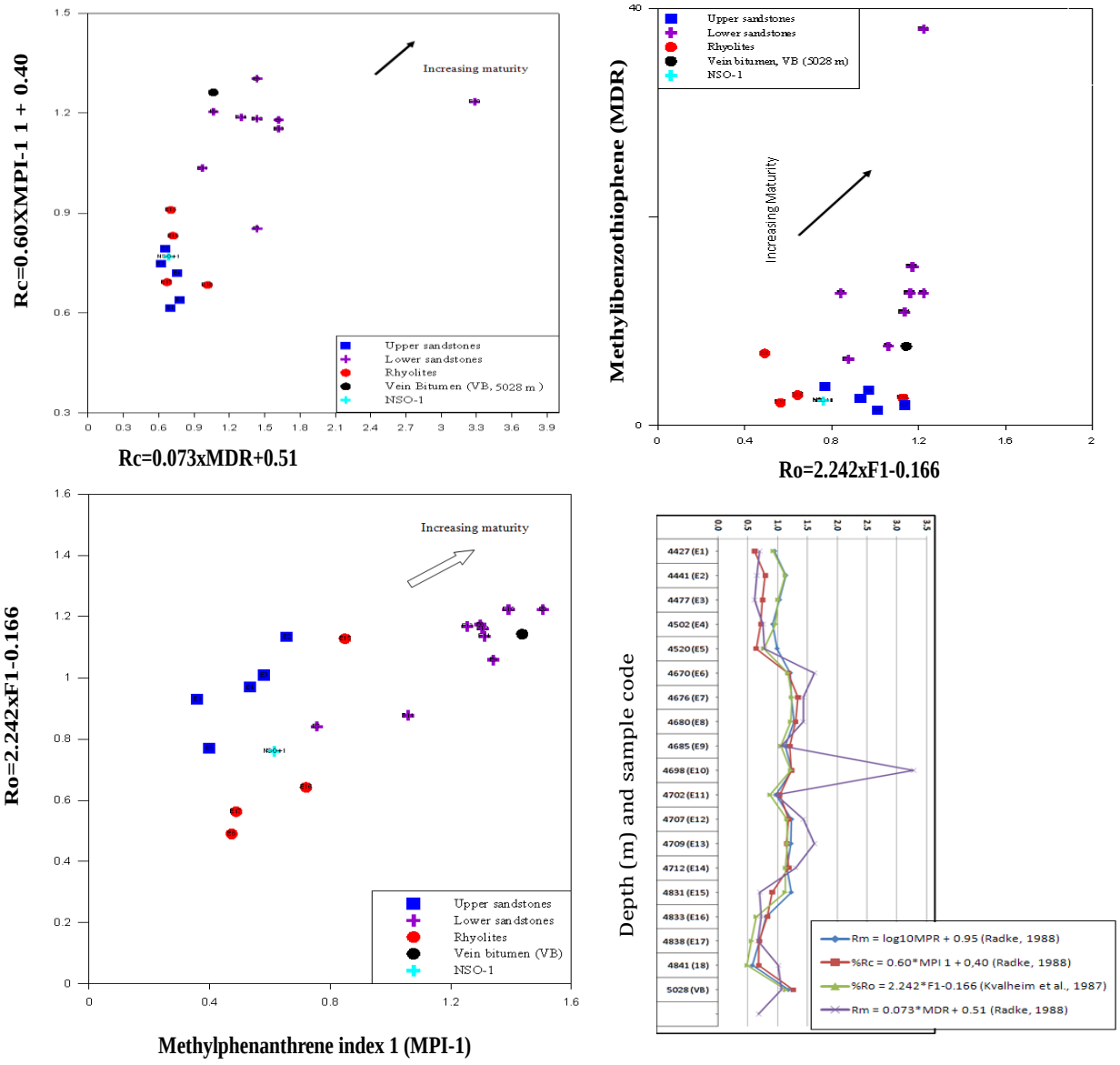

Figure 7.8: Cross plots of various vitrinite reflectance aromatic maturity parameters, all indicating that the samples from the lower sandstone are the most mature while samples from the rhyolite have the lowest maturity.

7.8. Summary of Maturities

Most of the studied Embla core samples have reached peak oil generation based on the biomarker maturities and the aromaticity. The Ts/(Ts + Tm) and diasteranes/(diasteranes +

regular sterane) values for the studied samples have reached equilibrium, which indicates that most of the samples have reached or surpassed oil generation. Some of the common biomarkers are more difficult to apply for the maturity assessment as their utilization is limited to medium maturity. However, there is a trend which clearly shows the maturity variation in the different Embla samples. The aromatic hydrocarbons based calculated vitrinite reflectances have proved to be very useful. For example Table 7.3 and Figure 7.9 clearly indicate the high maturity of the samples from the Lower sandstone. Accordingly, the following maturity trend (from most mature to less mature) can be concluded for the Embla samples: **Lower sandstone→VB →Upper sandstone→NSO-1 → Rhyolites.** The samples from the lower sandstones have calculated vitrinite reflectance values ranging from 0.88 to 1.62% (except sample E10 which has Rc value of 3.28%). This indicates that the samples have reached peak and even the condensate hydrocarbon generation stage. The **VB** sample (which was seen to have lower maturity according to the steranes and terpanes maturity parameters), however, is found to be one of the most mature samples based on the aromatic hydrocarbon data, which is more reliable for higher maturity assessment like the Embla samples.

Bharati, 1997 have also noted the limited use of serane and terapne parameters for the higly matured Embla samples and attributed this mainly due to low concentration of biomarkers identified by the GC-MS or theses samples have reached their maximum value, as hopanes and steranes are thermally degraded. Reduced biomarker concentrations commonly indicate increased maturity (Mackenzie et al., 1985a).

The maturities (Table 7.3) of the Embla samples are indicated to be towards the end of the oil window. These differences are believed to reflect different degree of burial of the source rocks, or to represent different stages of oil generation and /or diverse geothermal gradients. This is again linked to subsidence and overburden histories of the different source rock systems. Hence, the Embla petroleum have migrated from a hot, deeply buried source rock.

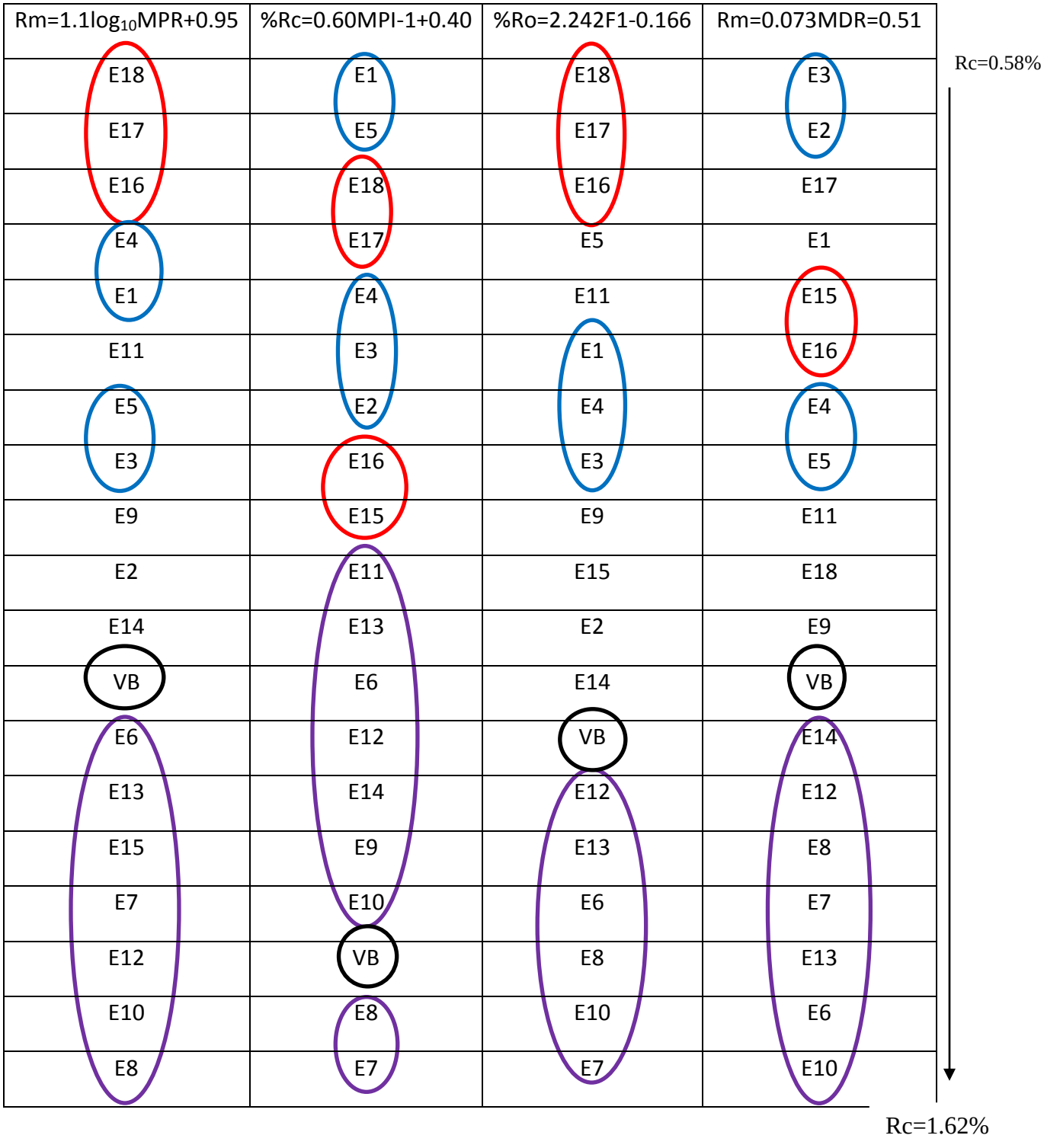

Figure 7.9 Summary and comparison of the maturity level in the Embla Field well 26S. The samples follow the trend: **Lower sandstone→VB →Upper sandstone→NSO-1 → Rhyolites,** the lower sandstone samples being the most mature while sample from the rhyolite are found to be less mature in the sample set. Note that the MDR based calculated R_c for E10 is 3.28%, extremely high compared to the other samples.

Sample	%Rc-MPI1	%Rc-MDR	Range in the oil	Lithology
E1	0.62	0.70	Peak oil	Upper
E2	0.79	0.65	Peak oil	,,
E3	0.75	0.62	Peak oil	,,
E4	0.72	0.76	Peak oil	,,
E5	0.64	0.78	Peak oil	,,
average	**0.70**	**0.70**	Peak oil	,,
E6	1.18	1.62	Condensate/wet gas	Lower
E7	1.34	1.43	Condensate/wet gas	,,
E8	1.30	1.43	Condensate	,,
E9	1.20	1.06	Late	,,
E10	1.23	3.28	Outside the range	,,
E11	1.03	0.97	Late/condensate	,,
E12	1.18	1.43	condensate	,,
E13	1.15	1.62	Condensate	,,
E14	1.19	1.30	Late	,,
Average	**1.20**	**1.57**	Condensate	,,
E15	0.91	0.70	Peak	Rhyolites
E16	0.83	0.72	Peak	,,
E17	0.69	0.67	Peak	,,
E8	0.68	1.01	Late	,,
average	**0.78**	**0.78**	Peak oil	,,
VB	1.26	1.06	Late	Vein Bitumen
NSO-1	0.77	0.68	Peak	NSO-1

Table 7.3 Summary of the maturities of the bitumen (maturity level). The samples from the Lower sandstone fall within the late oil to condensate level. The maturity level for the VB sample falls inside the late oil generative oil window. The Upper sandstone and rhyolite samples lie within the peak oil generative part of the oil window. See also Fig 5.12.

7.9. Organic facies

This section presents how biomarker and non-biomarker data are used to interpret the organic facies of the studied samples. The data of various analytical techniques (TLC-FID, GC-FID, and GC-MS) as applied on the studied samples will, in this section, be discussed in order to determine the organic facies and sedimentary environments of the bitumen in the samples.

Nonbiomarker and biomarker parameters are used together to provide the most reliable interpretation of source organic matter input, depositional environment, and the relationship between samples (Peters and Moldowan, 1993). Hunt, 1996 defined organic facies as mappable subdivisions of stratigraphic units distinguished from the adjacent subdivisions by the character of their organic matter. Different organic facies generate different amounts and types of hydrocarbons. Molecular parameters from analysis of the organic matter, kerogens, oil and gas, are useful in identifying the organic facies, because the living organisms that synthesized the precursors of the organic matter, were affected by the environment in which they lived (Waples and Machihara, 1991). The biomarkers and other organic compounds are modified in different ways after deposition, depending on the sedimentary setting and thermal influence.

Pristane/Phytane (Pr/Ph) ratios of oils or bitumens have been used to indicate the redox potential of the source sediments (Didyk et al., 1978) (see Figure 5.3). According to these authors, Pr/Ph ratios less than unity indicate anoxic deposition, particularly when accompanied by high sulfur contents. Oxic conditions are indicated by Pr/Ph > 1 (Peters and Moldowan, 1993). For samples within the oil generative window, high Pr/Ph ratios (>3) indicate terrestrial organic matter input under oxic conditions and low values (<0.6) typify anoxic condition (Peters and Moldowan, 1993). The same authors have noted that for samples with Pr/Ph ratio between the range of 0.8 and 2.5, the use of this parameter as paleoenvironment indicator is not recommended, unless other data are corroborating. Ten Haven et al, (1987) indicate that it is impossible to draw valid conclusions on the oxicity of the environment of deposition from Pr/Ph alone. Thermal maturity, among other variables, can change the Pr/Ph ratio (Peters and Moldowan, 1993). Typically the Pr/Ph ratio increase

with maturity (Connan, 1984). Ten Haven et al., (1987) indicate an increase in Pr/Ph and a decrease in Ph/n-C18 with thermal maturation. The Pr/Ph ratios typical for type II marine shales are 0.6-1.6 (Elvsborg et al., 1985).

The samples studied in this work have Pr/Ph ratio in the range between 0.96 to 1.94 (see Table 6.2). Sample E11 from the Lower sandstone unit has the lowest value, while VB sample has the highest ratio. The samples from the Upper and Lower sandstones have very similar Pr/Ph ratios (between 1.03-1.13) except for sample E11. During the GC-FID analysis for the rhyolite samples only one sample was able to provide detectable data on Pristane/Phytane ratio i.e. 1.58. More specifically, according to the Pr/Ph range explained by Elvsborg et al. (1985), all the samples from the Embla Field except the **VB** belong to type II marine shales. The higher Pr/Ph ratio for sample VB may indicate a more terrestrial input. Figure 7.10 is a plot of Pr/Ph and hopane/sterane, which indicates that the samples are derived from a marine source rock.

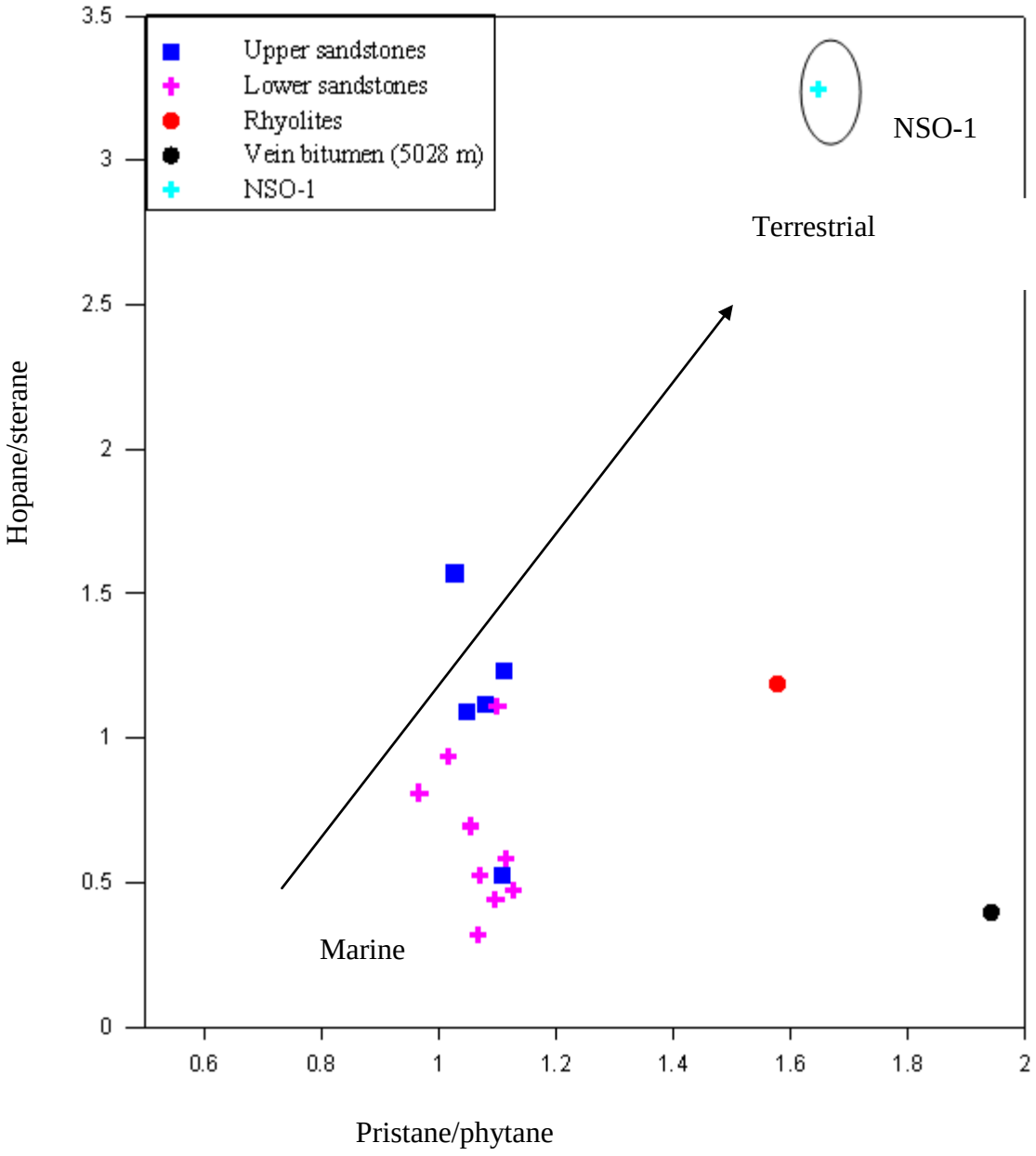

Figure 7.10. A cross plot of the facies parameters pristane/phytane versus hopane/sterane (parameter 9). A higher value indicates strong terrestrial input, while lower values indicate normal marine facies. The figure reveals that the samples from the Embla Field are of general marine type. The typical North Sea oil, NSO-1 is more terrestrial than the Embla samples; hence this may indicate the presence of a more marine alternative type oil source than the common Kimmeridge shale. The hopane/sterane ratio plays significant role in discriminating depositional environment of the samples.

The **Pr/n-C17 and Ph/n-C18** ratios can be used to interpret depositional environment of source rocks (Peters and Moldowan, 1993). Figure 7.11, shows plot of **Pr/n-C**17 **and Ph/n-C_{18}** for the studied samples. All of the samples from the Embla Field have originated from mixed organic sources, but very close to the marine setting. This is normal for transitional environments. Nevertheless, these ratios are influenced by both maturity (Peters and Moldowan, 1993) and evaporation loss, thus it is better to evaluate whether maturity or source facies has had the greatest influence on the samples. From Figure 7.11 it can be conclude that the hydrocarbons in the Embla reservoir are derived from source rocks with approximately the same facies. Still it seems that the source rock contains mixed organic matter deposited in a marine proximal setting. The maturity information of these samples as shown in figure 7.11 cannot be used for the case of Embla oils as the samples are also biodegraded.

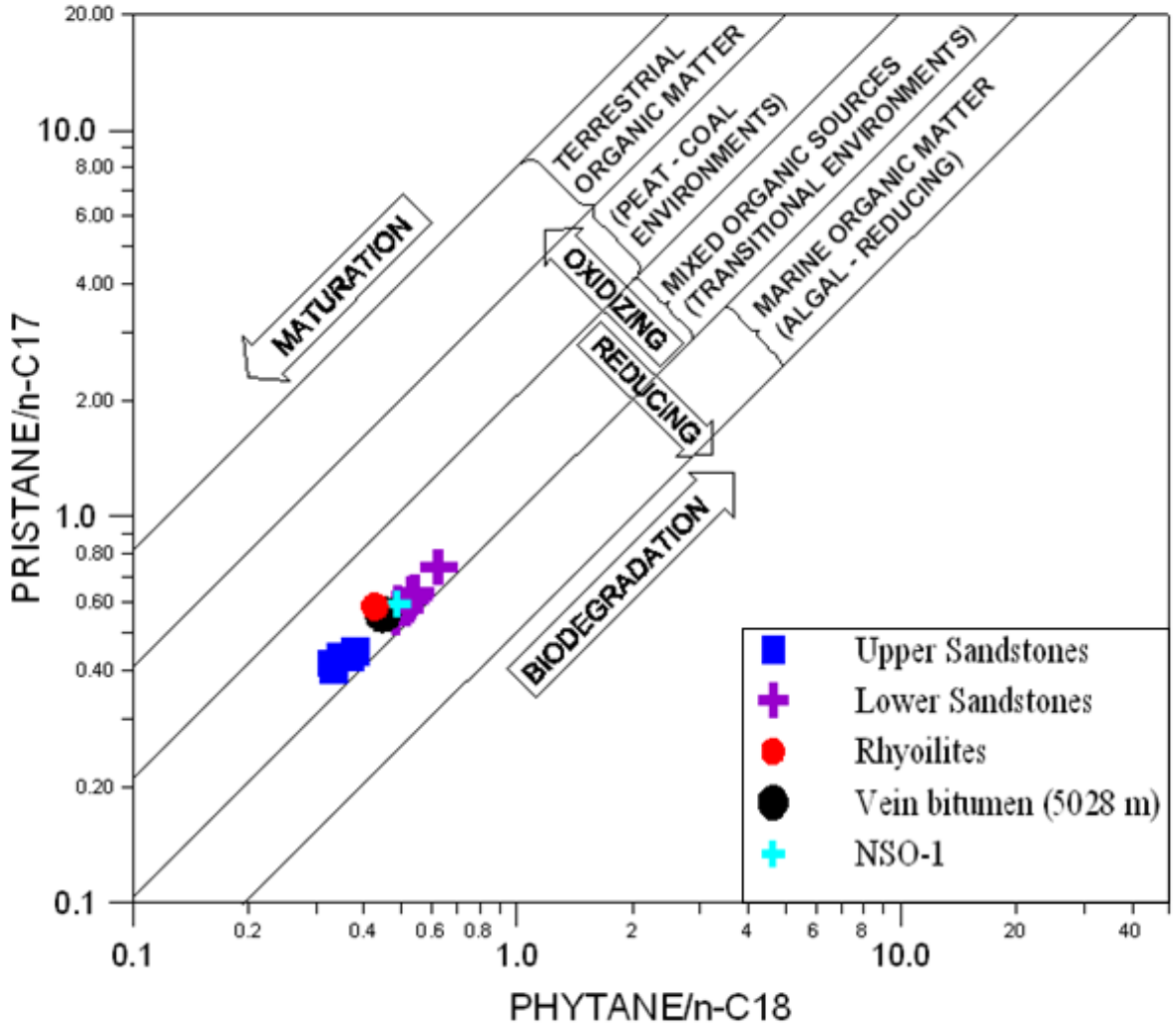

Figure 7.11. Cross plot of Pristane/n-C_{17} versus Phytane/n-C_{18}. Only one sample is plotted from the rhyolites due to lack of adequate GC-FID data. (From Shanmugam, 1984).

C27-C28-C29 Steranes

The relationship between C27, C28 and C29 ββ-steranes have been used to distinguish source rock facies of petroleum. Figure 7.12 is a ternary diagram showing the depositional environment (facies) of the samples studied. The diagram is divided into sub-areas where the individual areas are assigned to specific depositional environments (Shanmugam, 1984). It is indicated that all the Embla samples originated from marine planktonic source rock facies though, one sample from the Upper sandstone and another sample from the rhyolites belong

to an open marine facies source rock. Sample VB indicates that it was derived from a source rock that was tending to be estuarine. The NSO-1 sample lies in the open marine region.

The validity of the ternary diagram from Shanmugam (1984) is debated, and interpretation of source rock and its facies based entirely on sterane distributions alone is not recommended (Moldowan et al., 1985). Still, it is widely used and it continues to provide valid interpretations.

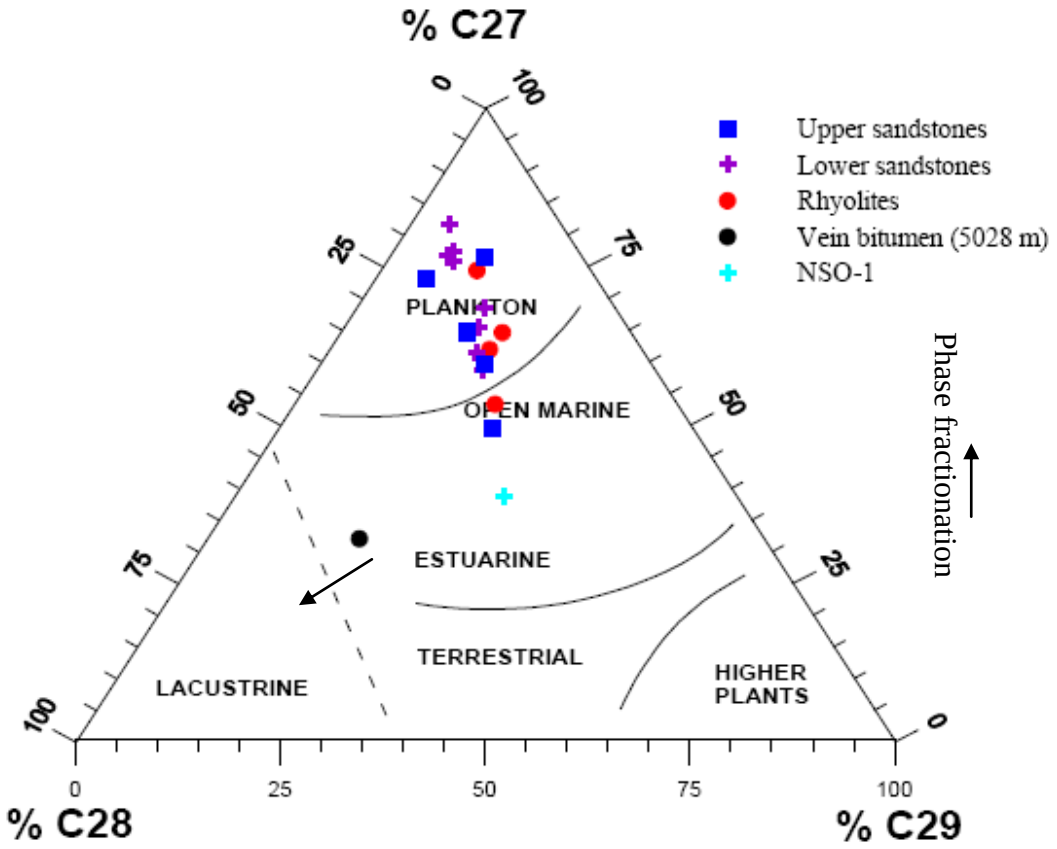

Figure 7.12. Ternary diagram, showing the relationship between the C_{27}, C_{28} and C_{29} ββ-steranes from the samples, illustrating the depositional environments for the sample set in the studied area, after Shanmugam (1984)

Sterane/ hopane ratio

Sterane/hopane ratio allows qualitative assessment of eukaryote versus prokaryote input to the organic matter because organisms vary widely in their steroid and hopanoid contents (Peters et al., 2005). In general, high ratios of sterane/hopane (≥ 1) typify marine organic matter with major contributions from planktonic and/or benthic algae (Moldowan et al., 1993).

The sterane/hopane ratio (Table 7.4) for the different parts of the reservoir (based on well 26S) in the Embla Field supports the above ternary plot in the sense that most of the samples from the Upper, the Lower sandstone and from the rhyolites originated from pure planktonic marine source organic matter than the typical Norwegian oil (NSO-1). Sample, VB from the vein filling plots more towards the lacustrine border. This could reflect that another source rock has involved as source for this bitumen. With a close examination on the sterane/hopane ratio there is a difference between the Upper and Lower sandstone samples. Considering the majority of the samples, the Upper sandstone with sterane/hopane ratios (0.64-1.91) and the Lower sandstone with sterane/hopane ratios (0.91-3.11) seem to have different sources and this could suggest that these two reservoir sections have at some time contained oil of different origin. Furthermore, possibly could the Kimmeridge oil charge have filled these two sub reservoir in different fashion.

Sample	Sterane/hopane	
E1	0,64	Upper sandstone
E2	0,91	„
E3	0,89	„
E4	0,81	„
E5	1,91	„
E6	2,26	Lower sandstone
E7	3,11	„
E8	1,71	„
E9	1,06	„
E10	1,44	„
E11	1,23	„
E12	2,10	„
E13	1,91	„
E14	0,90	„
E15	1,02	Rhyolites
E16	0,84	„
E17	1,32	„
E18	0,99	„
VB	2,51	Vein bitumen
NSO-1	0,31	Typical North Sea oil

Table 7.4: Sterane/hopane ratio as facies parameter (high sterane/ hopane ratio (≥ 1) indicate marine planktonic or algal input, while values (≤ 1)could represent reworked or terrigenous organic matter). The samples from the Upper sandstone could be originated from a different source rock than the Lower sandstone.

Figure 7.13 shows across plot of 3-MP/ 4-MDTP ratios versus Pr/Ph ratio. It is worth noting that all the samples from the lower sandstone have lower 3-MP/ 4-MDTP ratios which indicates the presence of a relatively high sulfur content (the thiophene 5-ring structure contains sulfur) associated with these samples, than most of the other samples. Still the

NSO-1 and one sample from the Upper sandstone contain high sulfur content as well. Since we have only one sample from the rhyolites which indicates results from the GC-FID and hence Pr/Ph ratio, we cannot tell about the sulfur content in the samples from the rhyolites. The samples from the Upper sandstones show relatively lower sulfur content (higher3-MP/ 4-MDTP) than the Lower sandstone counterparts. The extract from the vein bitumen also shows relatively lower sulfur content compared to the Lower sandstones. The typical North Sea oil, NSO-1 contains relatively lower sulfur content than the Lower sandstone sample of the Embla Field. It should be noted that biodegradation may result in sulfur enrichment, as benzothiophene derivates and high molecular weight hetero compounds are particularly resistant to bacterial degradation and hence they are selectively concentrated (Tissot and Welte, 1978).

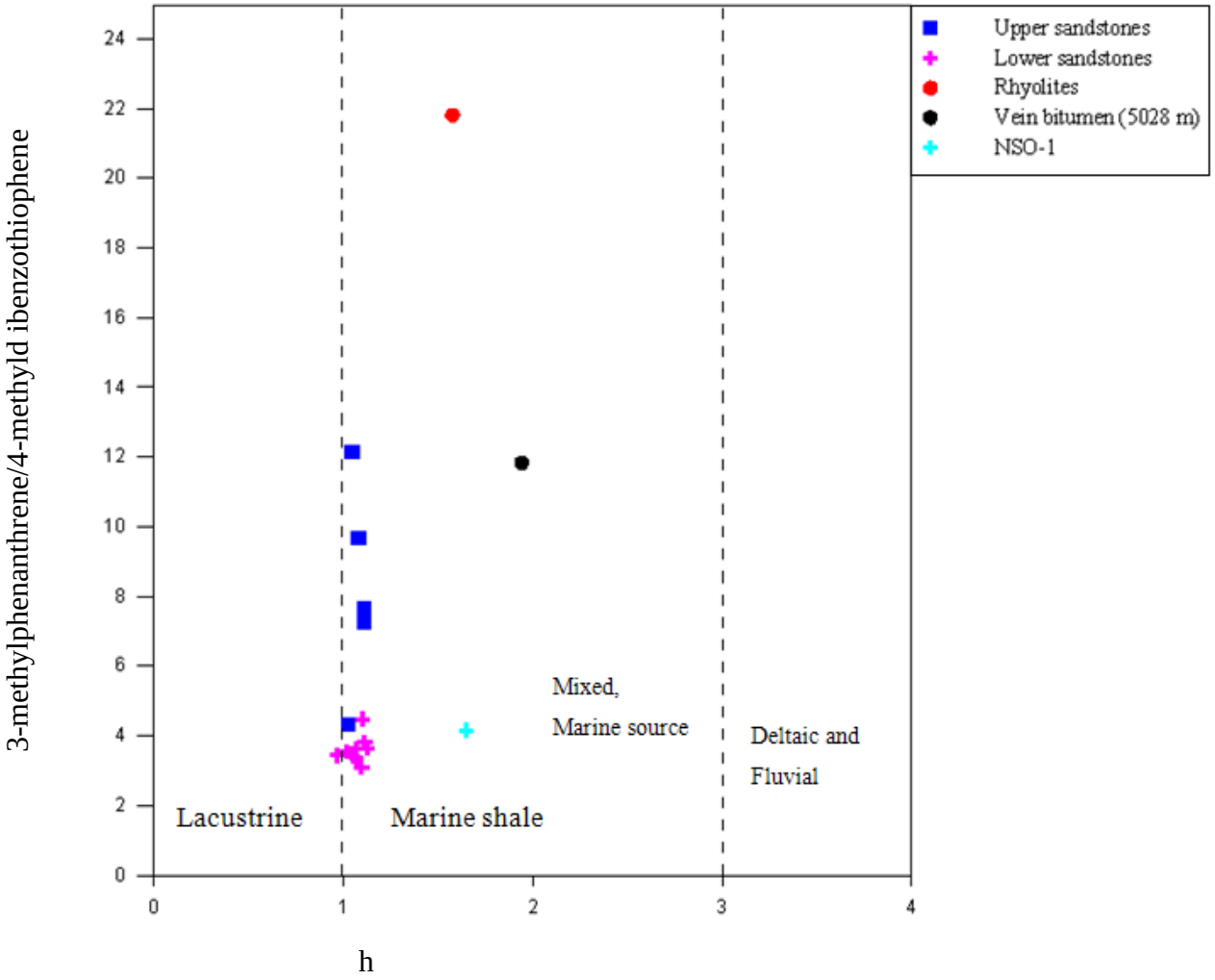

Figure 7.13. The Pr/Ph ratio plotted against the 3-MP/4-MDTP (parameter 26) ratio. This plot can indicate the source facies of the petroleum. All the samples have Pr/Ph ratios between 1 and 2, which indicate all the samples are of marine origin. (Modified from Hughes et al., 1995).

Low hopane/sterane ratios indicate marine, algae dominated organic matter, while higher ratios point to bacteria rich facies, bacterially reworked organic matter or a terrestrial input (Peters and Moldowan, 1993).

Obviously the samples from the Lower sandstone are more algae dominated organic than the other samples (Hopane/Sterane ratio ranges between 0.32 and 0.94), while sample E14 shows slightly higher ratio.

The sample from the Upper sandstone have hopane/sterane ratio (see parameter 9 of Table 6.3) values higher than 1, (except sample E5). Samples from the rhyolites also seem to form a group which informs about their common origin.

The VB sample (extract from Vein filled bitumen) shows the highest amount of bisnorhopane (see Table 6.3 and Figure 7.14) in the sample set. Peters and Moldowan (1993) state that higher amount of bisnorhopane is an indicator of anoxic conditions during deposition of the source rock. Several studies have confirmed this implication of the compound bisnorhopane (Dahl and Speers, 1985; Horstad, 1989), but anoxic source rocks have also been reported containing no bisnorhopane, and it is suggested that its occurrence is dependent upon a particular bacterial population or algal bloom (Waples and Machihara, 1991).

The NSO-sample considered here for reference shows a quite different value of the hopane/sterane ratio with value of 3.24 as compared to 0.83 (average hopane/sterane ratio for all the samples from the Embla considered here). This could indicate a different origin of the Embla bitumen relative to the widely known Upper Jurassic kimmeridge shale.

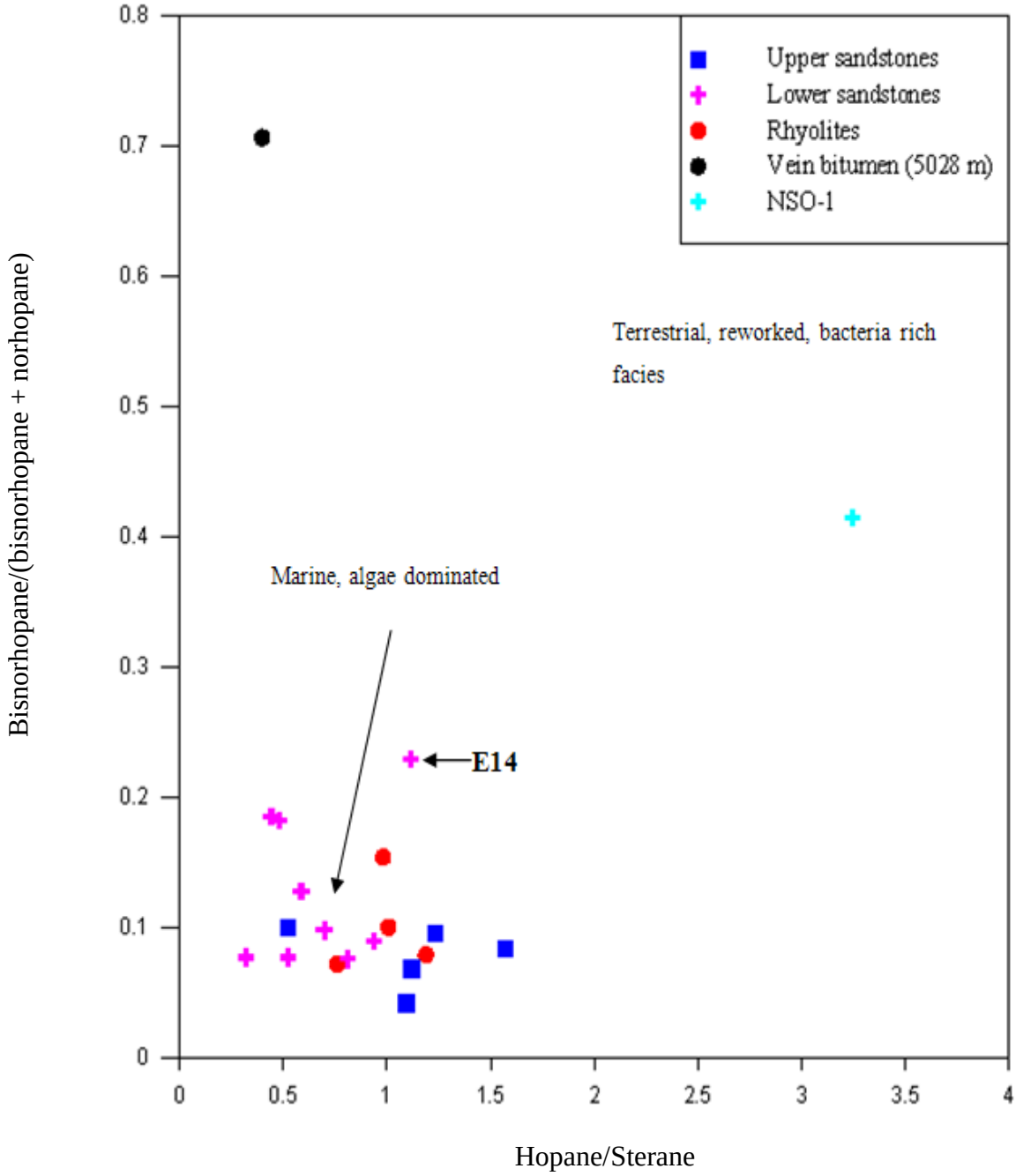

Figure 7.14.Cross-plot of the facies parameters hopane/sterane (parameter 9) versus bisnorhopane/(bisnorhopane + norhopane) (parameter 6). Note the high amount of bisnorhopane in the VB sample. See chapter 5.3.7 for explanation of the parameters.

Figures 7.15, 7.16 and 7.18 are cross plots of aromatic maturity data and facies related parameters. The plots clearly indicate the presence of two different oil populations in the Embla Field. Previous study by Bharati (1997) (page 64) using such diagrams, also indicated that the Upper sandstone and Lower sandstones (based on well 26S) of the Embla Field contain tow different types of bitumen. Hence this reservoir section may have experienced quite different filling histories.

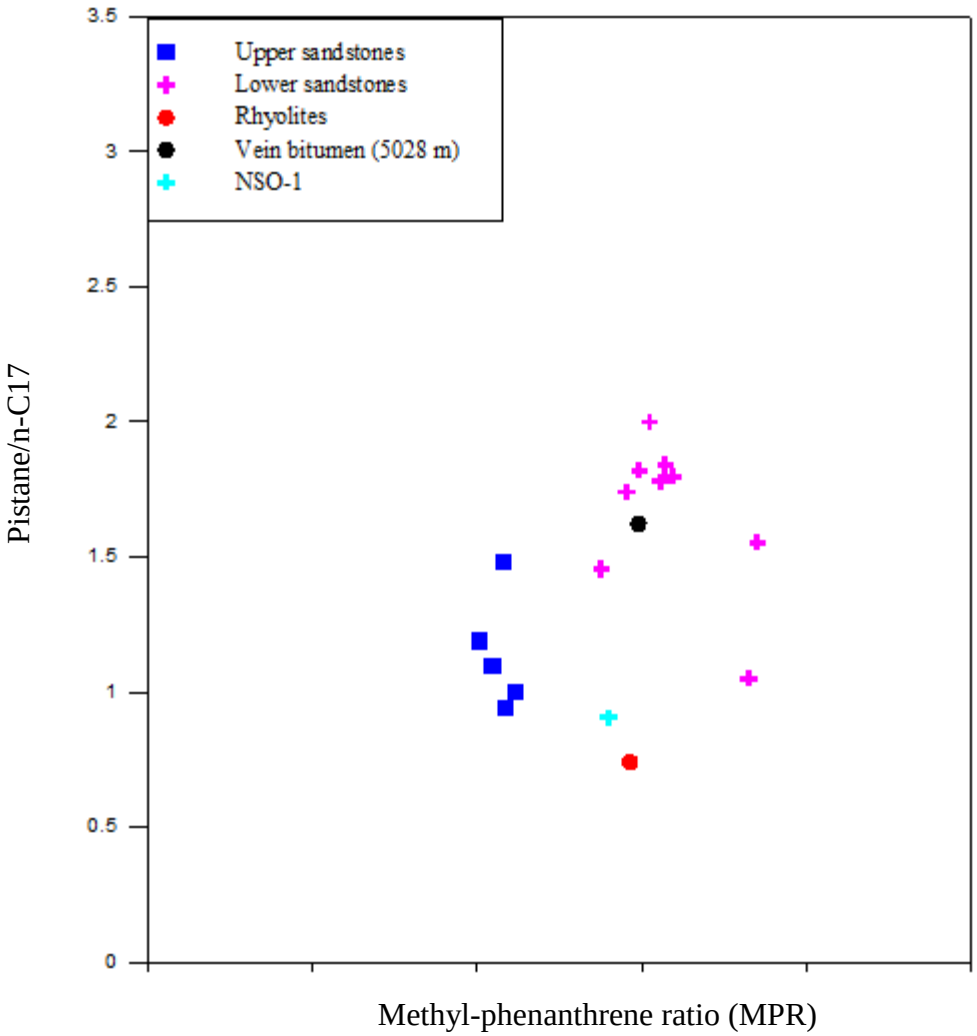

Figure 7.15. Pistane/n-C17 (source facies related parameter) versus MPR (maturity related parameter).

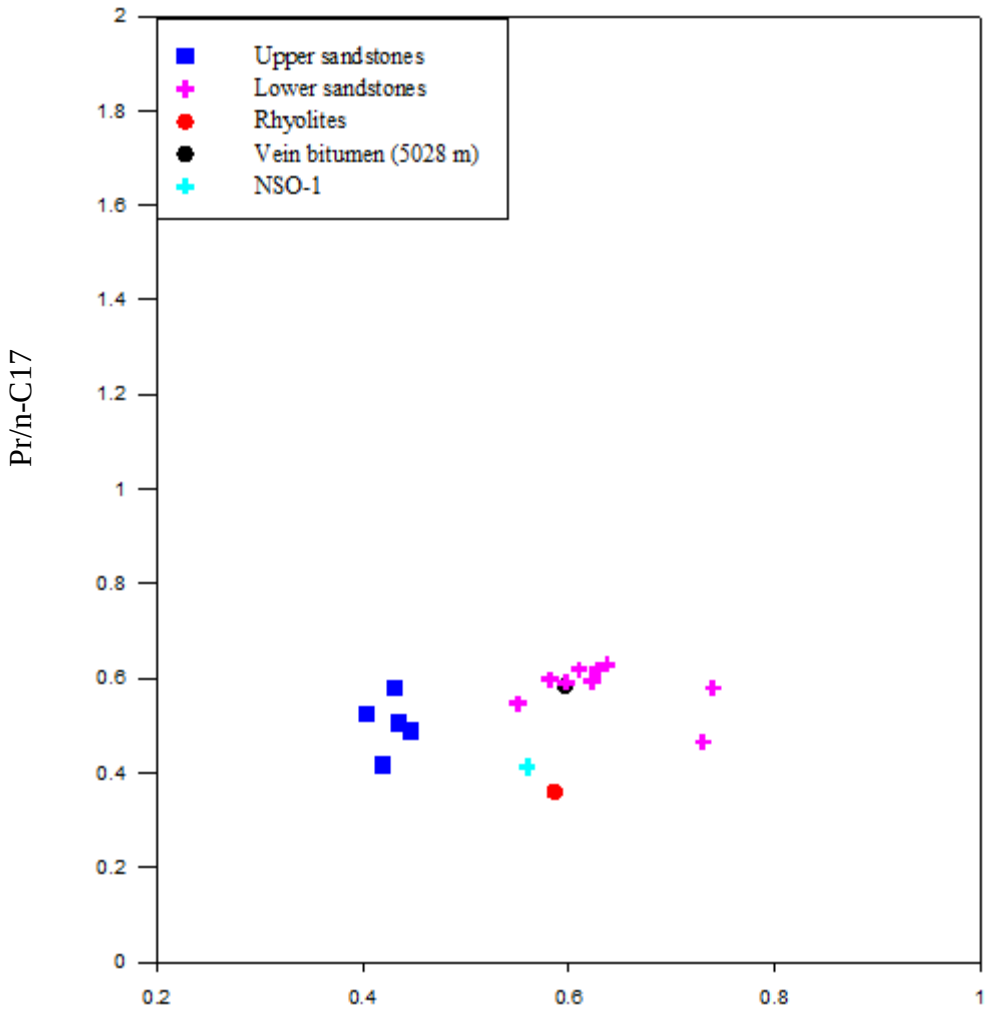

Figure 7.16 Pr/nc17 (facies related parameter) versus MPDF (maturity related parameter)

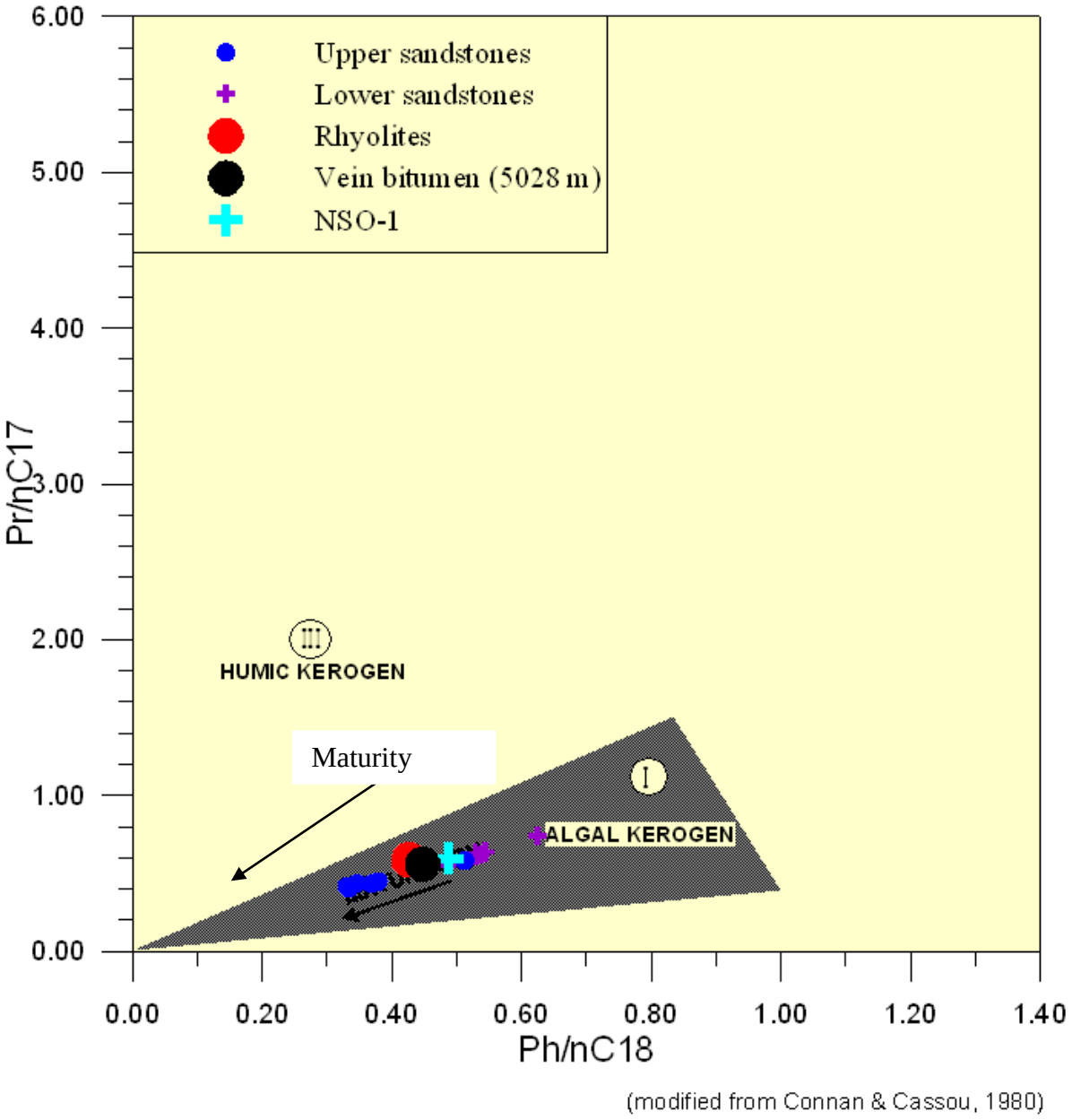

Figure 7.17. A plot of the Ph/n-C18 ratio versus the Pr/n-C17 ratio (modified from Connan and Cassou, 1980) indicating the type of kerogen present in the source rock from where the petroleum originated (Note that the figure does not maintain the previously suggested maturity trend). This is most likely due to paleo-biodegradation.

7.10. Summary of organic facies

From the discussion made regarding the organic facies, it was seen that there are variations in the source rock between the sample groups. It is evident that the samples which represent the different vertical sections of the Embla Field reservoir (well 26S) derived from a slightly different source material. Figure 7.18 represents a combination of results from both the GC-FID and GC-MS. Based on previous discussion and figures given in this section it is possible to allocate the different sample groups to their respective source rock.

The entire sample plots in the marine area, but with a potentially different terrestrial influx and/or mixing conditions.

The NSO-1sample (see for e.g. Figure 7.10 &7.12 shows the highest terrestrial influence followed by the Upper sandstone and rhyolite samples. There is no clear separation between the Upper sandstone and rhyolite samples as to which of these sample groups are more influenced by terrestrial inputs.

Finally, we can conclude that the depositional environment for the source rock that generated the petroleum in the samples is not unique by one singular source. There has been petroleum sources to contributing to the Embla reservoir at least from two sources, one being from highly marine while the other is transitional (meaning it is marine with terrestrial input). Shanmugam (1984) described the later to be typical for a proximal type II source rock. Even with the Lower part of the reservoir (Lower sandstone) there has been times fluxes from different source rocks (for example sample E14 which behaves to be more terrestrial).

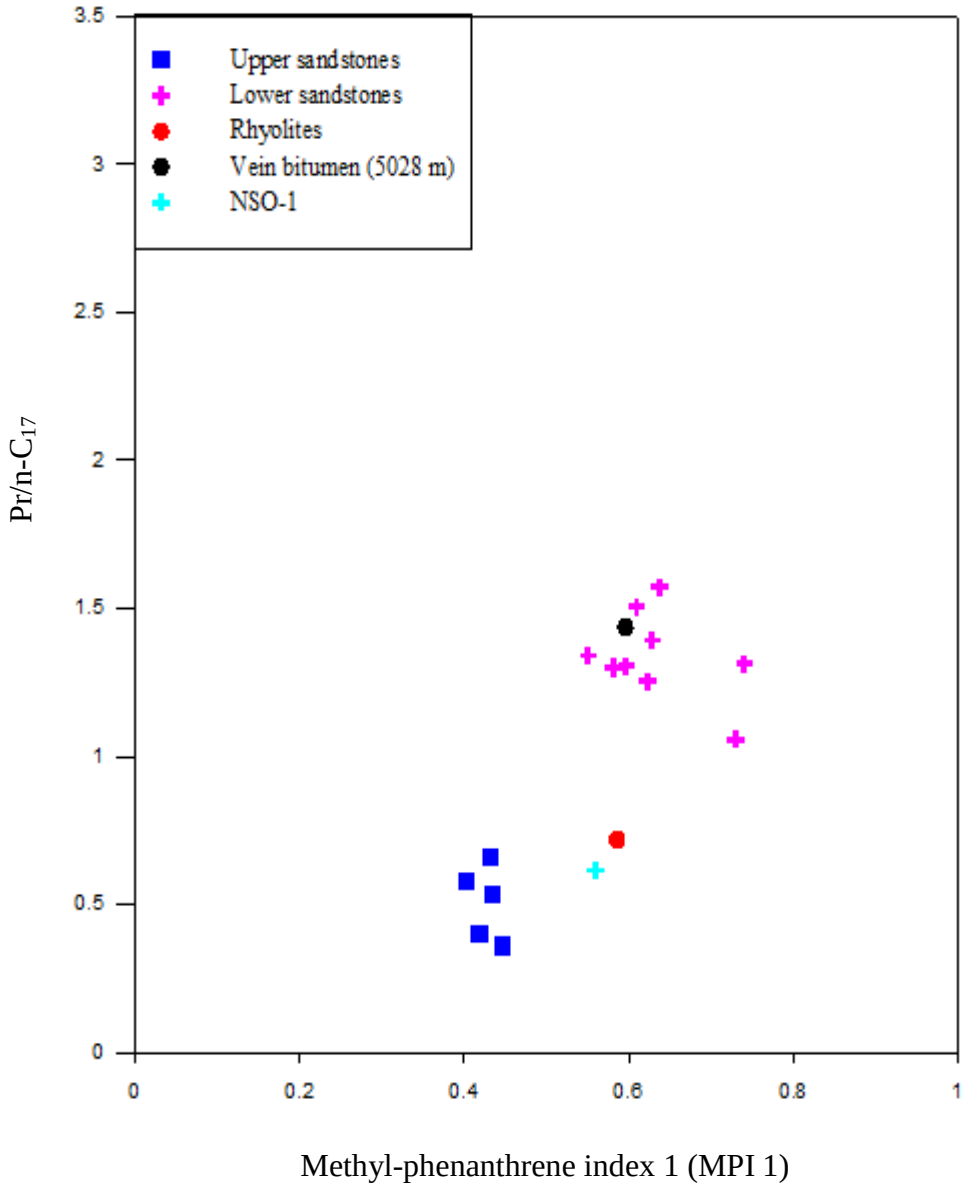

Figure 7.18 Pr/n-c_{17} (facies related parameter) against MPI1 (maturity related parameter).

MPI1=Methylphenanthrene index 1

7.11. Biodegradation of the samples

Biodegradation is the microbial alteration of crude oil, which occur if there is access to meteoric water, temperature range less than 65-80ºC, absence of H_2S and proximity to an oil-water contact (Ahsan, 1993; Connan, 1984). Biodegradation results in partial or total removal of n-alkanes, followed by isoparaffins, napthenes (such as steranes and terpanes), aromatics and eventually the polycyclic aromatics (Winters and Williams, 1969; 1971; Bailey et al., 1973; Chosson et al., 1992; Moldowan et al., 1992). Biodegradation of petroleum occur at low temperature (not more than about 80) and hence at shallow depth.

Loss of n-alkanes as indication of biodegradation

Winters and Williams, 1969 has noted the removal of n-alkanes by bacteria prior to any other compound class (thus increasing the relative concentration of acyclic isoprenoids, like pristane and phytane, compared to n-C17 and n-C18 respectively, with increasing biodegradation

The loss of n-alkanes is not pronounced in the studied samples from Embla. The removal of pristane and phytane are classified as extensive biodegradation, as observed in VB sample. The appearance of the unresolved complex mixture (UCM) hump may indicate other unresolved compounds rather than indication of biodegradation. The less degree of degradation could be due to the deep location of the samples and the source rocks could be even deeper below the current reservoir depth. The GC-FID chromatograms (Figures 7.19, 6.4-6.17 and Appendix A) reveal the presence of some biodegradation which could be anoxic but associated to water washing which contributed dissolved oxygen to enhance biodegradation at depth.

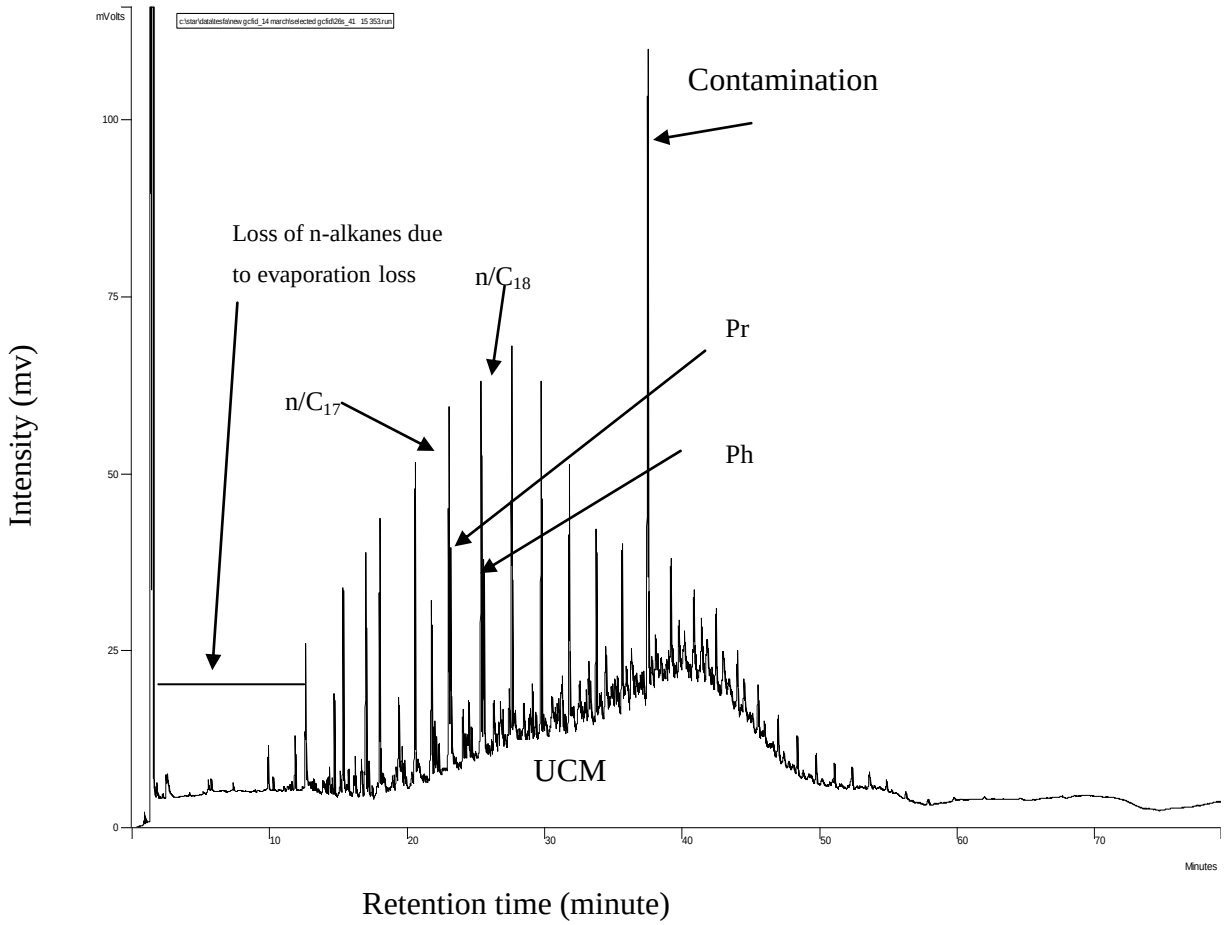

Figure 7.19. Biodegradation shown by the indicated UCM for the sample E7 of well 26S, Embla Field. Pr=Pristane, Ph=Phytane. See also Fig 7.20

UCM=Unresolved Complex Mixture, due to biodegradation

7.12. Summary of the samples

The samples show moderate evidence of biodegradation (see Fig 7.20). The unresolved complex mixture (UCM) is only partly present, and in a moderate degree. This testifies to the very moderate degree of biodegradation of the extracts from the well 26S of the Embla Field. This tells us that the Embla Field-currently deep and at 165°C; at some time must have contained oil at a reservoir temperature less than 80°C. This represents a paleo filling event and parts of the examined bitumen must be inherited from this event.

The samples represent variations in maturity, ranging from petroleum generated early to late-peak and condensate in the oil window. The general maturity trend is that the samples from the Lower sandstone of the reservoir are the most mature, followed by Upper sandston and rhyolite samples. The VB samples show different behavior. It does not follow the trend observed by the other, but it could be as mature as the Lower sandstone samples.

The depositional environment for the source rock that generated the petroleum in the samples is marine with mainly algal contribution. However, the lower sandstone has slightly different source facies than the Upper sandstone. The Lower sandstone is more mature, algae rich than the Upper sandstone. The study shows that the samples from the Embla Field are very mature and they are type 2 kerogen. The composition of the extracts (Table 6.1) for the lower and upper sandstones is different.

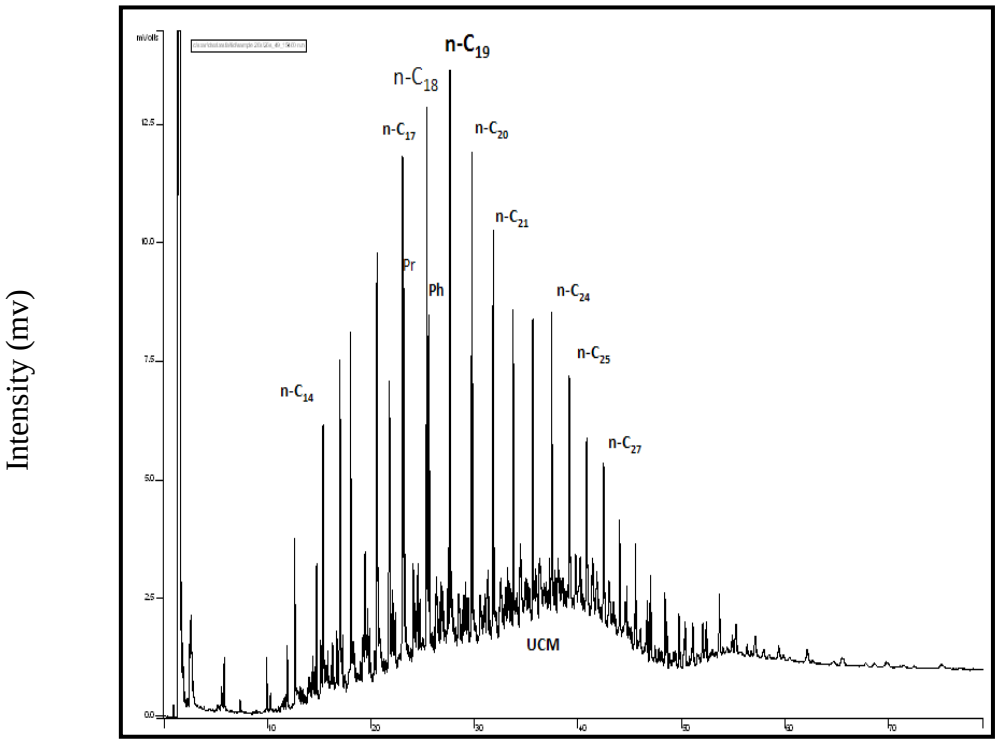

Figure 7.20. The GC-FID compounds, n-C17, pristine, n-C18 and phytane for sample E14 of the Embla samples. The lower n-alkanes (less than n-C_{12}) are not seen due to evaporation loss during storage.

8. Summary and conclusions

A total of 21 core samples from the Embla Field and one reference oil sample from Oseberg have been studied geochemically. The Embla Field consists of three reservoir units. The Uppermost, Upper and Lower Sandstones, separated vertically by a thick mudstone sequence. The Uppermost section is not found in the studied well, 2/7-26S. Therefore, the studied samples represent the Upper and Lower sandstones plus the mudstone sequence. Moreover, the well 26S penetrates down to the rhyolitic rocks. Four samples were from this unit. One sample (VB) represents bitumen in a rhyolite vein/fracture. The Oseberg oil (NSO-1) is standard oil in the North Sea and here it was considered as reference.

The objective of the study was to carry out geochemical analysis to characterize the Embla reservoir vertically based on the available core samples from the well 2/7-26S in terms of hydrocarbon abundance and composition, maturity, source facies and biodegradation.

From the geochemical studies the following conclusions can be drawn:

- The Upper sandstone in well 2/7-26S is richer than the Lower sandstone in migrated hydrocarbons. That is, comparing to the Lower sandstone the Upper sandstone contains more free hydrocarbons that can be extracted. On the contrary more polar compound have been observed in the Lower sandstone than the Upper sandstone.

- The order of hydrocarbon richness for the samples (more to less rich) is: Upper sandstone, Lower sandstone, VB, rhyolites.

- Compositionally the migrated hydrocarbons show variations vertically with depth. The relative non-hydrocarbon percentage increases dramatically with depth.

- Previous studies show that the rhyolite rocks are highly fractured, and bitumen is easily visible in the core samples of this lithology. However, the samples from the VB and rhyolite contains much less bitumen on a mg bitumen/g rock basis compared to the sandstones. This is in contrast to the bitumen visible by naked eyes in the rhyolite and VB core samples. Hence the conclusion is that the fact that less

hydrocarbon is extracted from the Lower sandstone, Rhyolites and VB is due to their high content of insoluble solid bitumen which has the capacity to reduce the permeability and porosity of the reservoir.

- The thick mudstone unit found between the Lower and Upper sandstones represent almost no extract compared to the extracts from the overlying and underlying sandstones, therefore, it is concluded that the petroleum in Embla has not invaded this unit and that it may represent a lateral intra-reservoir seal for vertical communication.

- The Embla samples are highly mature with vitrinite reflectance of more than 0.8%. The samples from the Upper and Lower sandstones show different maturity signatures. The lower sandstone being more mature.

- The applicability of the biomarker based maturity parameters is less useful for the highly mature Embla bitumen samples. Rather, aromatic hydrocarbon based maturity ratios reflect the maturity more reliably.

- On average the rhyolite samples show the lowest maturity and this could reflect that the oil entrapped in the rhyolites represent an early filling event.

- The following maturity trend for the studied samples is concluded (high to low): **Lower sandstone→VB →Upper sandstone→NSO-1 → Rhyolites.**

- The bitumen in the studied well of the Embla Field are concluded to be sourced from marine algal type 2 kerogen. The bitumen from the Lower sandstones is concluded to have originated partly from a more algal, restricted anoxic environment.

- The Upper and Lower sandstones show about similar values of n-alkane/isoprenoid and Pr/Ph ratios, hence no distinction on the degree of maturity can be made based on these parameters, and this suggests both units to contain oil of the same organic facies.

- The upper and lower sandstone samples show distinct facies which shows that the petroleum charges in the two units have not been mixing. The VB sample appeared to represent a higher degree of mixing than the other samples.

- The bitumen of the Embla Field are different from the NSO-1 trend in maturity and source rock facies, typically the oils of the Lower sandstone in well 2/7-26S were generated by different source facies with higher maturity than the normal North Sea Oils (NSO-1).

- The investigated samples generally show that the Embla bitumen are moderately biodegraded. Thus, the bitumen extracted show this biodegraded signature while the produced oil from the field today are non-degraded. This suggests that the bitumen extracted, which show this biodegraded signature, may in past reflect an earlier filling phase. This could explain also the discrepancy between the medium range and the biomarker parameters among the samples.

.

9. References

Ahsan, A, 1993: Petroleum biodegradation in the Tertiary Reservoirs of the North Sea. Cand. Scient. Thesis in Geology, Department of Geology, University of Oslo, Norway, 173 pp.

Alexander, R., Kagi, R.I., and Woodhouse, G.W., 1981, Factors influencing the evolution of petroleum aromatics from an immature crude oil during pyrolysis on a shale matrix: Journal of Analytical and Applied Pyrolysis, v. 3, p. 59-70.

Alexander, R., Kagi, R. I. and Woodhouse, G. W., 1981: Geochemical correlation of Windalia oil and extracts of Winning Group (Cretaceous) potential source rocks, Barrow Subbasin, Western Australia. *AAPG Bulletin,* **65,** 235-250.

Bharati, S., 1997, Mobile and immobile migrated hydrocarbons in the Embla field, North Sea: Trondheim, Faculty of Applied Earth Science and Petroleum Engineering, The Norwegian University of Science and Technology.

Bhullar, A. G., Karlsen, D. A., Backer-Owe, K., Le Tran, K., Skålnes, E., Berchelmann, H. H. and Kittelsen, J. E., 2000: Reservoir characterization by combined micro extraction – micro thin-layer chromatography (Iatroscan) method: A calibration study with examples from the Norwegian North Sea. *Journal of Petroleum Geology,* **23,** 221-244.

Clayton, J.L., and Bostick, N.H., 1986, Temperature effects on kerogen and on molecular and isotopic composition of organic matter in Pierre Shale near an igneous dike. Advances in organic geochemistry, 1985; Part I; Petroleum geochemistry., Ruellkotter, J., Ed., Pergamon, p. 135-143.

Cornford, C., Morrow, J.A., Turrington, A., Miles, J.A., and Brooks, J., 1983, Some geological controls on oil composition in the U.K. North Sea. Petroleum

geochemistry and exploration of Europe; International congress., Brooks, J., Ed.: Geological Society of London, p. 175-194.

Connan, J., 1984: Biodegradation of crude oils in reservoirs. Advances in petroleum geochemistry, Brooks, J. and Welte, D. H., Eds., Academic press, London, Vol. 1, 299-335.

Connan, J. and Cassou, A. M., 1980: Properties of gases and petroleum liquids derived from terrestrial kerogen at various maturation levels. *Geochimica et Cosmochimica Acta,* 44, 1-23.

Dahl, B. and Speers, G. C., 1985: Organic geochemistry of the Oseberg field. Petroleum geochemistry in exploration of the Norwegian Continental shelf, Thomas Bruce, M. E. A., Ed., Graham and Trotman, 185-195.

Elvsborg, A., Hagevang, T. and Throndsen, T., 1985: Origin of the gas-condensate of the Midgard Field at Haltenbanken. Petroleum geochemistry in exploration of the Norwegian Shelf., Larsen Rolf, M., Ed., Graham and Trotman, 213-219.

Didyk, B. M., Simoneit, B. R. T., Brassell, S. C., and Eglinton, G., 1978. Organic geochemical indicators of paleoenvironmental conditions of sedimentations: Nature, Vol. 272, p. 216-222

Fraser, A.J., Farnsworth, J., and Hodgson, N.A. Salt control on basin evolution – Central North Sea. In: A.M. Spenser, Editor, *Special Publication of the European Association of Petroleum Geoscientists No. 3* (1993

Gowers, M.B., Holtar, E., and Swensson, E., 1993, The structure of the norwegian central trough (central graben area), 1245-1254 p.

Gowers, M.B., and Sæbøe, A., 1985, On the structural evolution of the Central Trough in the Norwegian and Danish sectors of the North Sea: Marine and Petroleum Geology, v. 2, p. 298-318.

Ho, M.P. Rogers, H.V. Drushel and C.B. Koons, 1974. Evolution of sulfur compounds in crude oils. *Bulletin of the American Association of Petroleum Geologists* **58** (1974), pp. 2338–2348.

Horstad, I., 1989: Petroleum composition and heterogeneities within the Middle Jurassic reservoir in The Gullfaks field area, Norwegian North Sea, Department of Geology, University of Oslo.

Hughes, W.B., Use of thiophenic organosulfur compounds in characterizing crude oils derived from carbonate versus siliclastic sources. In: J.B. Palacas, Editor, *Petroleum Geochemistry and Source Rock Potential of Carbonate RocksAAPG, Studies in Geology* **18** (1984), pp. 181–196.

Hughes, W.B., Holba, A.G., and Dzou, L.I.P., 1995, The ratios of dibenzothiophene to phenanthrene and pristane to phytane as indicators of depositional environment and lithology of petroleum source rocks: Geochimica et Cosmochimica Acta, v. 59, p. 3581-3598.

Hunt, J.M., 1996, Petroleum geochemistry and geology: New York, W. H. Freeman, XX, 743 s. p.

Karlsen, D. A. and Larter, S. R., 1989: A rapid correlation method for petroleum population mapping within individual petroleum reservoirs – applications to petroleum reservoir description. Correlation in Hydrocarbon Exploration, Haresnape, J., Ed., 77-85

Karlsen, D. A. and Larter, S. R., 1991: Analysis of petroleum fractions by TLC-FID; applications to petroleum reservoir description. *Organic Geochemistry*, **17,** 603-617.

Karlsen, D., Nedkvitne, T., Larter, S., and Bjorlykke, K., 1995, The best paper award in organic geochemistry - hydrocarbon composition of authigenic inclusions - application to elucidation of petroleum reservoir filling history: Geochimica et Cosmochimica Acta, v. 59, p. 1439-1439.

Karlsen, D.A., Nedkvitne, T., Larter, S.R., and Bjorlykke, K., 1993, Hydrocarbon composition of authigenic inclusions - applications to elucidation of petroleum reservoir filling history: Geochimica et Cosmochimica Acta, v. 57, p. 3641-3659.

Karlsen, D. A., Skeie, J. E., Backer-Owe, K., Bjørlykke, K., Olstad, R., Berge, K., Cecchi, M., Vik, E. and Schaefer, R. G., 2004: Petroleum migration, faults and overpressure. Part II. Case history: The Haltenbanken Petroleum Province, offshore Norway. *Understanding Petroleum Reservoirs: towards an Integrated Reservoir Engineering and Geochemical Approach.* Cubitt, J. M., England, W. A. and Larter, S., Eds., Geological Society, London, Special Publications, **237,** 305-372

Karlsen, D.A., and Skeie, J.E., 2006, Petroleum migration, faults and overpressure, Part I: Calibrating basin modelling using petroleum in traps - A review: Journal of Petroleum Geology, v. 29, p. 227-255.

Knight, I.A., Allen, L.R., Coipel, J., Jacobs, L., and Scanlan, M.J., 1993, The embla field, 1433-1444 p.

Kvalheim, O. M., Telnaes, N., Bjorseth, A. and Christy, A. A., 1987: Interpretation of multivariate data; relationship between phenanthrenes in crude oils. Multivariate statistical workshop for geologists and geochemists., Kvalheim, O. M., Ed., Elsevier, 149-153.

Mackenzie, A. S., 1984: Applications of biological markers in petroleum geochemistry. Advances in petroleum geochemistry; Volume 1., Welte, D. H., Ed., Acad. Press, 115-214

Mackenzie, A.S, and Maxwell, J.R, 1981. Assessment of thermal maturation of sedimentary rocks by molecular measurement. In: J. Brooks, Editor, *Organic Maturation Studies and Fossil Fuel Exploration*, Academic Press, London (1981), pp. 239–254.

Mackenzie, A.S., Rullkoetter, J., Welte, D.H., and Mankiewicz, P., 1985, Reconstruction of oil formation and accumulation in North Slope, Alaska, using quantitative gas chromatography-mass spectrometry. Alaska North Slope oil-rock correlation study; analysis of North Slope crude, American Association of Petroleum Geologists, p. 319-377.

Mackenzie, A. S., Maxwell, J. R., Coleman, M. L. and Deegan, C. E., 1984: Biological marker and isotope studies of North Sea crude oils and sediments. *Proceedings – World Petroleum Congress = Actes et Documents – Congres Mondial du Petrole*, **11,** 45-56.

Moldowan, J. M., Fago, F. J., Carlson, R. M. K., Young, D. C., Van, D. G., Clardy, J., Schoell, M., Pillinger, C. T. and Watt, D. S., 1991: Rearranged hopanes in sediments and petroleum. *Geochimica et Cosmochimica Acta*, **55**, p. 3333 – 3353.

Pedersen, J. H., 2002: Atypical oils, unusual condensates and bitumens of the Norwegian Continental Shelf: an organic geochemical study, Cand. Scient. Thesis in Geology, Department of Geology, University of Oslo

Pedersen, J.H., Karlsen, D.A., Backer-Owe, K., Lie, J.E., and Brunstad, H., 2006, The geochemistry of two unusual oils from the Norwegian North Sea: implications for new source rock and play scenario: Petroleum Geoscience, v. 12, p. 85-96.

Peters, K.E., and Moldowan, J.M., 1993, The biomarker guide: interpreting molecular fossils in petroleum and ancient sediments: Englewood Cliffs, N.J., Prentice Hall, XVI, 363 s. p.

Peters, K.E., Moldowan, J.M., and Walters, C.C., 2005, The biomarker guide: Cambridge, Cambridge University Press, 2 b. p.

Radke, M. and Welte, D. H., 1983: The methylphenanthrene index (MPI); a maturity parameter based on aromatic hydrocarbons. Advances in organic geochemistry 1981., Speers, G., Ed., Wiley & Sons, 504-512.

Radke, M., Welte, D. H. and Willsch, H., 1982a: Geochemical study on a well in the western Canada Basin; relation of the aromatic distribution pattern to maturity of organic matter. *Geochimica et Cosmochimica Acta*, **46,** 1-10.

Radke, M., 1988, Application of aromatic compounds as maturity indicators in source rocks and crude oils: Marine and Petroleum Geology, v. 5, p. 224-236.

Sears, R.A., Harbury, A.R., Protoy, A.J.G. & Stewart, D.J. 1993: Structural styles from the Central Graben in the UK and Norway. In: Parker, J.R. (ed.): Petroleum geology of Northwest Europe: proceedings of the 4th conference, 1231–1243. London: Geological Society.

Seifert, W.K., and Moldowan, J.M., 1986, Use of biological markers in petroleum exploration. In: Johns, R. B. (Editor): Methods in Geochemistry and Geophysics, v. 24, p. 261-290.

Shanmugam, G., 1984: Significance of terrestrial environments and related organic matter in generating commercial quantities of oil, Gippsland Basin, Australia. Society of Economic Paleontologists and Mineralogists First annual midyear meeting. Society of Economic Paleontologists and Mineralogists, 73.

Sutton, P.A., Lewis, C.A., and Rowland, S.J., 2005, Isolation of individual hydrocarbons from the unresolved complex hydrocarbon mixture of a biodegraded crude oil using preparative capillary gas chromatography: Organic Geochemistry, v. 36, p. 963-970.

ten Haven, H. L., J. W. de Leeuw, T. M. Peakman, and J. R. Maxwell, 1986, Anomalies in steroid and hopanoid maturity indices: Geochemica et Cosmochimica Acta, v. 50, p. 853-855.

ten Haven, H. L., De Leeuw, J. W., Rullkoetter, J. and Sinninghe Damste, J. S., 1987: Restricted utility of the pristane/phytane ratio as a palaeoenvironmental indicator. *Nature (London),* **330,** 641-643.

Tissot, B. P. and Welte, D. H., 1978: Petroleum formation and occurrence: a new approach to oil and gas exploration. Springer- Verlag, 538 pp.

Tissot, B. P., Welte, D. H., 1984, Petroleum formation and occurrence, (2nd edition) Springer-Verlag, p. 380-381.

Waples, D. W. and Machihara, T., 1991: Biomarkers for geologists – A practical guide to the application of steranes and triterpanes in petroleum geology. Vol. 9, *AAPG Methods in Exploration,* AAPG, 91 pp.

Weiss, H. M., Wilhelms, A., Mills, N., Scotchmer, J., Hall, P. B., Lind, K. and Brekke, T., 2000: NIGOGA – The Norwedian Industry Guide to Organic Geochemical Analyses [online]. Norsk Hydro, Statoil, Geolab Nor, SINTEF Petroleum Research and the Norwegian Petroleum Directorate. Available from World Wide Web: http://www.npd.no/ **4.0**, 1-102.

Winters, J. C. and Williams, J. A., 1969: Microbiological alteration of crude oil in the reservoir. American Chemical Society, division of petroleum chemistry, New York Meeting Preprints, **14(4),** E22-E31.

Østensen, M., 2005, A geochemical assessment of petroleum from underground oil storage caverns in relation to petroleum from natural reservoirs offshore Norway.

APPENDIX

Appendix A GC-FID Chromatograms

NSO-1

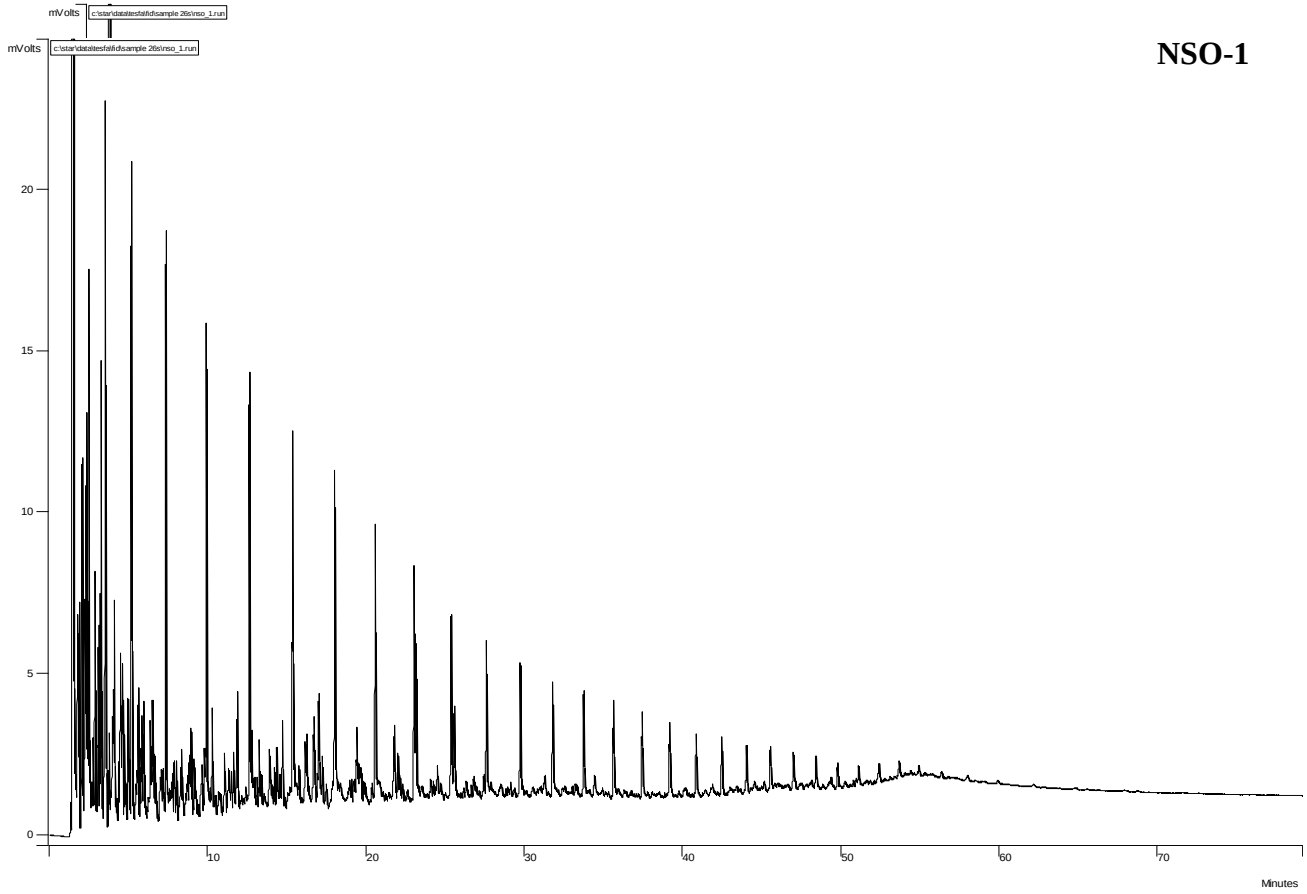
mVolts
c:\star\data\tesfa\fcds\sample 26s\nso_1.run
mVolts
c:\star\data\tesfa\fcds\sample 26s\nso_1.run
20
15
10
5
0
10
20
30
40
50
60
70
Minutes

Sample E1

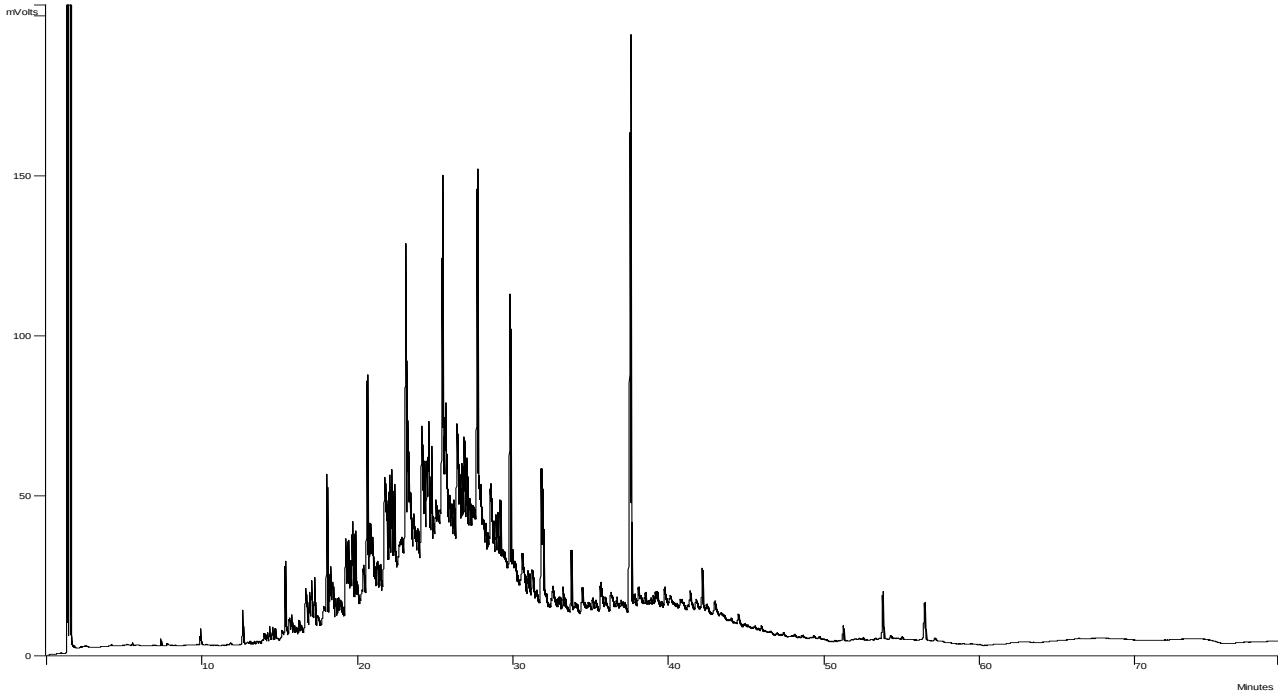

Sample E2

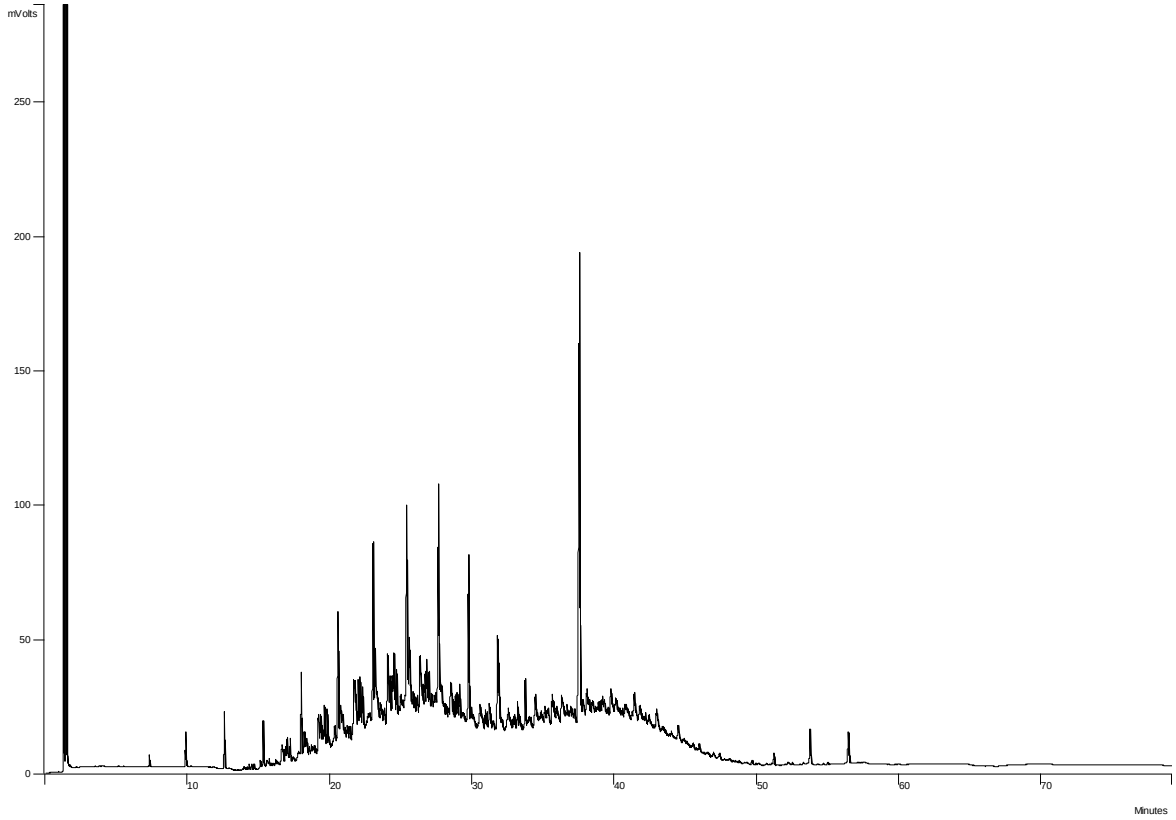

Sample E3

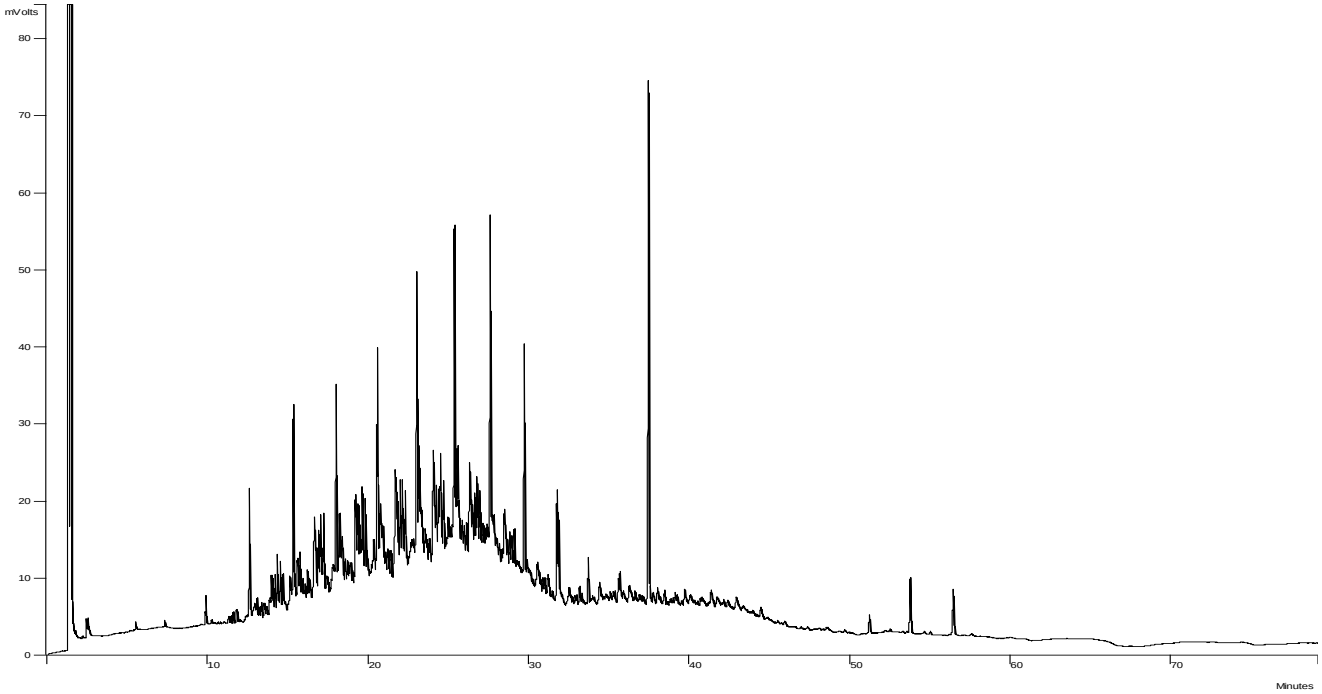

Sample E4

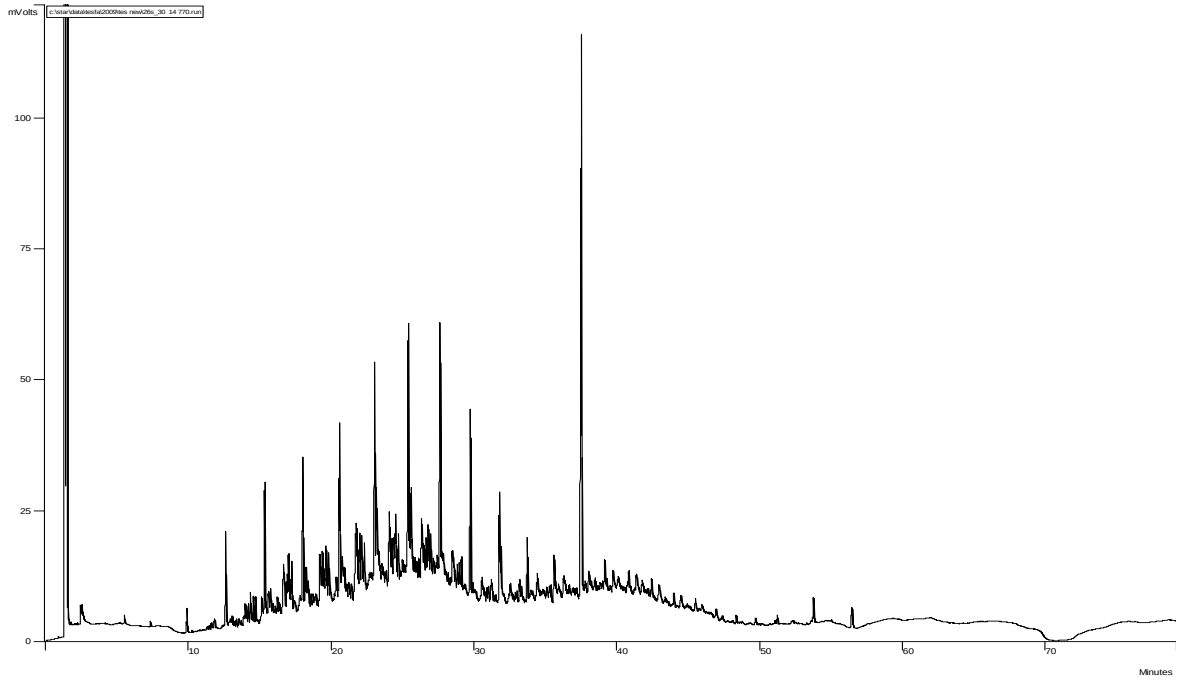

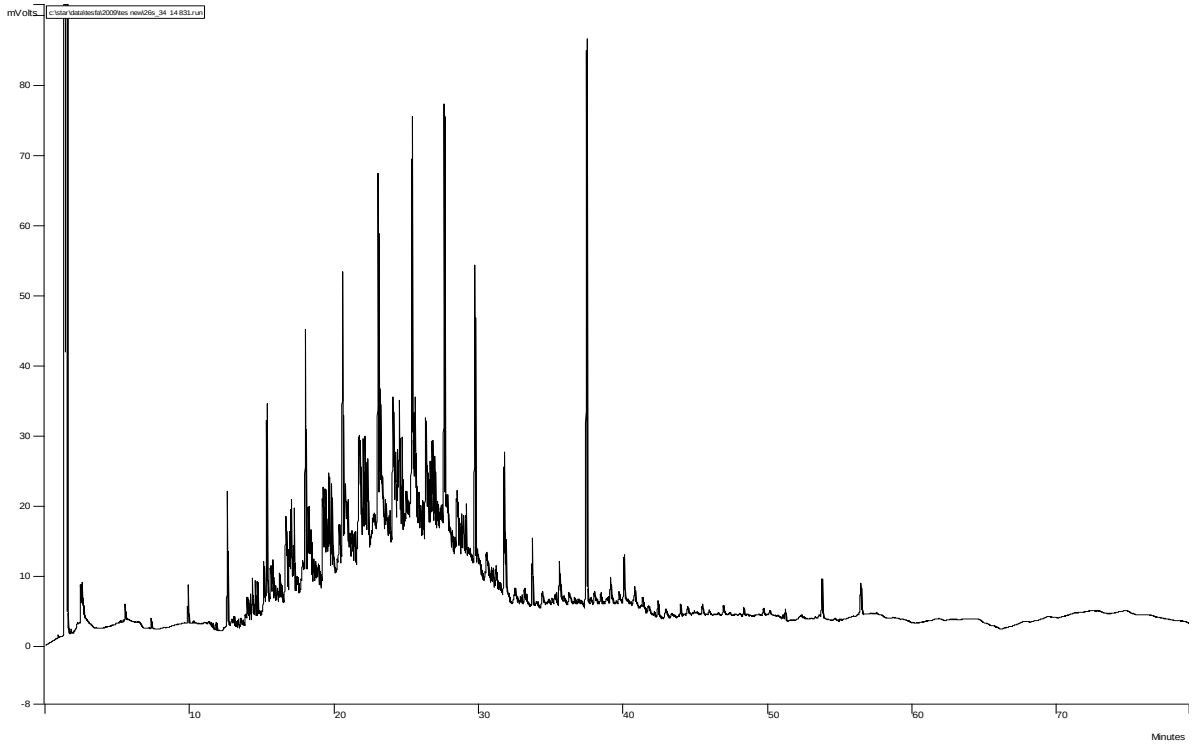

Sample E5

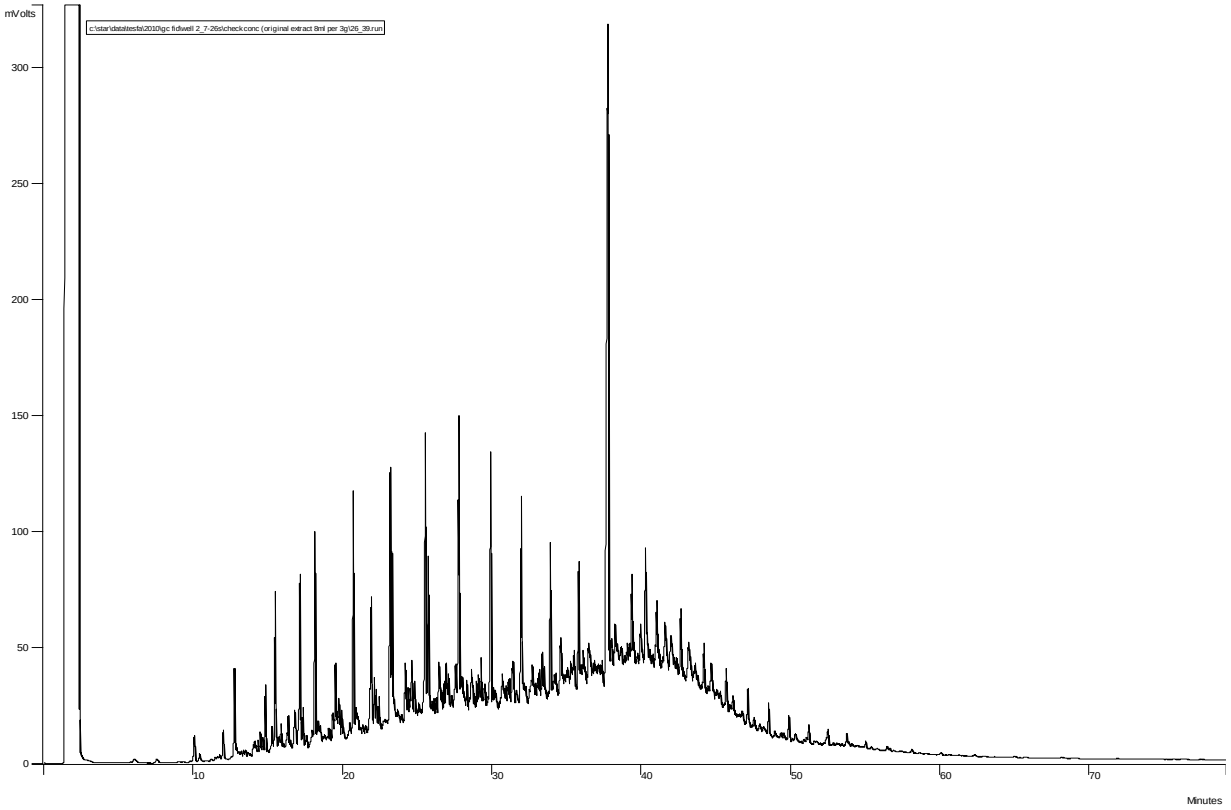
mVolts
c:\star\datatest\st2010\gc fidwell 2_7-26s\check conc (original extract 8ml per 3g\26_39.run
300
250
200
150
100
50
0
10
20
30
40
50
60
70
Minutes

Sample E6

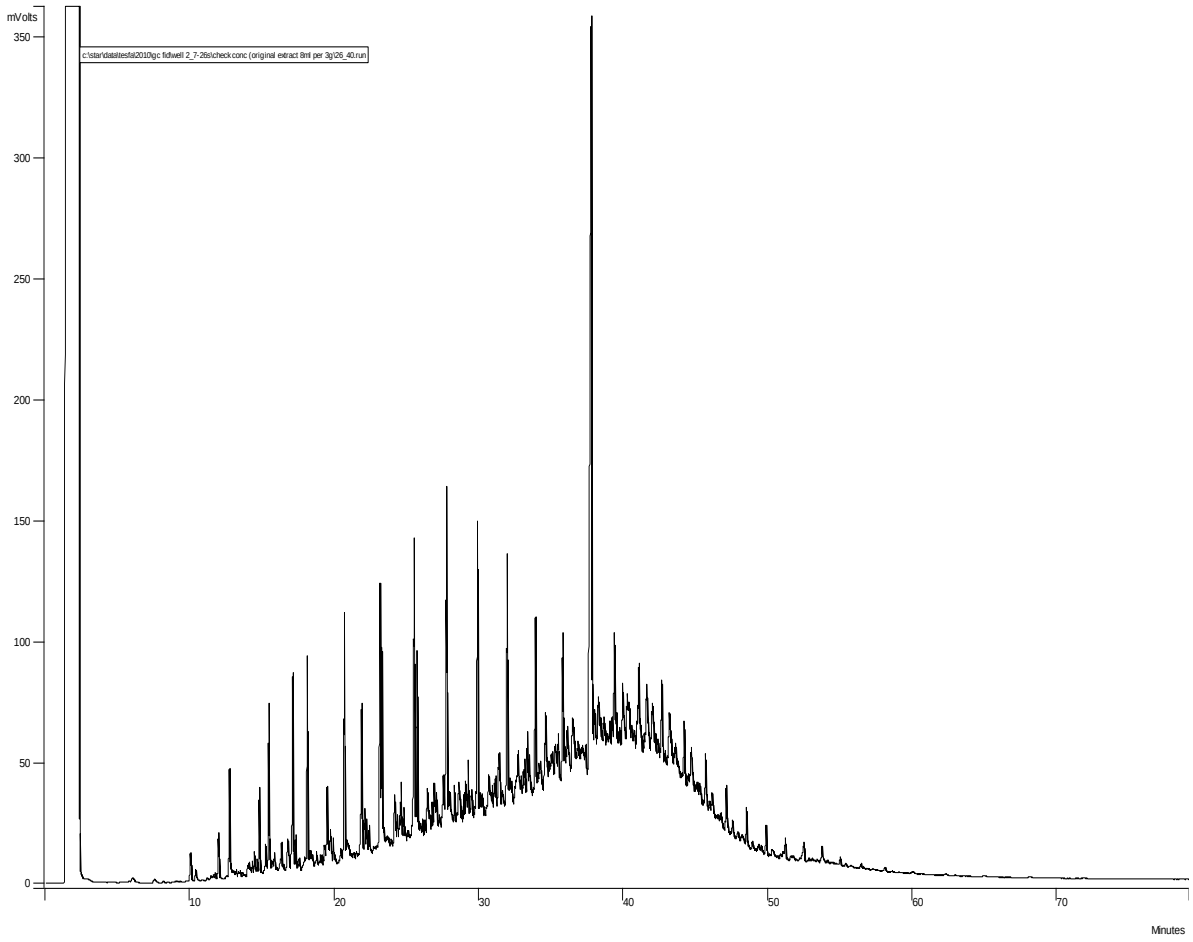
mVolts
350
300
250
200
150
100
50
0
c:\star\data\test\fall2010\gc fidwell 2_7-26b\checkconc (original extract 8ml per 3g\26_40.run
10
20
30
40
50
60
70
Minutes

Sample E7

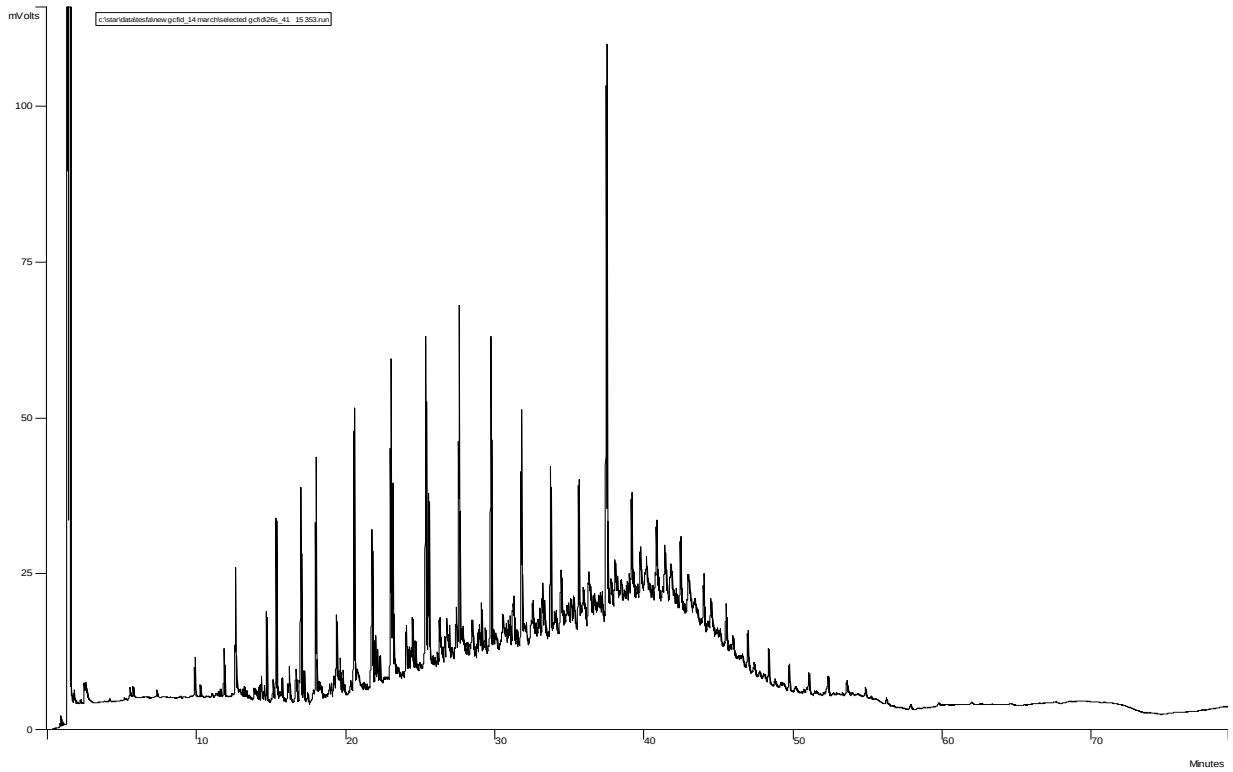
mVolts
c:\star\datatestfalnew.gc\fid_14 march\selected.gc\fid2\fs_41 15 353.run
100
75
50
25
0
10
20
30
40
50
60
70
Minutes

Sample E8

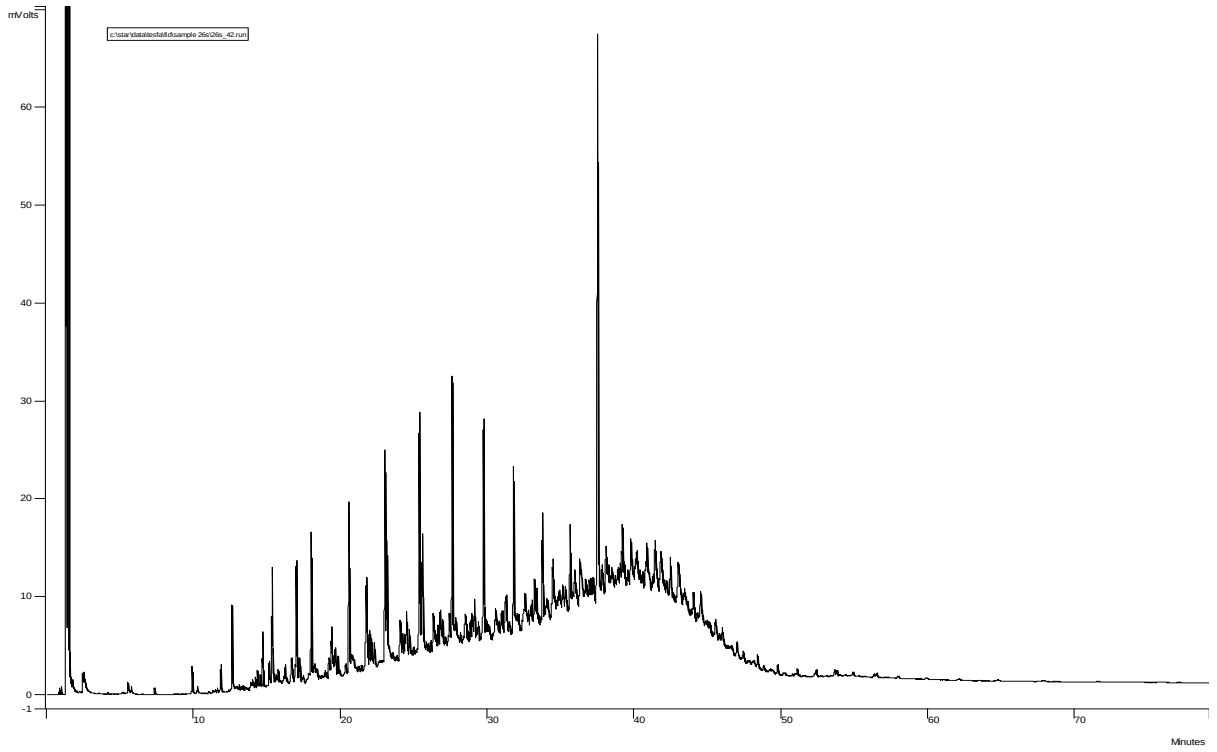
mVolts
c:\star\data\esfa\fid\sample 26s\26s_42.run
60
50
40
30
20
10
0
-1
10
20
30
40
50
60
70
Minutes

Sample E9

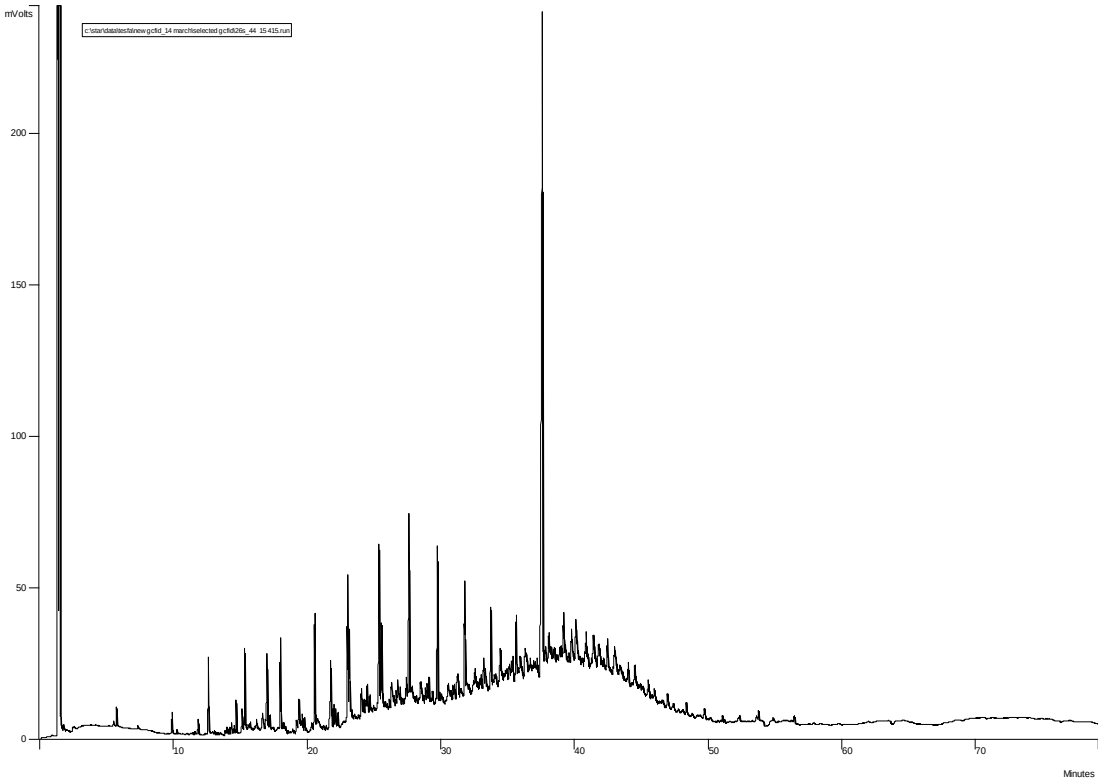

Sample E10

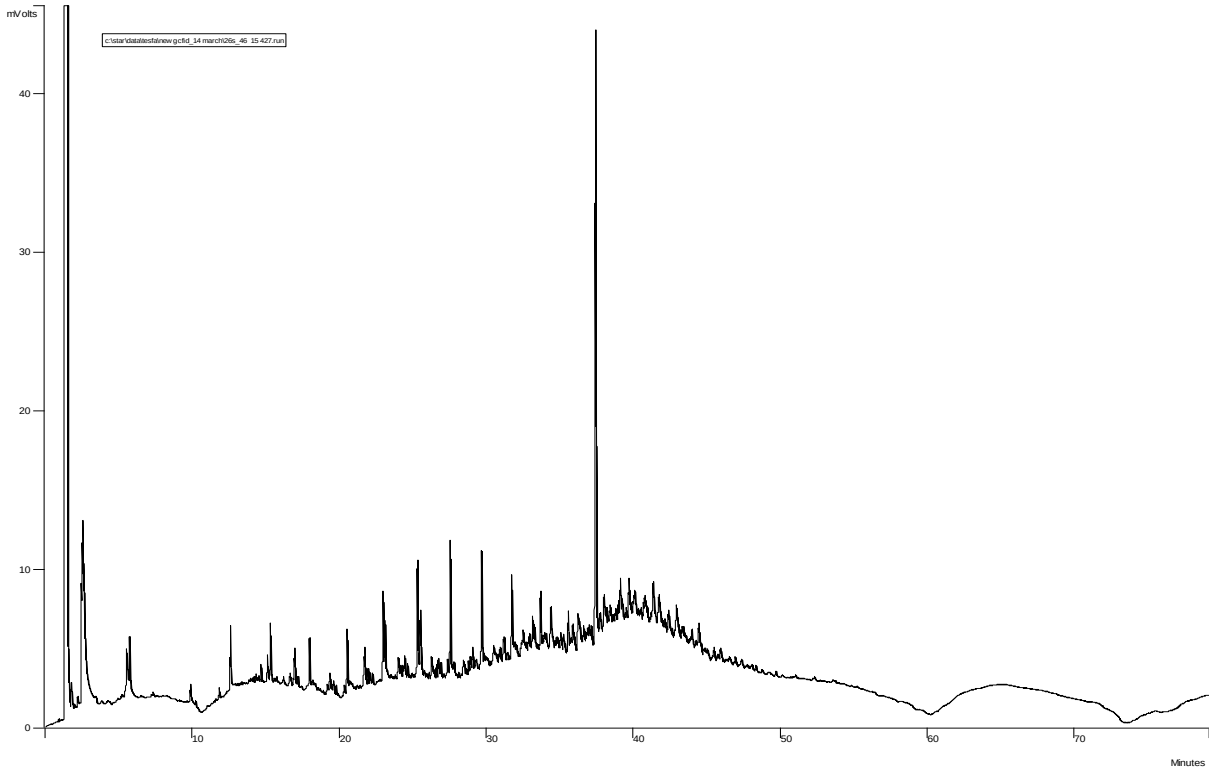
mVolts
c:\star\datatestfs\new gc\fid_14 march\26s_46 15 427.run
40
30
20
10
0
10
20
30
40
50
60
70
Minutes

Sample E11

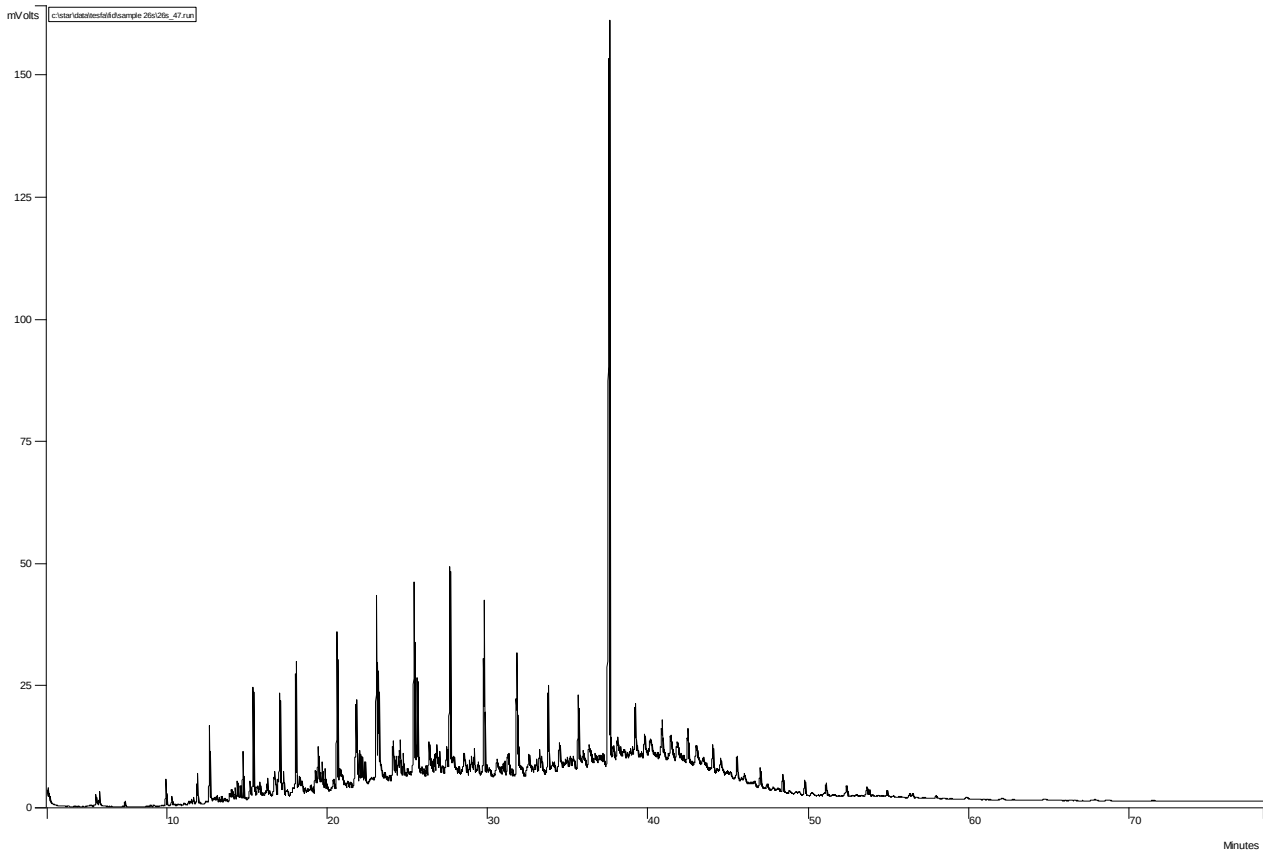
mVolts
c:\star\data\testfa\lid\sample 26s\26s_47.run
150
125
100
75
50
25
0
10
20
30
40
50
60
70
Minutes

Sample E12

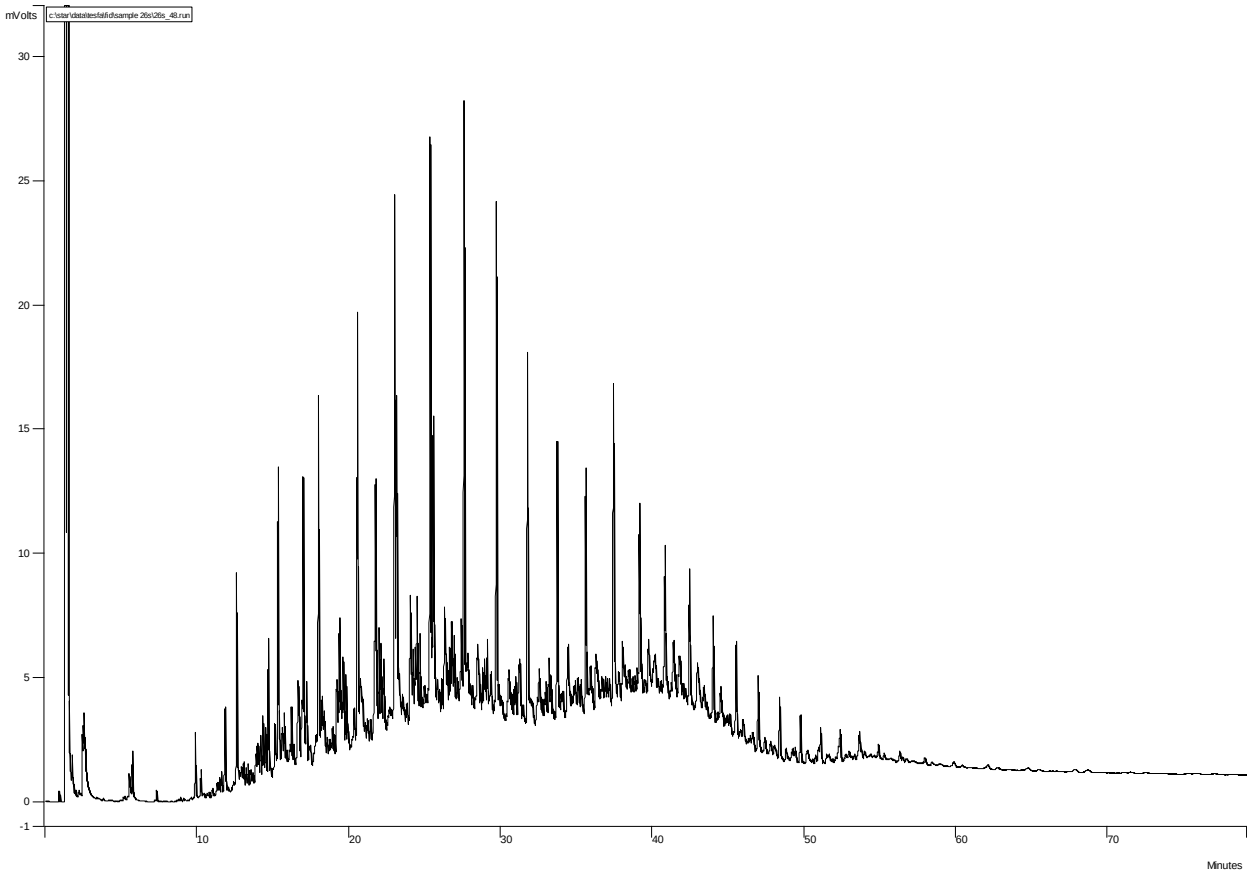
mVolts
c:\star\data\tes\fafid\sample 26s\26s_48.run
30
25
20
15
10
5
0
-1
10
20
30
40
50
60
70
Minutes

Sample E13

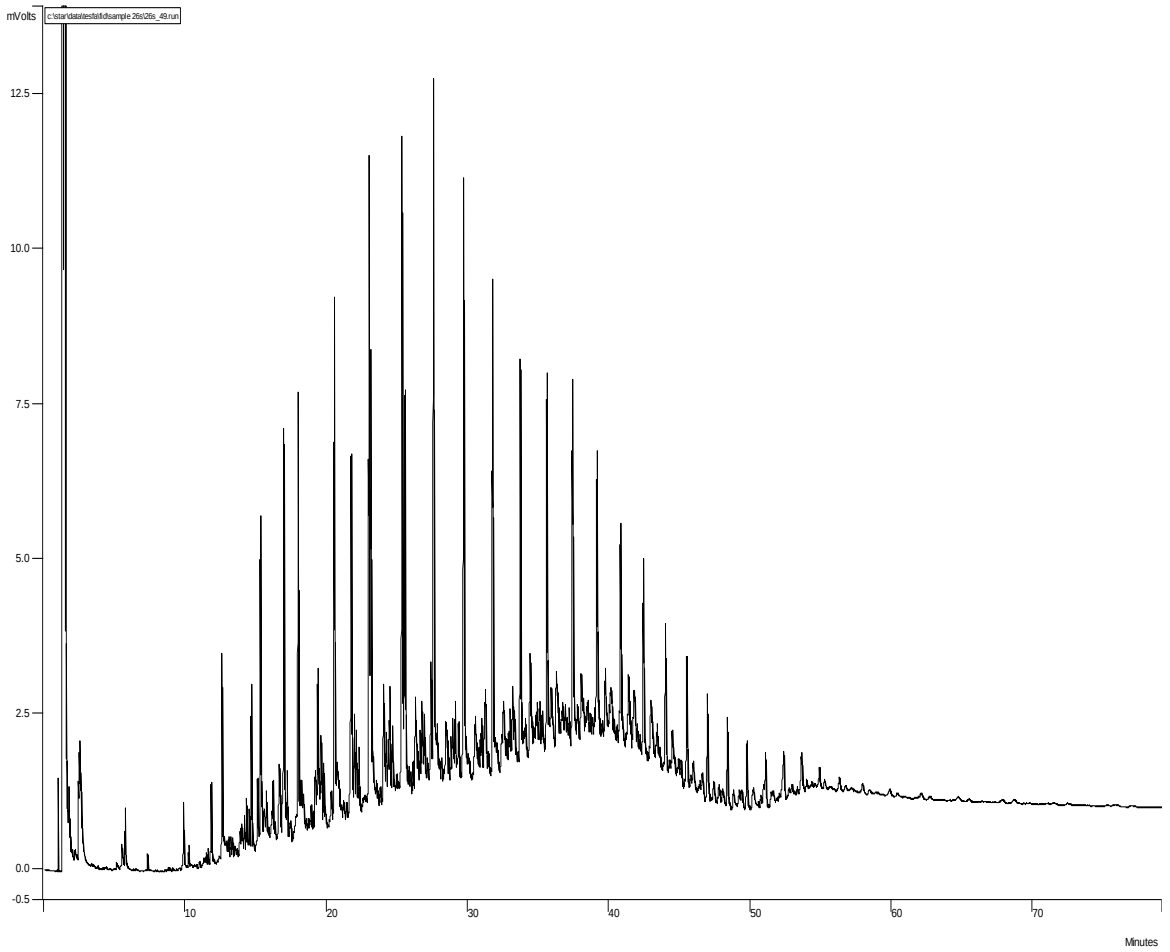
mVolts
c:\star\data\esta\ds\sample 26s\26s_49.run
12.5
10.0
7.5
5.0
2.5
0.0
-0.5
10
20
30
40
50
60
70
Minutes

Sample E14

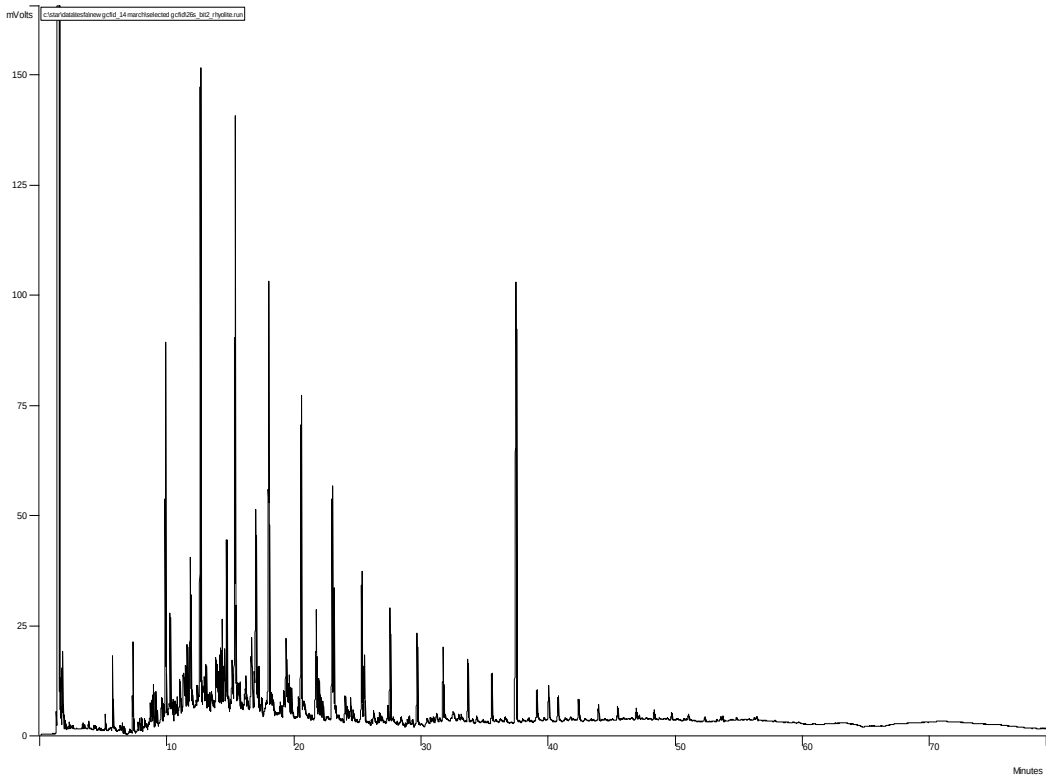

Vein Butimen (VB)

APPENDIX B GC-MS chromatograms

NSO-1

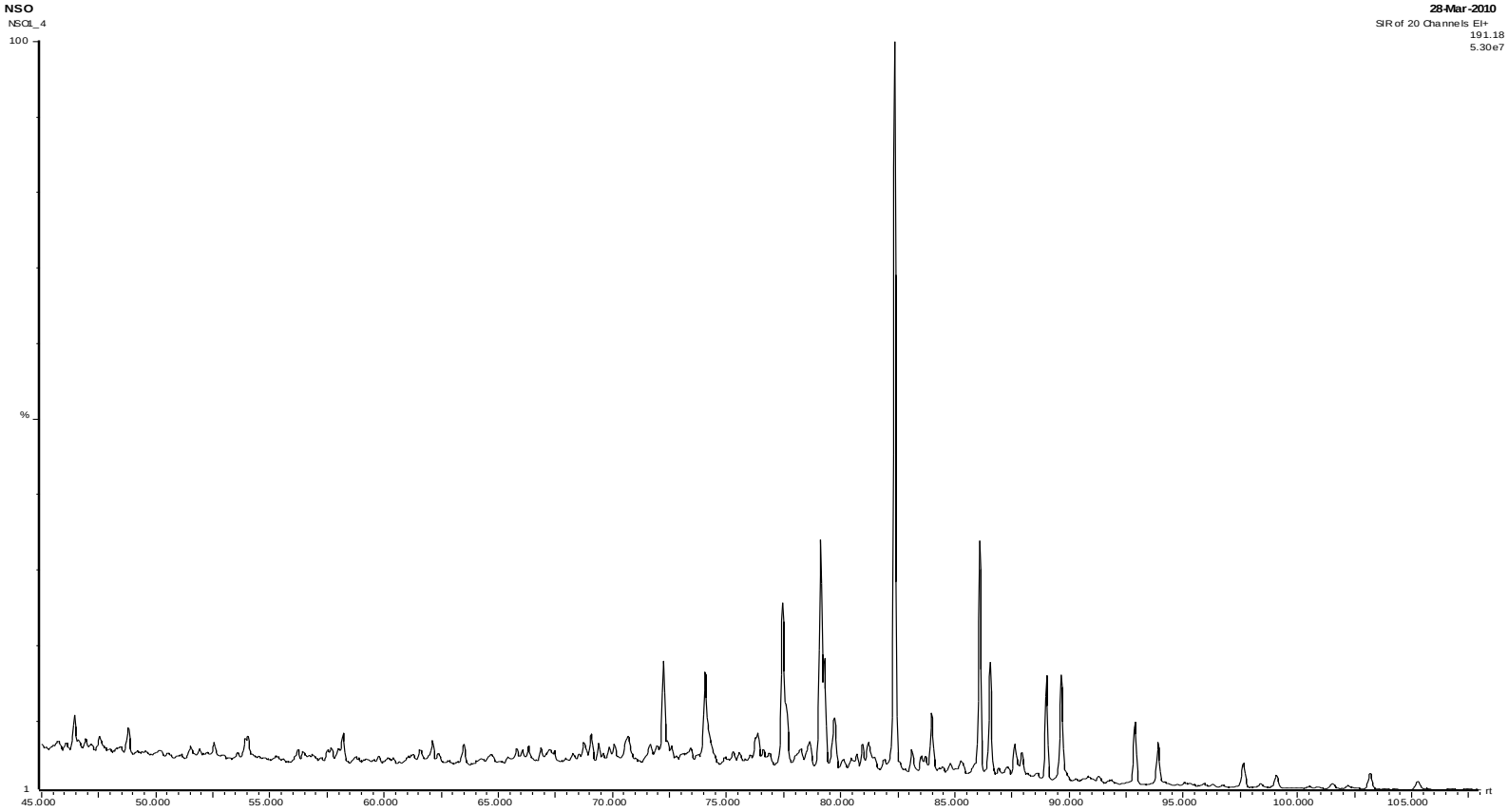
NSO
NSOL_4
28-Mar-2010
SIR of 20 Channels EI+
191.18
5.30e7
100
%
1
45.000
50.000
55.000
60.000
65.000
70.000
75.000
80.000
85.000
90.000
95.000
100.000
105.000
rt

166

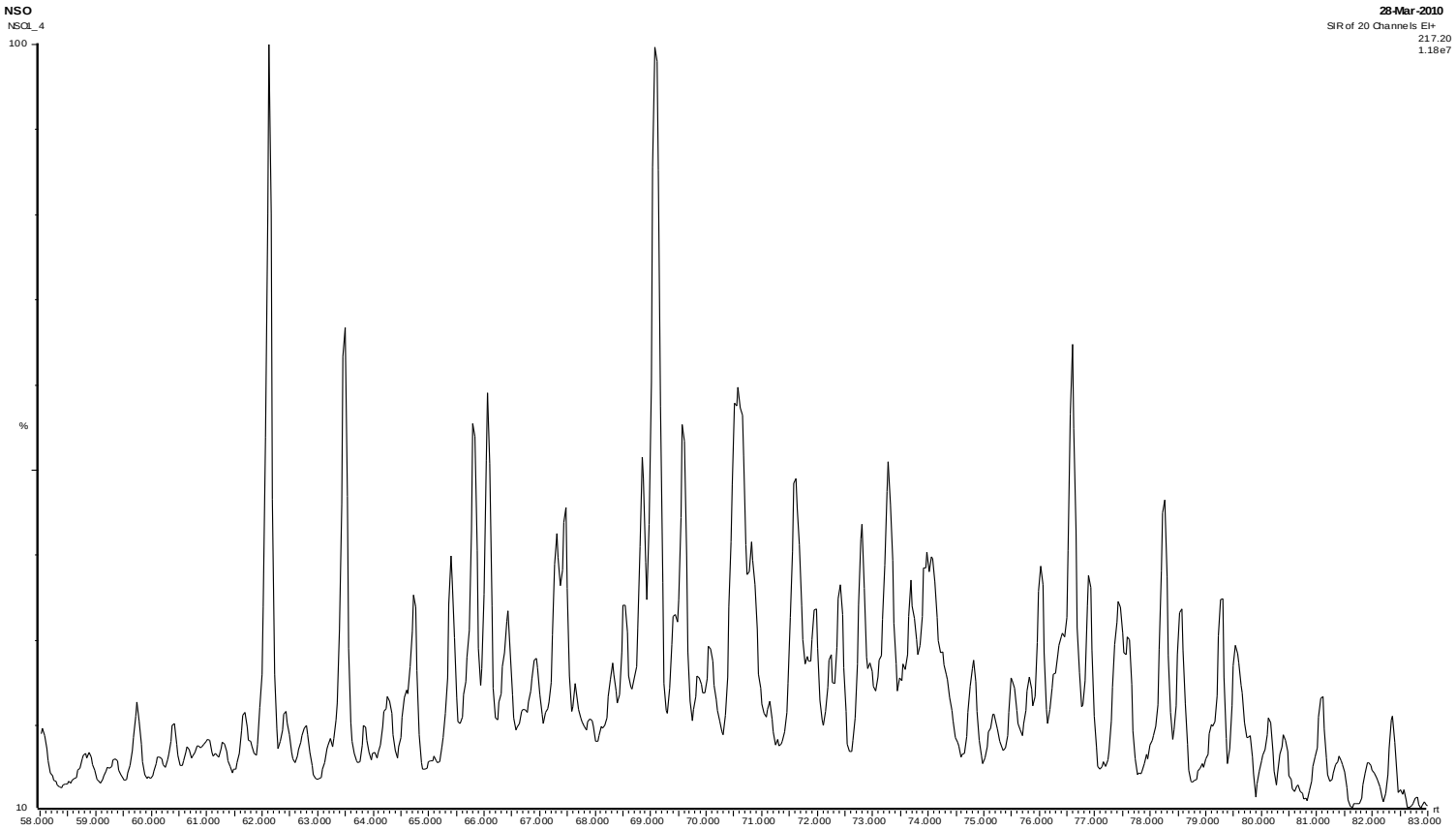
NSO
NSOL_4
28-Mar-2010
SIR of 20 Channels EI+
217.20
1.18e7
100
%
10
58.000
59.000
60.000
61.000
62.000
63.000
64.000
65.000
66.000
67.000
68.000
69.000
70.000
71.000
72.000
73.000
74.000
75.000
76.000
77.000
78.000
79.000
80.000
81.000
82.000
83.000
rt

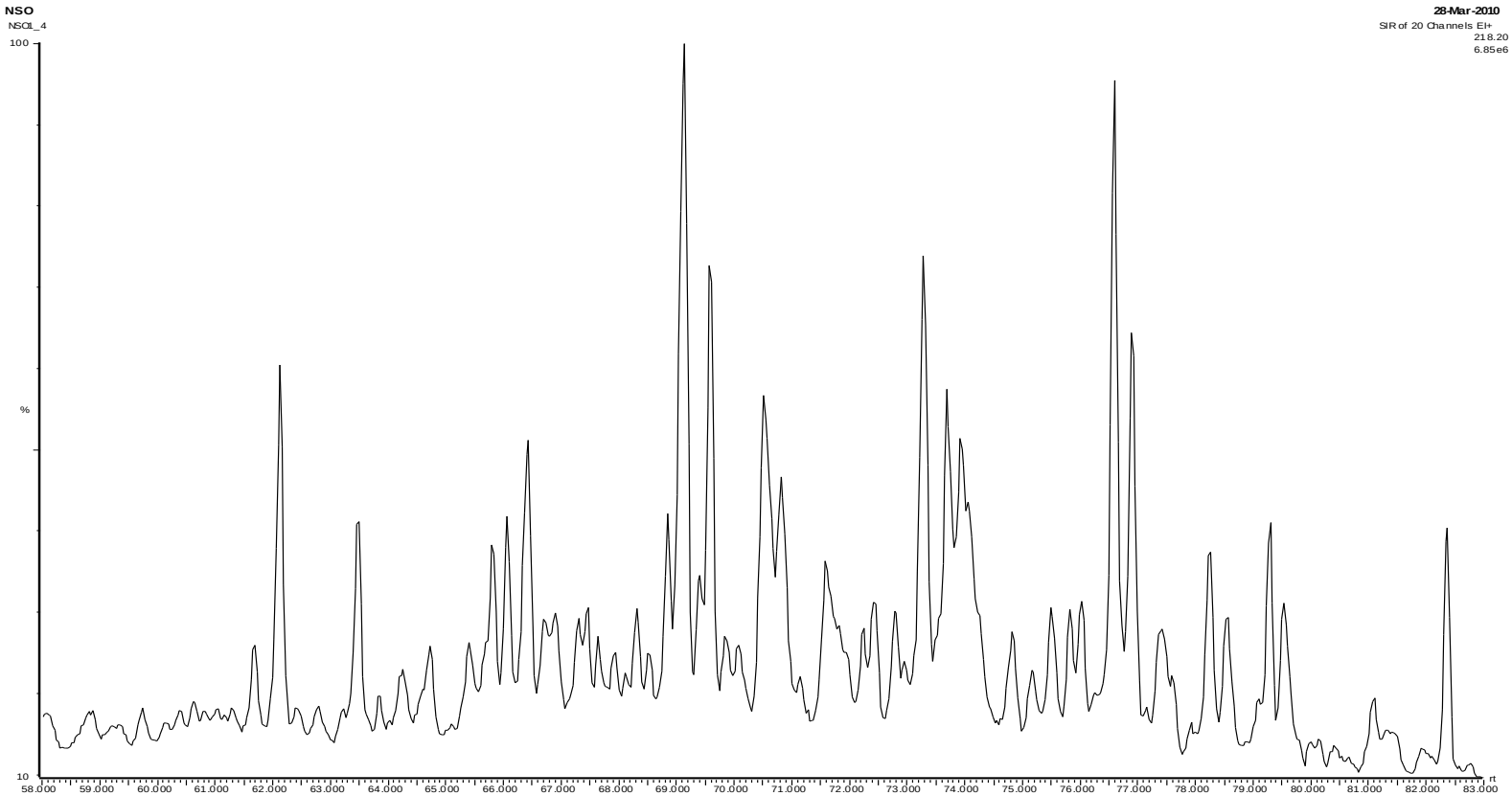
NSO
NSOIL_4
28-Mar-2010
SIR of 20 Channels EI+
218.20
6.85e6
100
%
10
58.000
59.000
60.000
61.000
62.000
63.000
64.000
65.000
66.000
67.000
68.000
69.000
70.000
71.000
72.000
73.000
74.000
75.000
76.000
77.000
78.000
79.000
80.000
81.000
82.000
83.000
rt

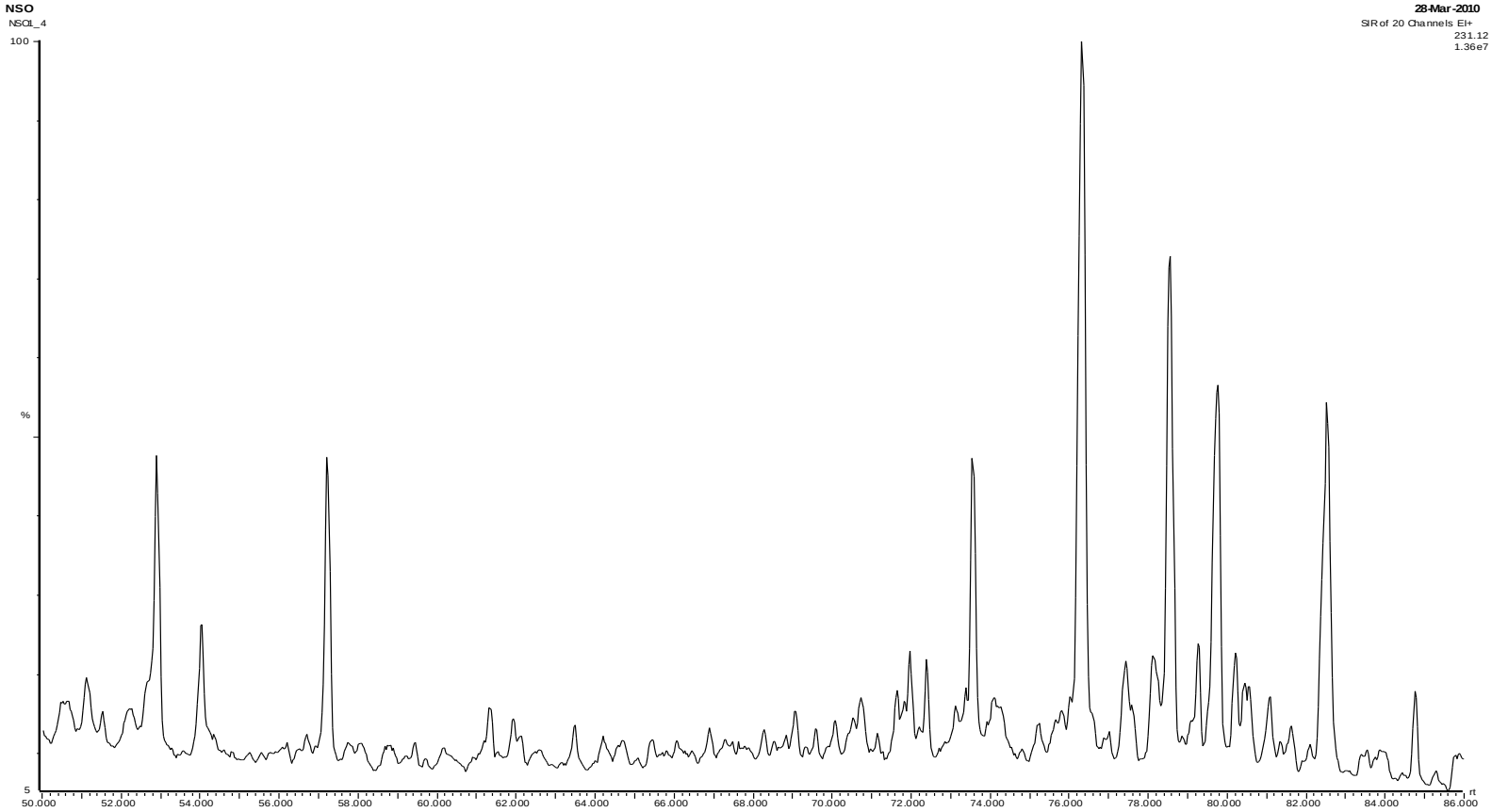
NSO
NSO1_4
28-Mar-2010
SIR of 20 Channels EI+
231.12
1.36e7
100
%
5
50.000
52.000
54.000
56.000
58.000
60.000
62.000
64.000
66.000
68.000
70.000
72.000
74.000
76.000
78.000
80.000
82.000
84.000
86.000
rt

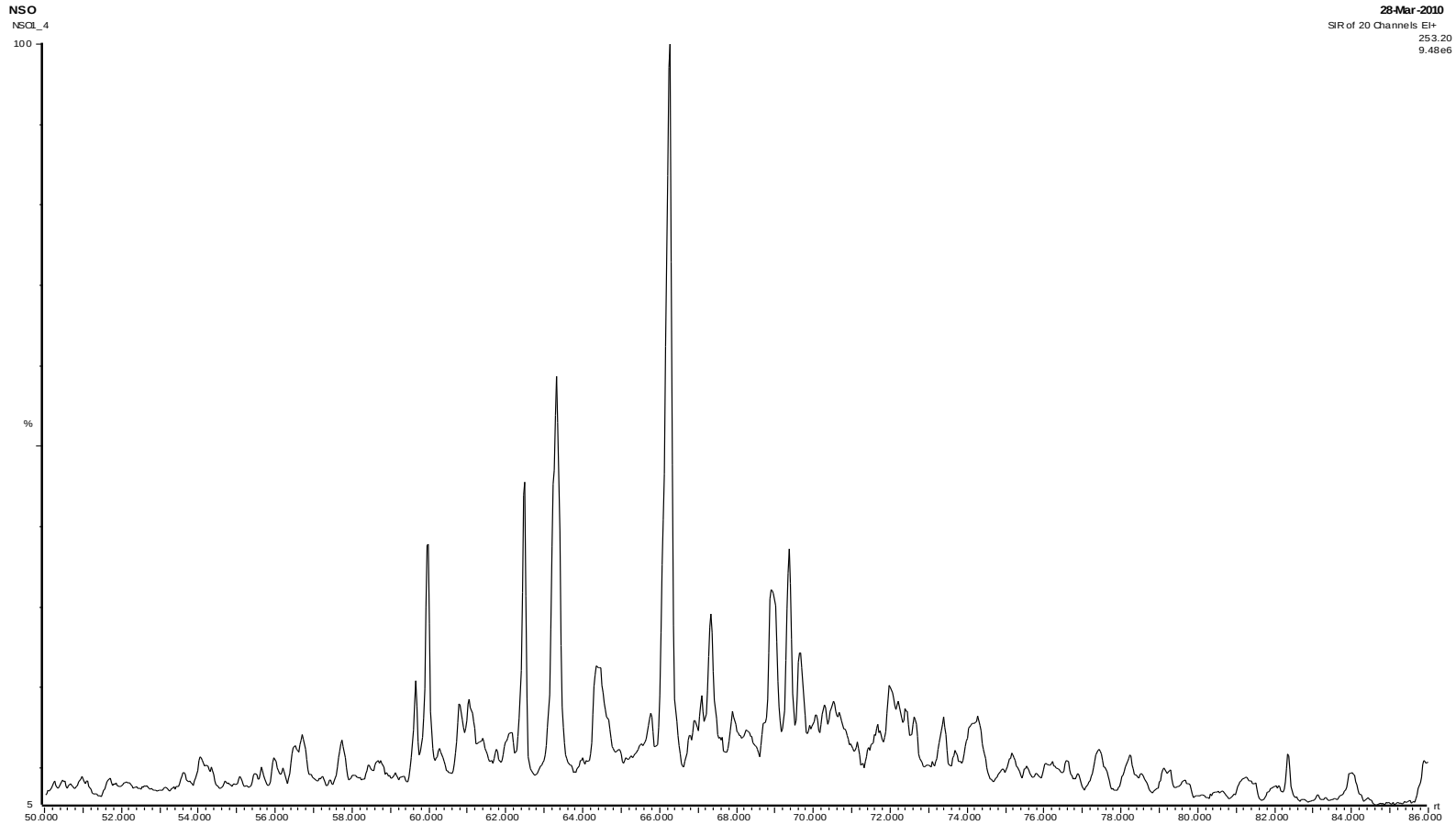
NSO
NSOL_4
28-Mar-2010
SIR of 20 Channels EI+
253.20
9.48e6
100
%
5
50.000
52.000
54.000
56.000
58.000
60.000
62.000
64.000
66.000
68.000
70.000
72.000
74.000
76.000
78.000
80.000
82.000
84.000
86.000
rt

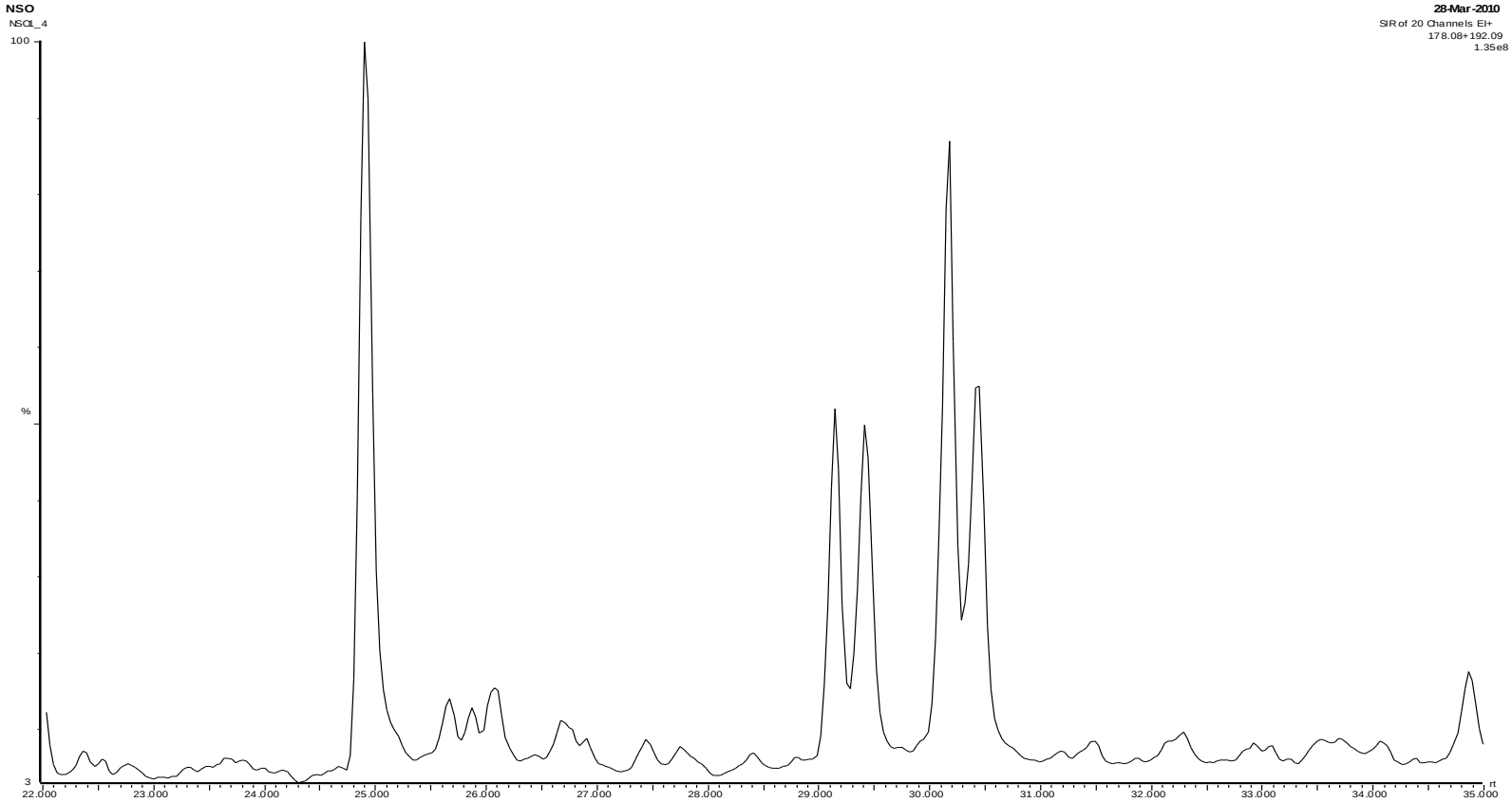
NSO
NSOL_4
28-Mar-2010
SIR of 20 Channels EI+
178.08+192.09
1.35e8
100
%
3
22.000
23.000
24.000
25.000
26.000
27.000
28.000
29.000
30.000
31.000
32.000
33.000
34.000
35.000
rt

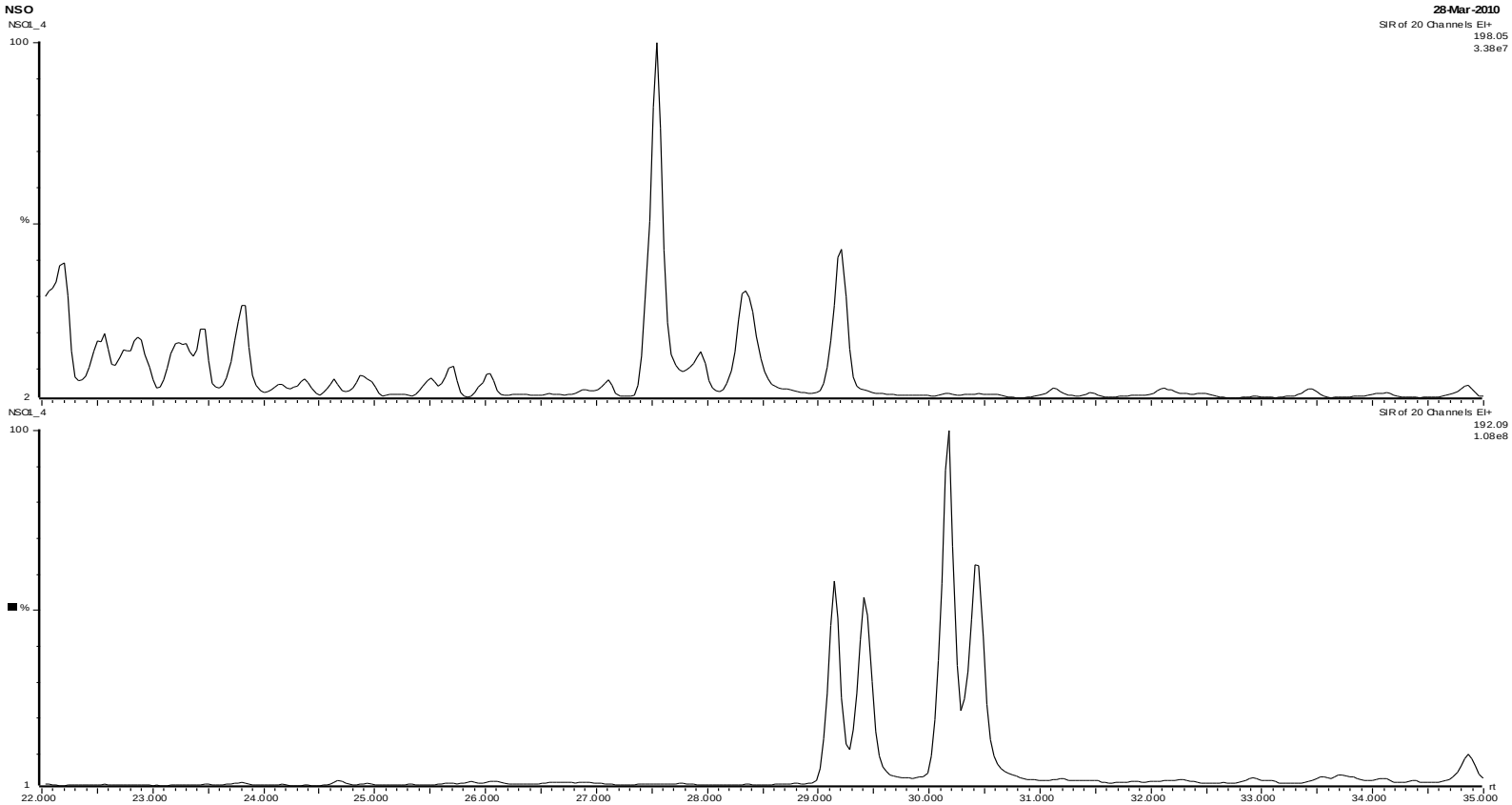
NSO
28-Mar-2010
NSO1_4
SIR of 20 Channels EI+
198.05
3.38e7
100
%
2
NSO1_4
SIR of 20 Channels EI+
192.09
1.08e8
100
%
1
22.000
23.000
24.000
25.000
26.000
27.000
28.000
29.000
30.000
31.000
32.000
33.000
34.000
35.000
rt

GC-MS Chromatograms for sample E2

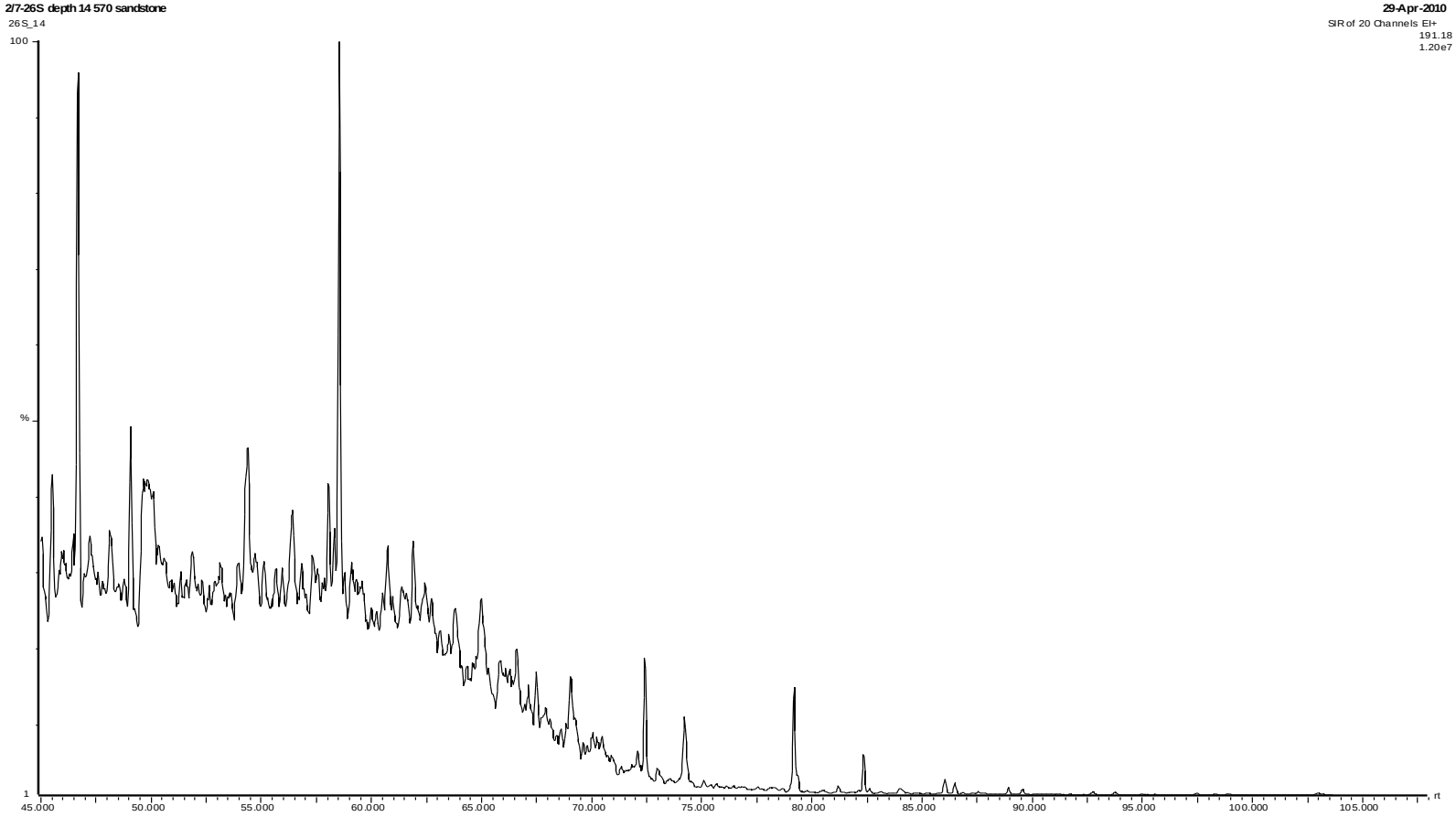
2/7-26S depth 14 570 sandstone
26S_14
29-Apr-2010
SIR of 20 Channels EI+
191.18
1.20e7
100
%
1
45.000
50.000
55.000
60.000
65.000
70.000
75.000
80.000
85.000
90.000
95.000
100.000
105.000
rt

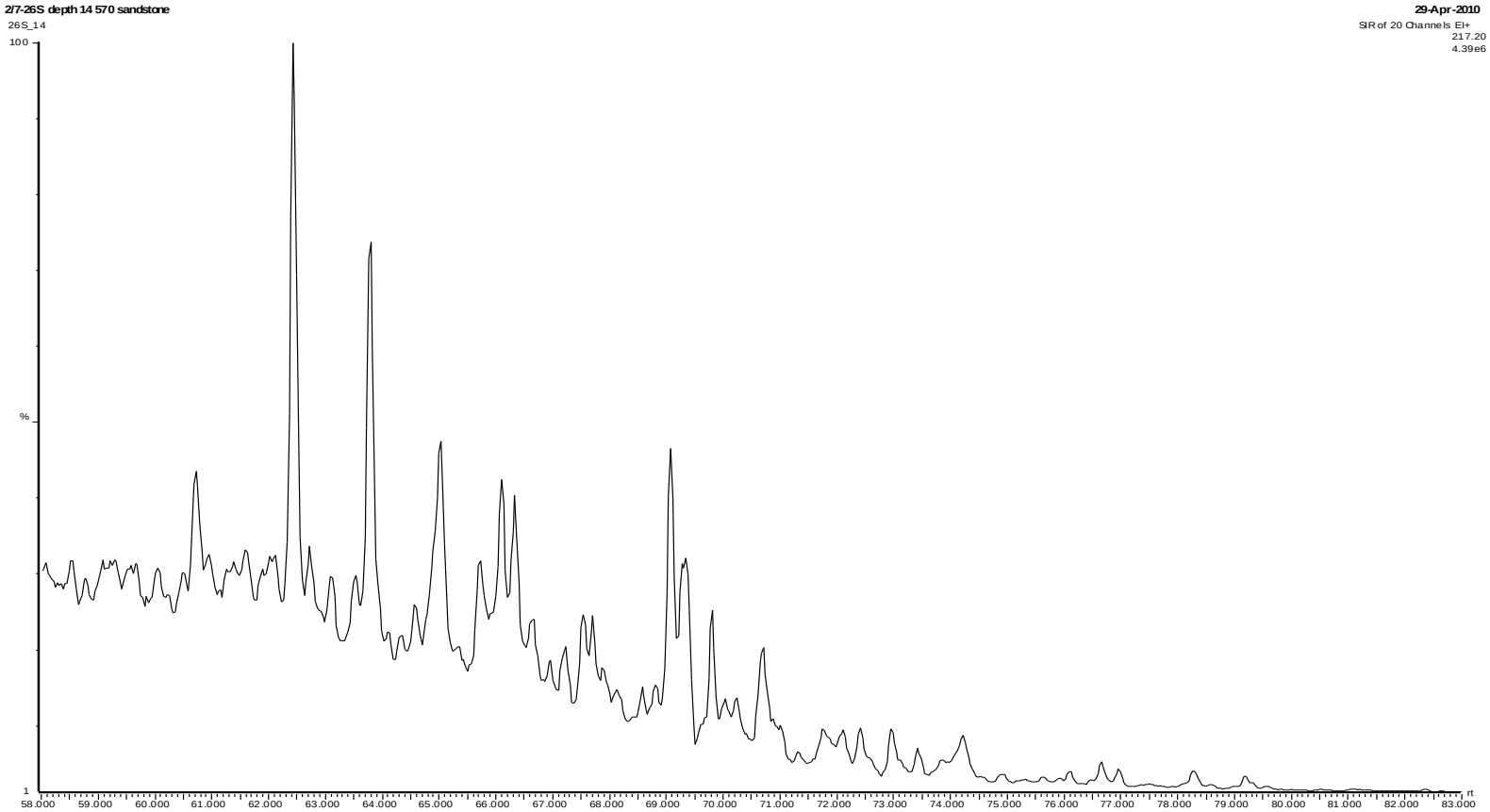
2/7-26S depth 14 570 sandstone
29-Apr-2010
26S_14
SIR of 20 Channels EI+
217.20
4.39e6
100
%
1
58.000
59.000
60.000
61.000
62.000
63.000
64.000
65.000
66.000
67.000
68.000
69.000
70.000
71.000
72.000
73.000
74.000
75.000
76.000
77.000
78.000
79.000
80.000
81.000
82.000
83.000
rt

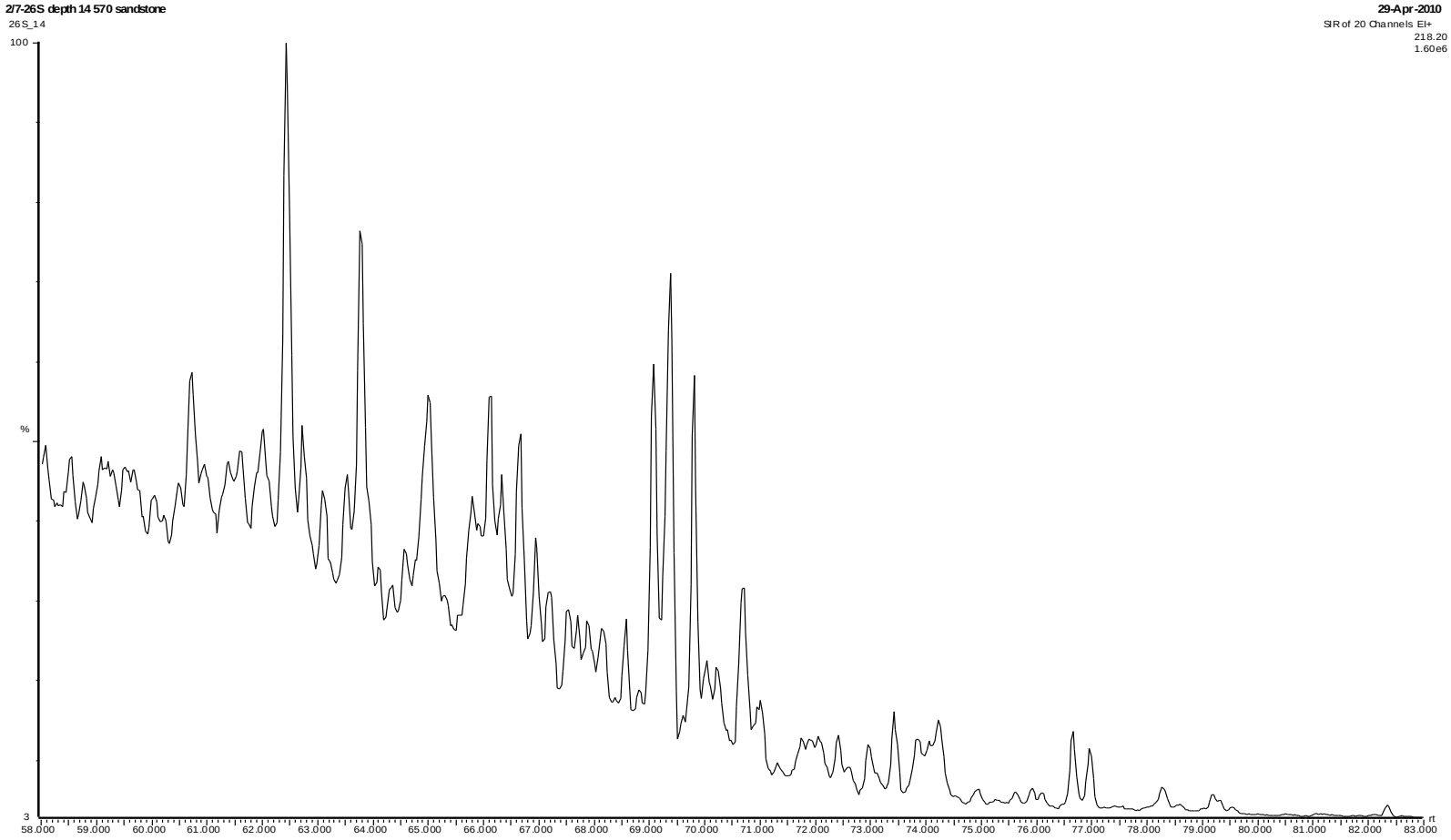
2/7-26S depth 14 570 sandstone
29-Apr-2010
26S_14
SIR of 20 Channels El+
218.20
1.60e6
100
%
3
58.000
59.000
60.000
61.000
62.000
63.000
64.000
65.000
66.000
67.000
68.000
69.000
70.000
71.000
72.000
73.000
74.000
75.000
76.000
77.000
78.000
79.000
80.000
81.000
82.000
83.000
ft

‘

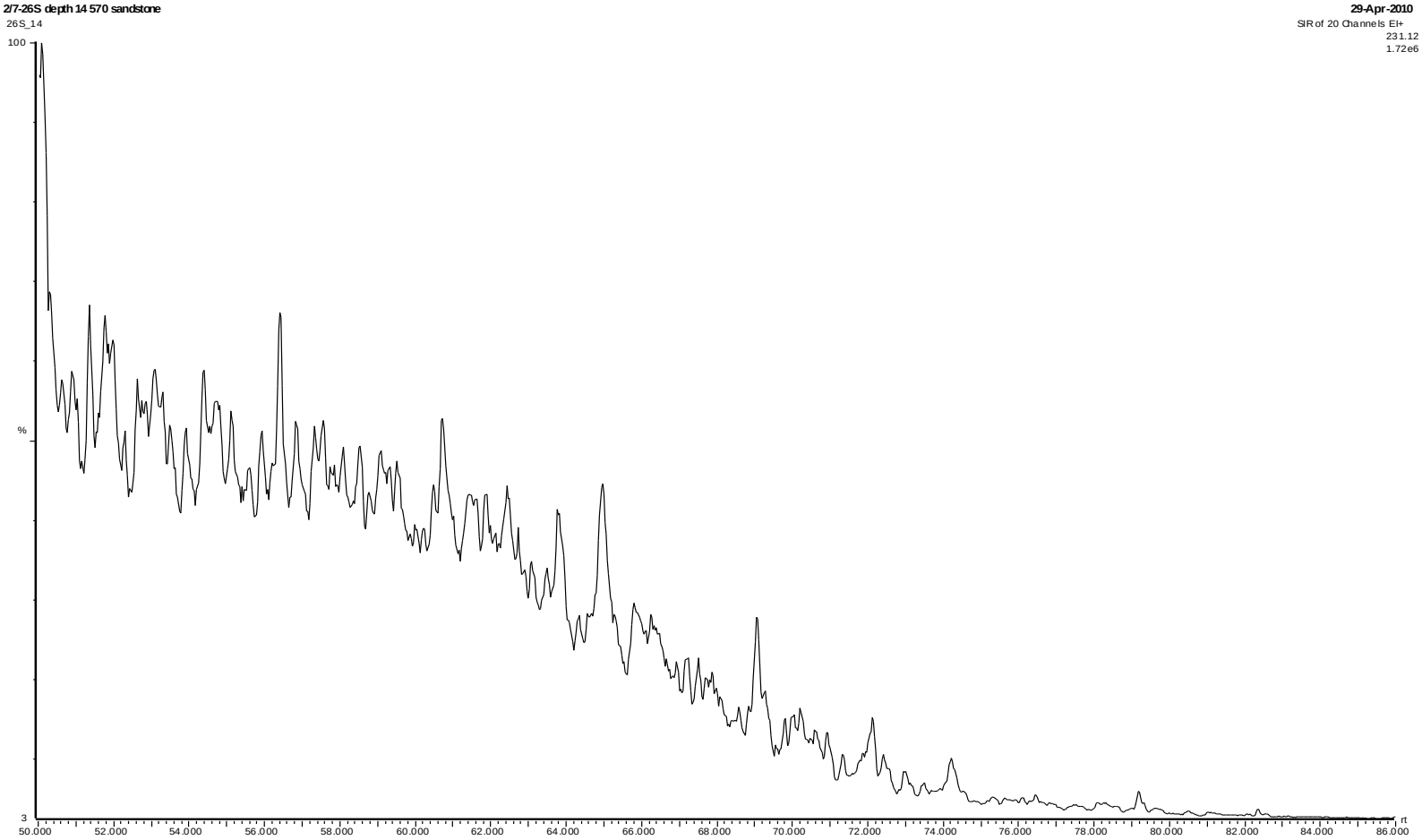
2/7-26S depth 14 570 sandstone
29-Apr-2010
26S_14
SIR of 20 Channels EI+
231.12
1.72e6
100
%
3
50.000
52.000
54.000
56.000
58.000
60.000
62.000
64.000
66.000
68.000
70.000
72.000
74.000
76.000
78.000
80.000
82.000
84.000
86.000
ft

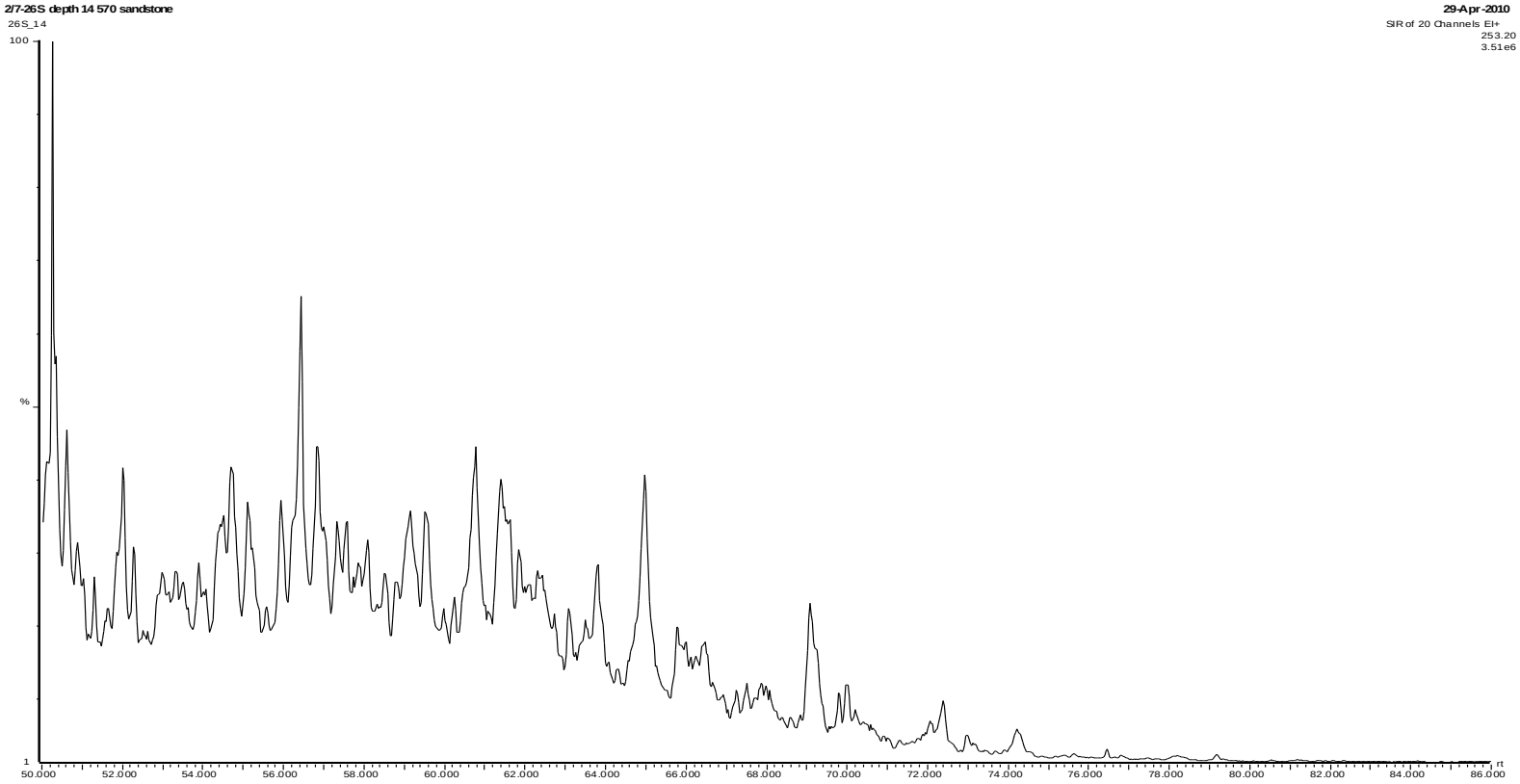
2/7-26S depth 14 570 sandstone
29-Apr-2010
26S_14
SIR of 20 Channels EI+
253.20
3.51e6
100
%
1
50.000
52.000
54.000
56.000
58.000
60.000
62.000
64.000
66.000
68.000
70.000
72.000
74.000
76.000
78.000
80.000
82.000
84.000
86.000
rt

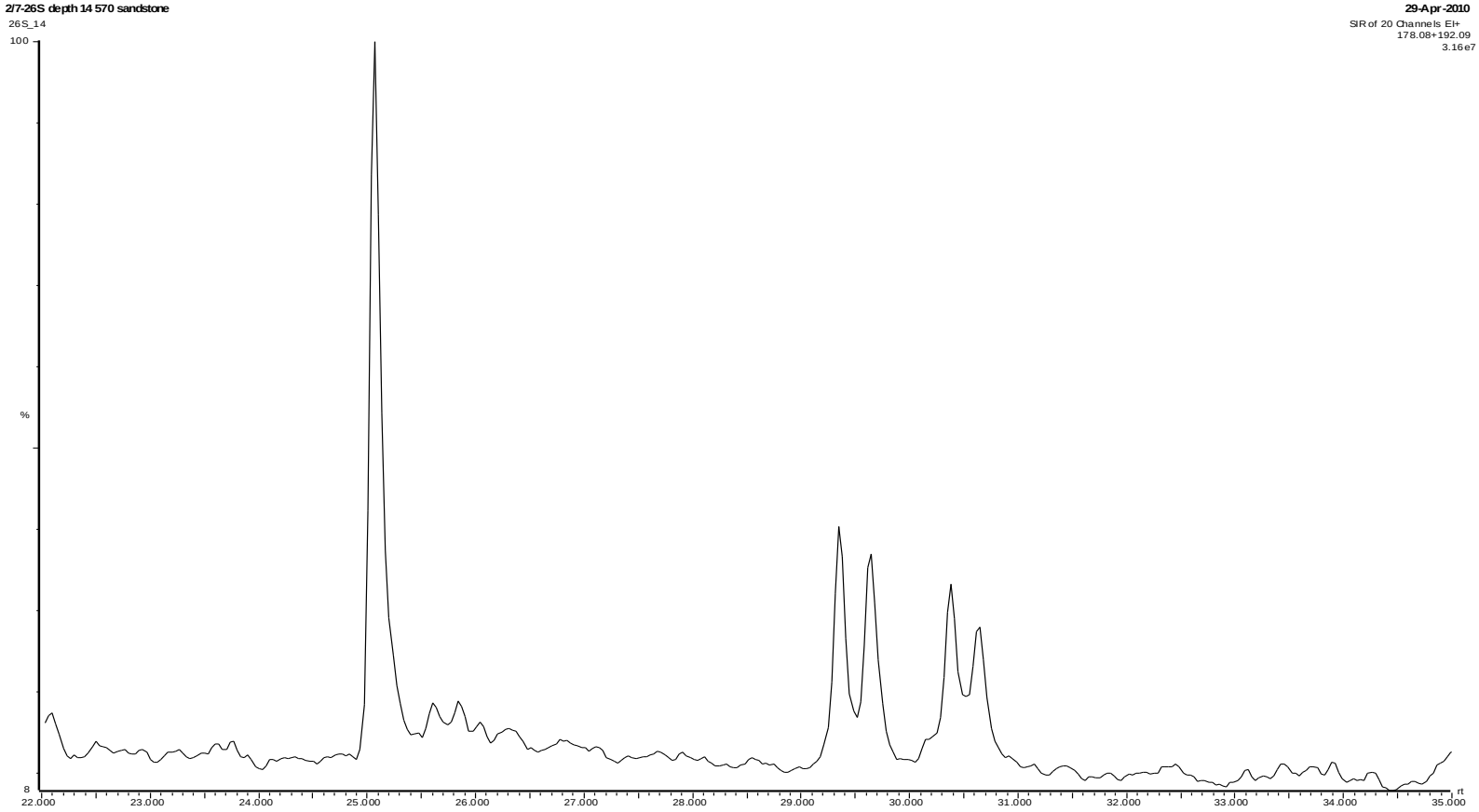
2/7-26S depth 14 570 sandstone
26S_14
29-Apr-2010
SIR of 20 Channels EI+
178.08+192.09
3.16e7
100
%
8
22.000
23.000
24.000
25.000
26.000
27.000
28.000
29.000
30.000
31.000
32.000
33.000
34.000
35.000
rt

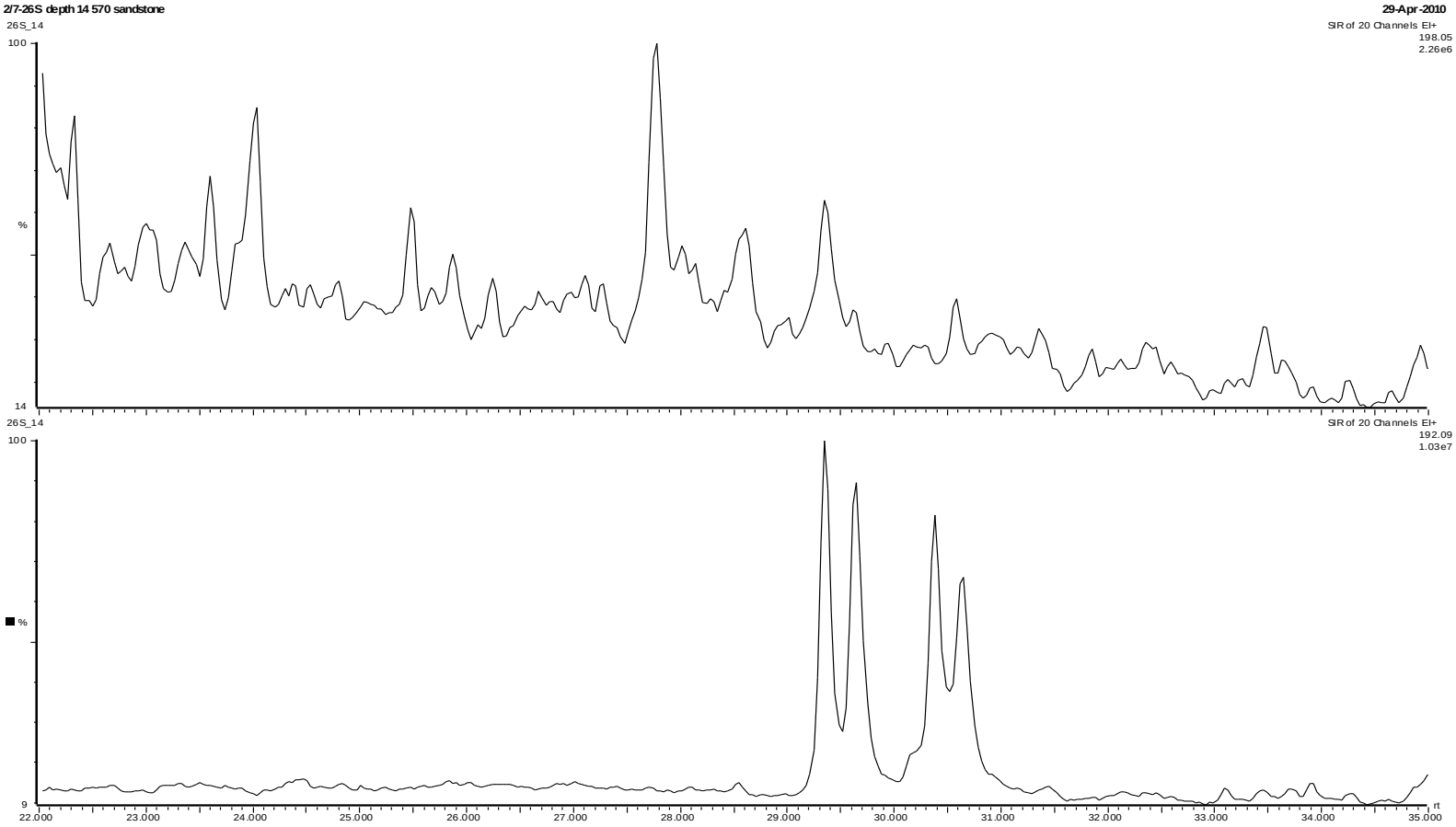
2/7-26S depth 14 570 sandstone
29-Apr-2010
26S_14
SIR of 20 Channels EI+
198.05
2.26e6
100
%
14
26S_14
SIR of 20 Channels EI+
192.09
1.03e7
100
%
9
22.000
23.000
24.000
25.000
26.000
27.000
28.000
29.000
30.000
31.000
32.000
33.000
34.000
35.000
rt

GC-MS Chromatograms for sample E4

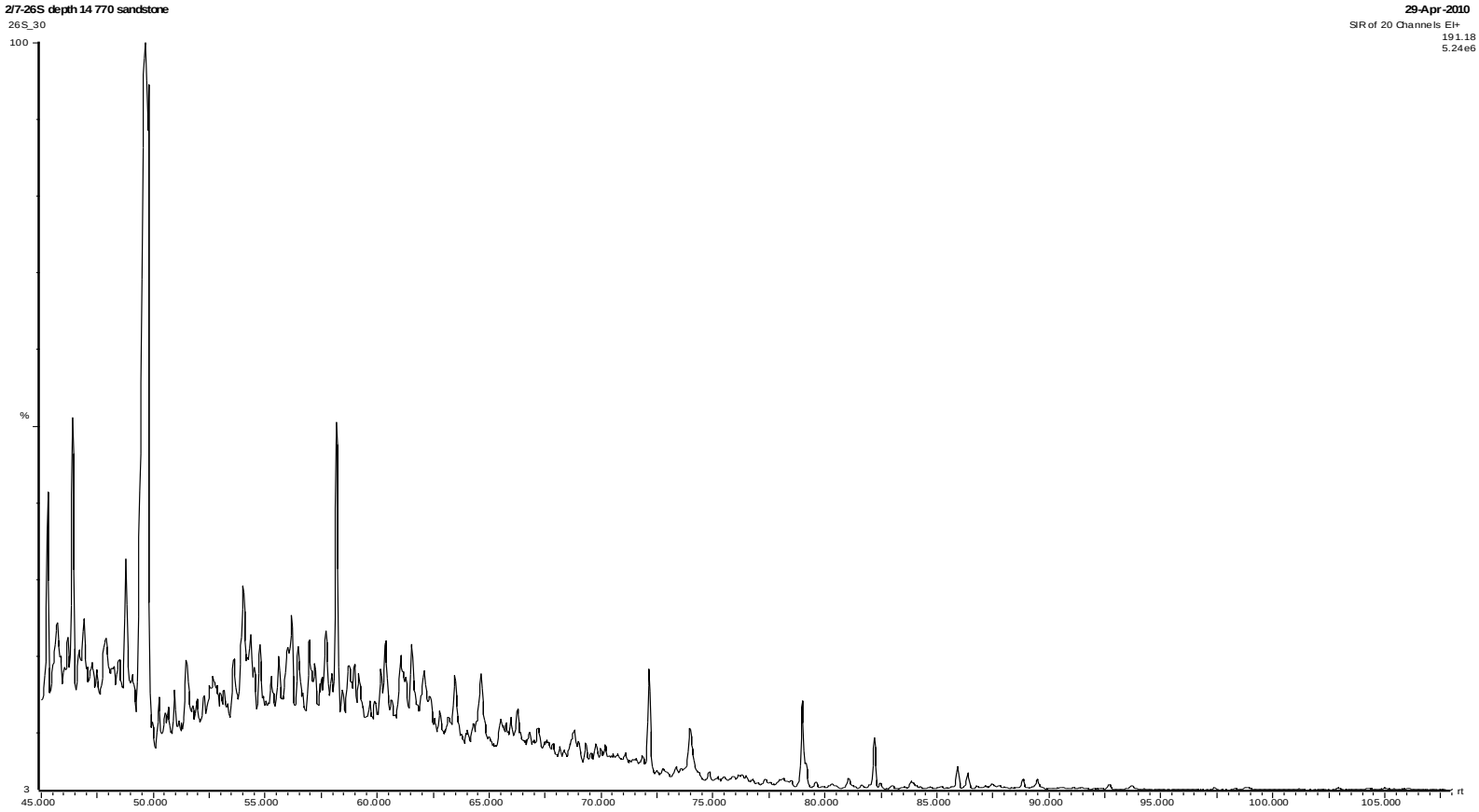
2/7-26S depth 14 770 sandstone
29-Apr-2010
26S_30
SIR of 20 Channels EI+
191.18
5.24e6
100
%
3
45.000
50.000
55.000
60.000
65.000
70.000
75.000
80.000
85.000
90.000
95.000
100.000
105.000
rt

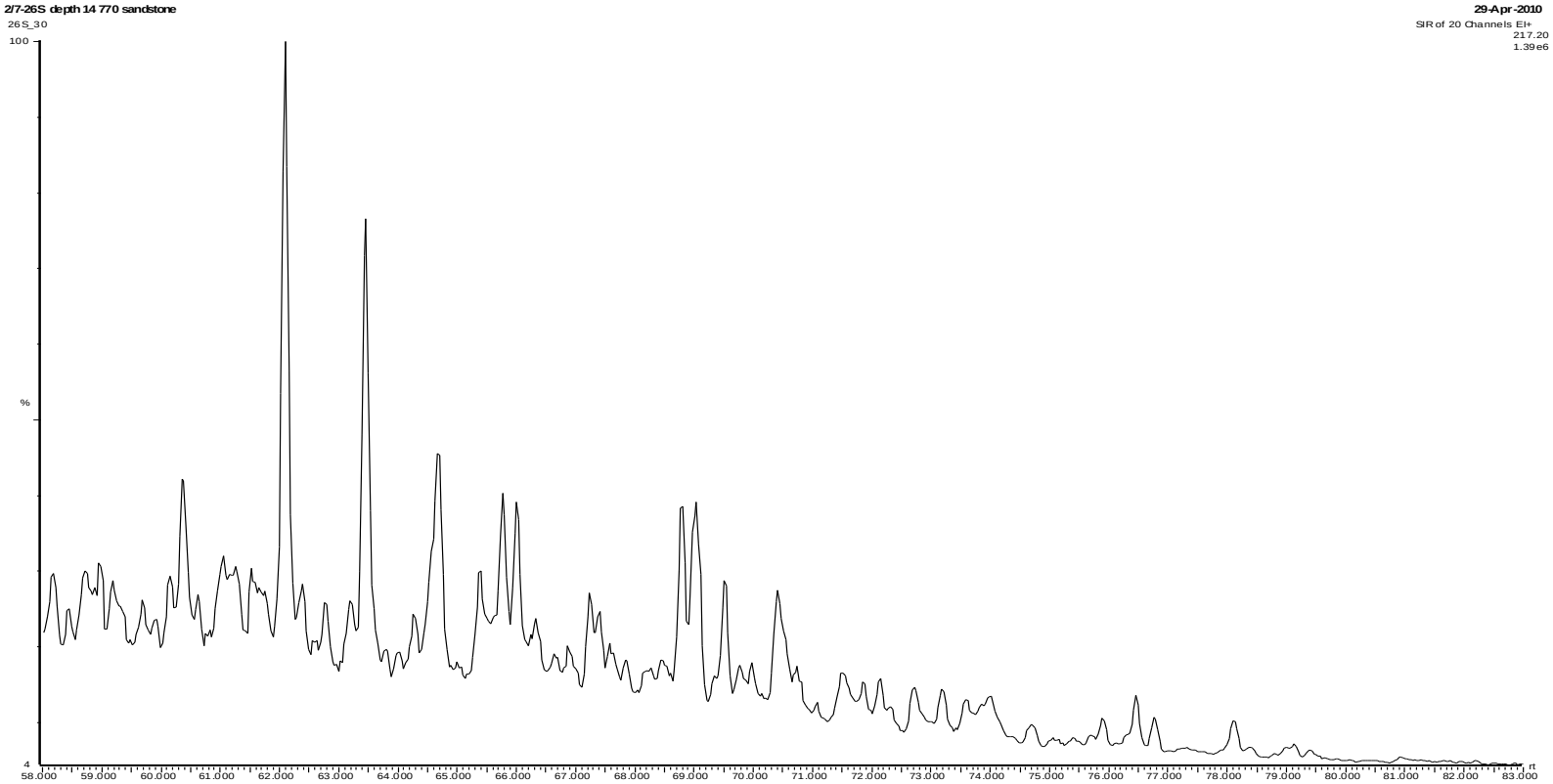
2/7-26S depth 14 770 sandstone
29-Apr-2010
26S_30
SIR of 20 Channels EI+
217.20
1.39e6
100
%
4
58.000
59.000
60.000
61.000
62.000
63.000
64.000
65.000
66.000
67.000
68.000
69.000
70.000
71.000
72.000
73.000
74.000
75.000
76.000
77.000
78.000
79.000
80.000
81.000
82.000
83.000
rt

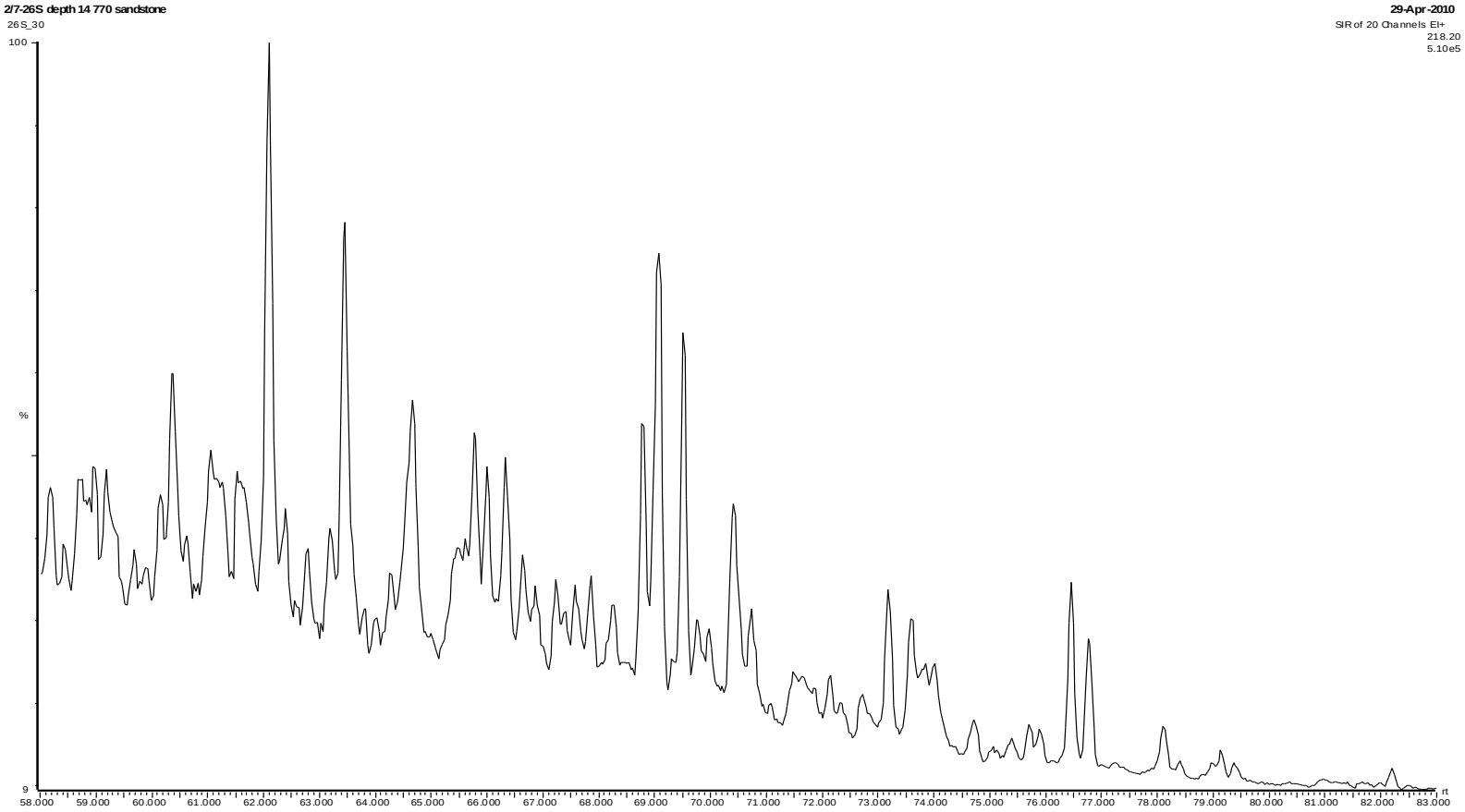
2/7-26S depth 14 770 sandstone
29-Apr-2010
26S_30
SIR of 20 Channels EI+
218.20
5.10e5
100
%
9
58.000
59.000
60.000
61.000
62.000
63.000
64.000
65.000
66.000
67.000
68.000
69.000
70.000
71.000
72.000
73.000
74.000
75.000
76.000
77.000
78.000
79.000
80.000
81.000
82.000
83.000
rt

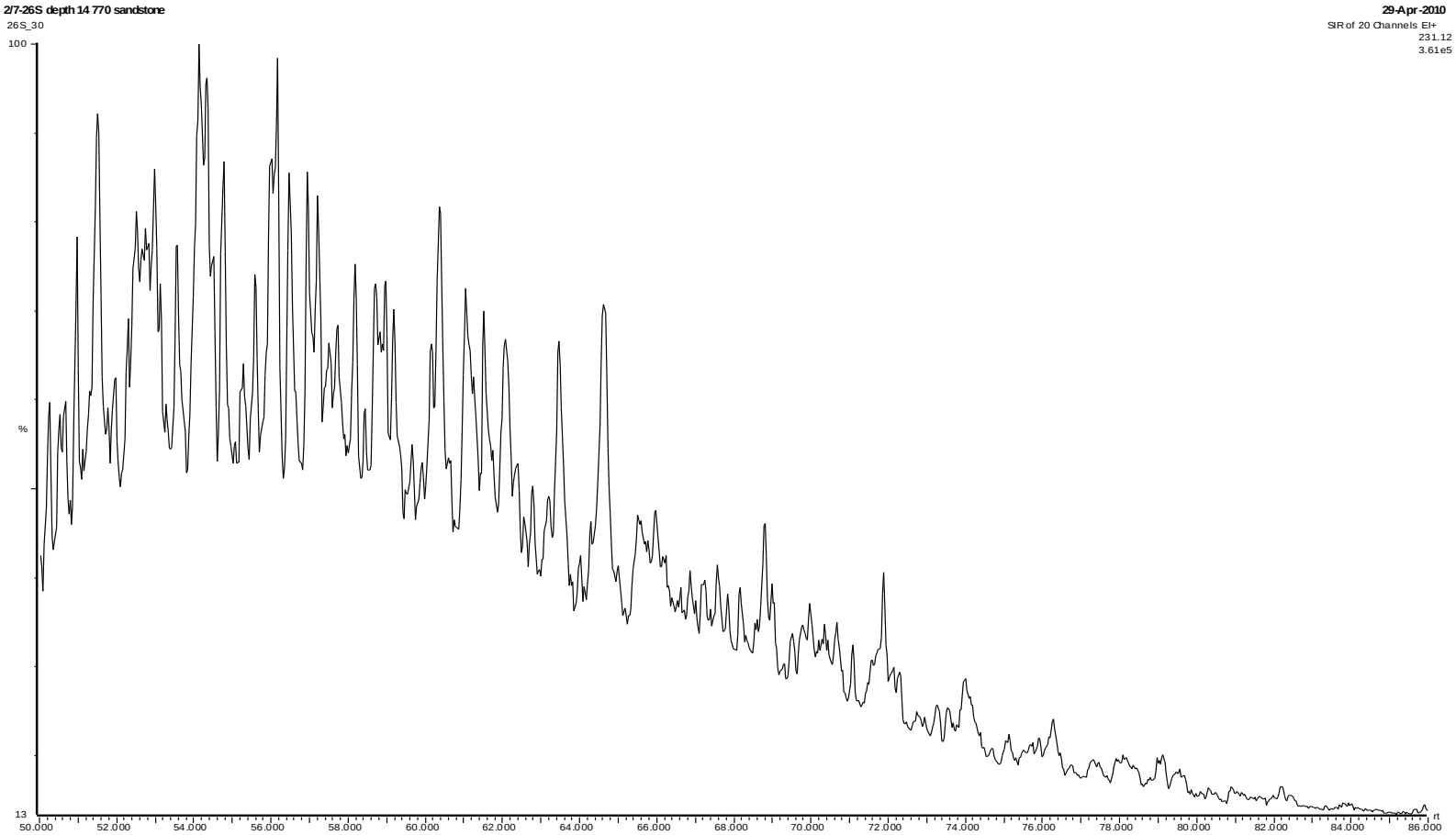
2/7-26S depth 14 770 sandstone
26S_30
29-Apr-2010
SIR of 20 Channels EI+
231.12
3.61e5
100
%
13
50.000
52.000
54.000
56.000
58.000
60.000
62.000
64.000
66.000
68.000
70.000
72.000
74.000
76.000
78.000
80.000
82.000
84.000
86.000
rt

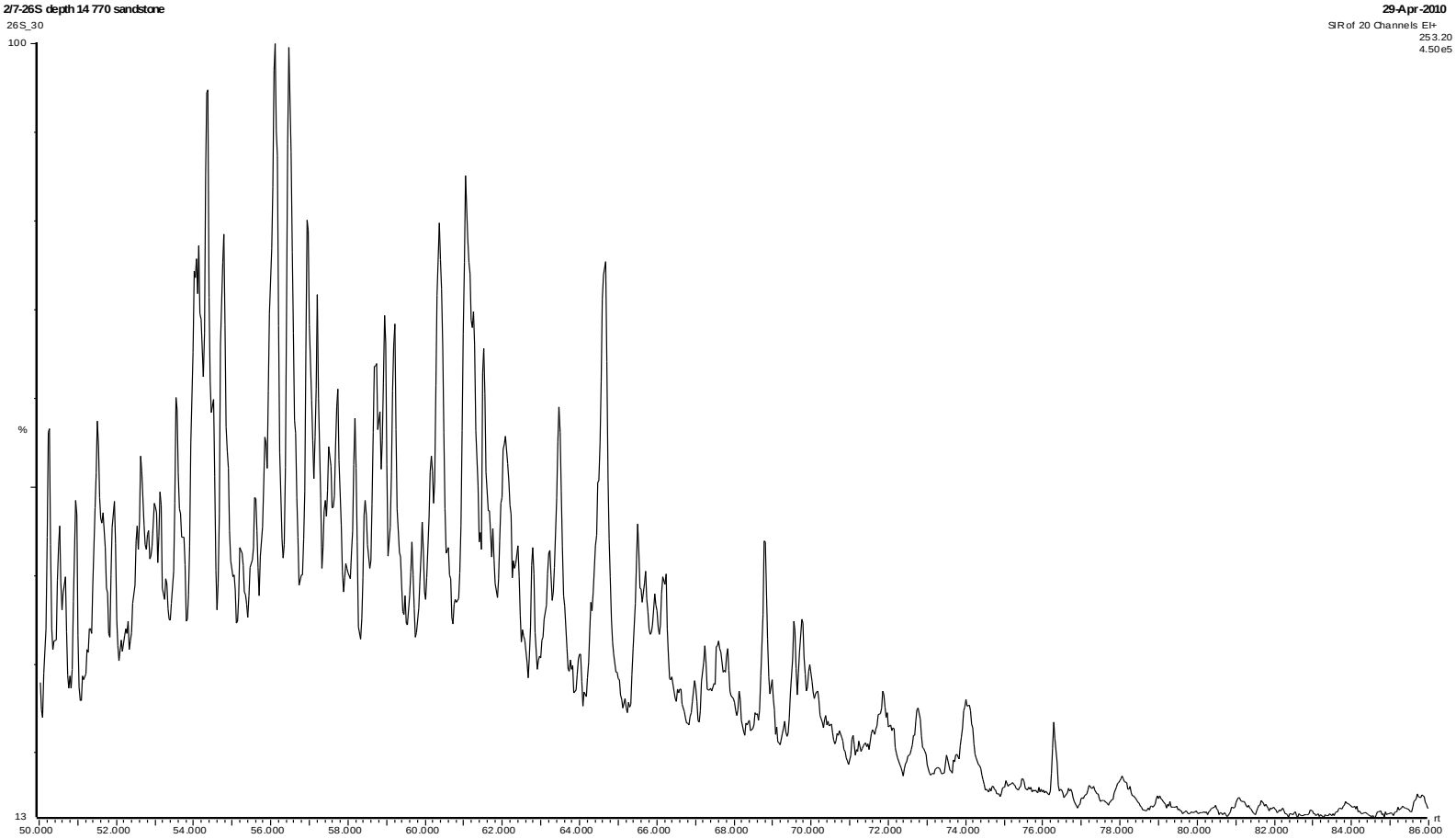
2/7-26S depth 14 770 sandstone
29-Apr-2010
26S_30
SIR of 20 Channels EI+
253.20
4.50e5
100
%
13
50.000
52.000
54.000
56.000
58.000
60.000
62.000
64.000
66.000
68.000
70.000
72.000
74.000
76.000
78.000
80.000
82.000
84.000
86.000
rt

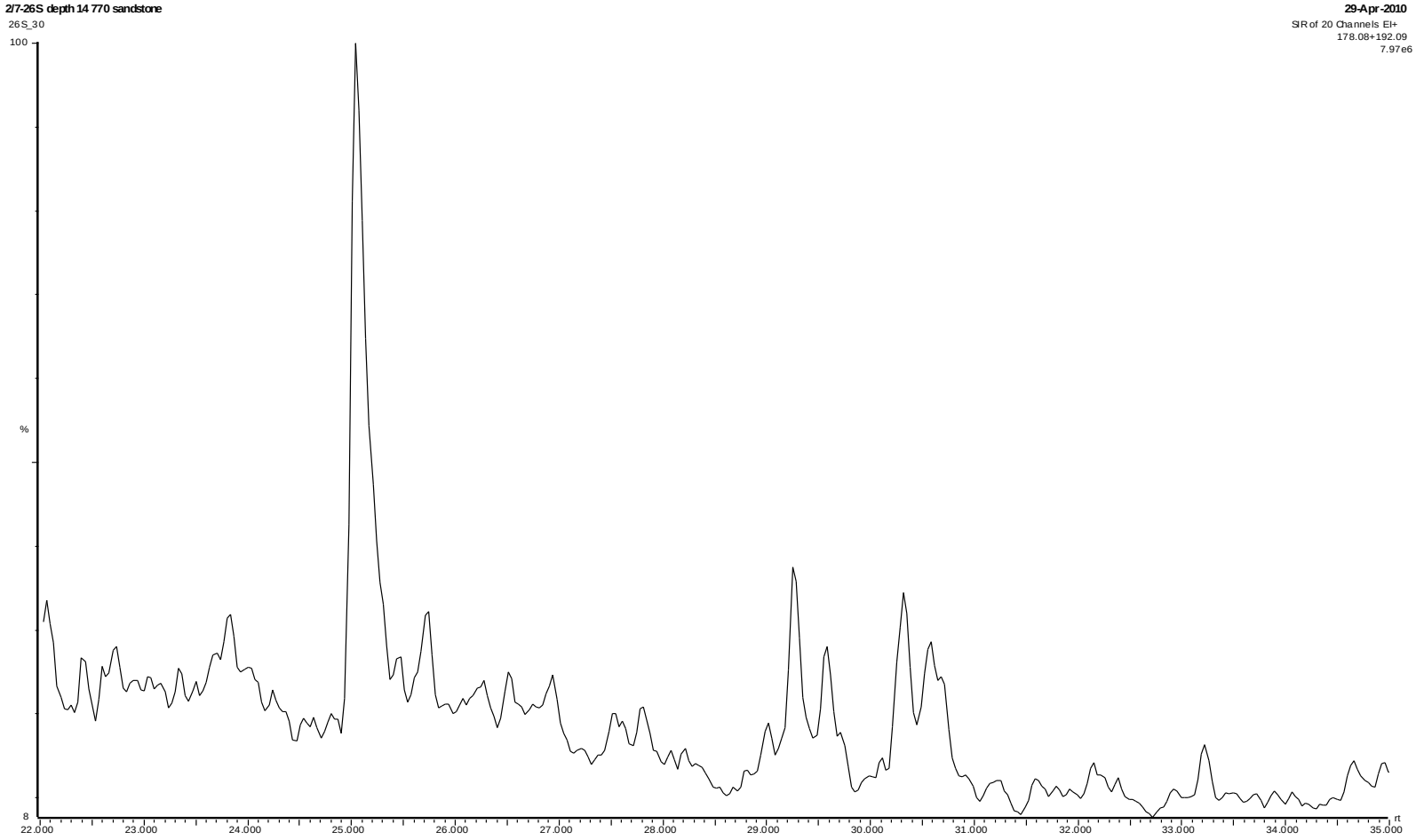
2/7-26S depth 14 770 sandstone
26S_30
29-Apr-2010
SIR of 20 Channels EI+
178.08+192.09
7.97e6
100
%
8
22.000
23.000
24.000
25.000
26.000
27.000
28.000
29.000
30.000
31.000
32.000
33.000
34.000
35.000
rt

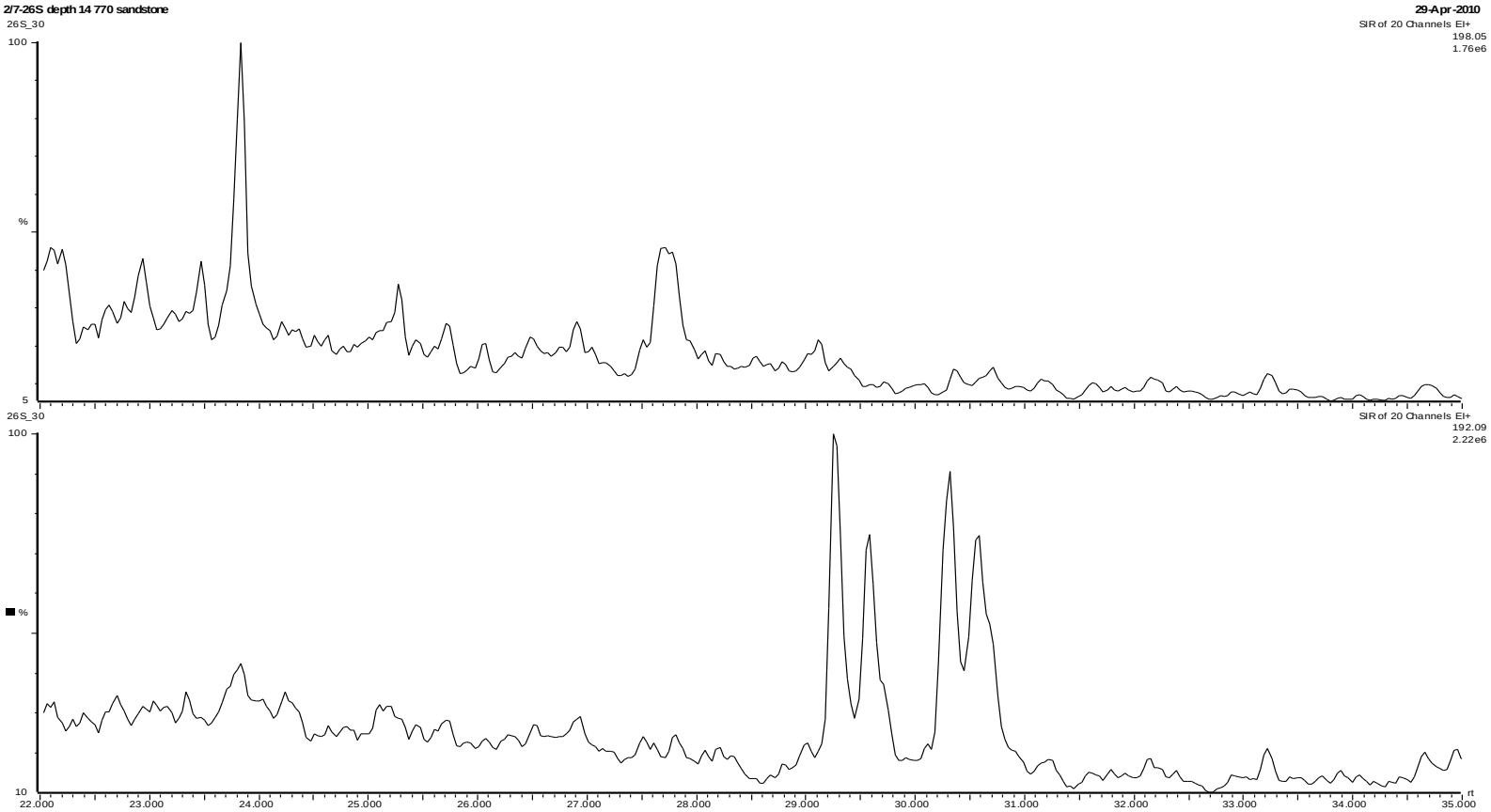
2/7-26S depth 14 770 sandstone
29-Apr-2010
26S_30
SIR of 20 Channels EI+
198.05
1.76e6
100
%
5
26S_30
SIR of 20 Channels EI+
192.09
2.22e6
100
%
10
22.000
23.000
24.000
25.000
26.000
27.000
28.000
29.000
30.000
31.000
32.000
33.000
34.000
35.000
rt

GC-MS Chromatograms for sample E5

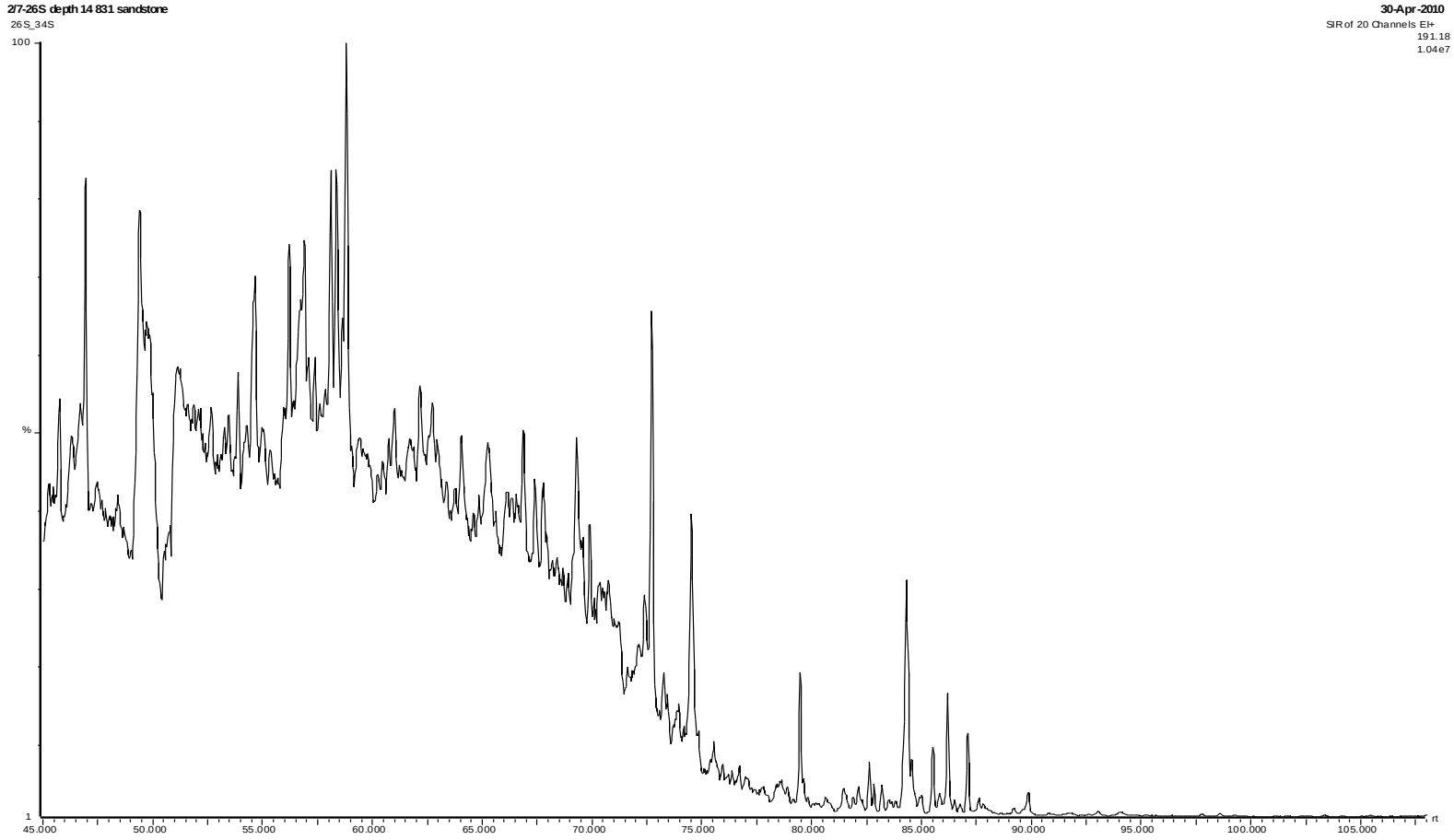
2/7-26S depth 14 831 sandstone
26S_34S
100
%
1
45.000
50.000
55.000
60.000
65.000
70.000
75.000
80.000
85.000
90.000
95.000
100.000
105.000
rt
30-Apr-2010
SIR of 20 Channels EI+
191.18
1.04e7

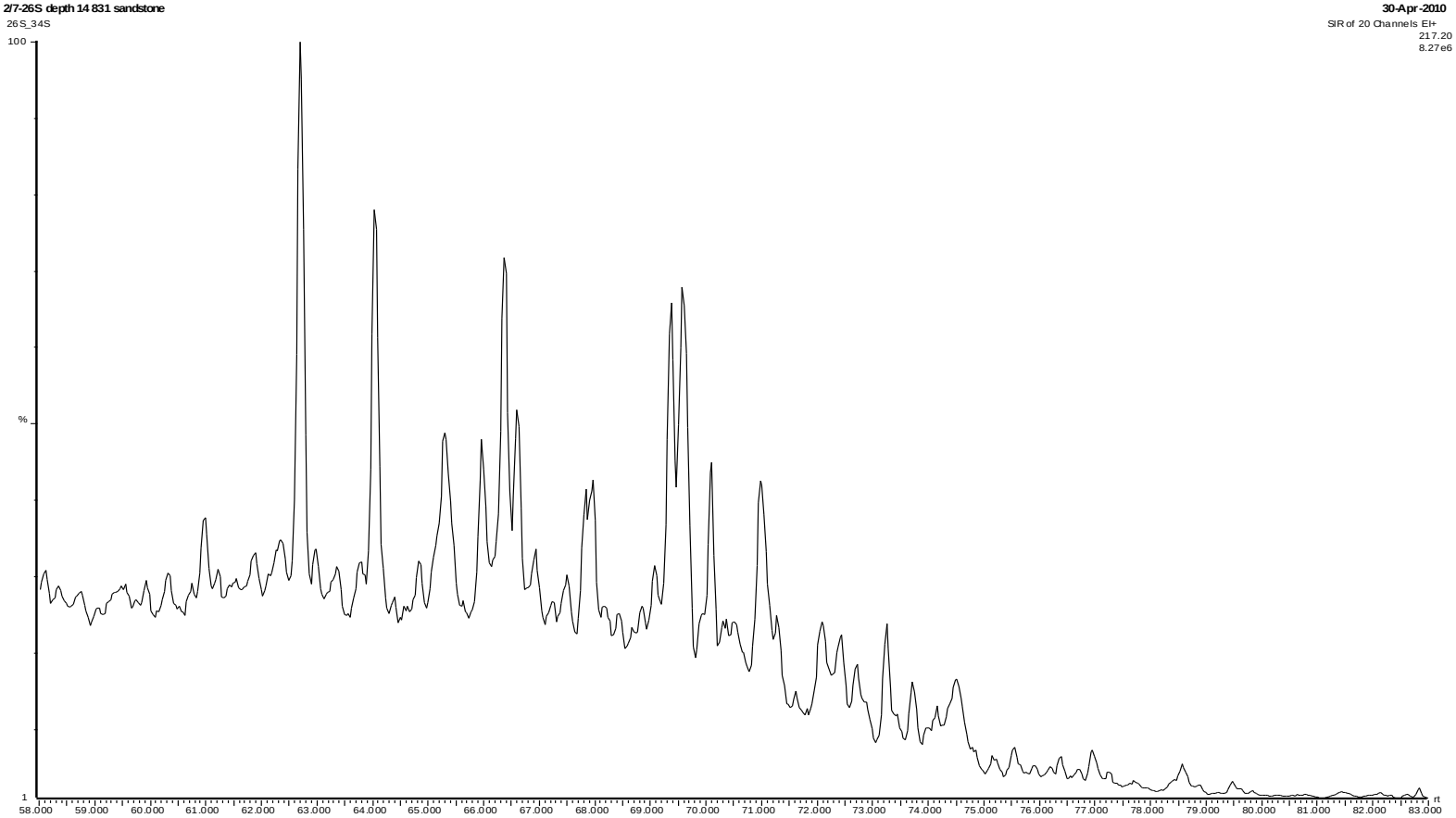
2/7-26S depth 14 831 sandstone
30-Apr-2010
26S_34S
SIR of 20 Channels EI+
217.20
8.27e6
100
%
1
58.000
59.000
60.000
61.000
62.000
63.000
64.000
65.000
66.000
67.000
68.000
69.000
70.000
71.000
72.000
73.000
74.000
75.000
76.000
77.000
78.000
79.000
80.000
81.000
82.000
83.000
rt

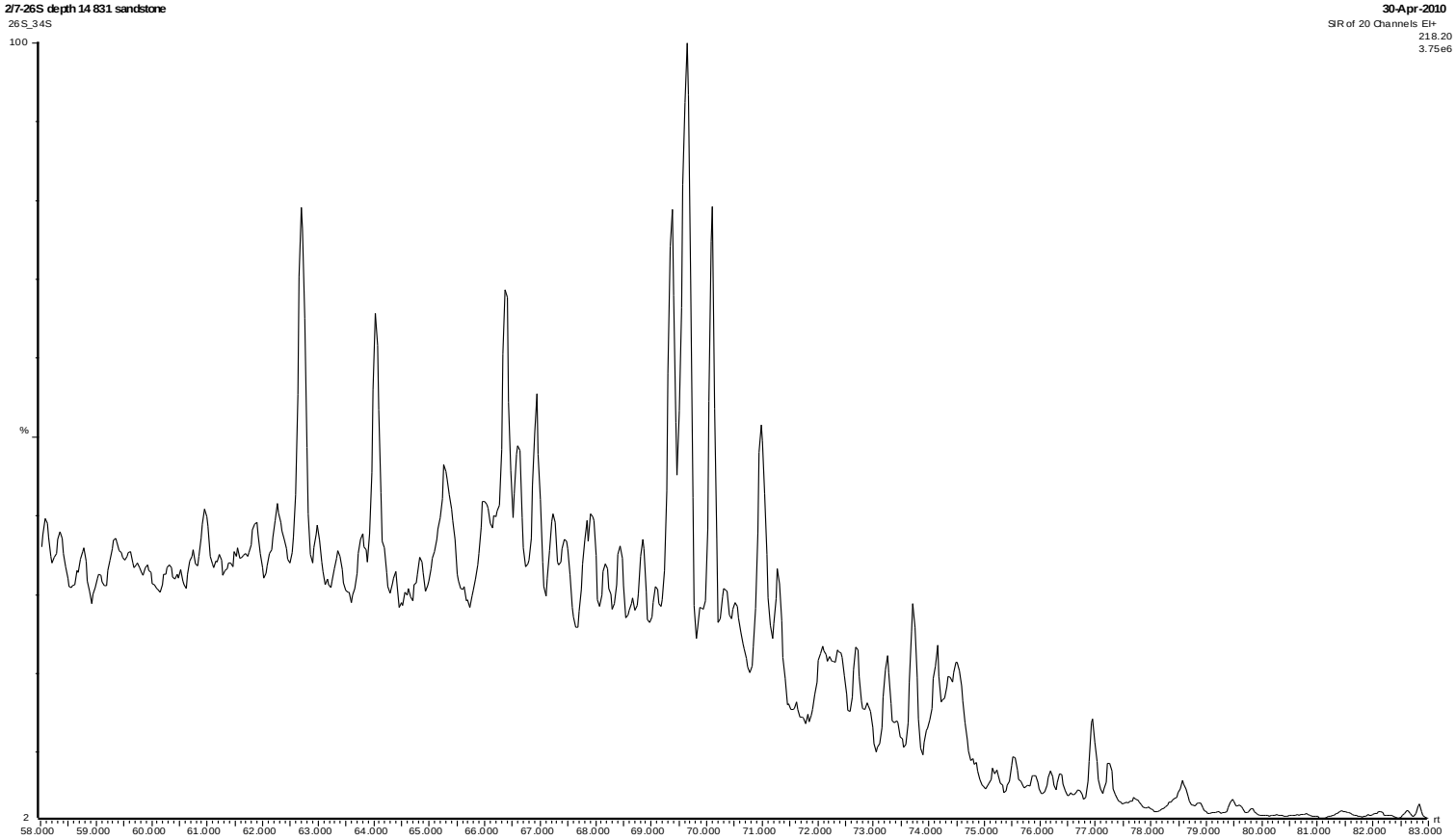
2/7-26S depth 14 831 sandstone
26S_34S
30-Apr-2010
SIR of 20 Channels EI+
218.20
3.75e6
100
%
2
58.000
59.000
60.000
61.000
62.000
63.000
64.000
65.000
66.000
67.000
68.000
69.000
70.000
71.000
72.000
73.000
74.000
75.000
76.000
77.000
78.000
79.000
80.000
81.000
82.000
83.000
rt

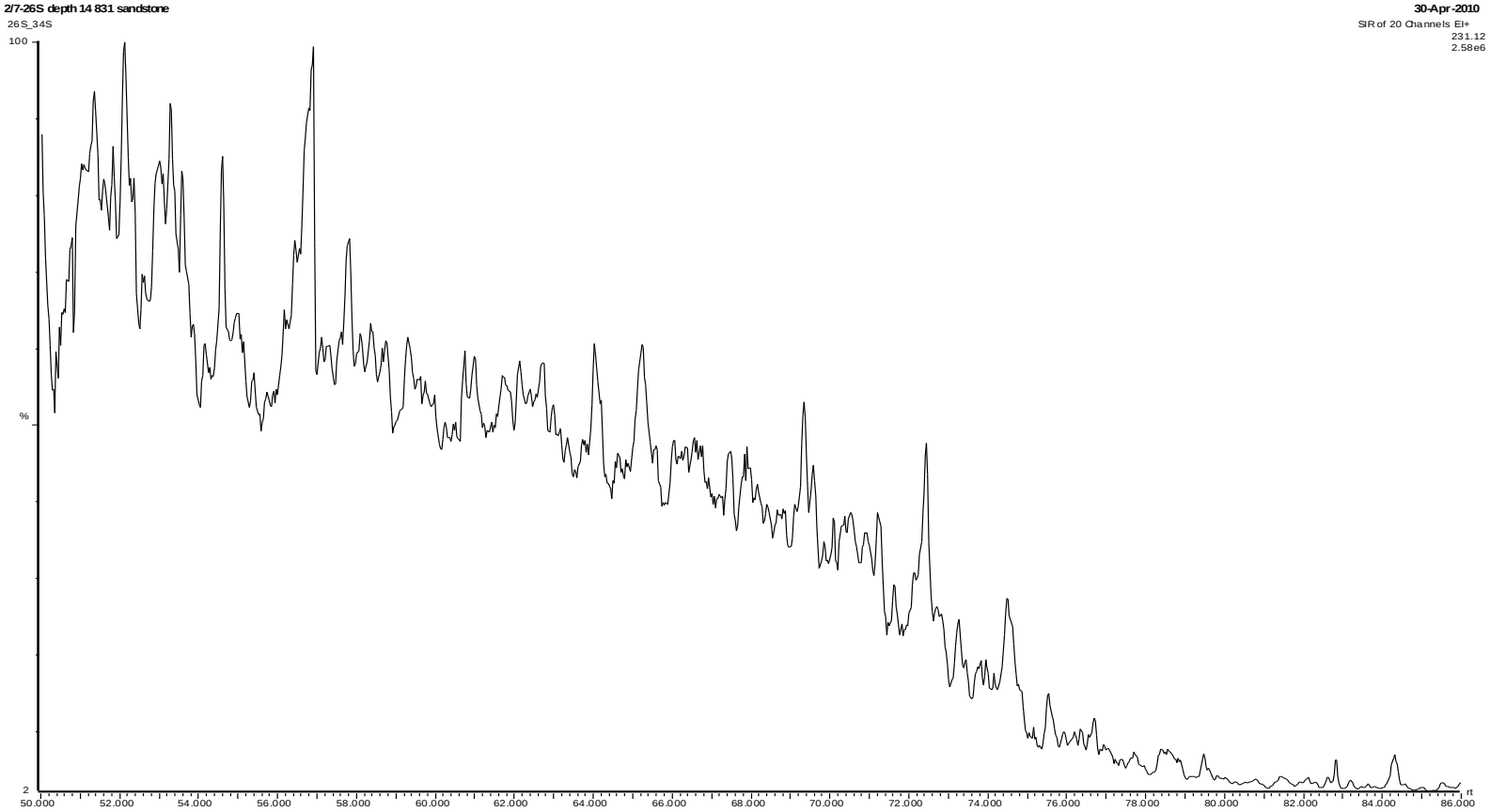
2/7-26S depth 14 831 sandstone
26S_34S
100
%
2
50.000
52.000
54.000
56.000
58.000
60.000
62.000
64.000
66.000
68.000
70.000
72.000
74.000
76.000
78.000
80.000
82.000
84.000
86.000
rt
30-Apr-2010
SIR of 20 Channels EI+
231.12
2.58e6

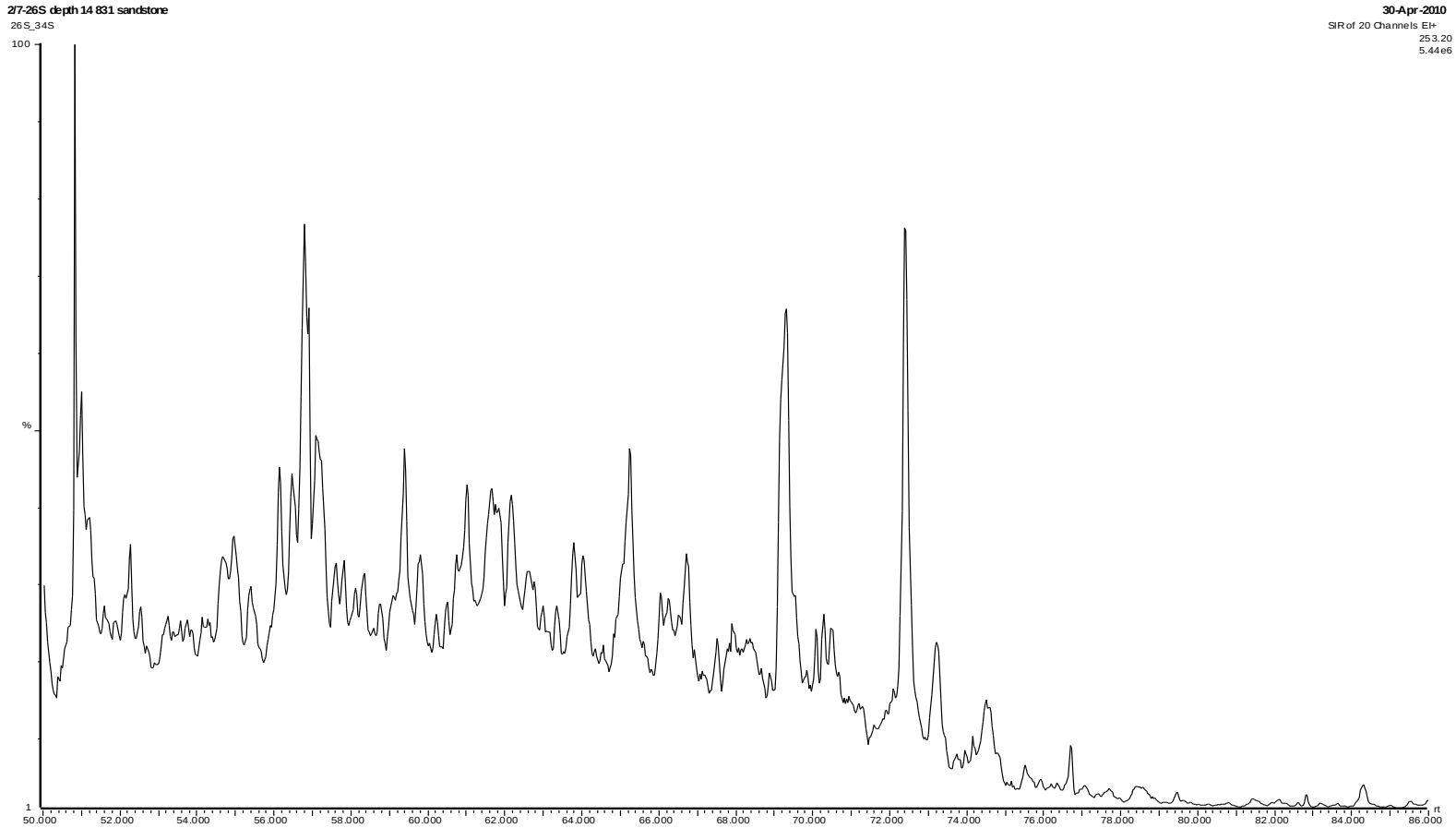
2/7-26S depth 14 831 sandstone
26S_34S
30-Apr-2010
SIR of 20 Channels EI+
253.20
5.44e6
100
%
1
50.000
52.000
54.000
56.000
58.000
60.000
62.000
64.000
66.000
68.000
70.000
72.000
74.000
76.000
78.000
80.000
82.000
84.000
86.000
rt

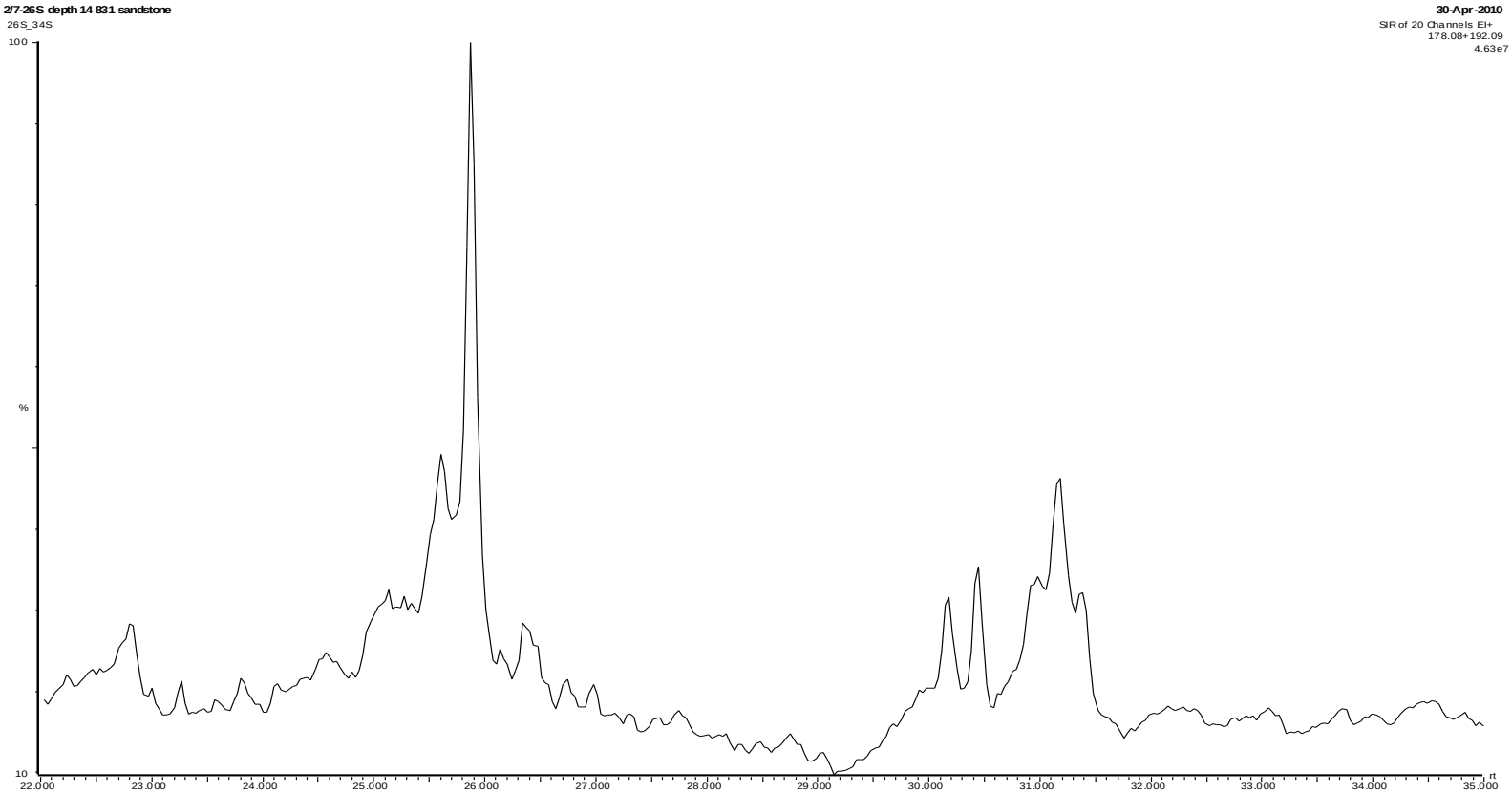
2/7-26S depth 14 831 sandstone
26S_34S
100
%
10
22.000
23.000
24.000
25.000
26.000
27.000
28.000
29.000
30.000
31.000
32.000
33.000
34.000
35.000
ft
30-Apr-2010
SIR of 20 Channels El+
178.08+192.09
4.63e7

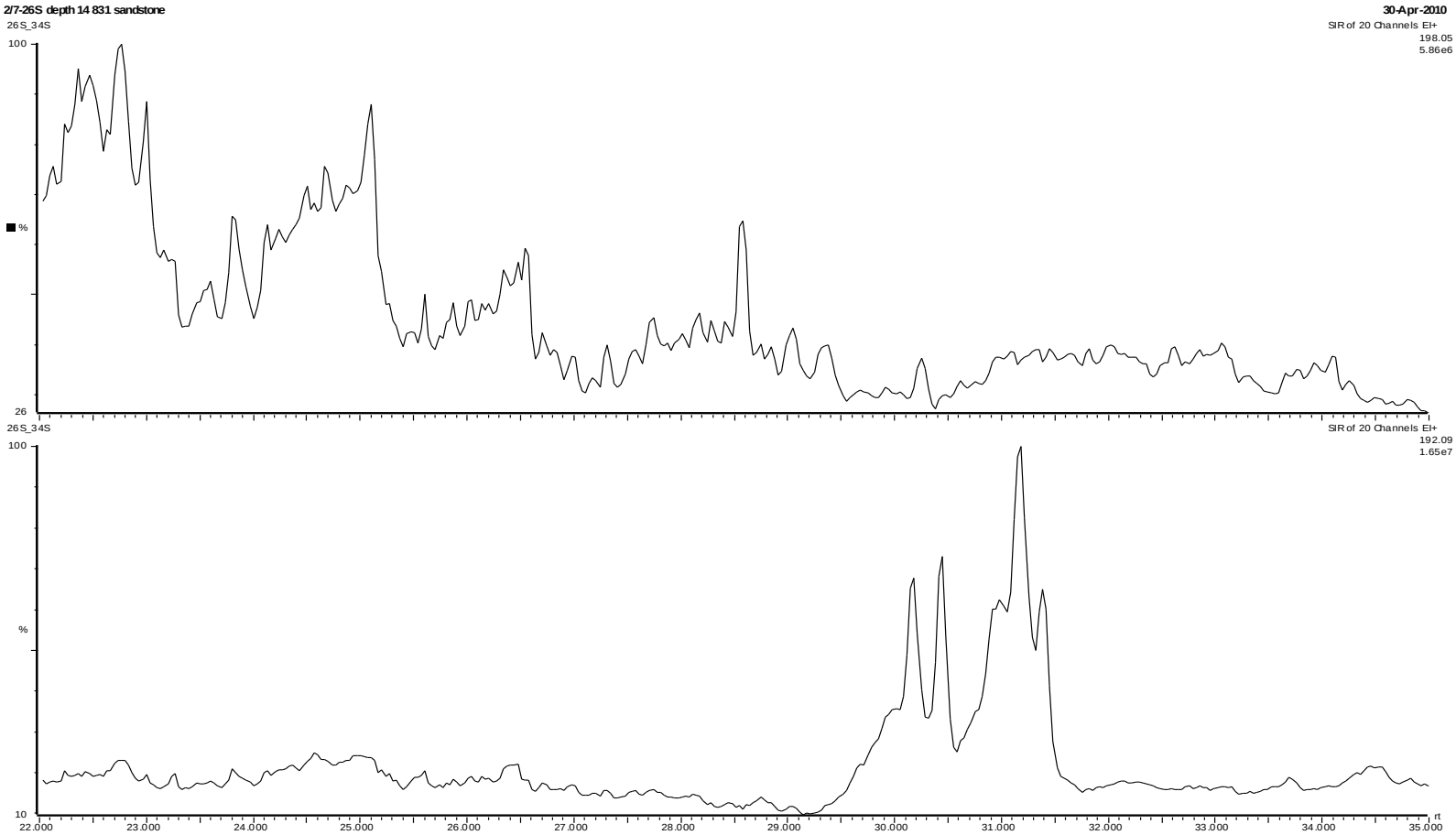
2/7-26S depth 14 831 sandstone
30-Apr-2010
26S_34S
SIR of 20 Channels EI+
198.05
5.86e6
100
%
26
26S_34S
SIR of 20 Channels EI+
192.09
1.65e7
100
%
10
22.000
23.000
24.000
25.000
26.000
27.000
28.000
29.000
30.000
31.000
32.000
33.000
34.000
35.000
rt

GC-MS Chromatograms for sample E6

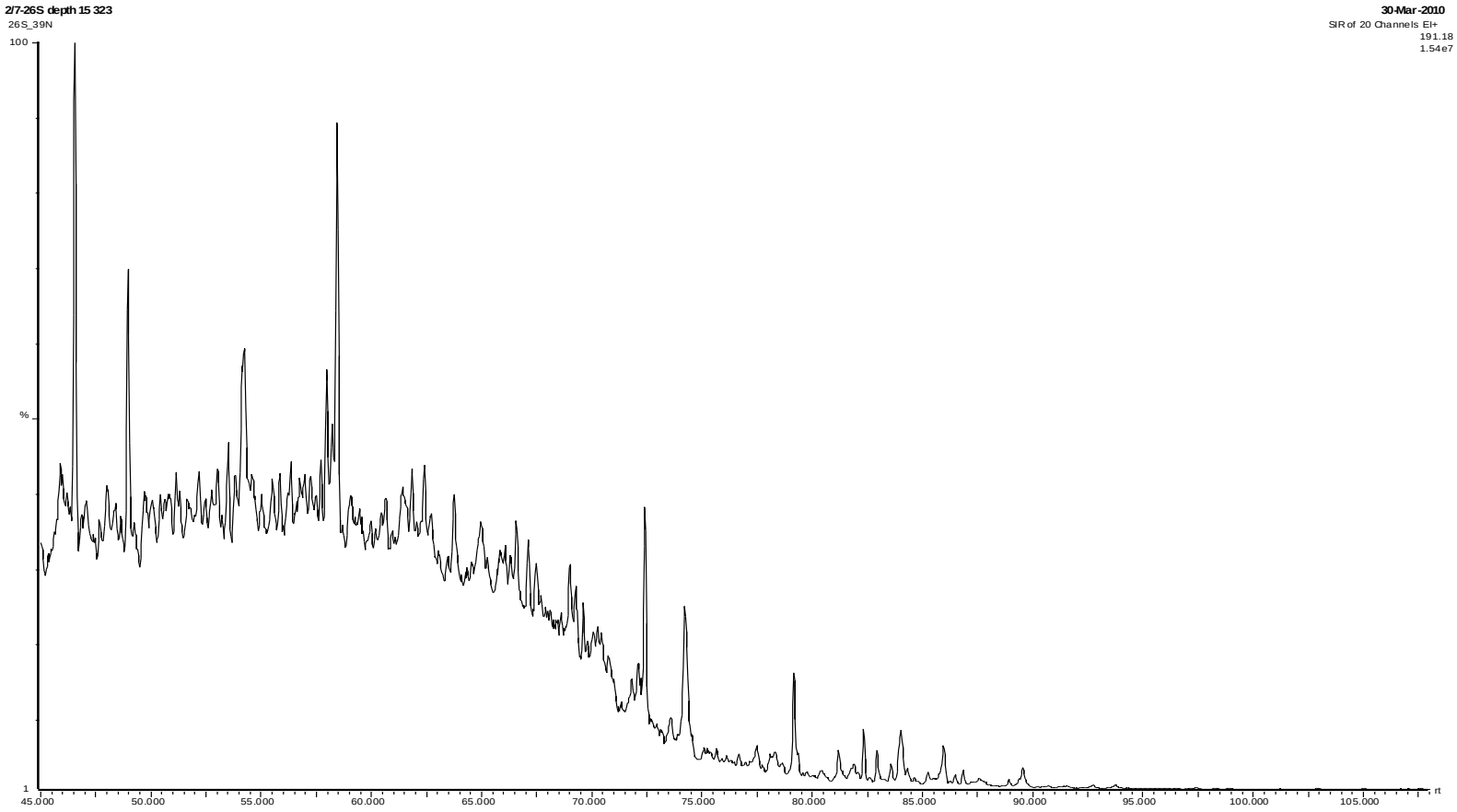
2/7-26S depth 15 323
26S_39N
30-Mar-2010
SIR of 20 Channels EI+
191.18
1.54e7
100
%
1
45.000
50.000
55.000
60.000
65.000
70.000
75.000
80.000
85.000
90.000
95.000
100.000
105.000
rt

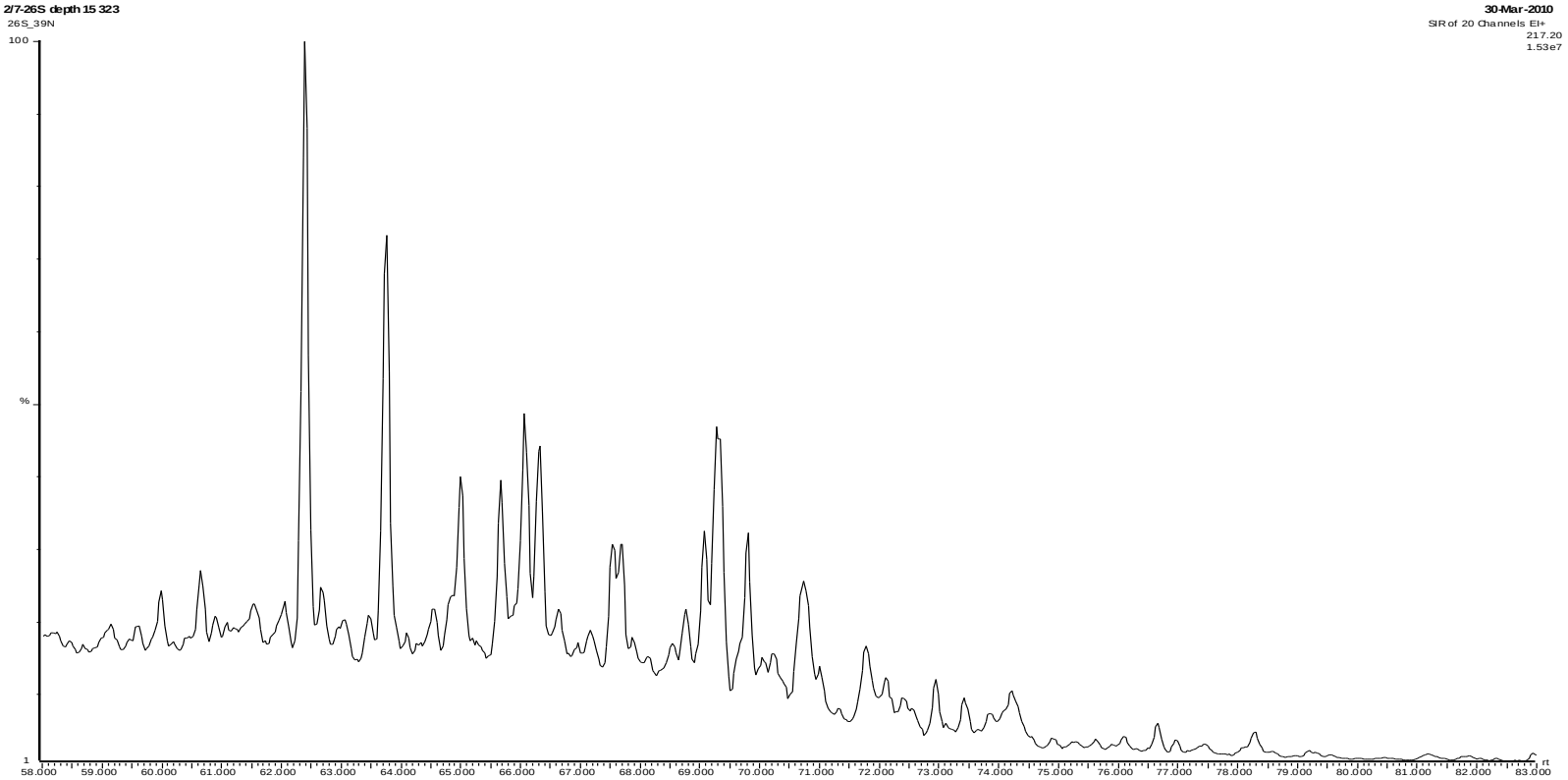
2/7-26S depth 15 323
26S_39N
100
%
1
58.000
59.000
60.000
61.000
62.000
63.000
64.000
65.000
66.000
67.000
68.000
69.000
70.000
71.000
72.000
73.000
74.000
75.000
76.000
77.000
78.000
79.000
80.000
81.000
82.000
83.000
rt
30-Mar-2010
SIR of 20 Channels EI+
217.20
1.53e7

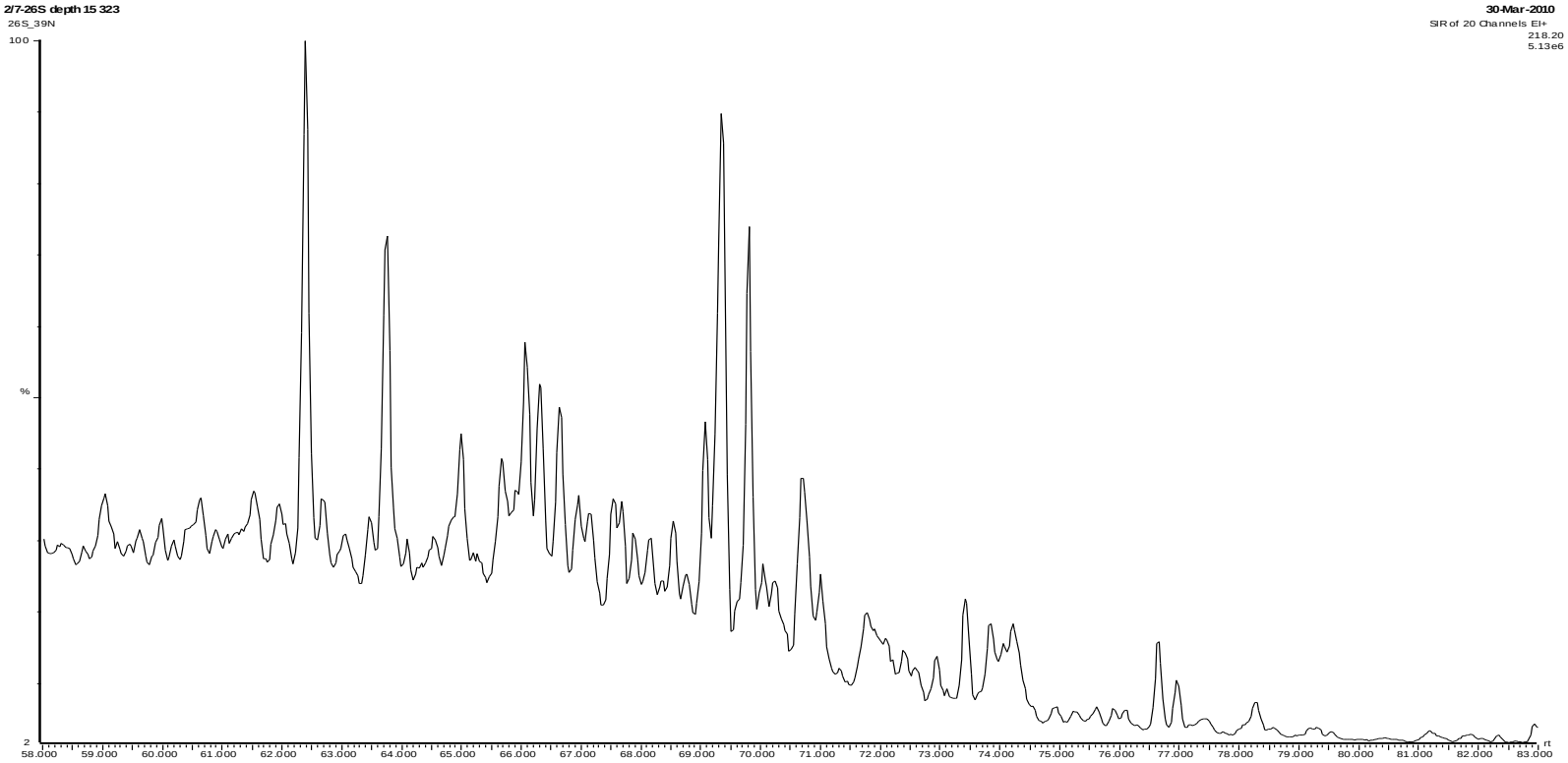
2/7-26S depth 15 323
26S_39N
100
%
2
30-Mar-2010
SIR of 20 Channels EI+
218.20
5.13e6
58.000
59.000
60.000
61.000
62.000
63.000
64.000
65.000
66.000
67.000
68.000
69.000
70.000
71.000
72.000
73.000
74.000
75.000
76.000
77.000
78.000
79.000
80.000
81.000
82.000
83.000
rt

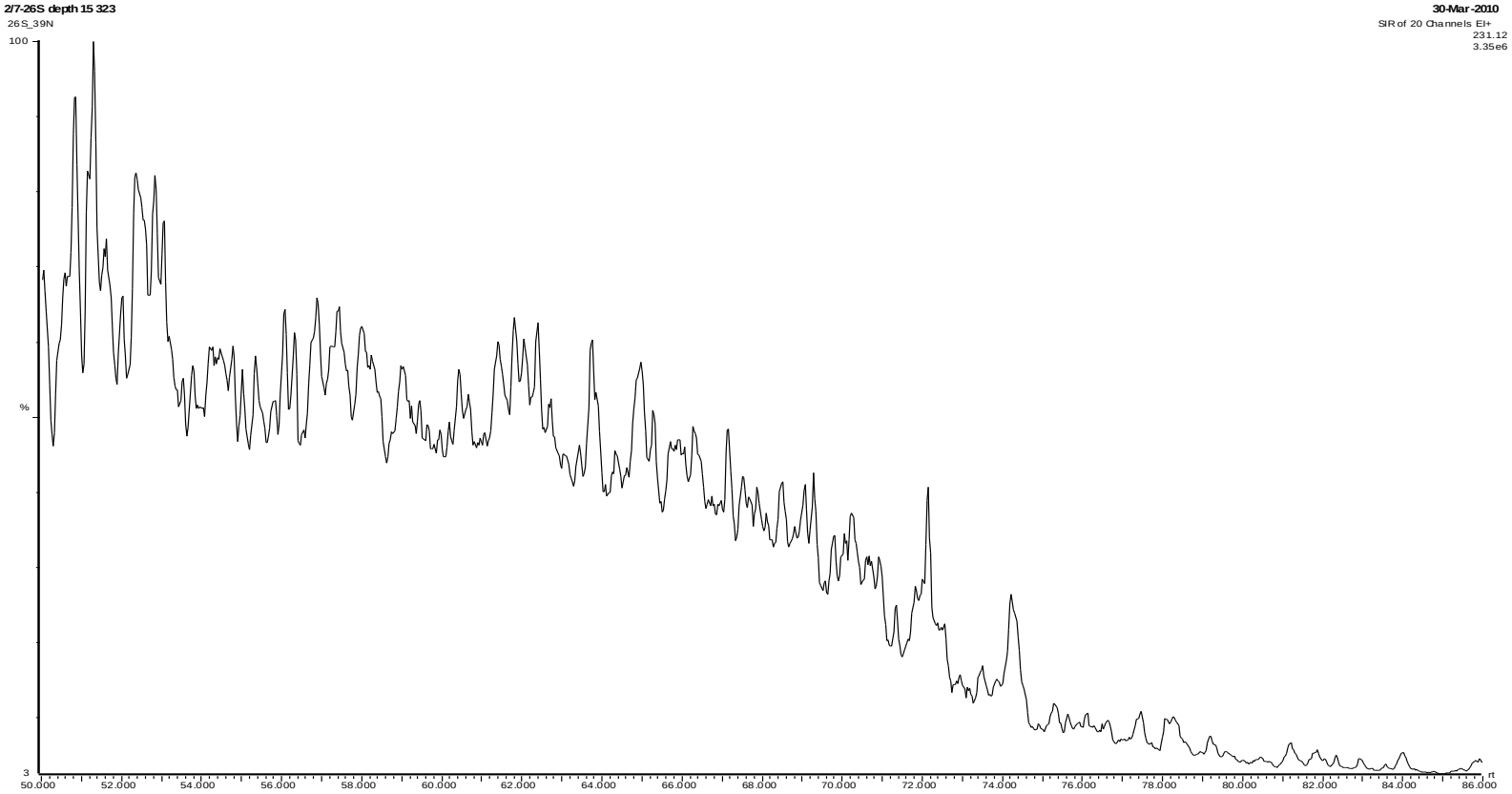
2/7-26S depth 15 323
26S_39N
30-Mar-2010
SIR of 20 Channels EI+
231.12
3.35e6
100
%
3
50.000
52.000
54.000
56.000
58.000
60.000
62.000
64.000
66.000
68.000
70.000
72.000
74.000
76.000
78.000
80.000
82.000
84.000
86.000
rt

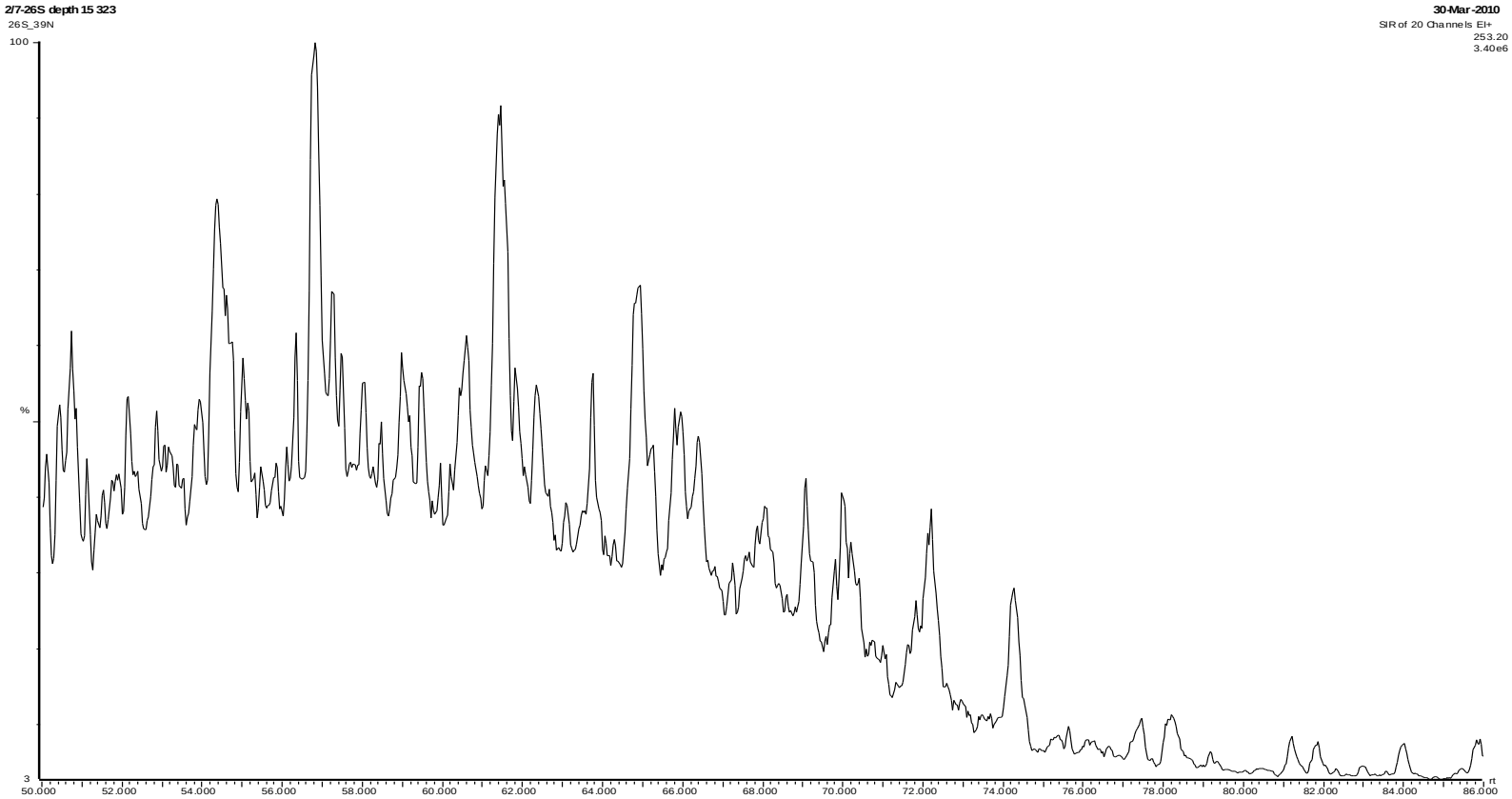
2/7-26S depth 15 323
26S_39N
30-Mar-2010
SIR of 20 Channels EI+
253.20
3.40e6
100
%
3
50.000
52.000
54.000
56.000
58.000
60.000
62.000
64.000
66.000
68.000
70.000
72.000
74.000
76.000
78.000
80.000
82.000
84.000
86.000
rt

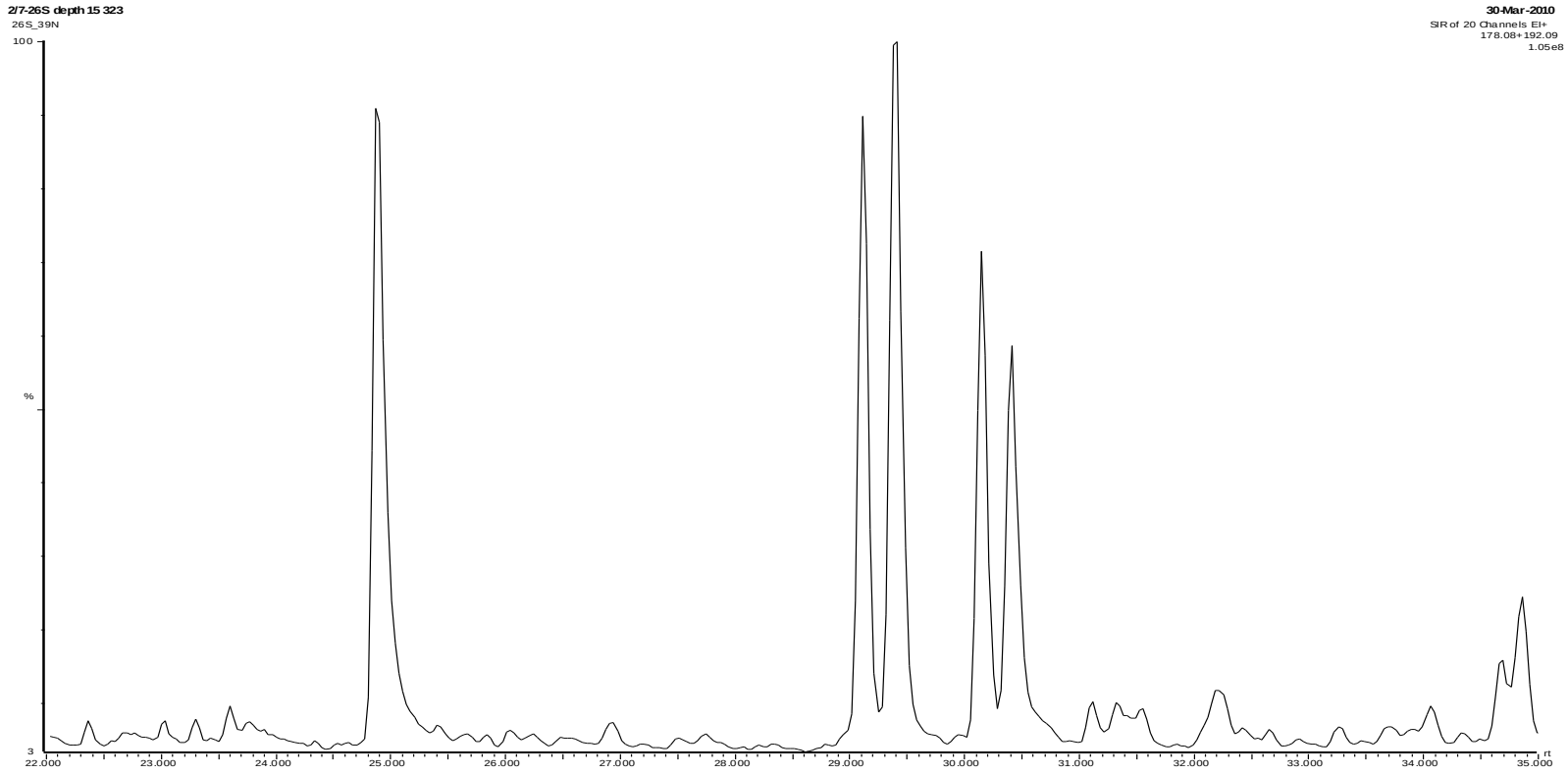
2/7-26S depth 15 323
26S_39N
100
%
3
22.000
23.000
24.000
25.000
26.000
27.000
28.000
29.000
30.000
31.000
32.000
33.000
34.000
35.000
rt
30-Mar-2010
SIR of 20 Channels EI+
178.08+192.09
1.05e8

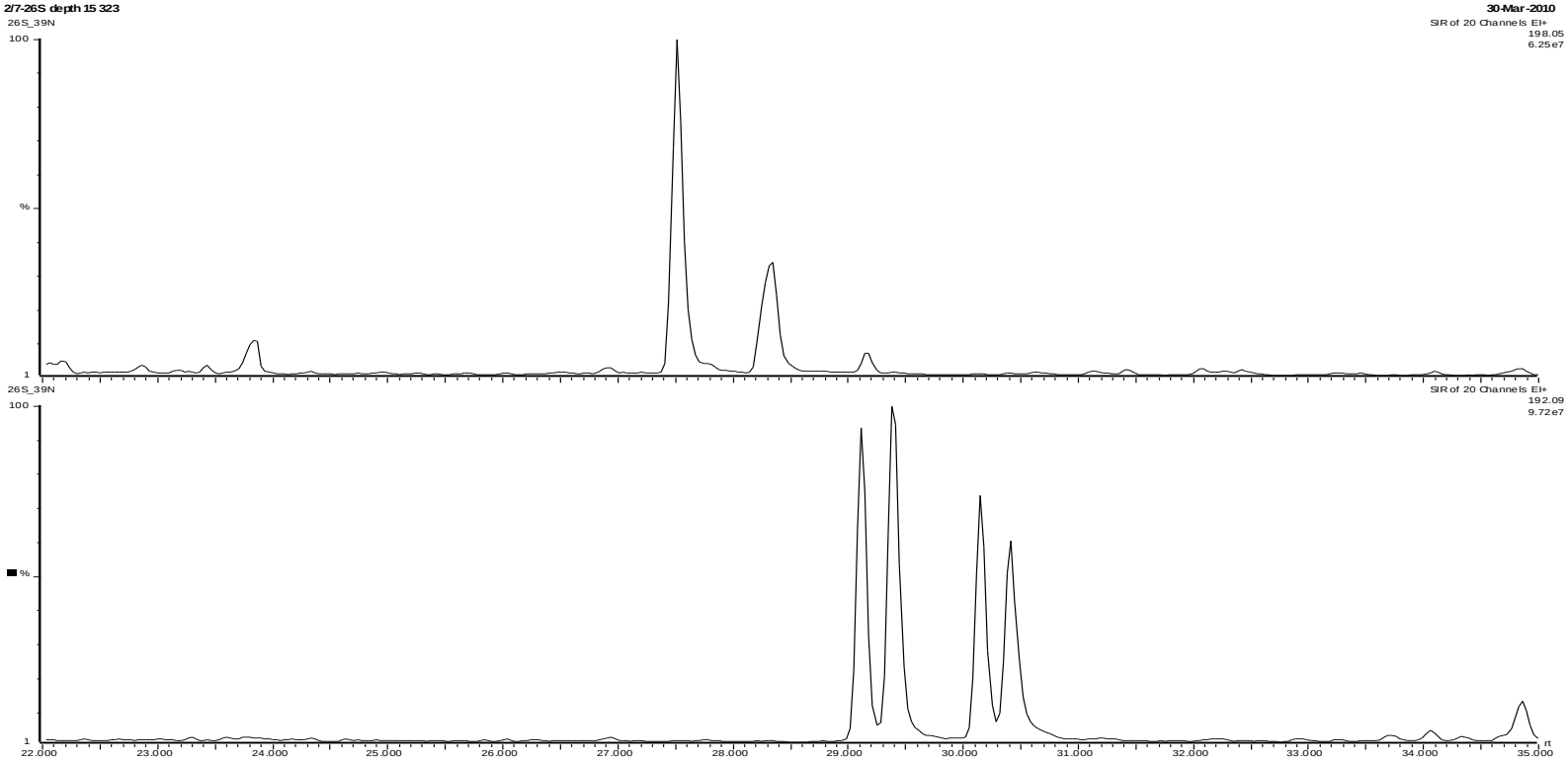
2/7-26S depth 15 323
30-Mar-2010
26S_39N
SIR of 20 Channels EI+
198.05
6.25e7
100
%
1
26S_39N
SIR of 20 Channels EI+
192.09
9.72e7
100
%
1
22.000
23.000
24.000
25.000
26.000
27.000
28.000
29.000
30.000
31.000
32.000
33.000
34.000
35.000
rt

GC-MS Chromatograms for sample E7

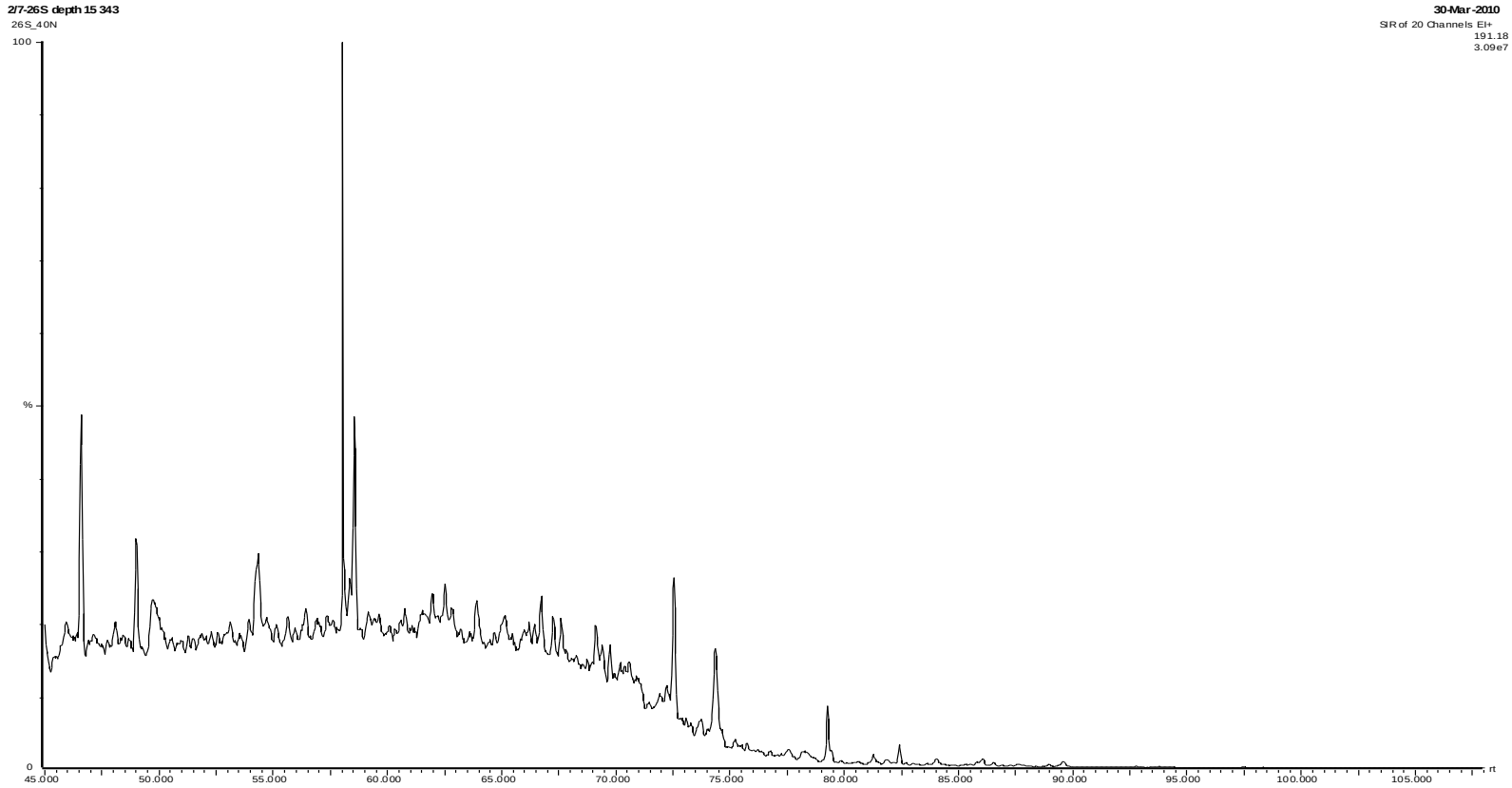
2/7-26S depth 15 343
26S_40N
30-Mar-2010
SIR of 20 Channels EI+
191.18
3.09e7
100
%
0
45.000
50.000
55.000
60.000
65.000
70.000
75.000
80.000
85.000
90.000
95.000
100.000
105.000
rt

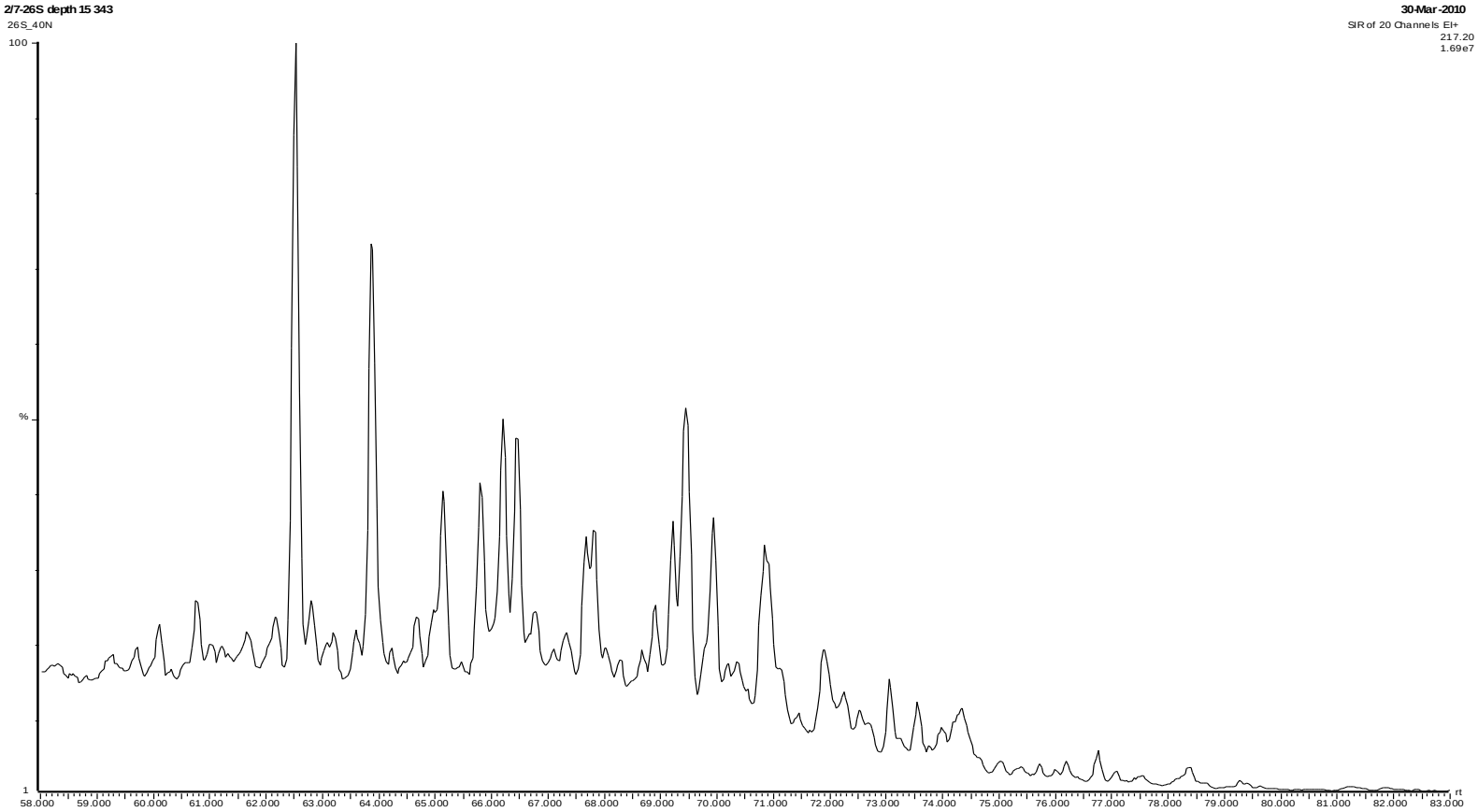
2/7-26S depth 15 343
26S_40N
30-Mar-2010
SIR of 20 Channels EI+
217.20
1.69e7
100
%
1
58.000
59.000
60.000
61.000
62.000
63.000
64.000
65.000
66.000
67.000
68.000
69.000
70.000
71.000
72.000
73.000
74.000
75.000
76.000
77.000
78.000
79.000
80.000
81.000
82.000
83.000
rt

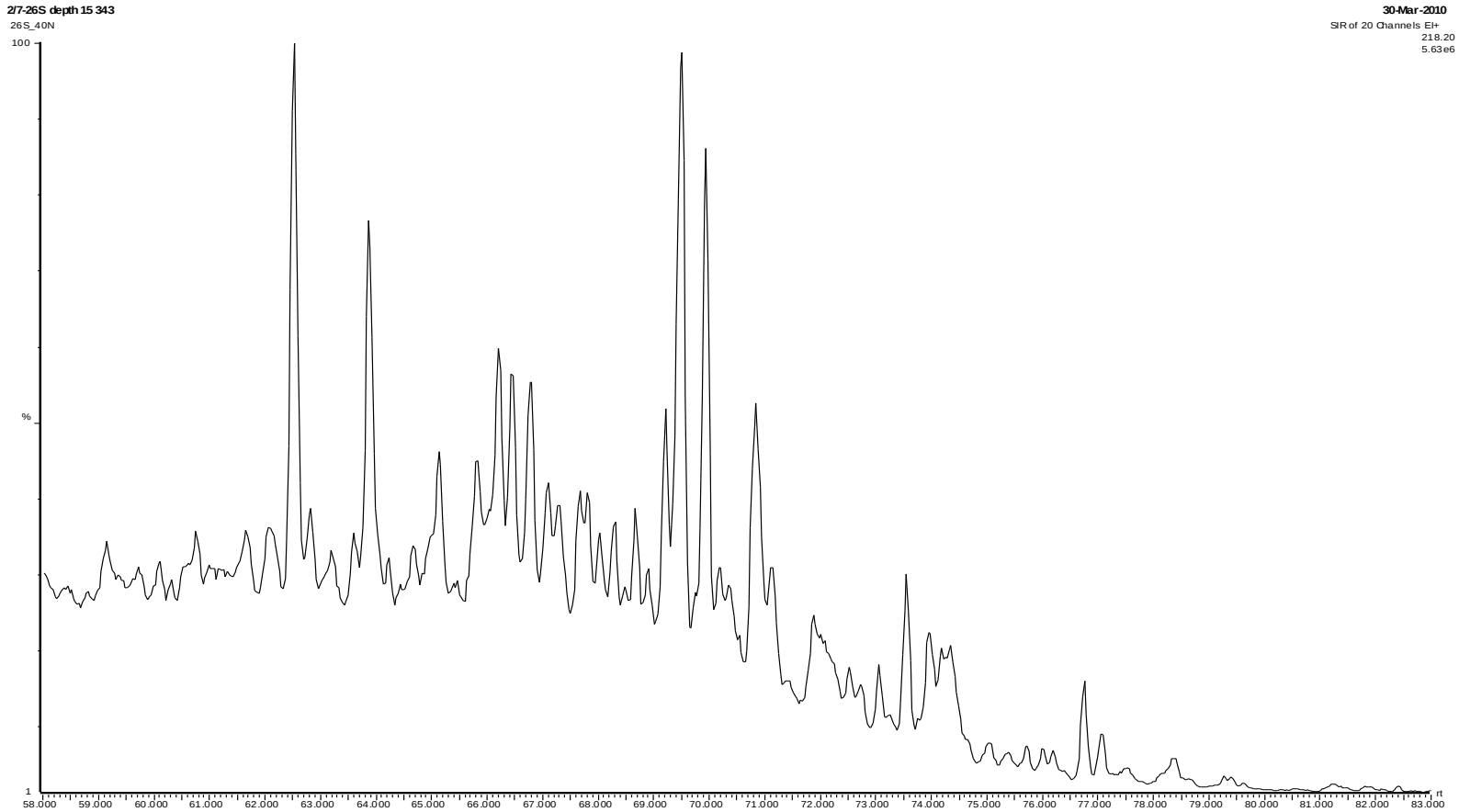
2/7-26S depth 15 343
26S_40N
30-Mar-2010
SIR of 20 Channels EI+
218.20
5.63e6
100
%
1
58.000
59.000
60.000
61.000
62.000
63.000
64.000
65.000
66.000
67.000
68.000
69.000
70.000
71.000
72.000
73.000
74.000
75.000
76.000
77.000
78.000
79.000
80.000
81.000
82.000
83.000
rt

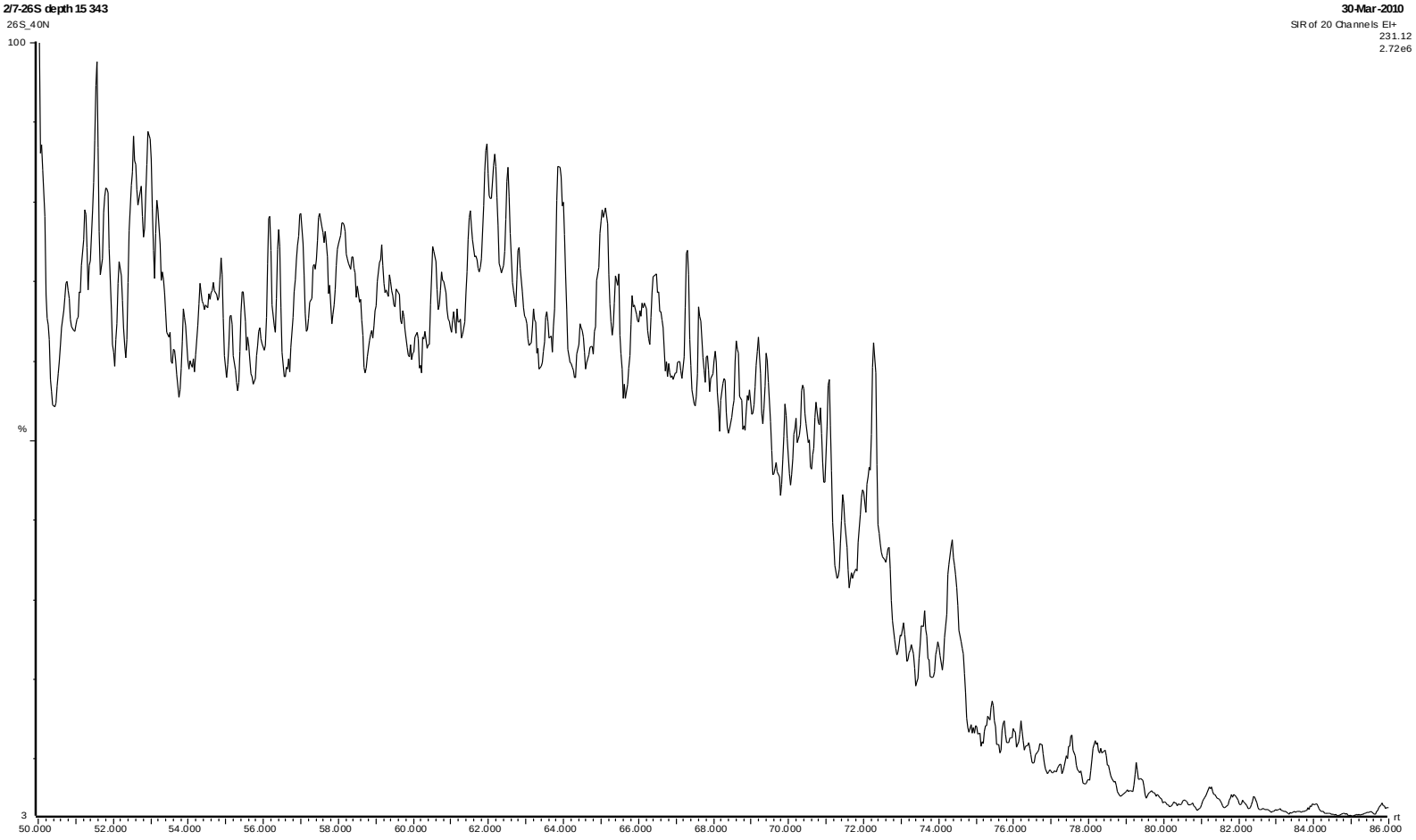
2/7-26S depth 15 343
26S_40N
30-Mar-2010
SIR of 20 Channels EI+
231.12
2.72e6
100
%
3
50.000
52.000
54.000
56.000
58.000
60.000
62.000
64.000
66.000
68.000
70.000
72.000
74.000
76.000
78.000
80.000
82.000
84.000
86.000
rt

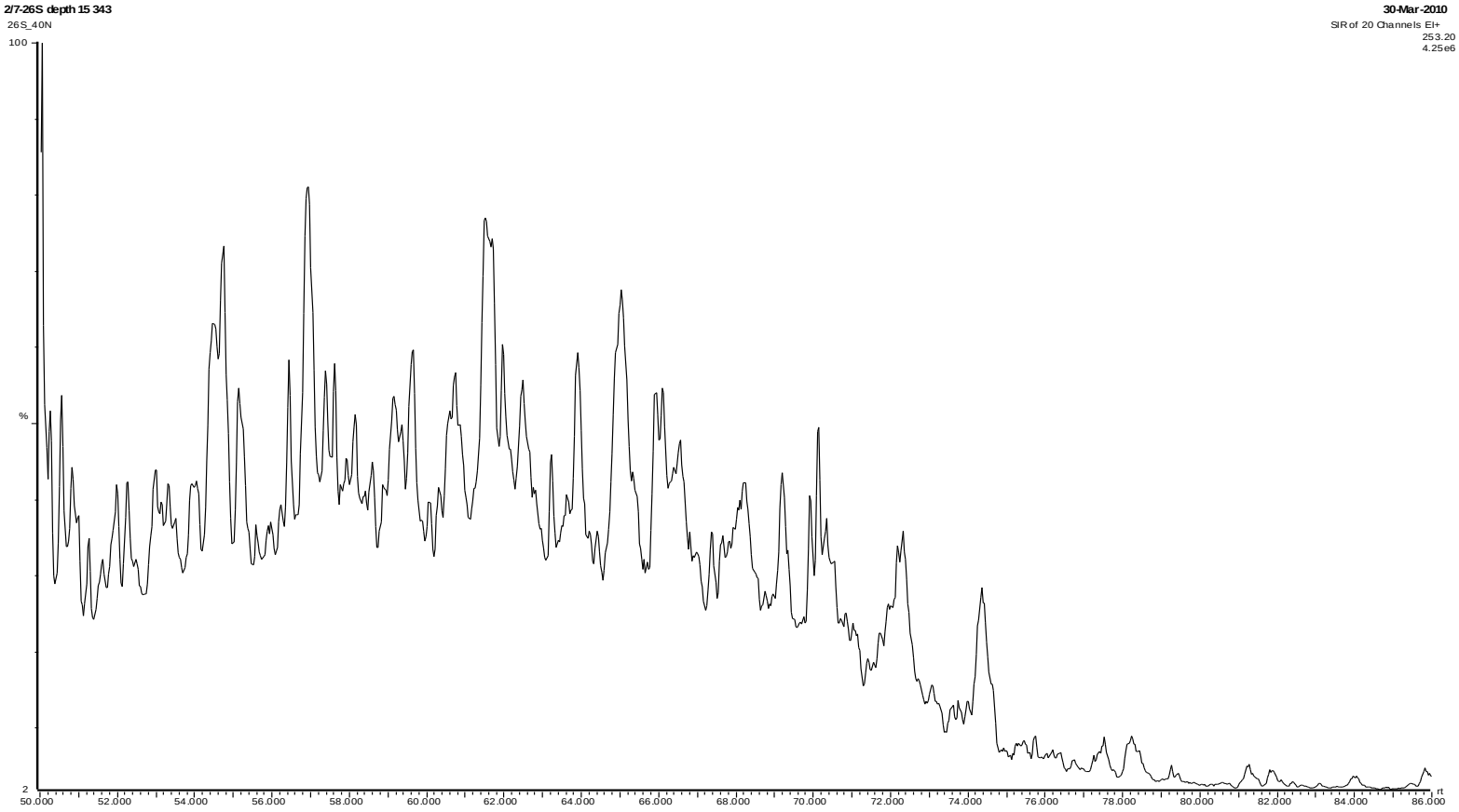
2/7-26S depth 15 343
26S_40N
30-Mar-2010
SIR of 20 Channels EI+
253.20
4.25e6
100
%
2
50.000
52.000
54.000
56.000
58.000
60.000
62.000
64.000
66.000
68.000
70.000
72.000
74.000
76.000
78.000
80.000
82.000
84.000
86.000
rt

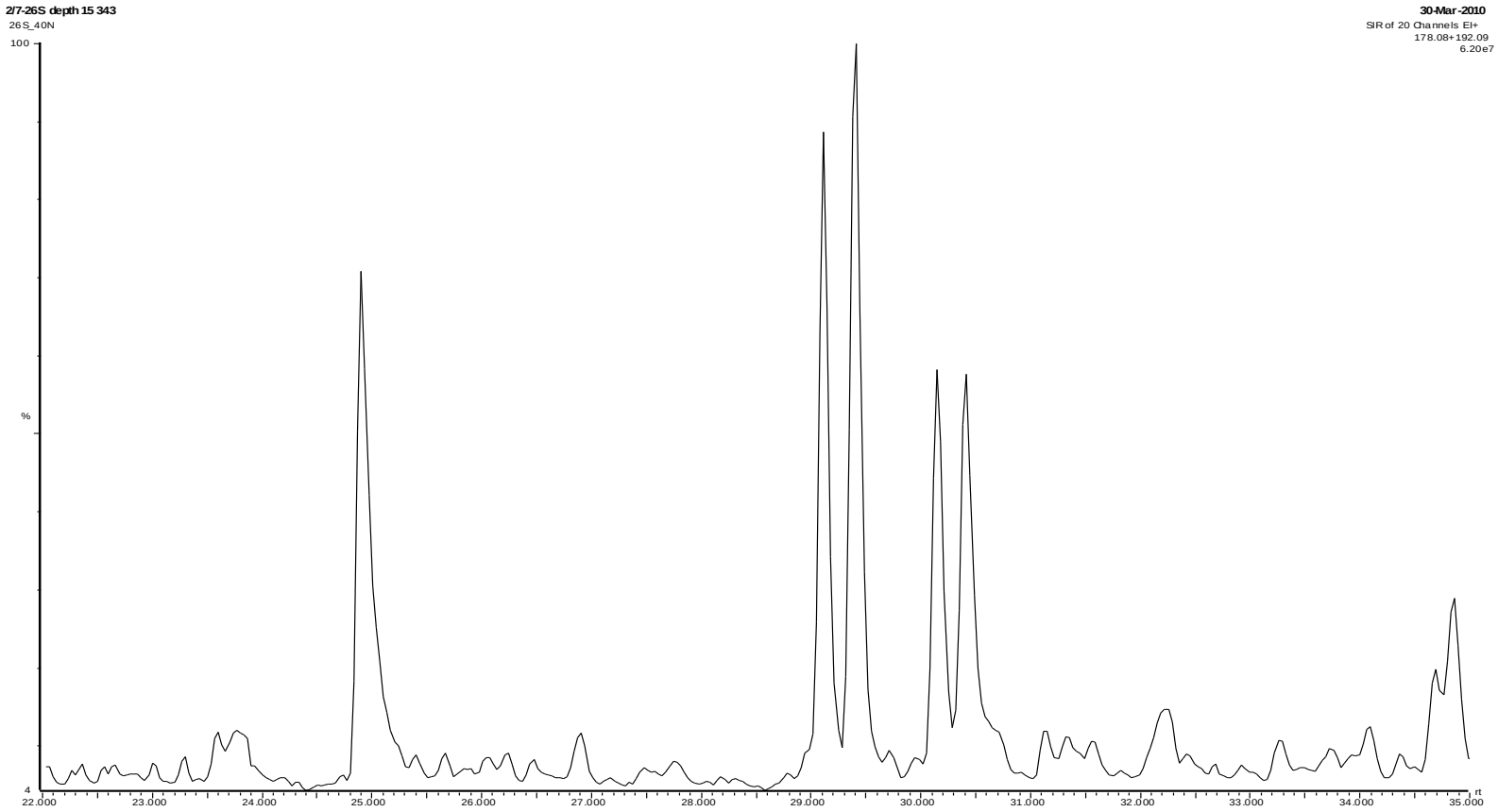
2/7-26S depth 15 343
26S_40N
30-Mar-2010
SIR of 20 Channels EI+
178.08+192.09
6.20e7
100
%
4
22.000
23.000
24.000
25.000
26.000
27.000
28.000
29.000
30.000
31.000
32.000
33.000
34.000
35.000
rt

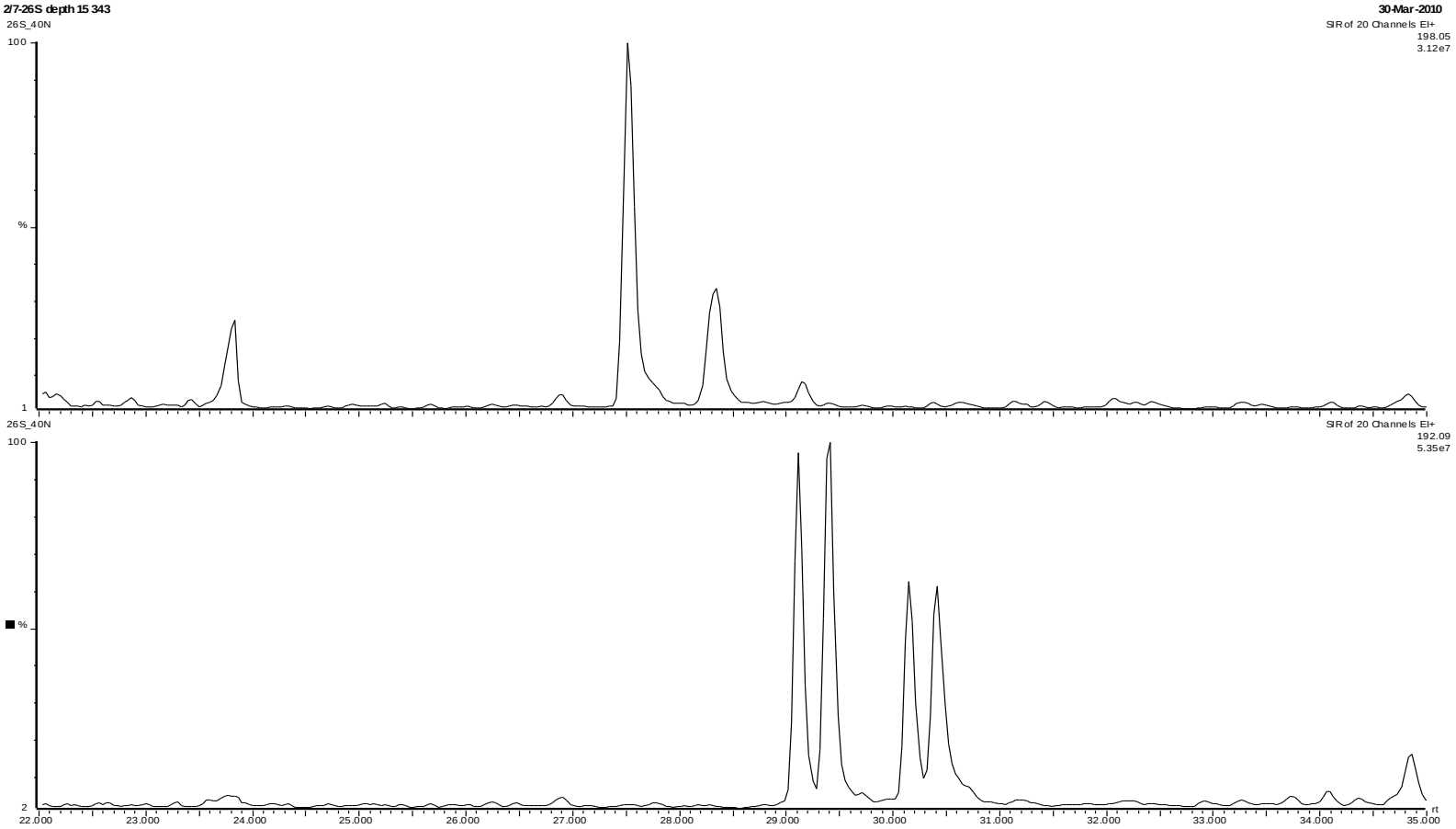
2/7-26S depth 15 343
30-Mar-2010
26S_40N
SIR of 20 Channels EI+
198.05
3.12e7
100
%
1
26S_40N
SIR of 20 Channels EI+
192.09
5.35e7
100
%
2
22.000
23.000
24.000
25.000
26.000
27.000
28.000
29.000
30.000
31.000
32.000
33.000
34.000
35.000
rt

GC-MS Chromatograms for sample E8

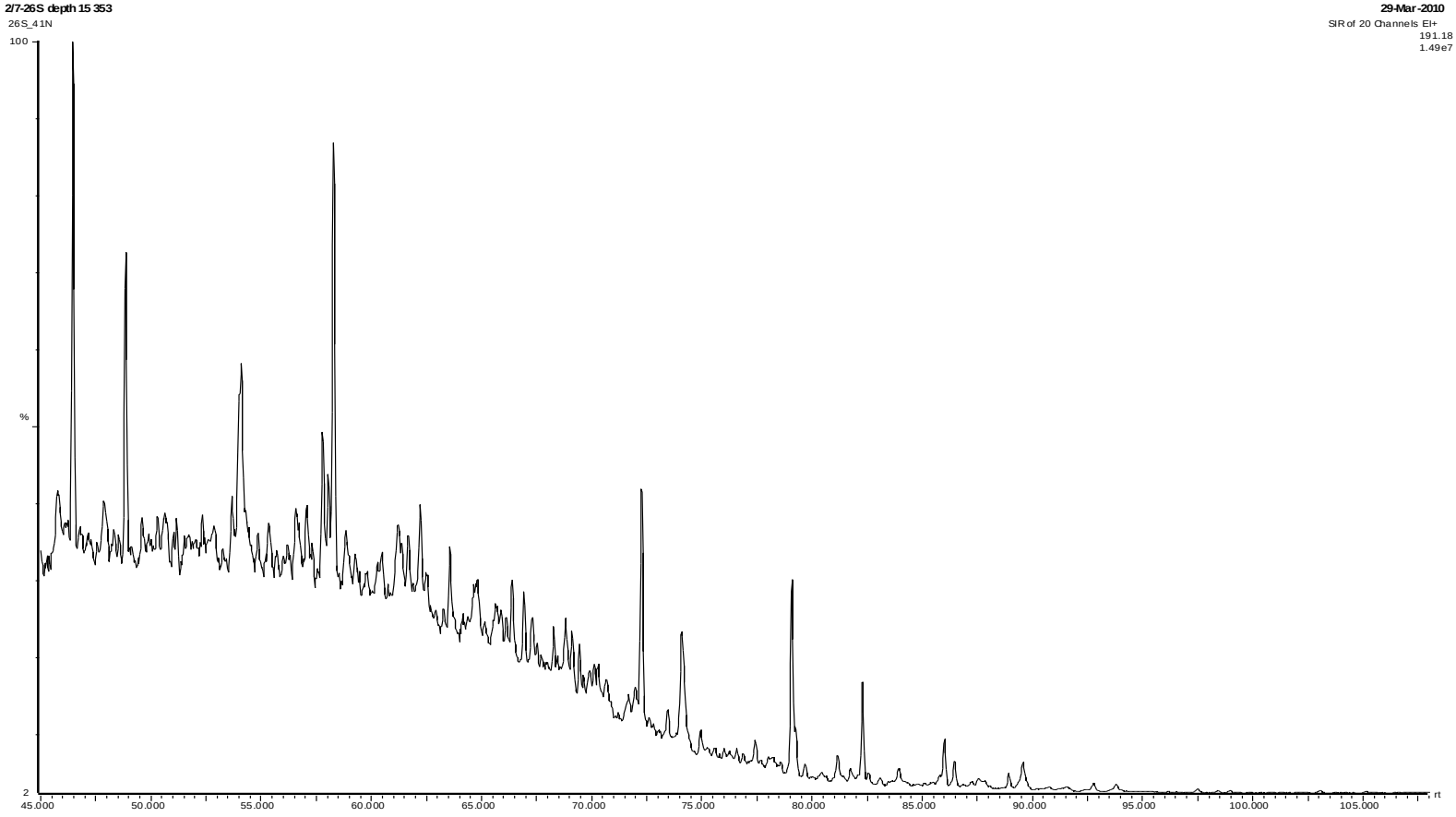
2/7-26S depth 15 353
26S_41N
29-Mar-2010
SIR of 20 Channels EI+
191.18
1.49e7
100
%
2
45.000
50.000
55.000
60.000
65.000
70.000
75.000
80.000
85.000
90.000
95.000
100.000
105.000
rt

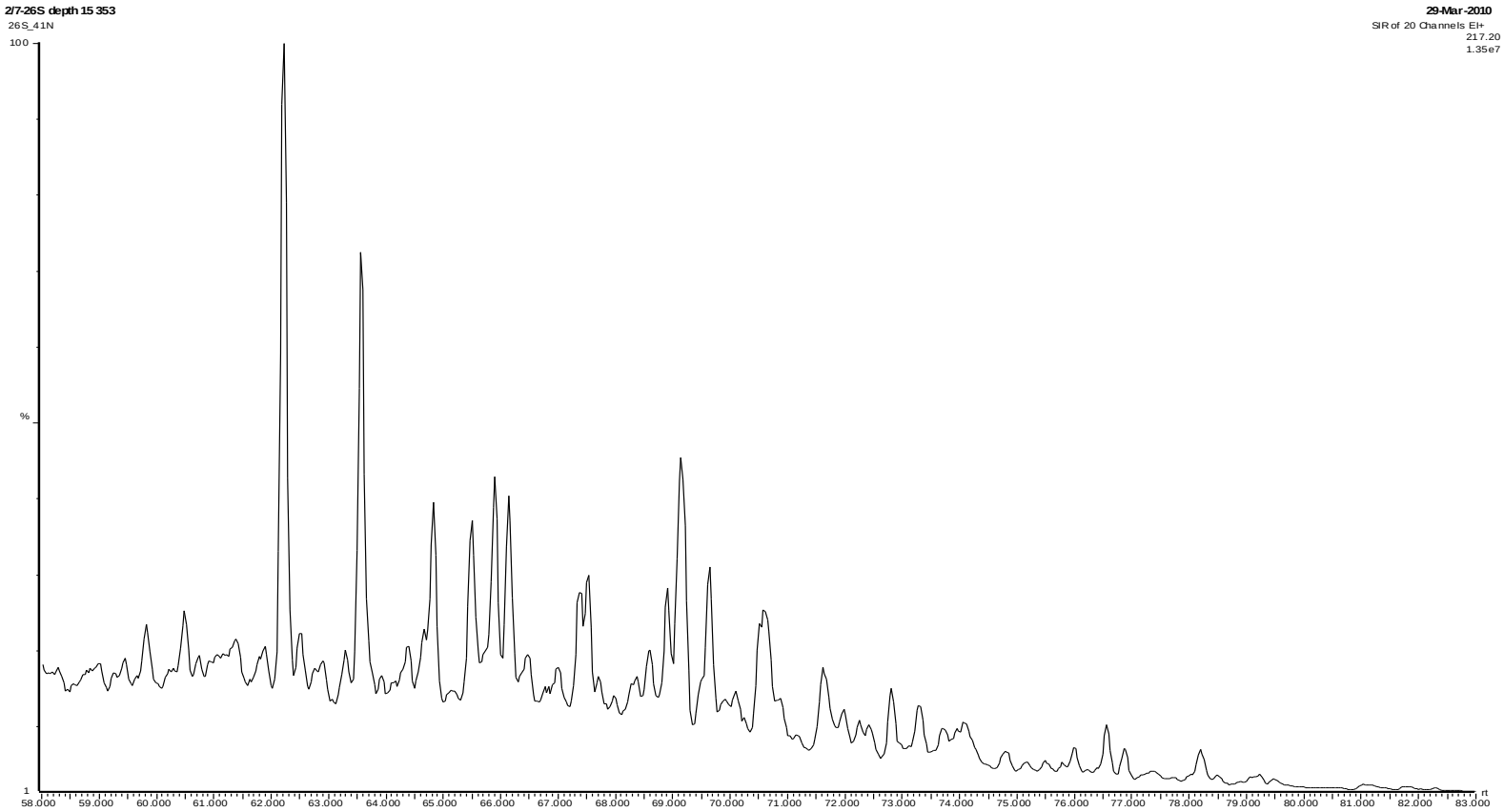
2/7-26S depth 15 353
26S_41N
29-Mar-2010
SIR of 20 Channels EI+
217.20
1.35e7
100
%
1
58.000
59.000
60.000
61.000
62.000
63.000
64.000
65.000
66.000
67.000
68.000
69.000
70.000
71.000
72.000
73.000
74.000
75.000
76.000
77.000
78.000
79.000
80.000
81.000
82.000
83.000
rt

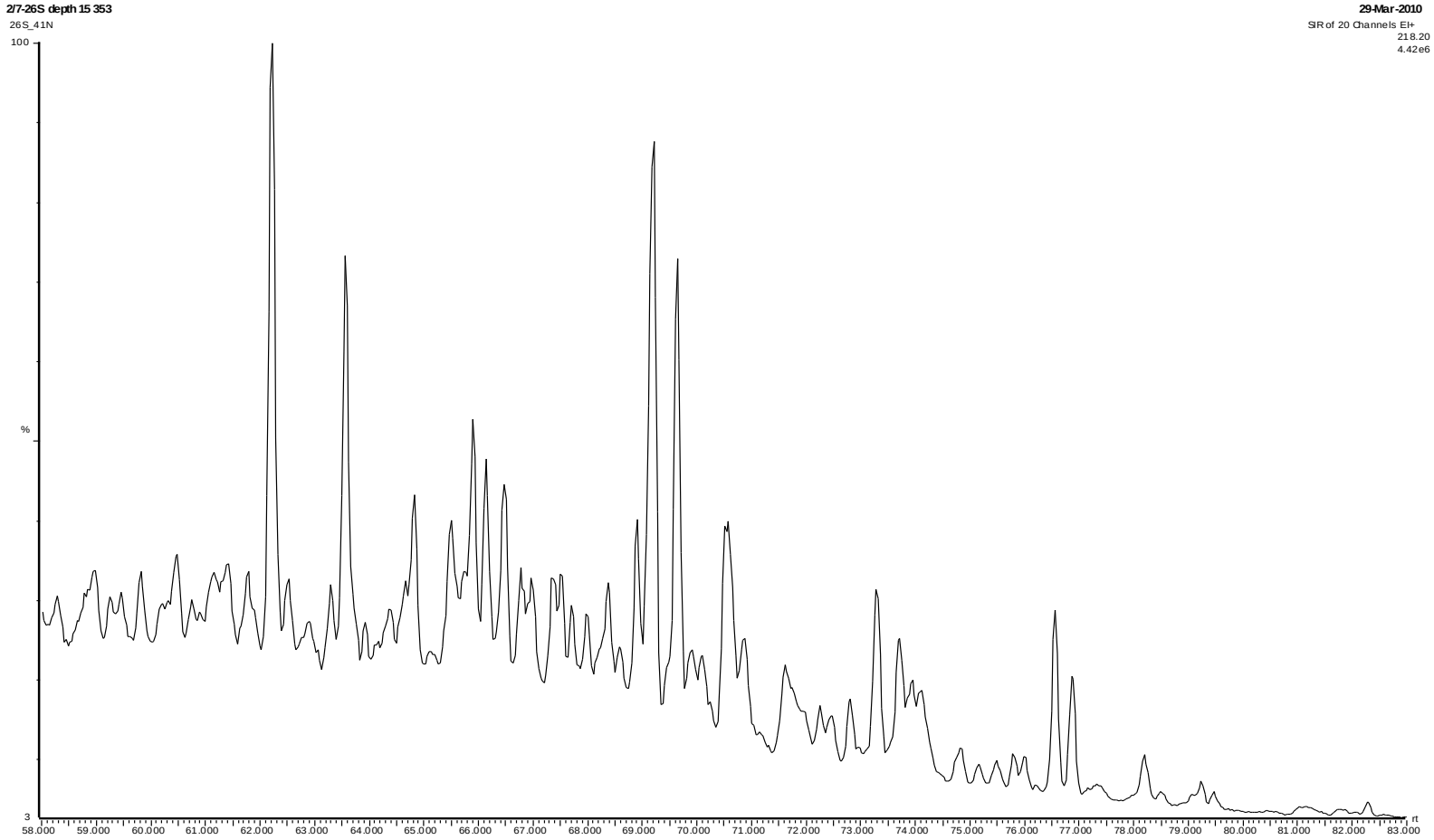
2/7-26S depth 15 353
26S_41N
29-Mar-2010
SIR of 20 Channels EI+
218.20
4.42e6
100
%
3
58.000
59.000
60.000
61.000
62.000
63.000
64.000
65.000
66.000
67.000
68.000
69.000
70.000
71.000
72.000
73.000
74.000
75.000
76.000
77.000
78.000
79.000
80.000
81.000
82.000
83.000
rt

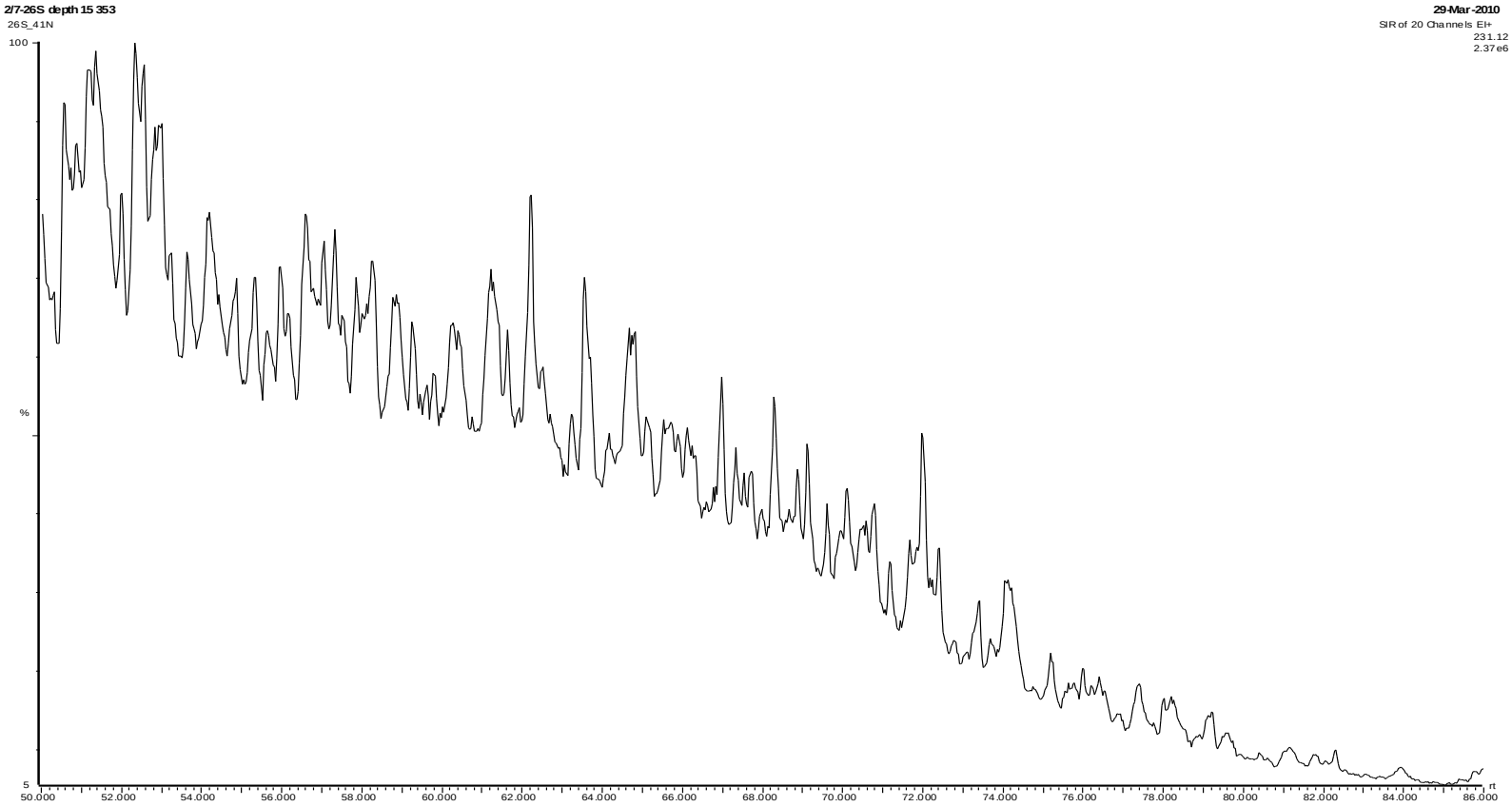
2/7-26S depth 15 353
26S_41N
29-Mar-2010
SIR of 20 Channels EI+
231.12
2.37e6
100
%
5
50.000
52.000
54.000
56.000
58.000
60.000
62.000
64.000
66.000
68.000
70.000
72.000
74.000
76.000
78.000
80.000
82.000
84.000
86.000
rt

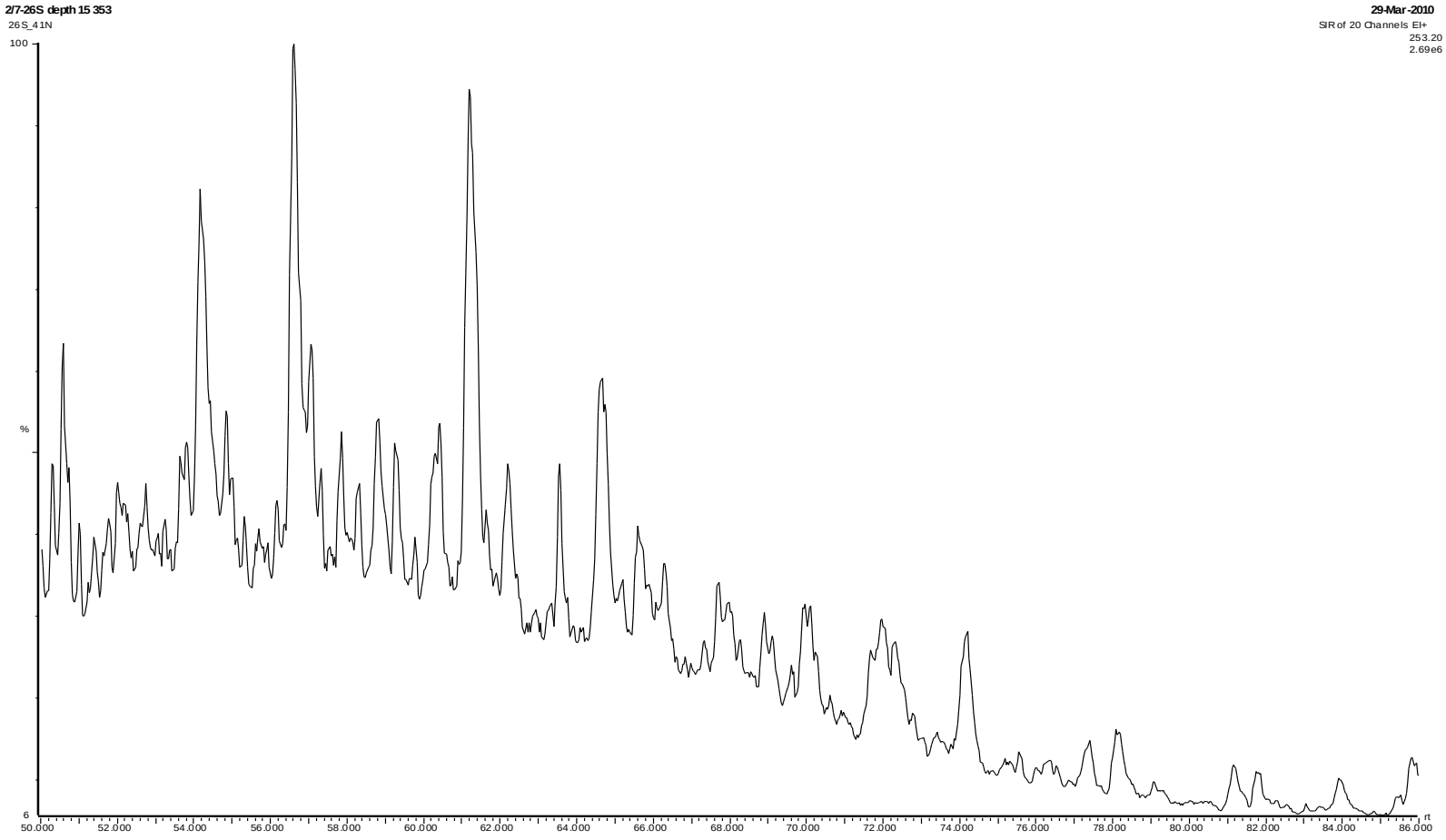
2/7-26S depth 15 353
26S_41N
29-Mar-2010
SIR of 20 Channels EI+
253.20
2.69e6
100
%
6
50.000
52.000
54.000
56.000
58.000
60.000
62.000
64.000
66.000
68.000
70.000
72.000
74.000
76.000
78.000
80.000
82.000
84.000
86.000
rt

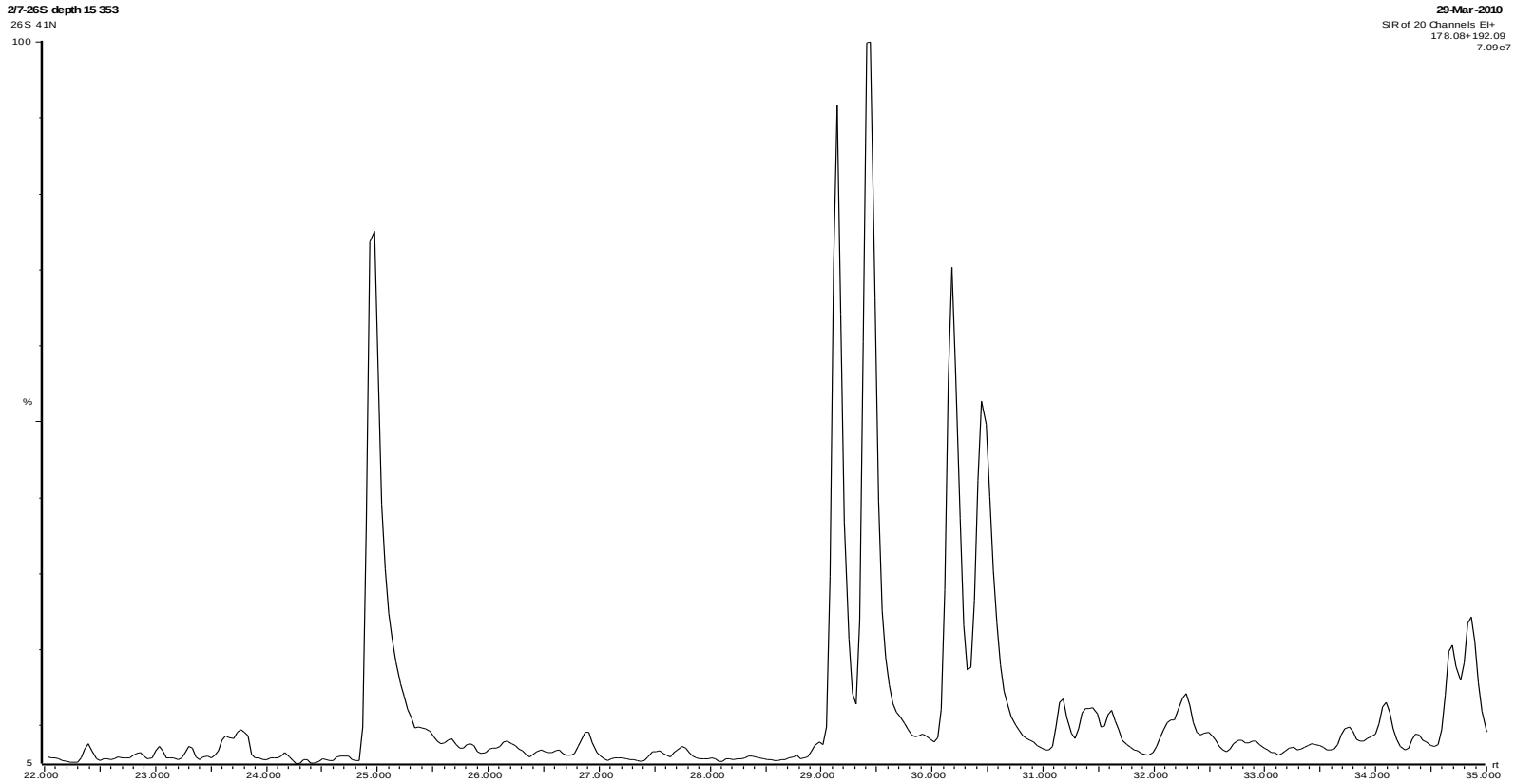
2/7-26S depth 15 353
26S_41N
29-Mar-2010
SIR of 20 Channels EI+
178.08+192.09
7.09e7
100
%
5
22.000
23.000
24.000
25.000
26.000
27.000
28.000
29.000
30.000
31.000
32.000
33.000
34.000
35.000
rt

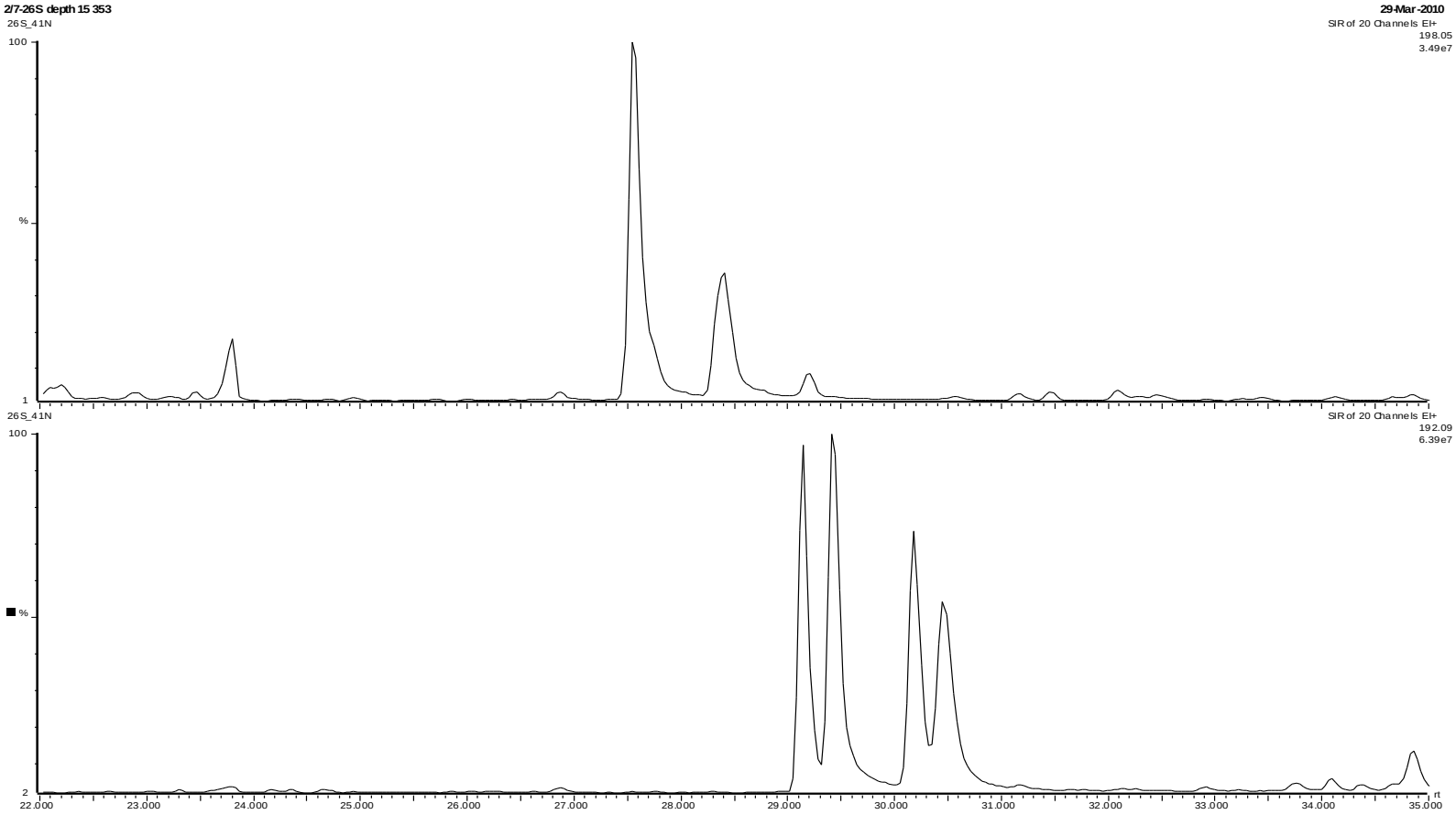
2/7-26S depth 15 353
29-Mar-2010
26S_41N
SIR of 20 Channels EI+
198.05
3.49e7
100
%
1
26S_41N
SIR of 20 Channels EI+
192.09
6.39e7
100
%
2
22.000
23.000
24.000
25.000
26.000
27.000
28.000
29.000
30.000
31.000
32.000
33.000
34.000
35.000
rt

GC_MS Chromatograms for sample E9

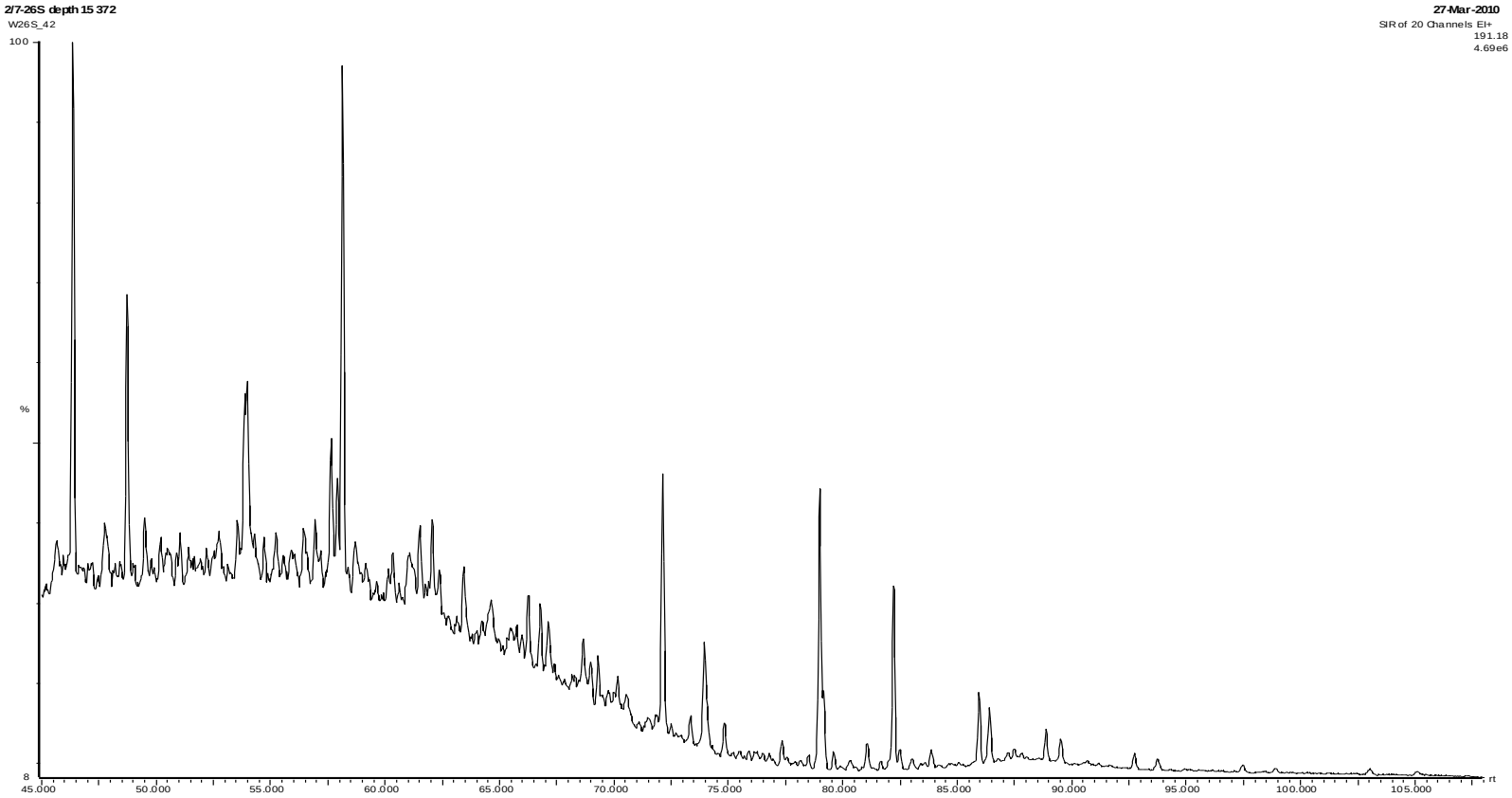
2/7-26S depth 15 372
W26S_42
27-Mar-2010
SIR of 20 Channels ES+
191.18
4.69e6
100
%
8
45.000
50.000
55.000
60.000
65.000
70.000
75.000
80.000
85.000
90.000
95.000
100.000
105.000
rt

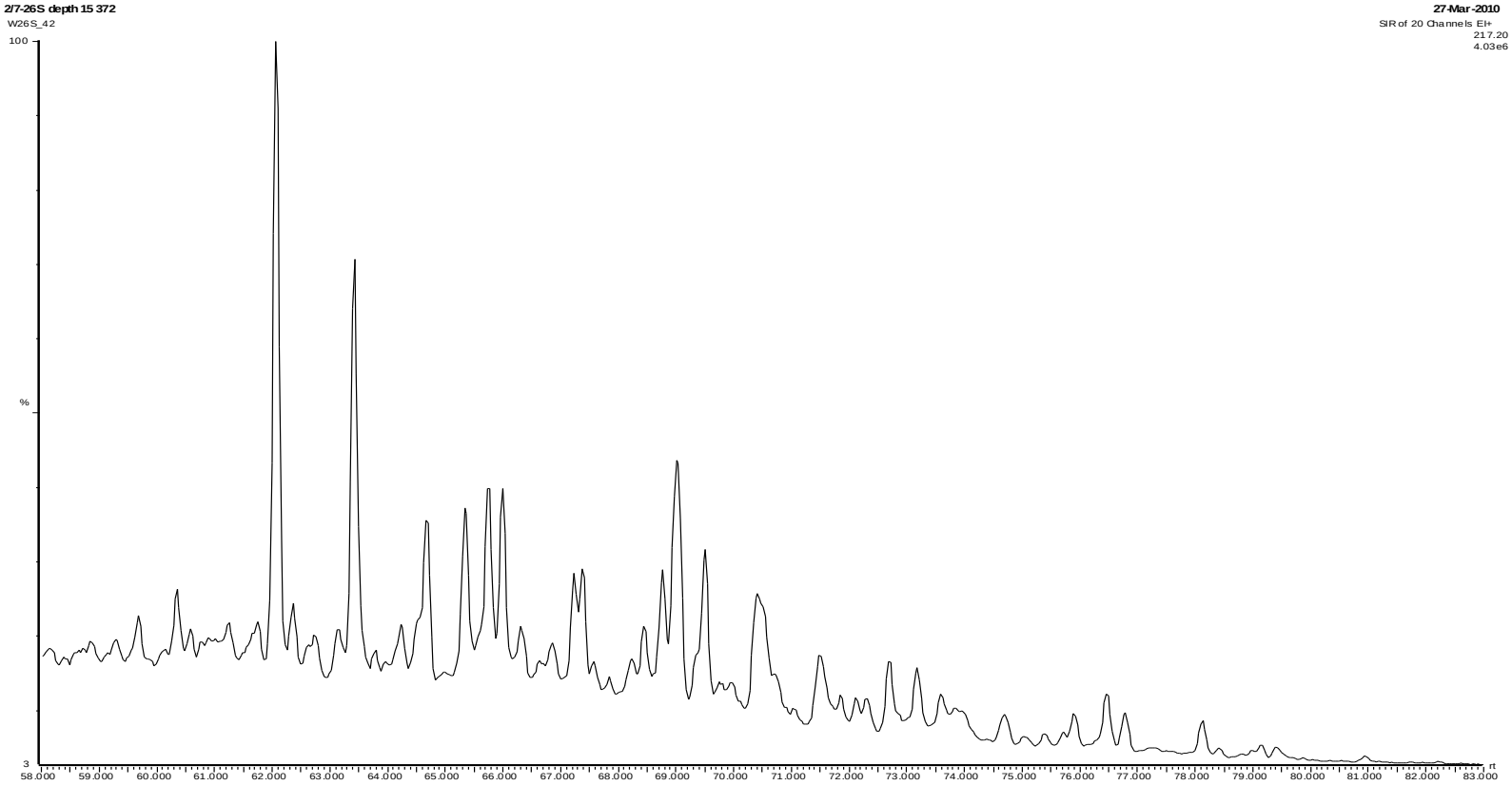
2/7-26S depth 15 372
W26S_42
27-Mar-2010
SIR of 20 Channels EI+
217.20
4.03e6
100
%
3
58.000
59.000
60.000
61.000
62.000
63.000
64.000
65.000
66.000
67.000
68.000
69.000
70.000
71.000
72.000
73.000
74.000
75.000
76.000
77.000
78.000
79.000
80.000
81.000
82.000
83.000
rt

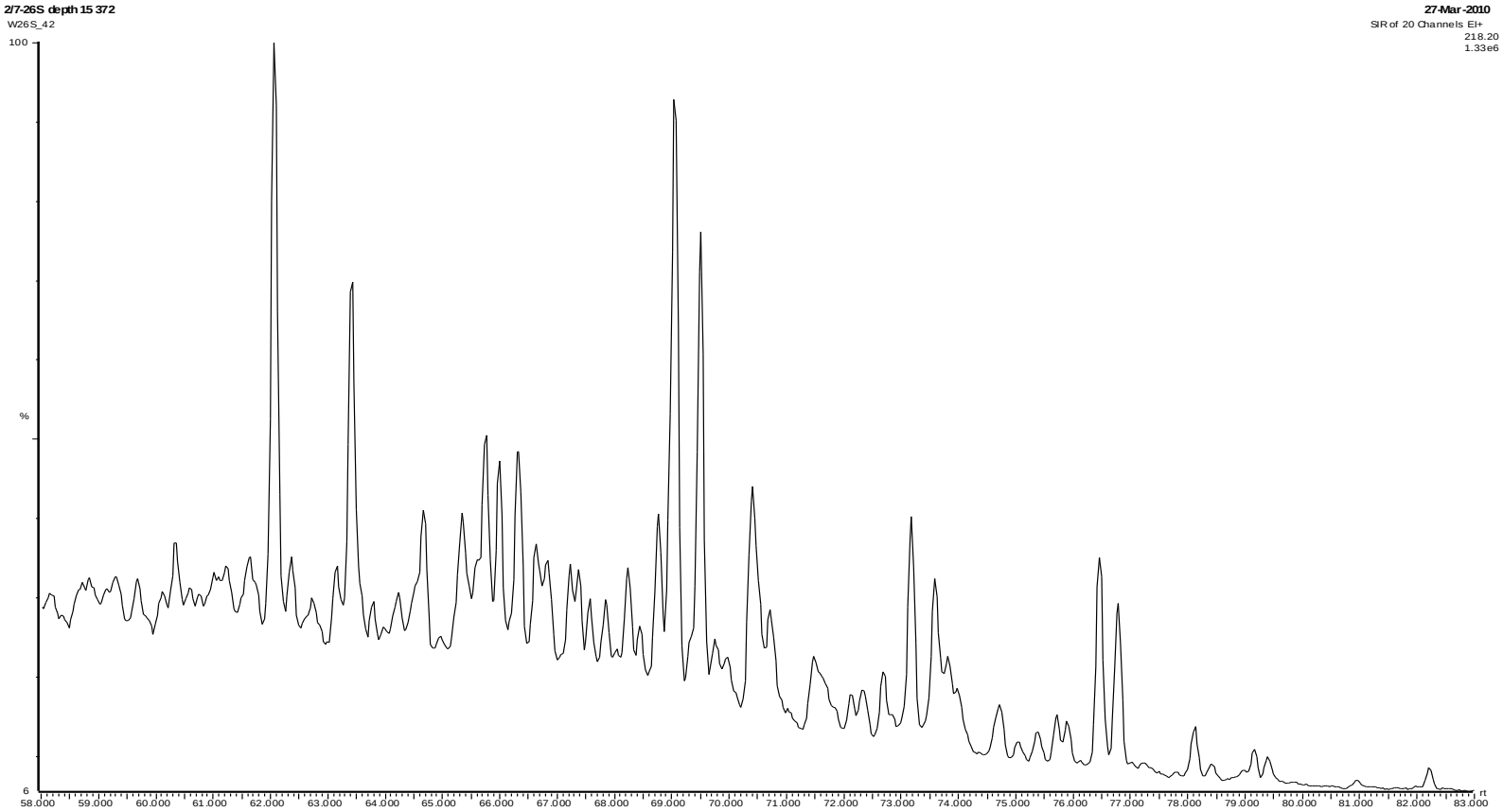
2/7-26S depth 15 372
W26S_42
27-Mar-2010
SIR of 20 Channels EI+
218.20
1.33e6
100
%
6
58.000
59.000
60.000
61.000
62.000
63.000
64.000
65.000
66.000
67.000
68.000
69.000
70.000
71.000
72.000
73.000
74.000
75.000
76.000
77.000
78.000
79.000
80.000
81.000
82.000
83.000
rt

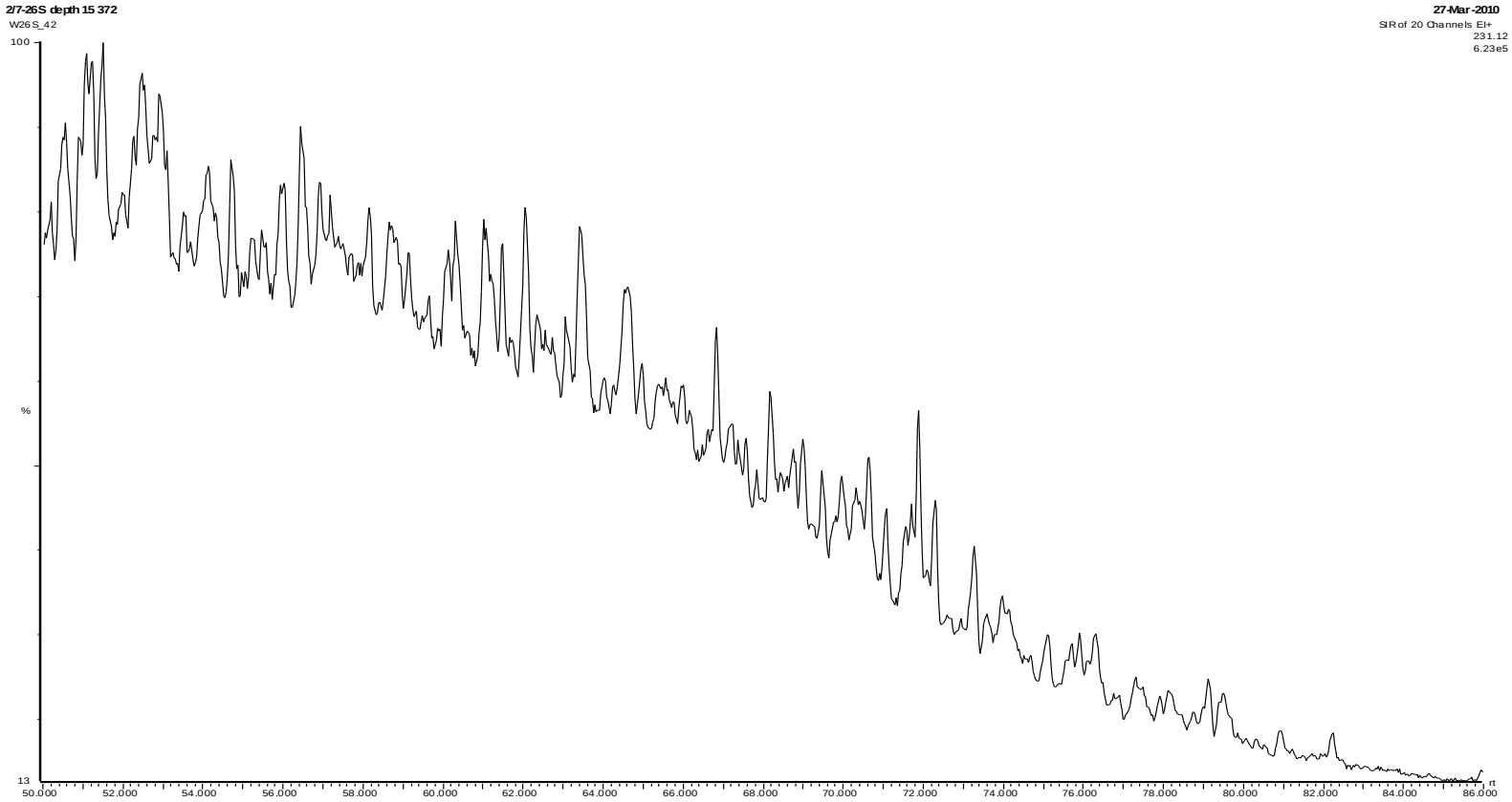
2/7-26S depth 15 372
W26S_42
27-Mar-2010
SIR of 20 Channels EI+
231.12
6.23e5
100
%
13
50.000
52.000
54.000
56.000
58.000
60.000
62.000
64.000
66.000
68.000
70.000
72.000
74.000
76.000
78.000
80.000
82.000
84.000
86.000
rt

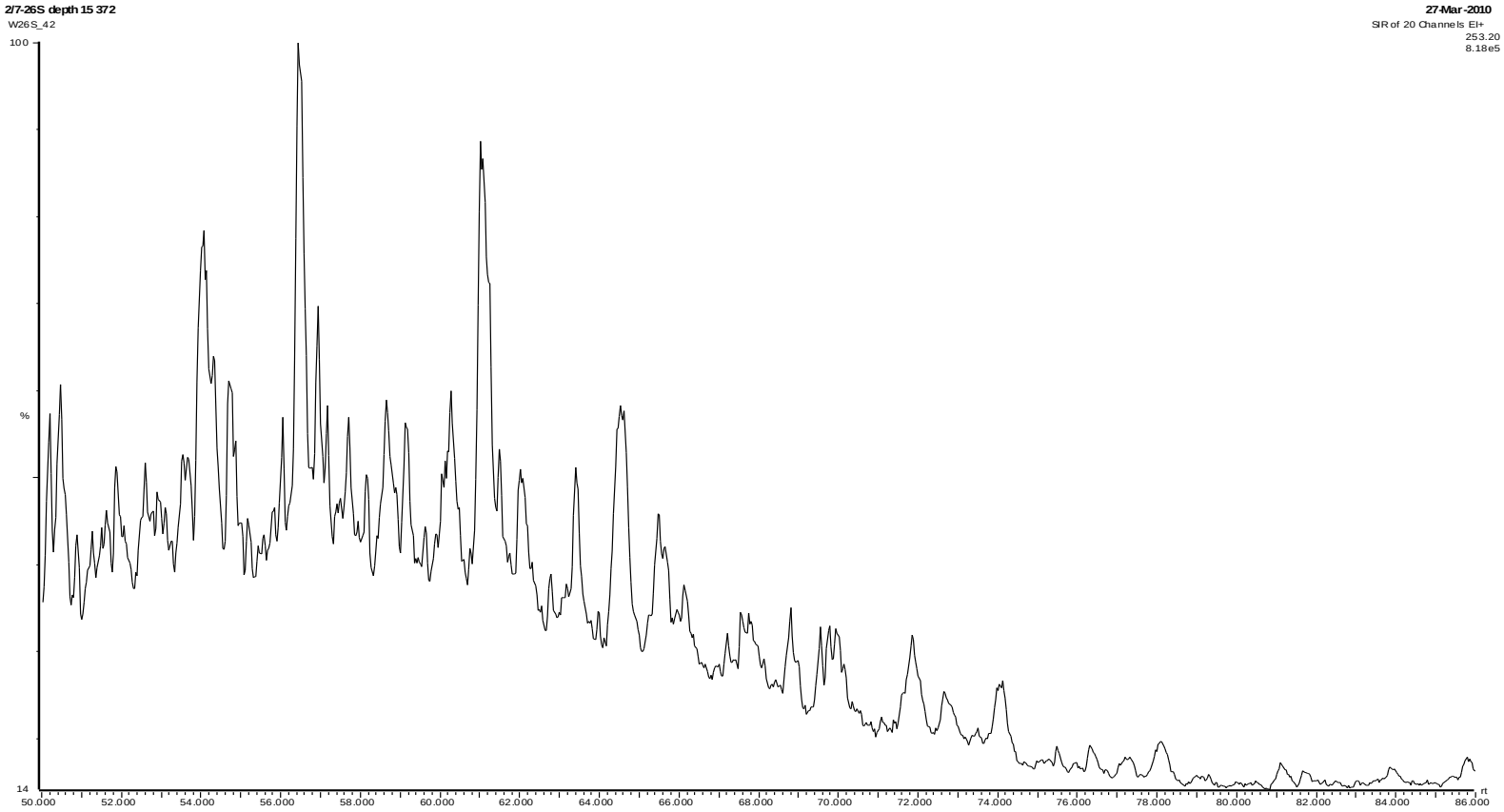
2/7-26S depth 15 372
W26S_42
27-Mar-2010
SIR of 20 Channels EI+
253.20
8.18e5
100
%
14
50.000
52.000
54.000
56.000
58.000
60.000
62.000
64.000
66.000
68.000
70.000
72.000
74.000
76.000
78.000
80.000
82.000
84.000
86.000
rt

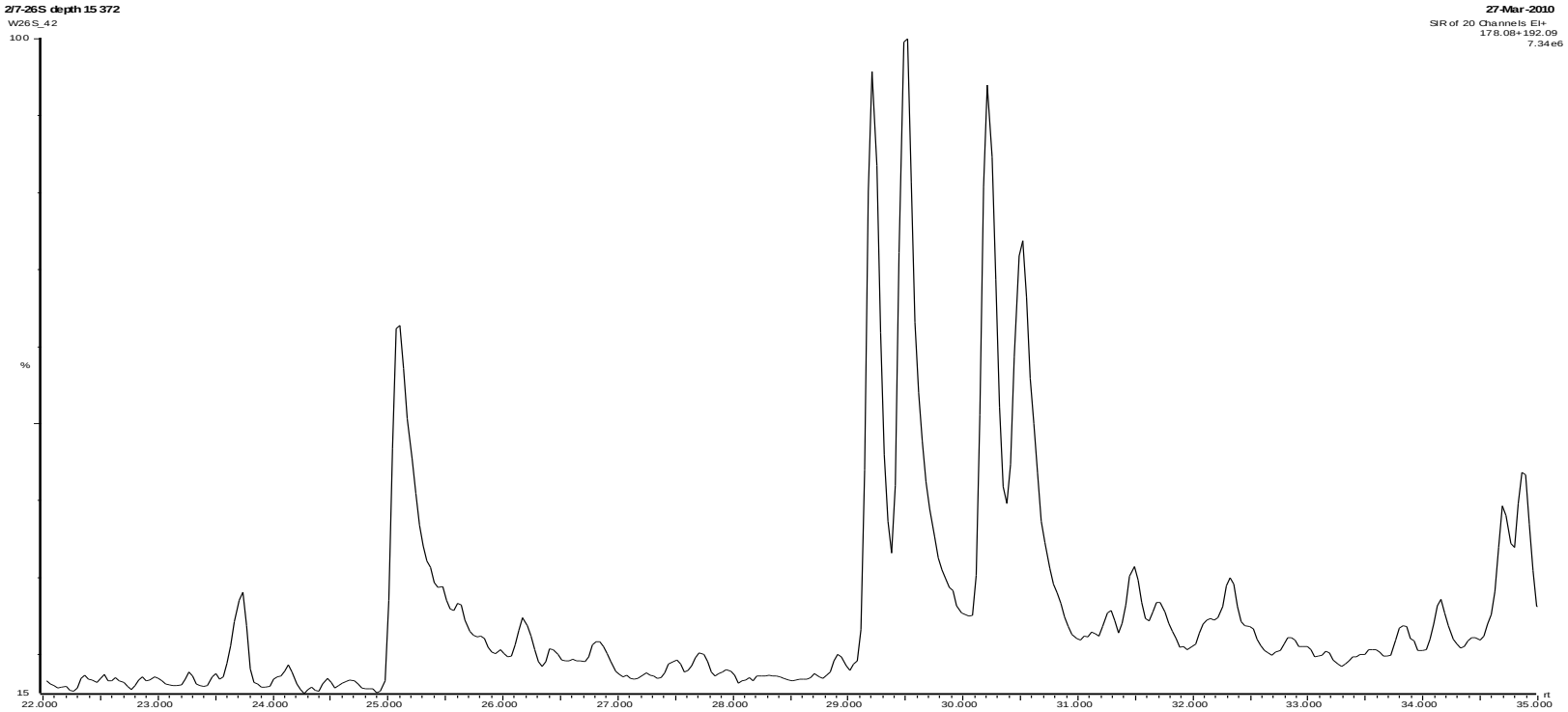
2/7-26S depth 15 372
W26S_42
27-Mar-2010
SIR of 20 Channels EI+
178.08+192.09
7.34e6
100
%
15
22.000
23.000
24.000
25.000
26.000
27.000
28.000
29.000
30.000
31.000
32.000
33.000
34.000
35.000
rt

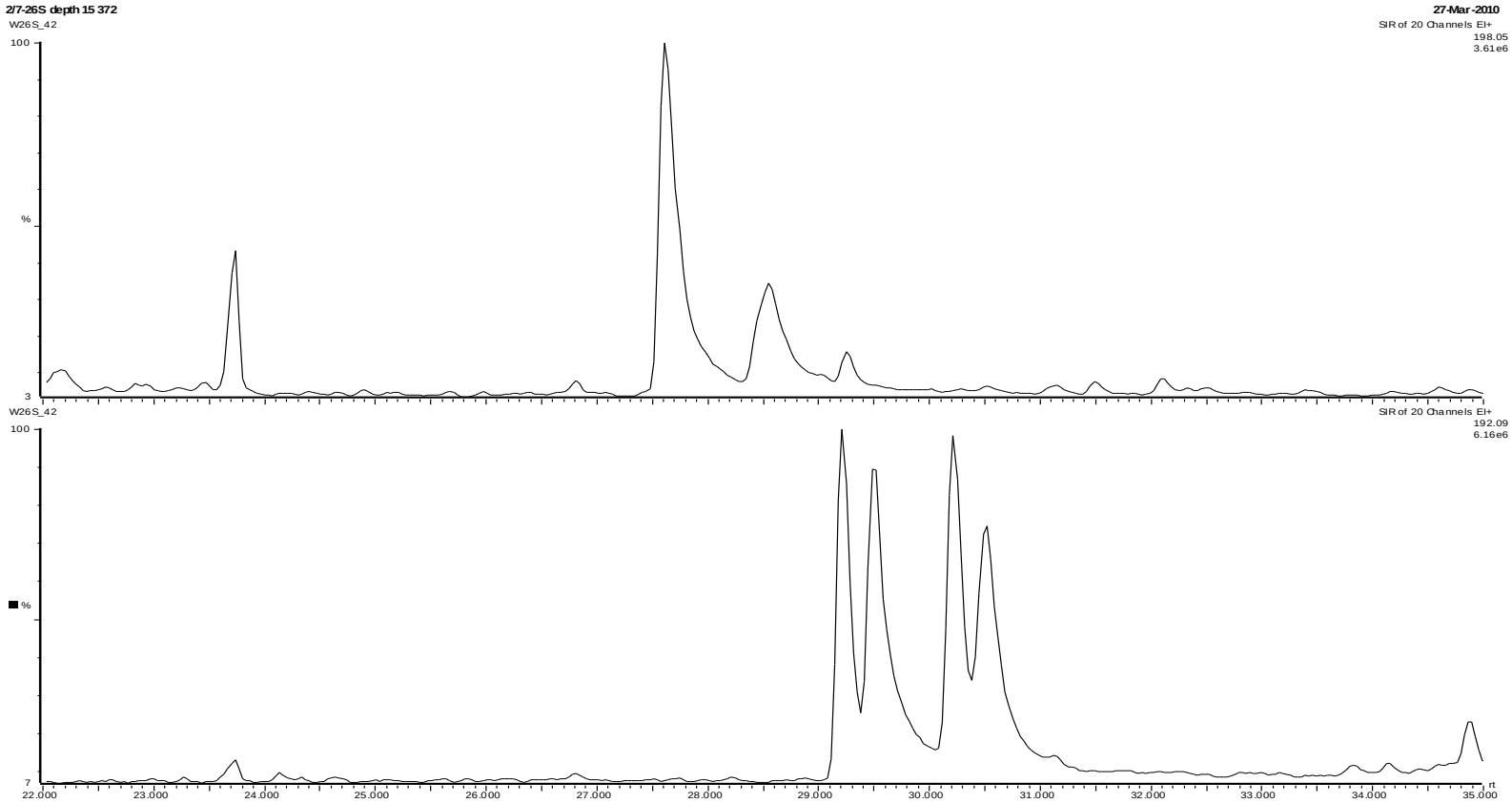
2/7-26S depth 15 372
27-Mar-2010
W26S_42
SIR of 20 Channels EI+
198.05
3.61e6
100
%
3
W26S_42
SIR of 20 Channels EI+
192.09
6.16e6
100
%
7
22.000
23.000
24.000
25.000
26.000
27.000
28.000
29.000
30.000
31.000
32.000
33.000
34.000
35.000
rt

GC-MS Chromatograms for sample E10

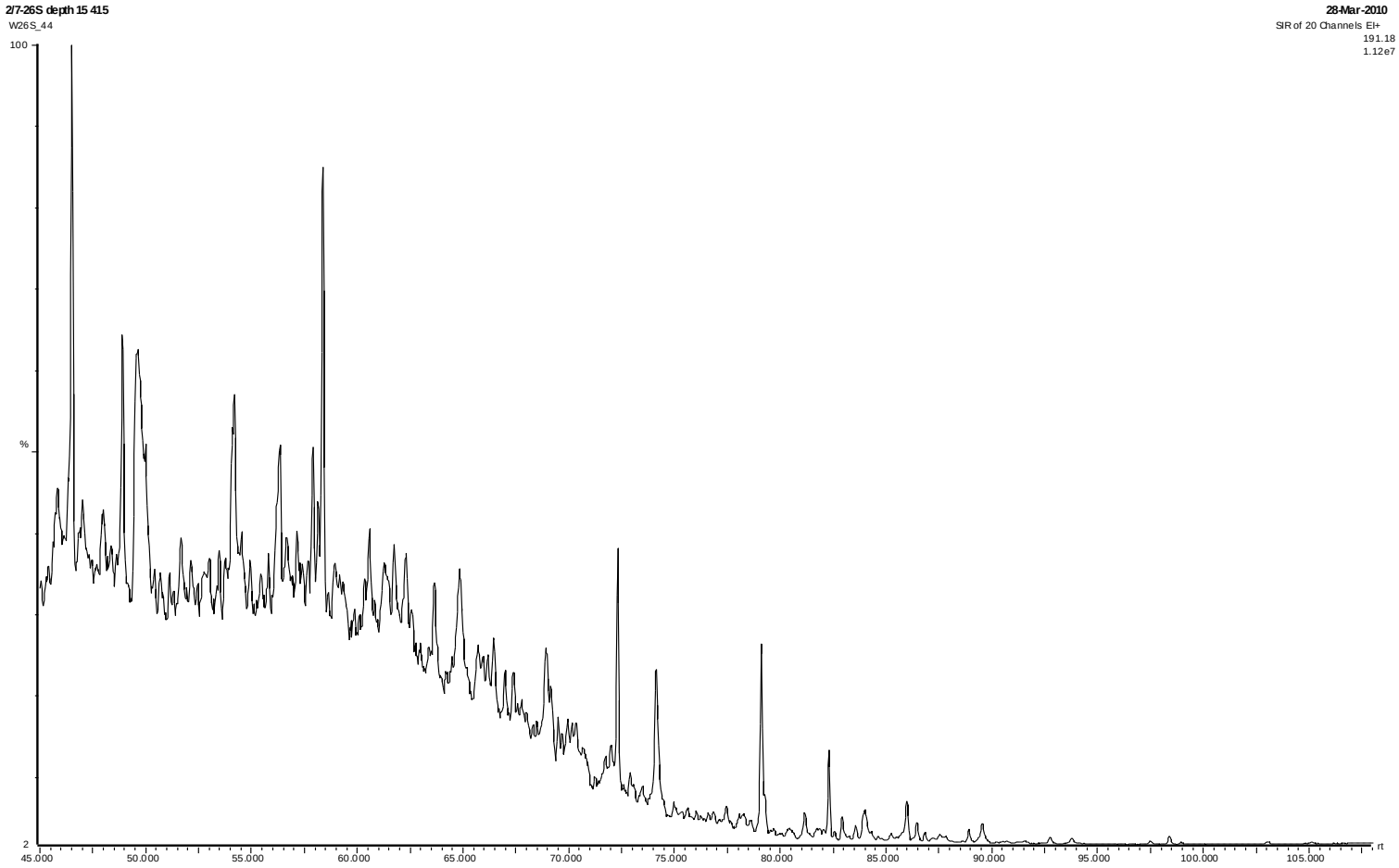
2/7-26S depth 15 415
W26S_44
28-Mar-2010
SIR of 20 Channels EI+
191.18
1.12e7
100
%
2
45.000
50.000
55.000
60.000
65.000
70.000
75.000
80.000
85.000
90.000
95.000
100.000
105.000
rt

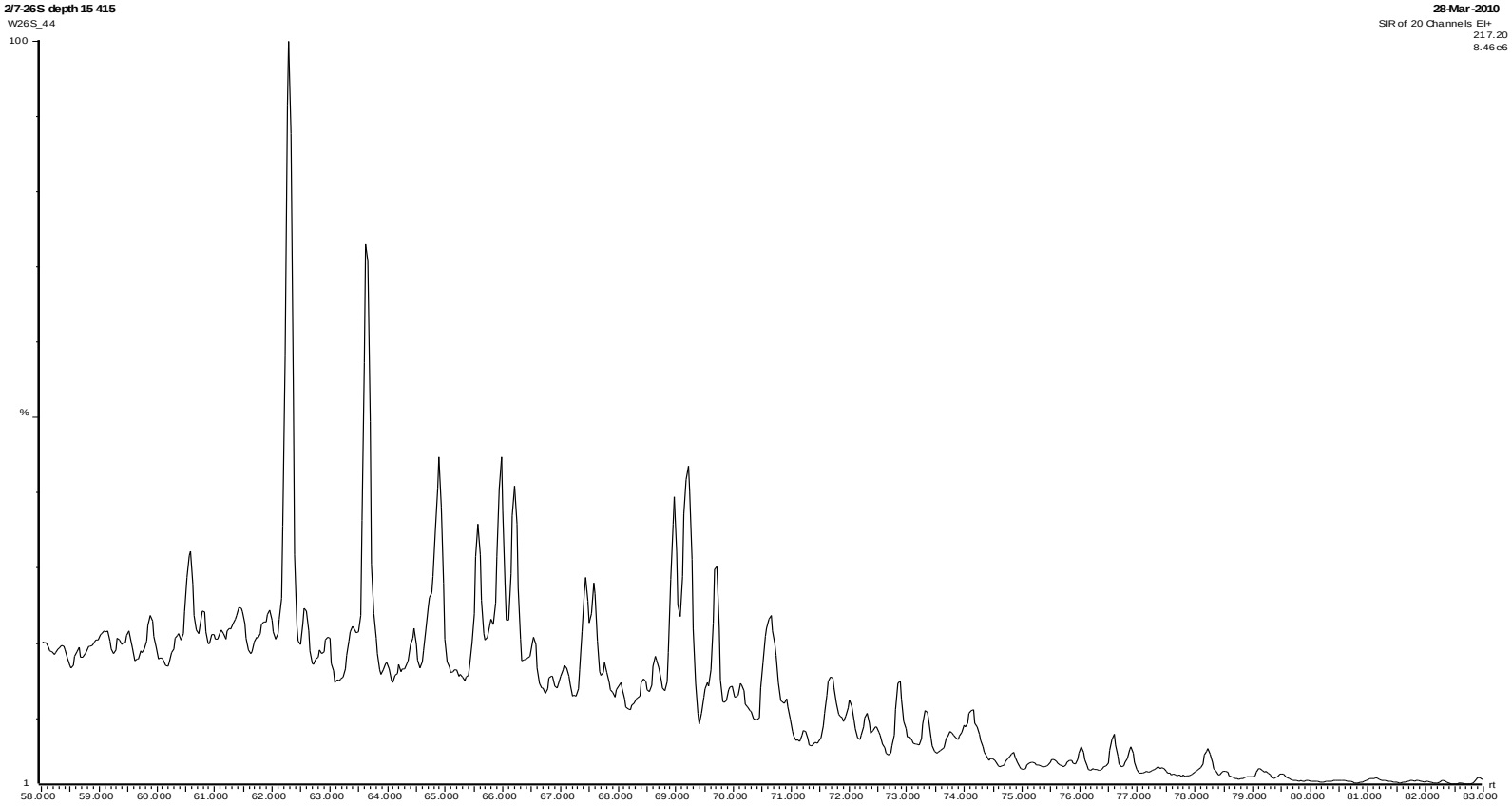
2/7-26S depth 15 415
W26S_44
28-Mar-2010
SIR of 20 Channels EI+
217.20
8.46e6
100
%
1
58.000
59.000
60.000
61.000
62.000
63.000
64.000
65.000
66.000
67.000
68.000
69.000
70.000
71.000
72.000
73.000
74.000
75.000
76.000
77.000
78.000
79.000
80.000
81.000
82.000
83.000
rt

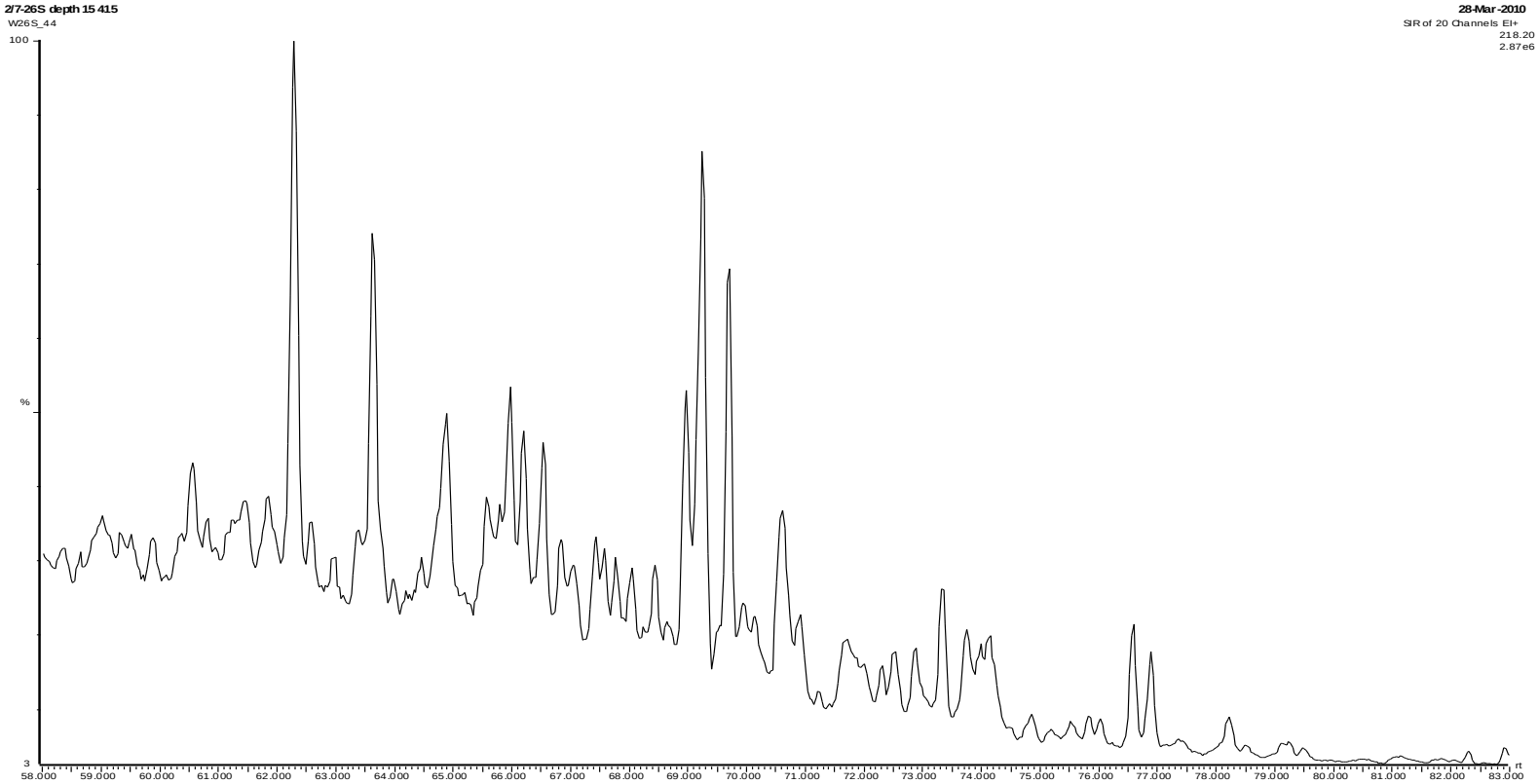
2/7-26S depth 15 415
W26S_44
28-Mar-2010
SIR of 20 Channels EI+
218.20
2.87e6
100
%
3
58.000
59.000
60.000
61.000
62.000
63.000
64.000
65.000
66.000
67.000
68.000
69.000
70.000
71.000
72.000
73.000
74.000
75.000
76.000
77.000
78.000
79.000
80.000
81.000
82.000
83.000
rt

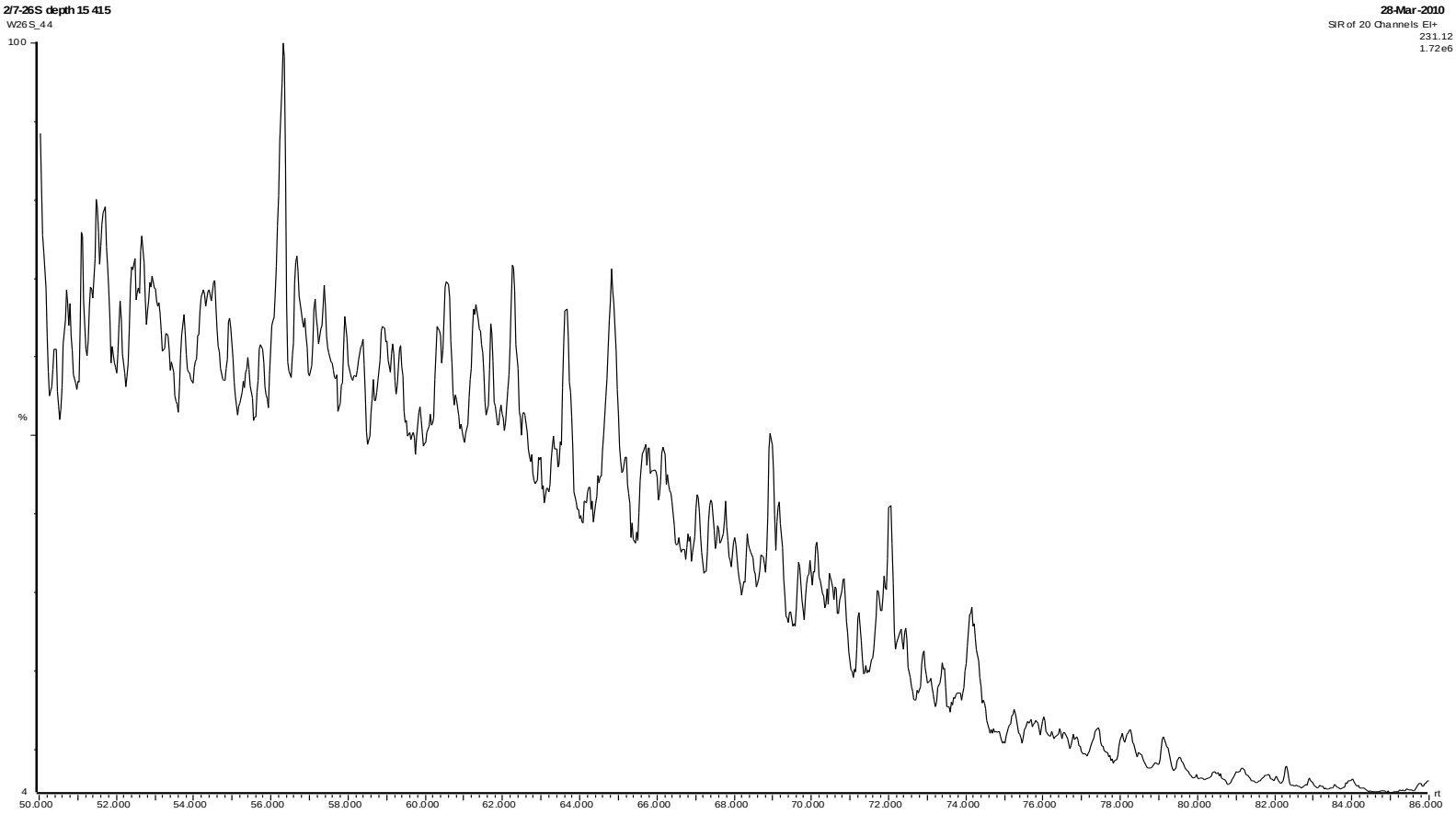
2/7-26S depth 15 415
W26S_44
28-Mar-2010
SIR of 20 Channels EI+
231.12
1.72e6
100
%
4
50.000
52.000
54.000
56.000
58.000
60.000
62.000
64.000
66.000
68.000
70.000
72.000
74.000
76.000
78.000
80.000
82.000
84.000
86.000
rt

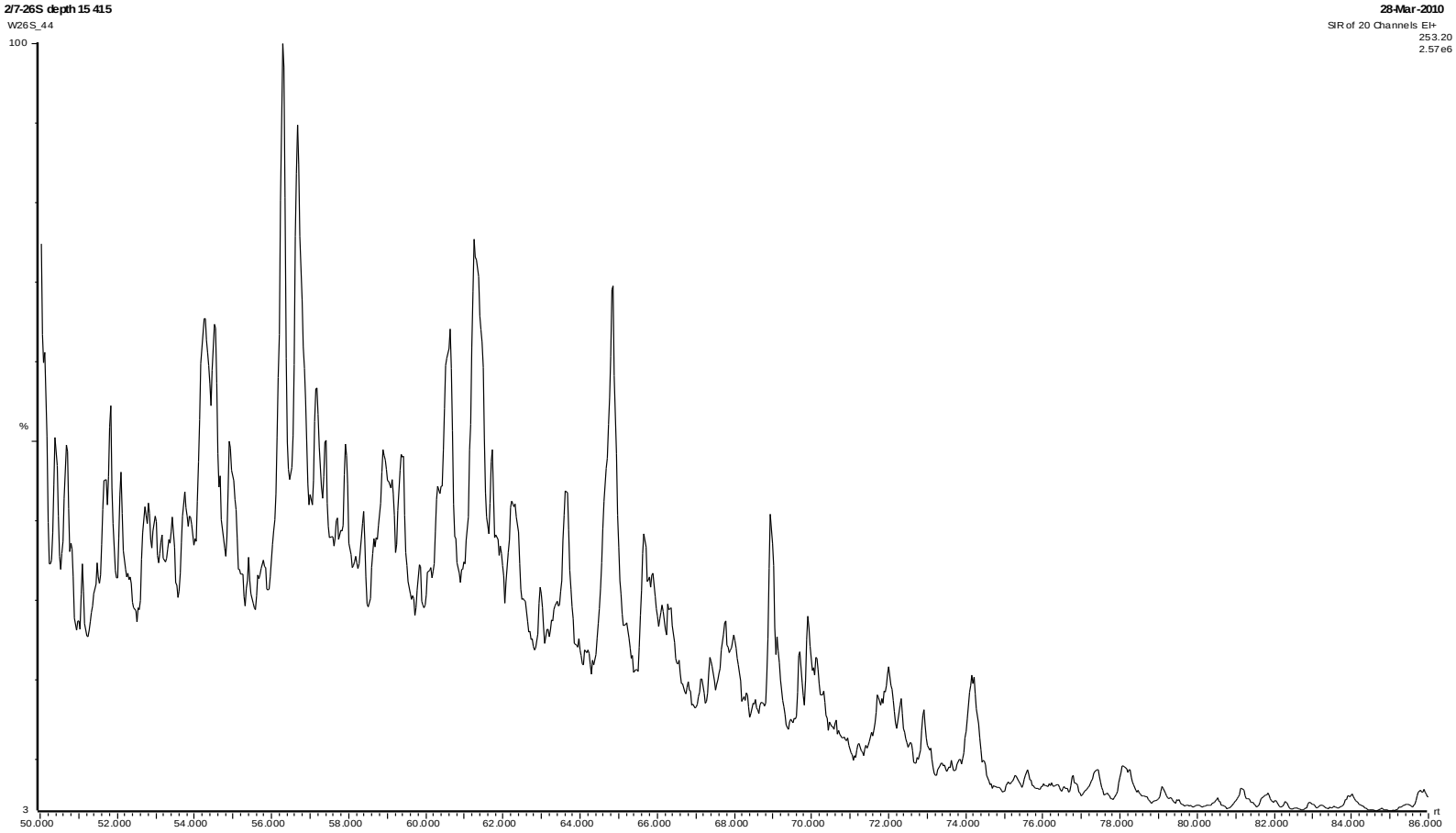
2/7-26S depth 15 415
W26S_44
28-Mar-2010
SIR of 20 Channels EI+
253.20
2.57e6
100
%
3
50.000
52.000
54.000
56.000
58.000
60.000
62.000
64.000
66.000
68.000
70.000
72.000
74.000
76.000
78.000
80.000
82.000
84.000
86.000
rt

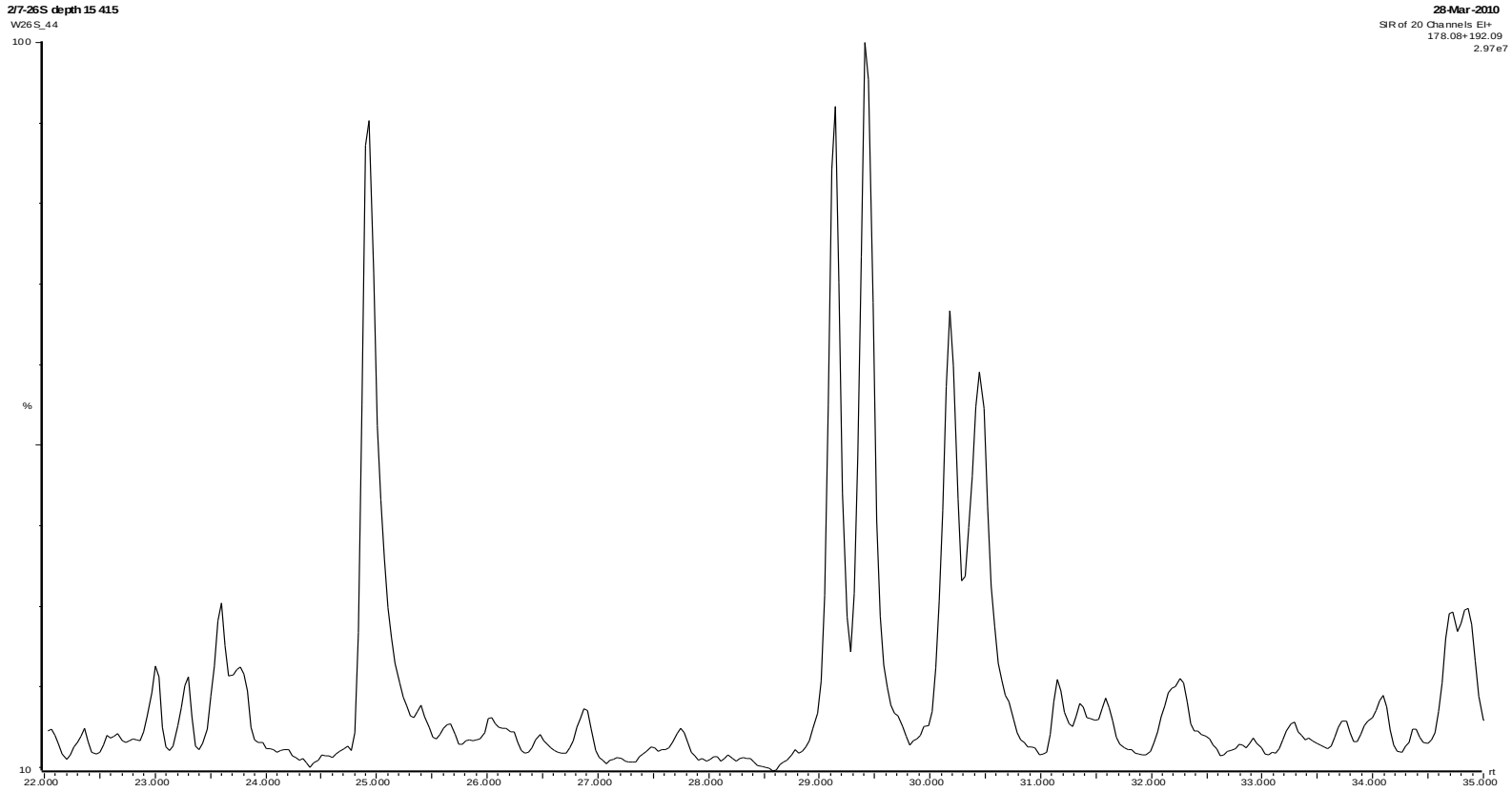
2/7-26S depth 15 415
W26S_44
28-Mar-2010
SIR of 20 Channels EI+
178.08+192.09
2.97e7
100
%
10
22.000
23.000
24.000
25.000
26.000
27.000
28.000
29.000
30.000
31.000
32.000
33.000
34.000
35.000
rt

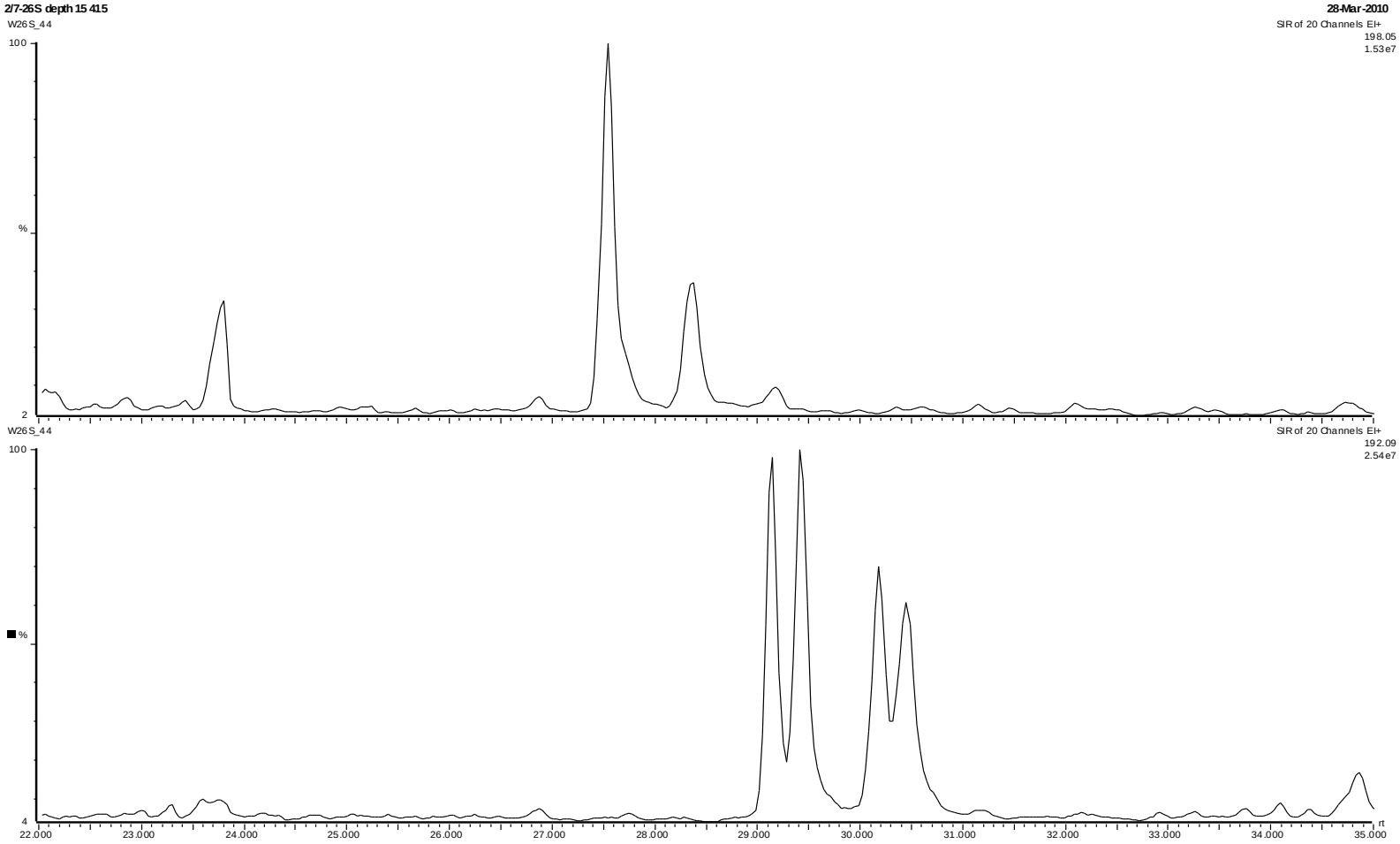
2/7-26S depth 15 415
28-Mar-2010
W26S_44
SIR of 20 Channels EI+
198.05
1.53e7
100
%
2
W26S_44
SIR of 20 Channels EI+
192.09
2.54e7
100
%
4
22.000
23.000
24.000
25.000
26.000
27.000
28.000
29.000
30.000
31.000
32.000
33.000
34.000
35.000
rt

GC-MS Chromatograms for sample E11

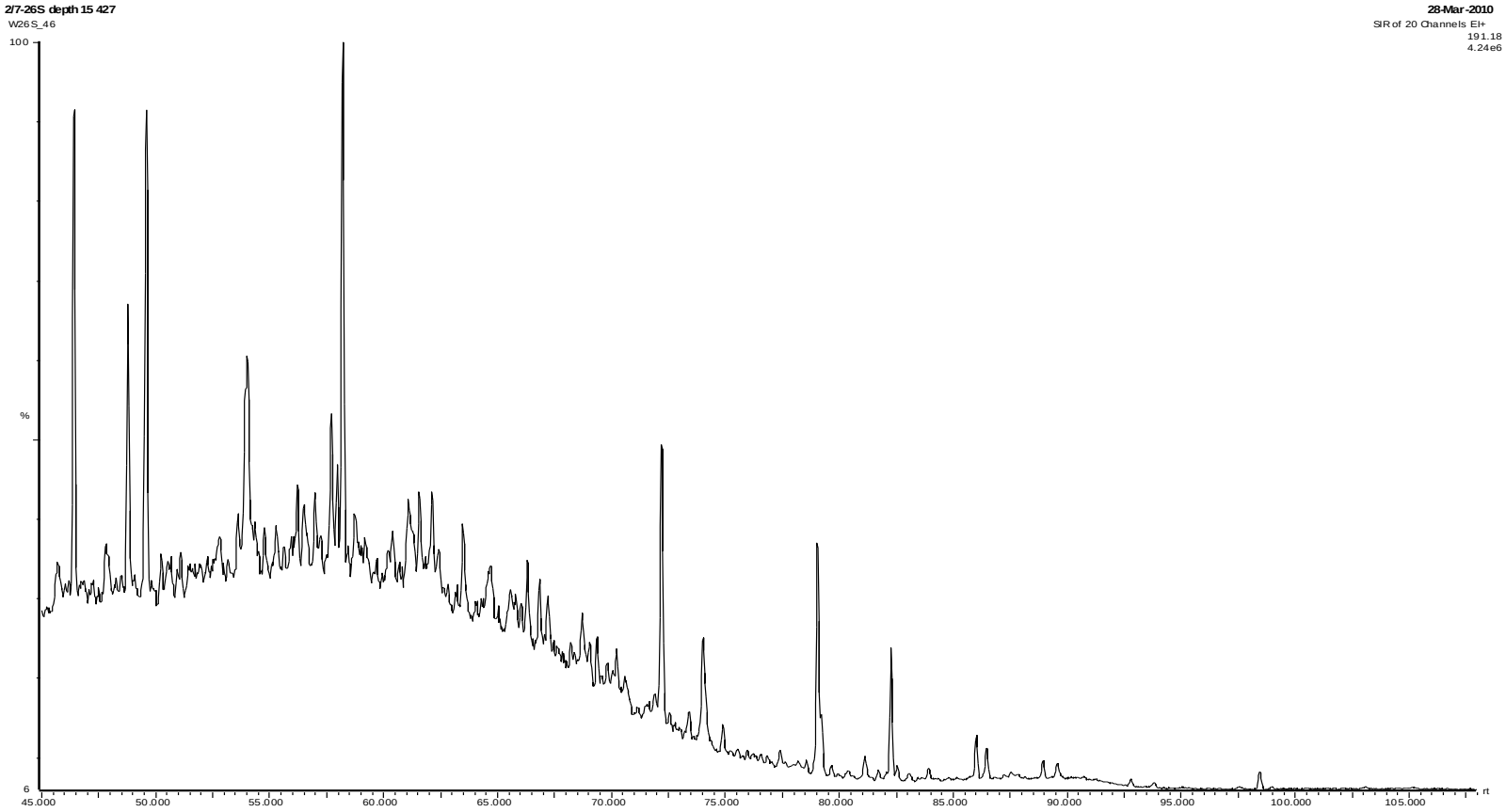
2/7-26S depth 15 427
W26S_46
28-Mar-2010
SIR of 20 Channels ES+
191.18
4.24e6
100
%
6
45.000
50.000
55.000
60.000
65.000
70.000
75.000
80.000
85.000
90.000
95.000
100.000
105.000
rt

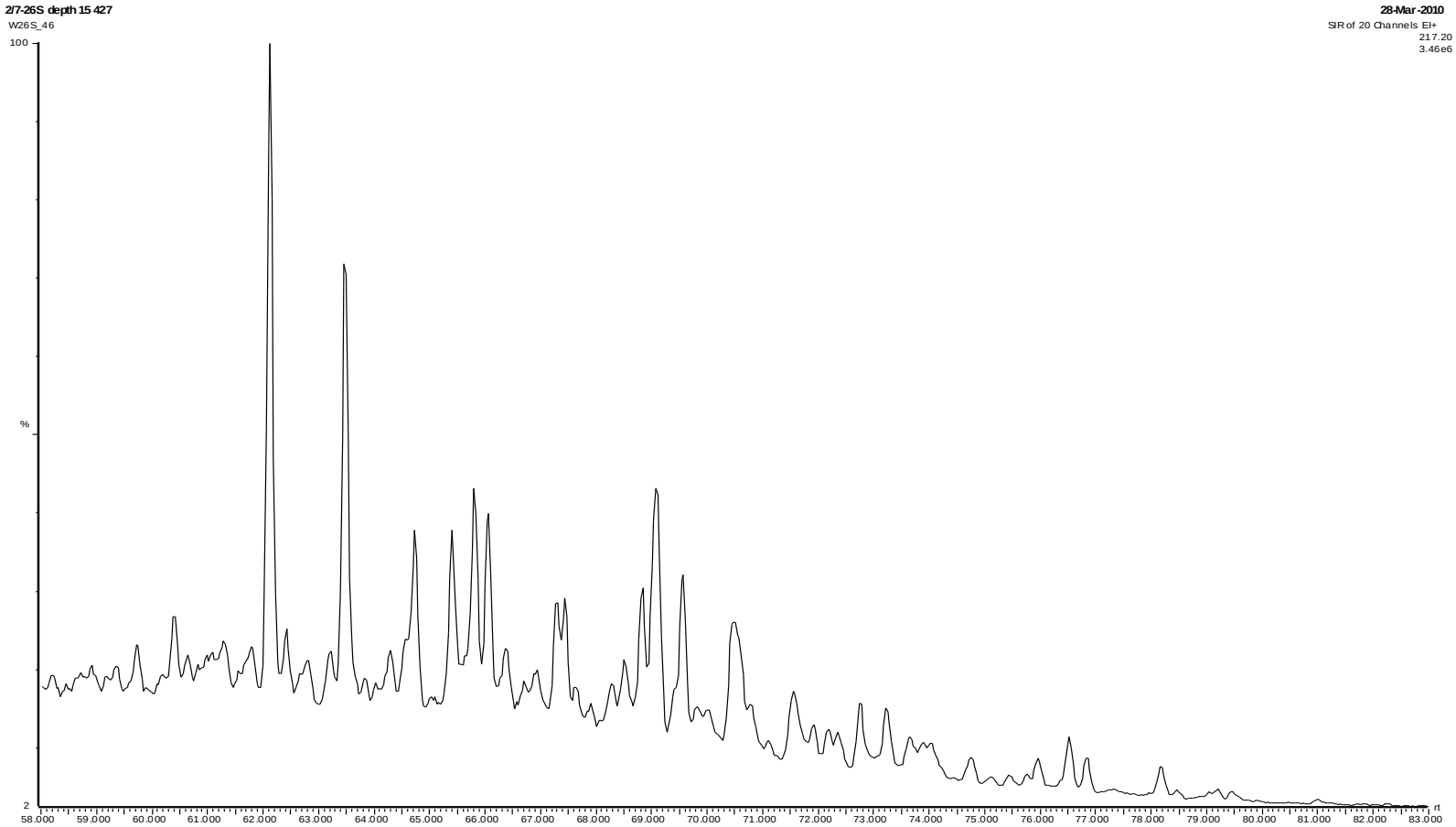
2/7-26S depth 15 427
W26S_46
28-Mar-2010
SIR of 20 Channels EI+
217.20
3.46e6
100
%
2
58.000
59.000
60.000
61.000
62.000
63.000
64.000
65.000
66.000
67.000
68.000
69.000
70.000
71.000
72.000
73.000
74.000
75.000
76.000
77.000
78.000
79.000
80.000
81.000
82.000
83.000
rt

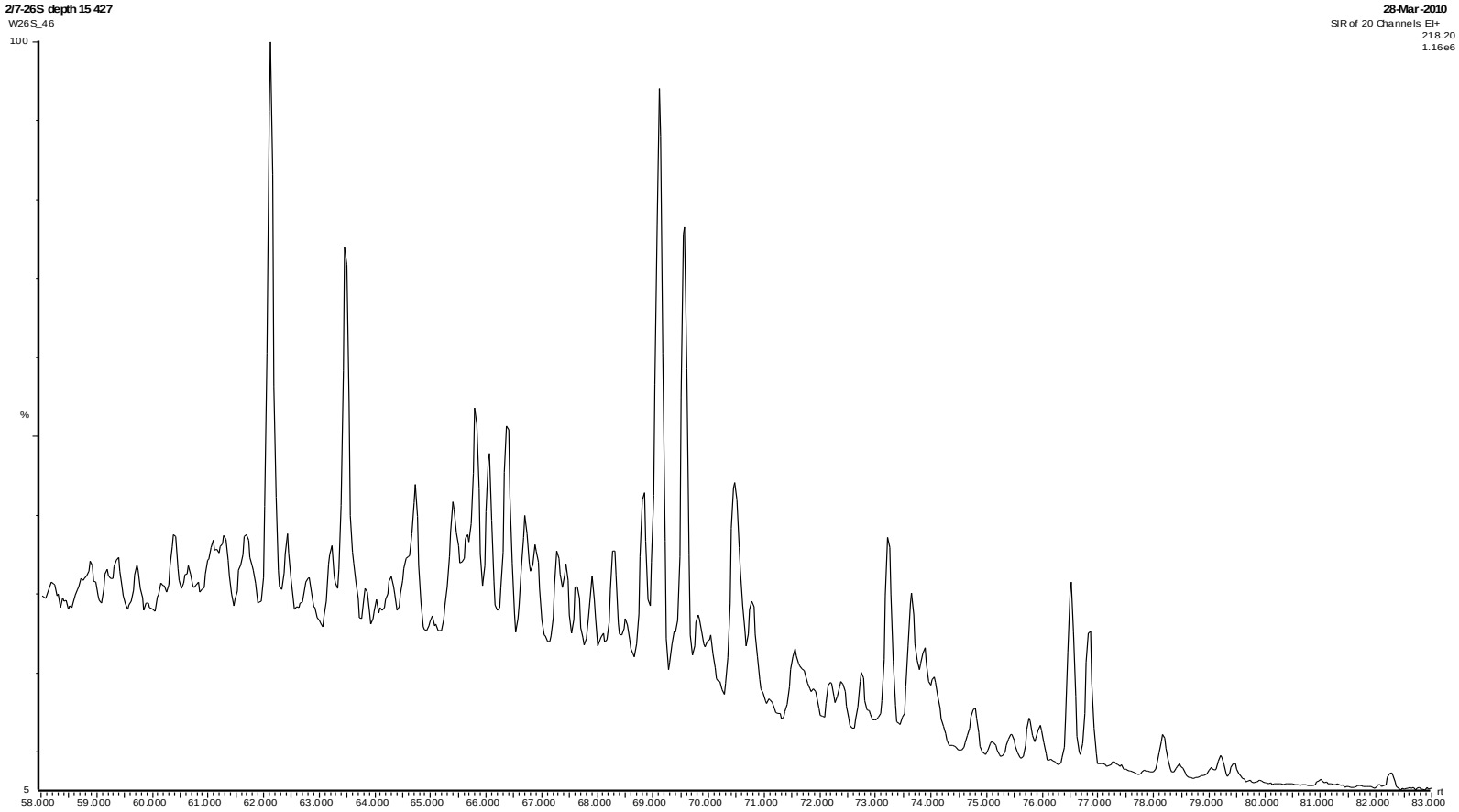
2/7-26S depth 15 427
W26S_46
28-Mar-2010
SIR of 20 Channels EI+
218.20
1.16e6
100
%
5
58.000
59.000
60.000
61.000
62.000
63.000
64.000
65.000
66.000
67.000
68.000
69.000
70.000
71.000
72.000
73.000
74.000
75.000
76.000
77.000
78.000
79.000
80.000
81.000
82.000
83.000
rt

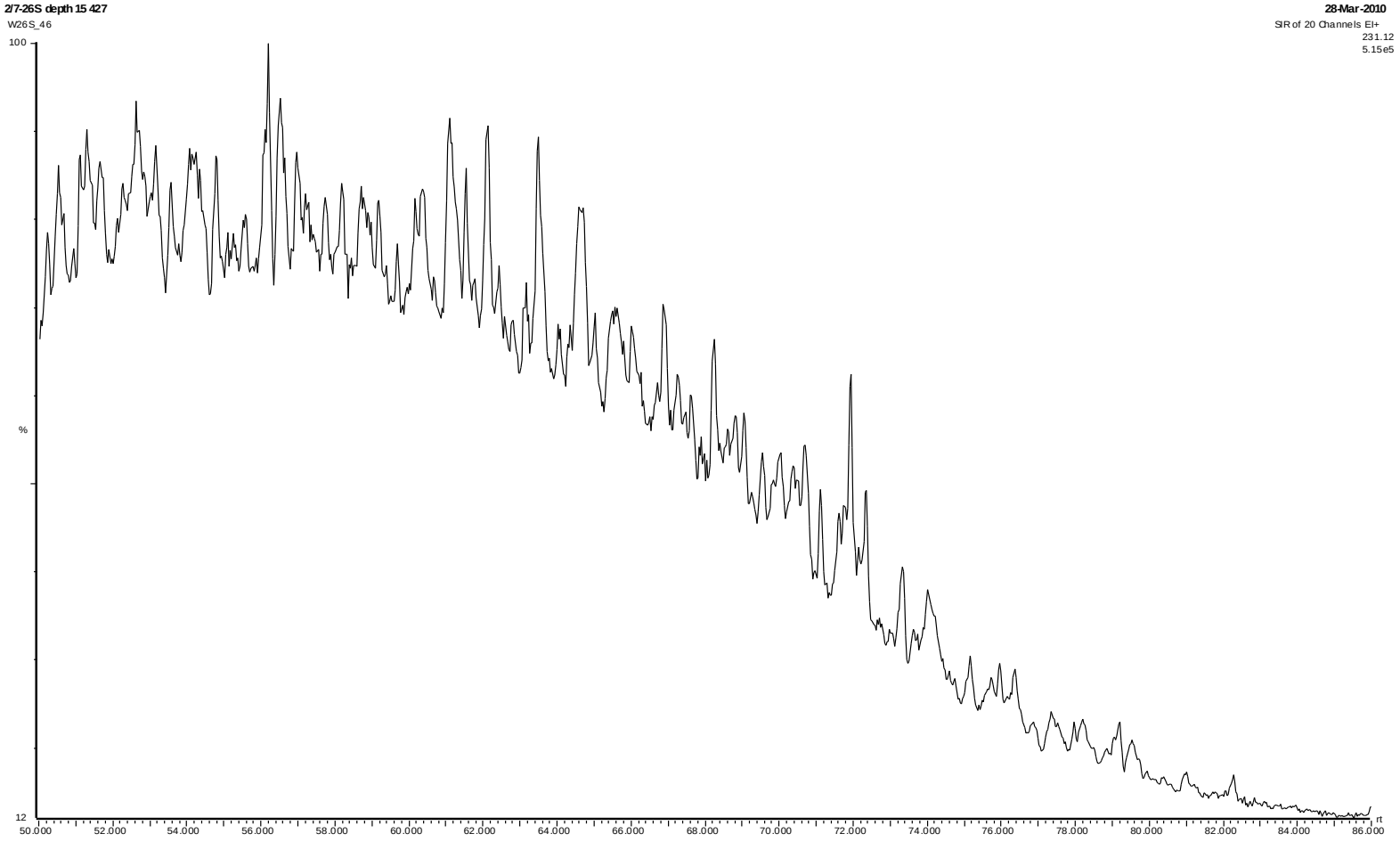
2/7-26S depth 15 427
W26S_46
28-Mar-2010
SIR of 20 Channels EI+
231.12
5.15e5
100
%
12
50.000
52.000
54.000
56.000
58.000
60.000
62.000
64.000
66.000
68.000
70.000
72.000
74.000
76.000
78.000
80.000
82.000
84.000
86.000
rt

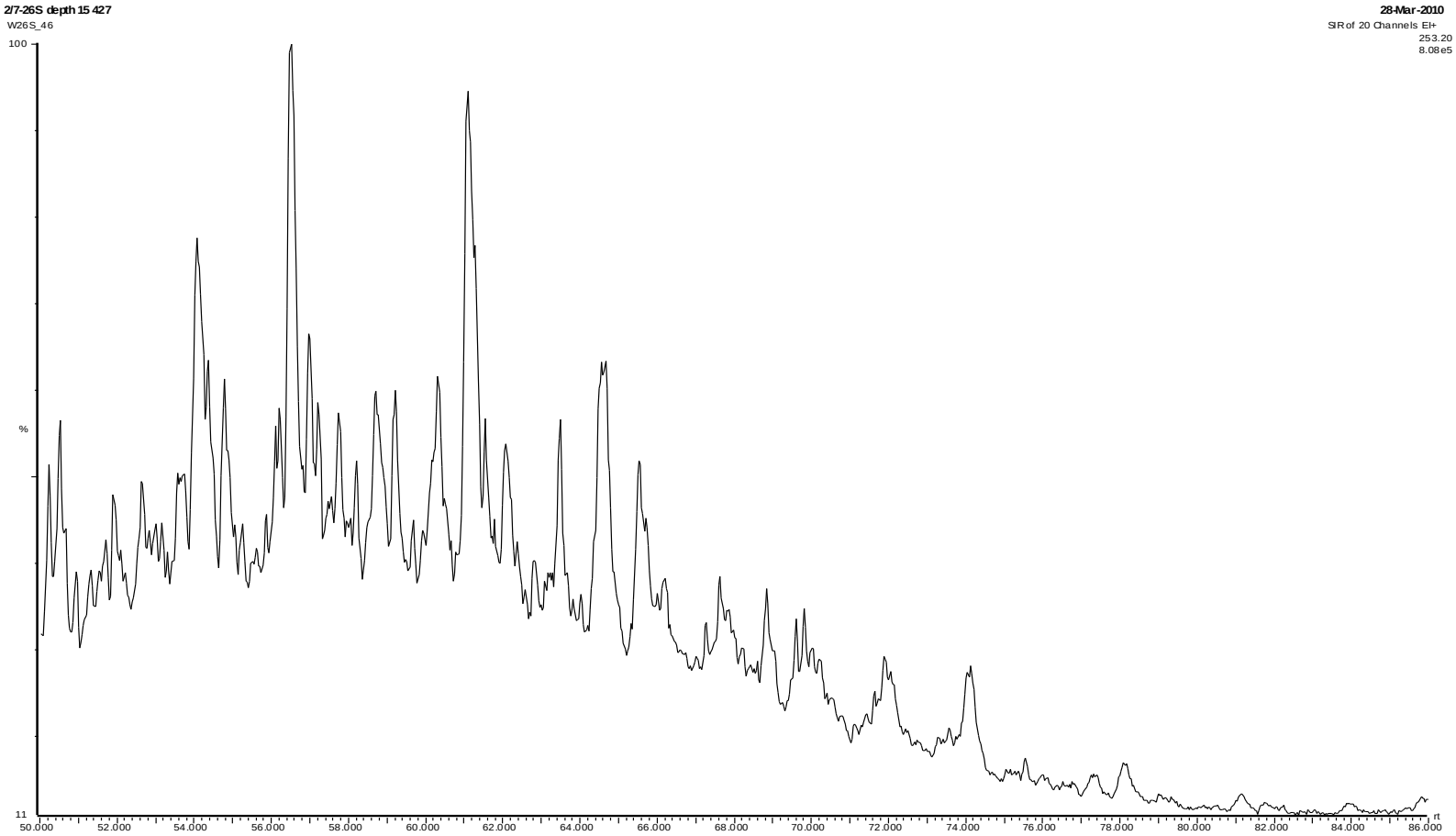
2/7-26S depth 15 427
W26S_46
28-Mar-2010
SIR of 20 Channels EI+
253.20
8.08e5
100
%
11
50.000
52.000
54.000
56.000
58.000
60.000
62.000
64.000
66.000
68.000
70.000
72.000
74.000
76.000
78.000
80.000
82.000
84.000
86.000
rt

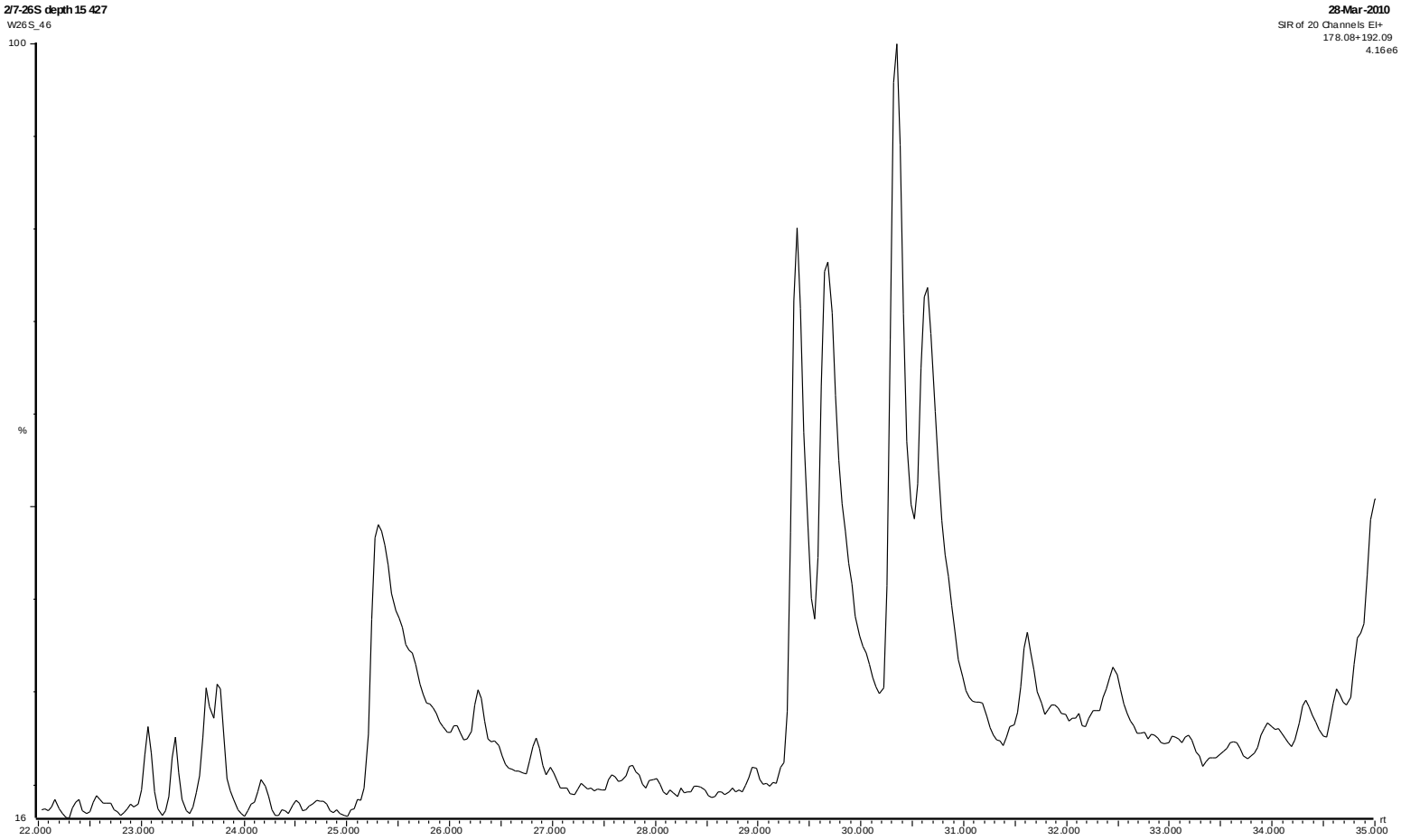
2/7-26S depth 15 427
W26S_46
28-Mar-2010
SIR of 20 Channels EI+
178.08+192.09
4.16e6
100
%
16
22.000
23.000
24.000
25.000
26.000
27.000
28.000
29.000
30.000
31.000
32.000
33.000
34.000
35.000
rt

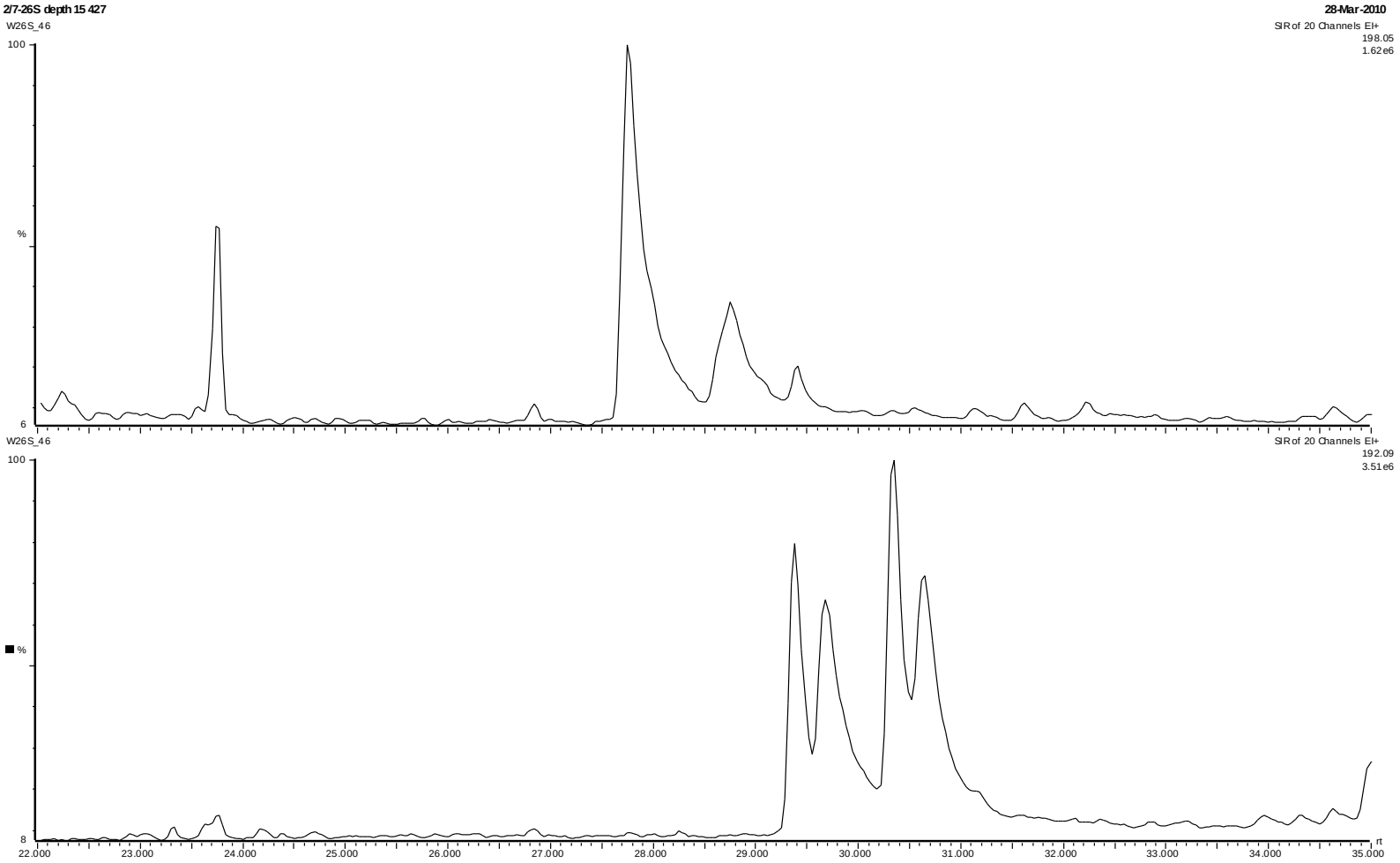
2/7-26S depth 15 427
28-Mar-2010
W26S_46
SIR of 20 Channels EI+
198.05
1.62e6
100
%
6
W26S_46
SIR of 20 Channels EI+
192.09
3.51e6
100
%
8
22.000
23.000
24.000
25.000
26.000
27.000
28.000
29.000
30.000
31.000
32.000
33.000
34.000
35.000
rt

GC-MS Chromatograms for sample E12

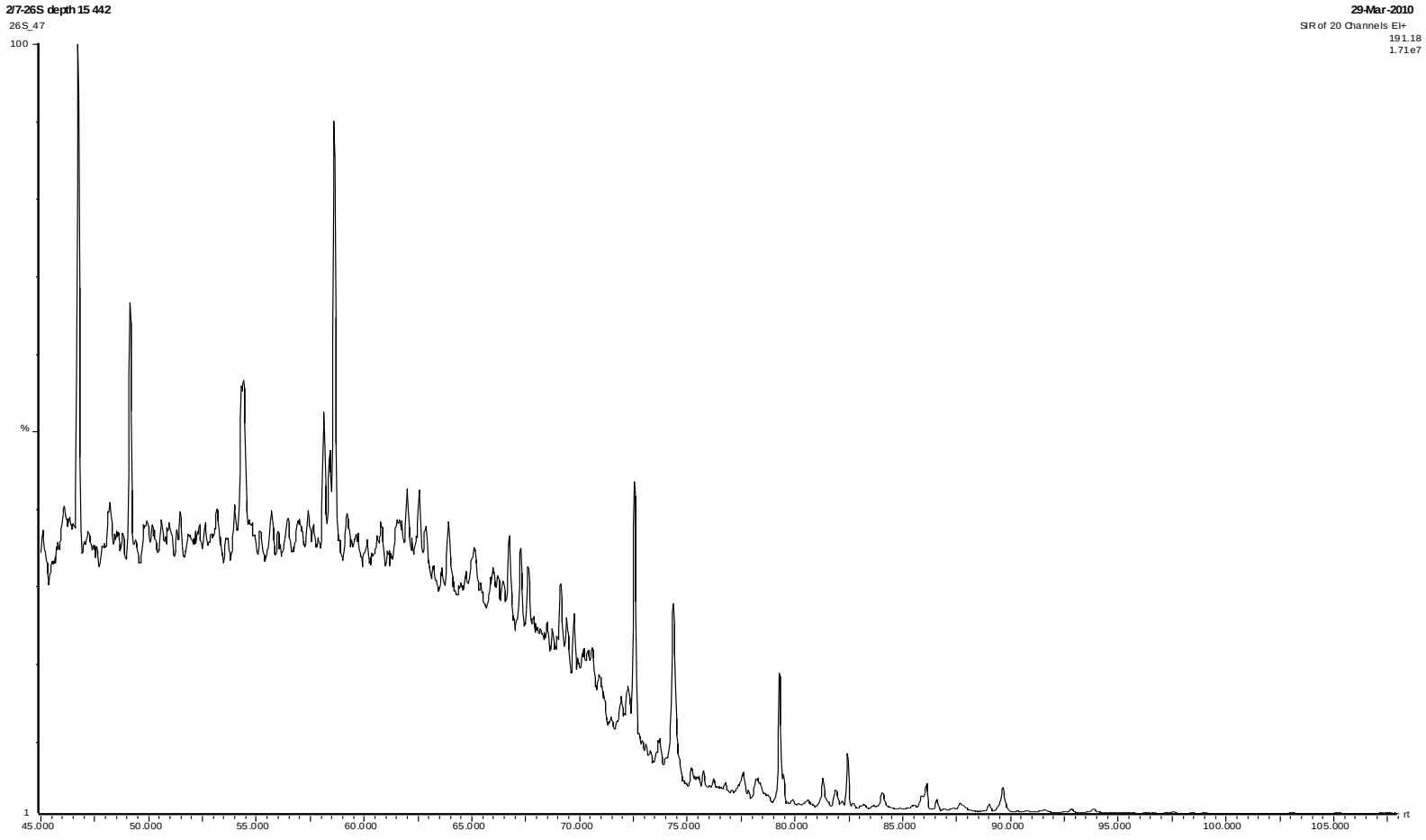
2/7-26S depth 15 442
26S_47
29-Mar-2010
SIR of 20 Channels ES+
191.18
1.71e7
100
%
1
45.000
50.000
55.000
60.000
65.000
70.000
75.000
80.000
85.000
90.000
95.000
100.000
105.000
rt

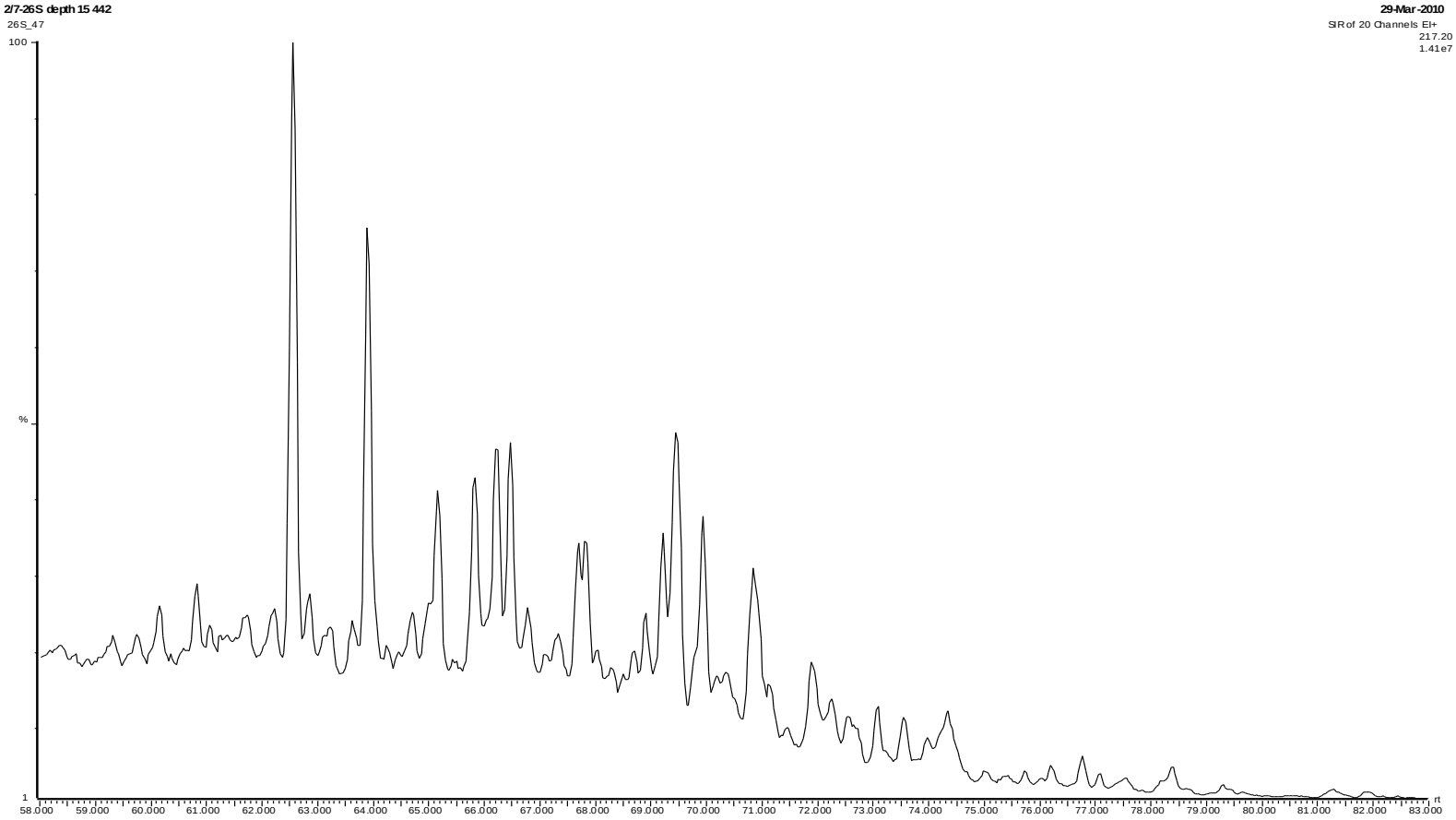
2/7-26S depth 15 442
26S_47
100
%
1
58.000
59.000
60.000
61.000
62.000
63.000
64.000
65.000
66.000
67.000
68.000
69.000
70.000
71.000
72.000
73.000
74.000
75.000
76.000
77.000
78.000
79.000
80.000
81.000
82.000
83.000
rt
29-Mar-2010
SIR of 20 Channels EI+
217.20
1.41e7

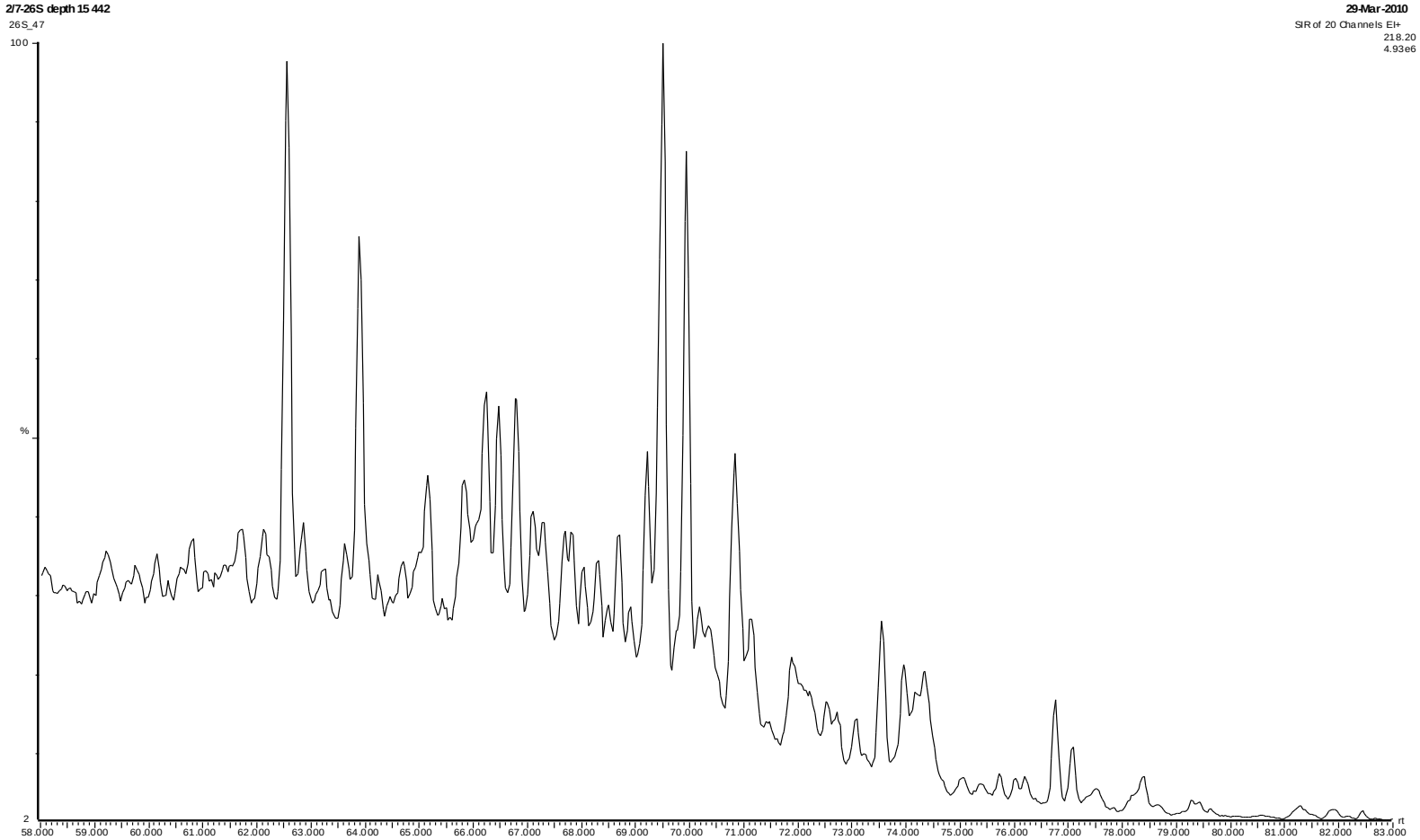
2/7-26S depth 15 442
26S_47
100
%
2
29-Mar-2010
SIR of 20 Channels EI+
218.20
4.93e6
58.000
59.000
60.000
61.000
62.000
63.000
64.000
65.000
66.000
67.000
68.000
69.000
70.000
71.000
72.000
73.000
74.000
75.000
76.000
77.000
78.000
79.000
80.000
81.000
82.000
83.000
rt

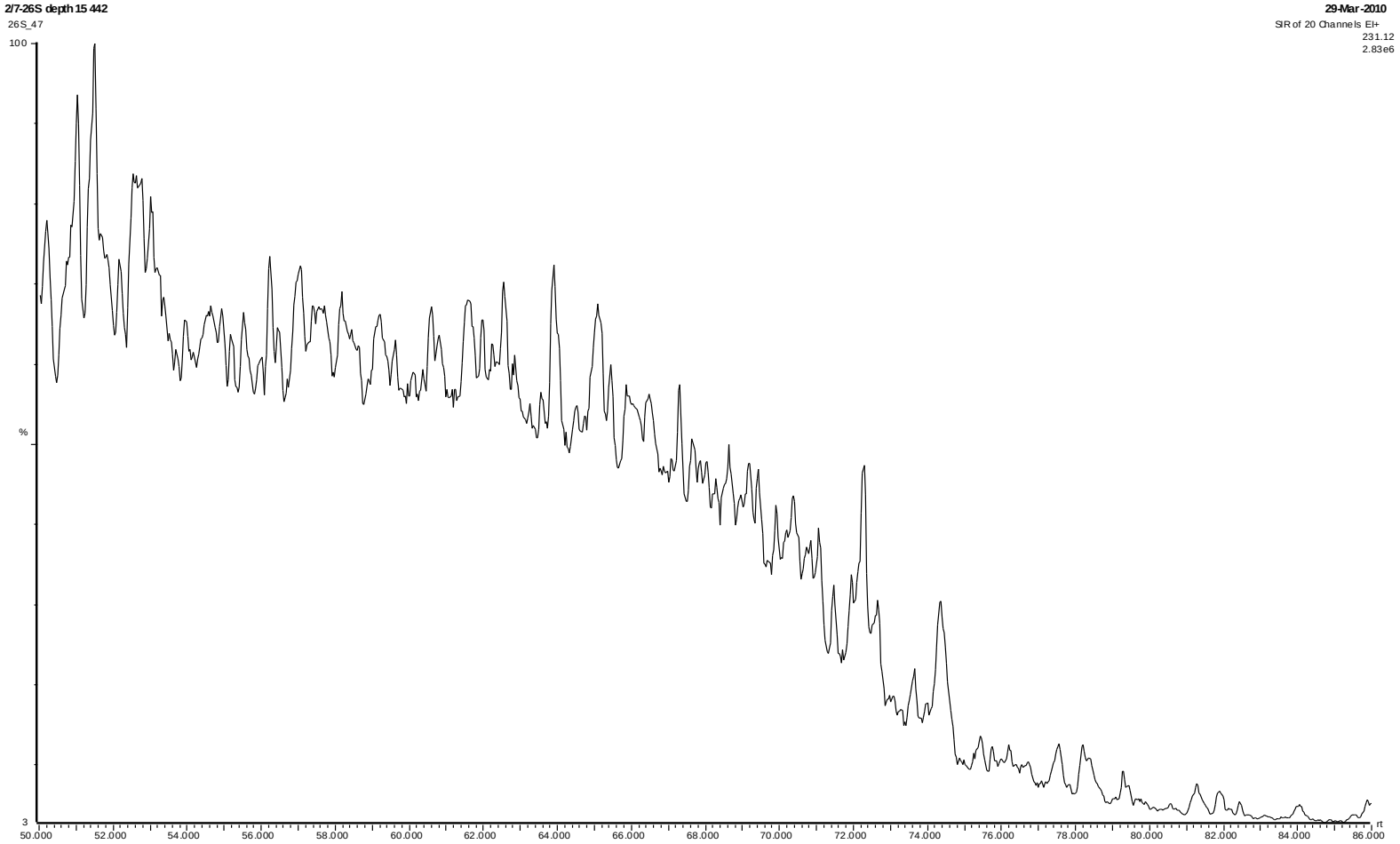
2/7-26S depth 15 442
26S_47
29-Mar-2010
SIR of 20 Channels EI+
231.12
2.83e6
100
%
3
50.000
52.000
54.000
56.000
58.000
60.000
62.000
64.000
66.000
68.000
70.000
72.000
74.000
76.000
78.000
80.000
82.000
84.000
86.000
rt

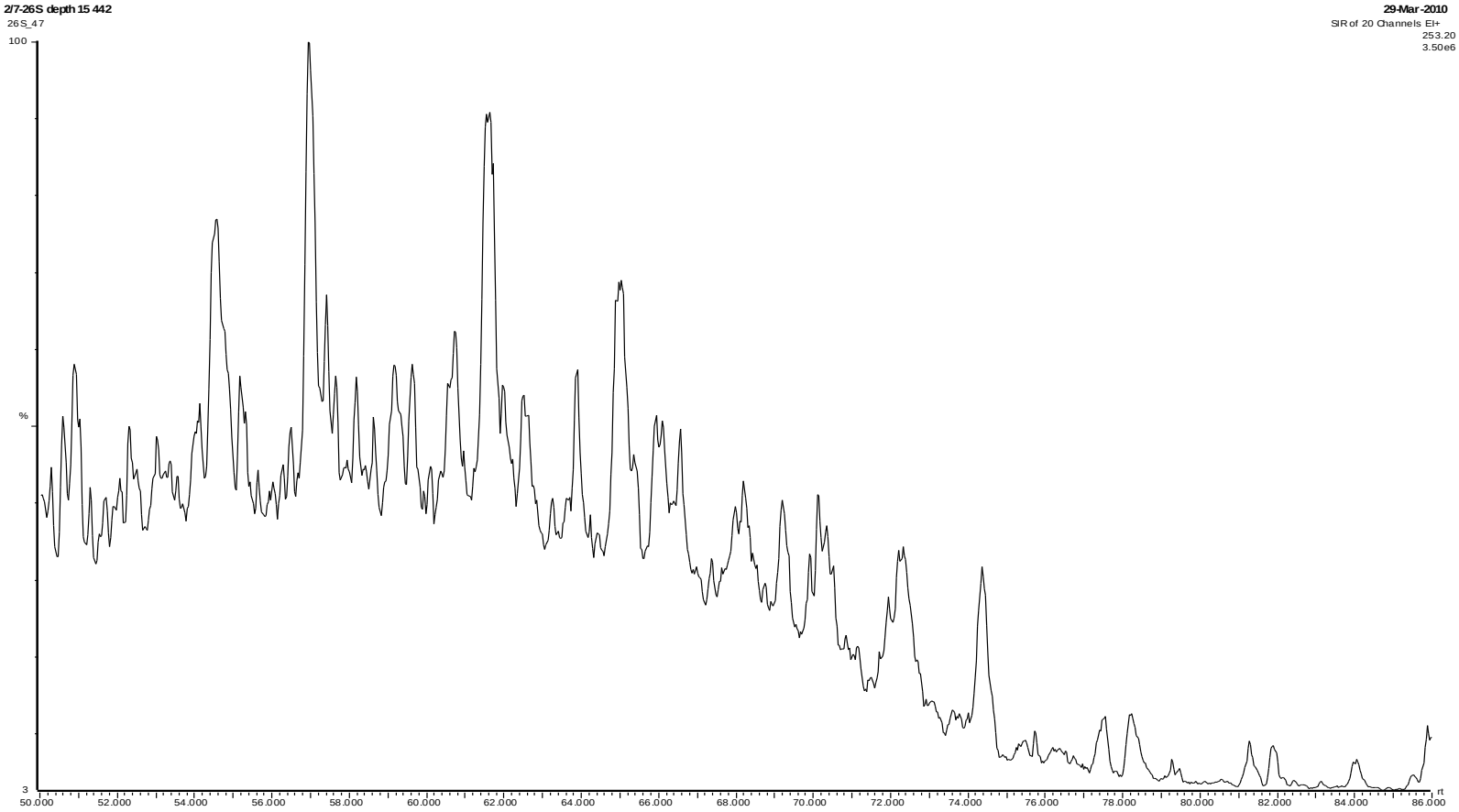
2/7-26S depth 15 442
26S_47
100
%
3
29-Mar-2010
SIR of 20 Channels EI+
253.20
3.50e6
50.000
52.000
54.000
56.000
58.000
60.000
62.000
64.000
66.000
68.000
70.000
72.000
74.000
76.000
78.000
80.000
82.000
84.000
86.000
rt

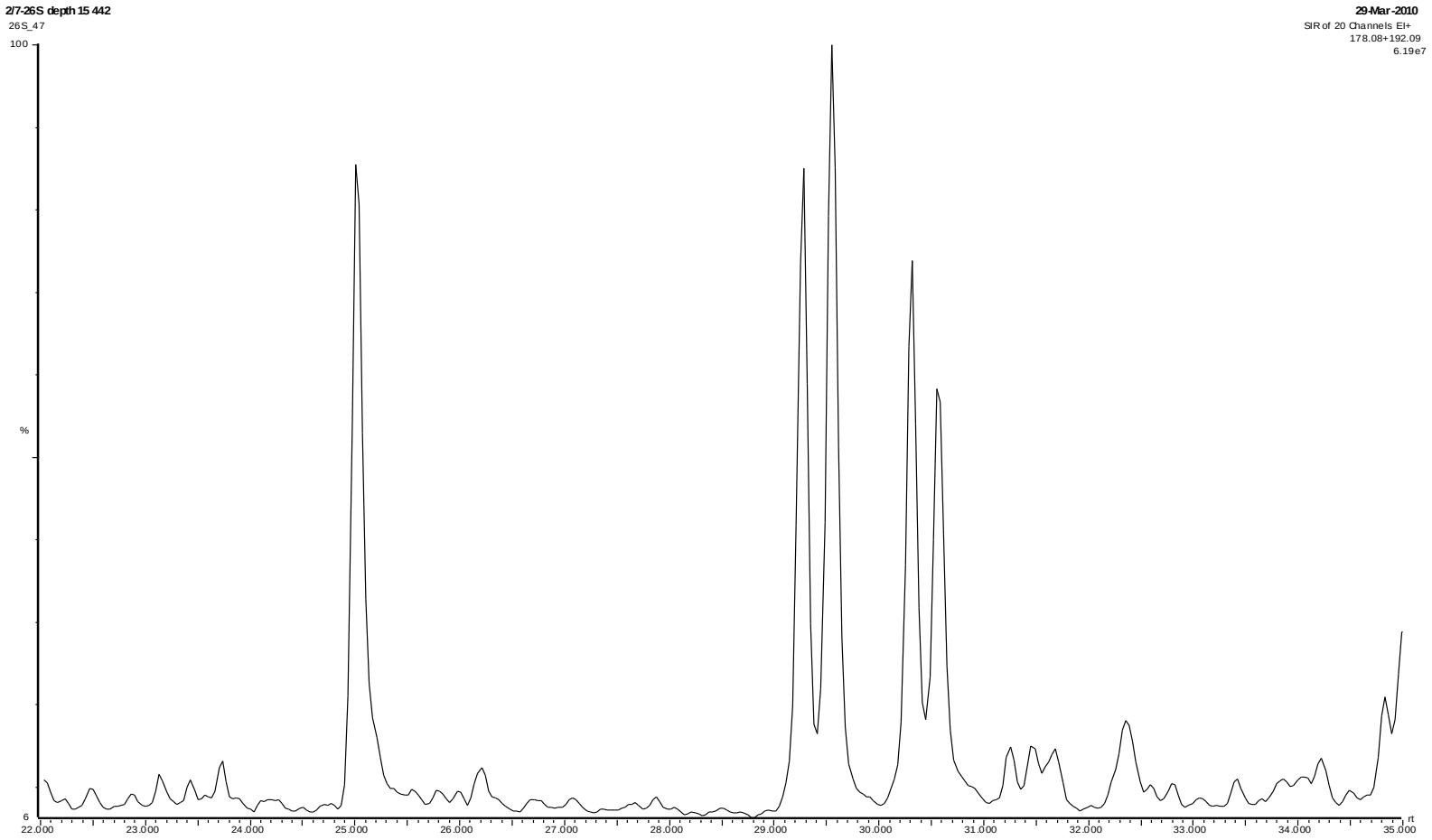
2/7-26S depth 15 442
26S_47
29-Mar-2010
SIR of 20 Channels EI+
178.08+192.09
6.19e7
100
%
6
22.000
23.000
24.000
25.000
26.000
27.000
28.000
29.000
30.000
31.000
32.000
33.000
34.000
35.000
rt

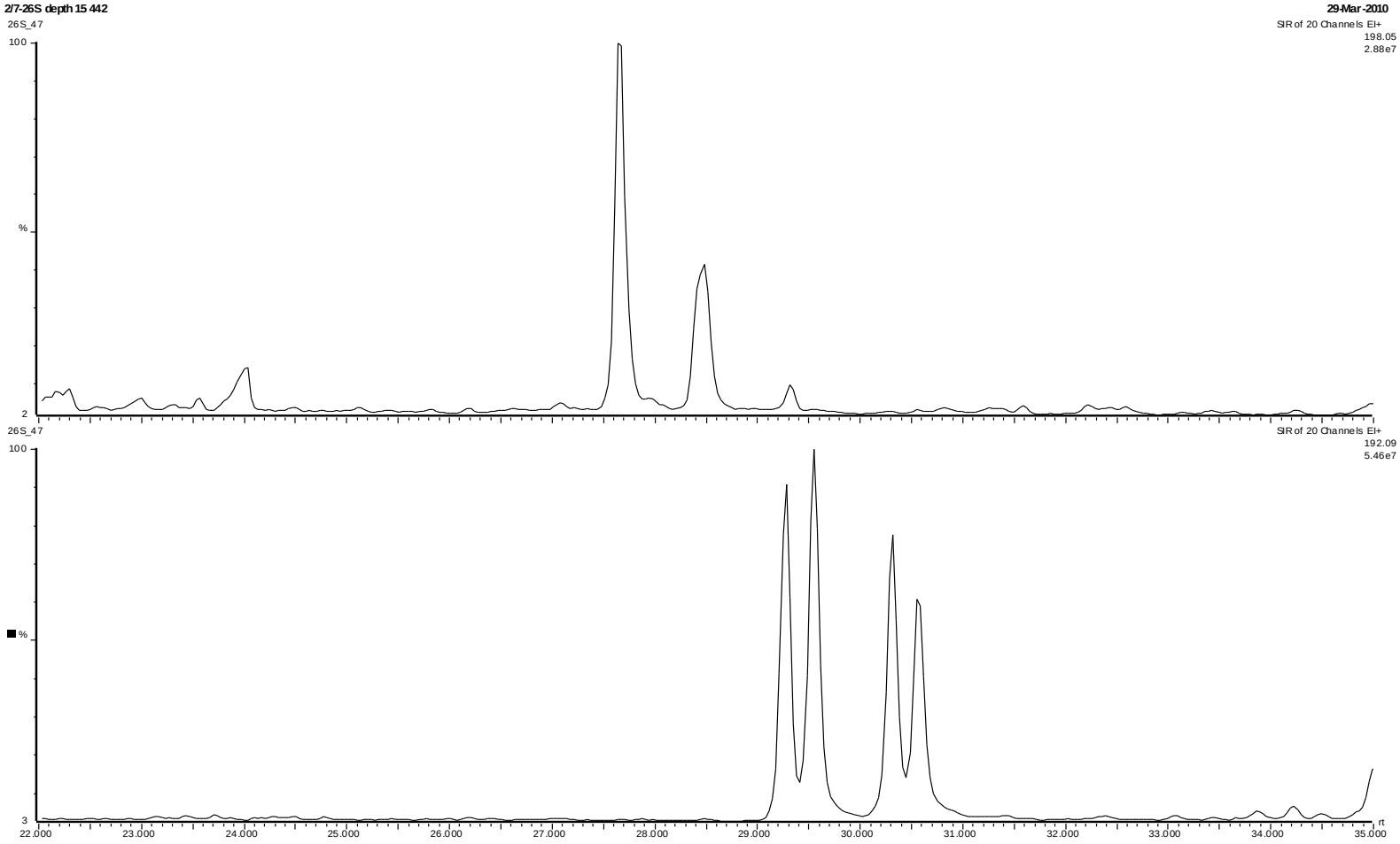
2/7-26S depth 15 442
29-Mar-2010
26S_47
SIR of 20 Channels EI+
198.05
2.88e7
100
%
2
26S_47
SIR of 20 Channels EI+
192.09
5.46e7
100
%
3
22.000
23.000
24.000
25.000
26.000
27.000
28.000
29.000
30.000
31.000
32.000
33.000
34.000
35.000
rt

GC-MS Chromatograms for sample E13

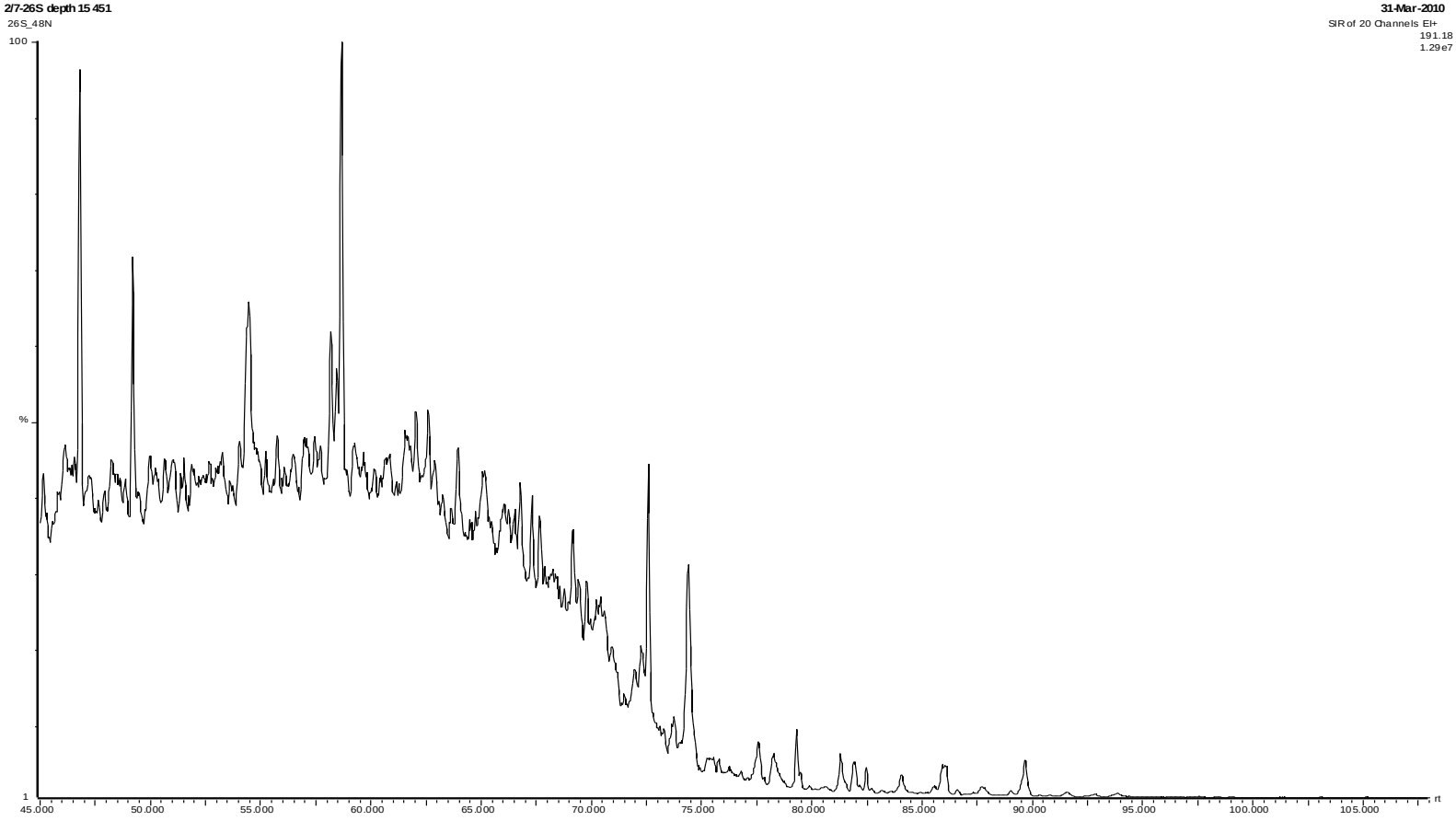
2/7-26S depth 15 451
26S_48N
31-Mar-2010
SIR of 20 Channels EI+
191.18
1.29e7
100
%
1
45.000
50.000
55.000
60.000
65.000
70.000
75.000
80.000
85.000
90.000
95.000
100.000
105.000
rt

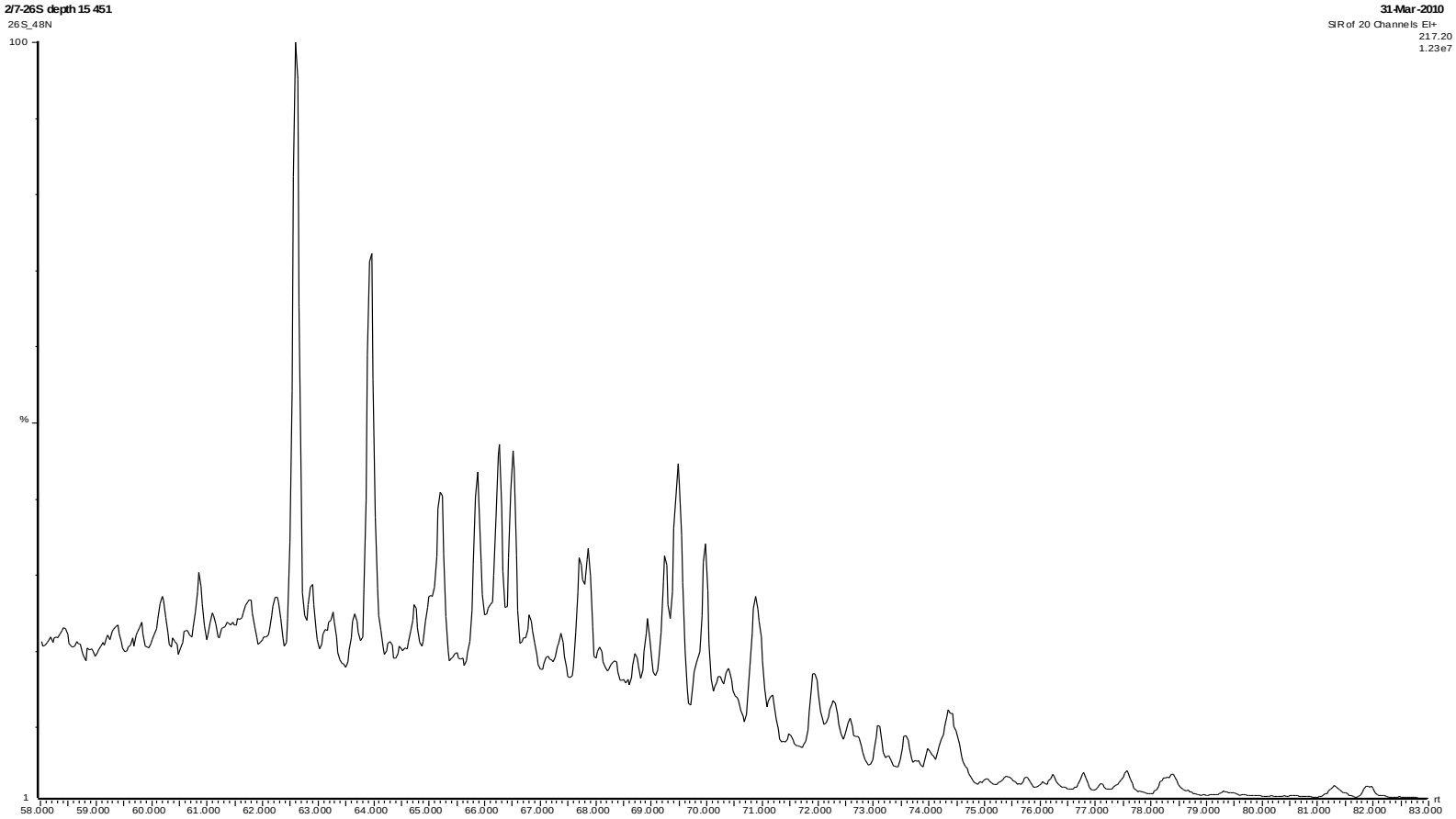
2/7-26S depth 15 451
26S_48N
31-Mar-2010
SIR of 20 Channels EI+
217.20
1.23e7
100
%
1
58.000
59.000
60.000
61.000
62.000
63.000
64.000
65.000
66.000
67.000
68.000
69.000
70.000
71.000
72.000
73.000
74.000
75.000
76.000
77.000
78.000
79.000
80.000
81.000
82.000
83.000
rt

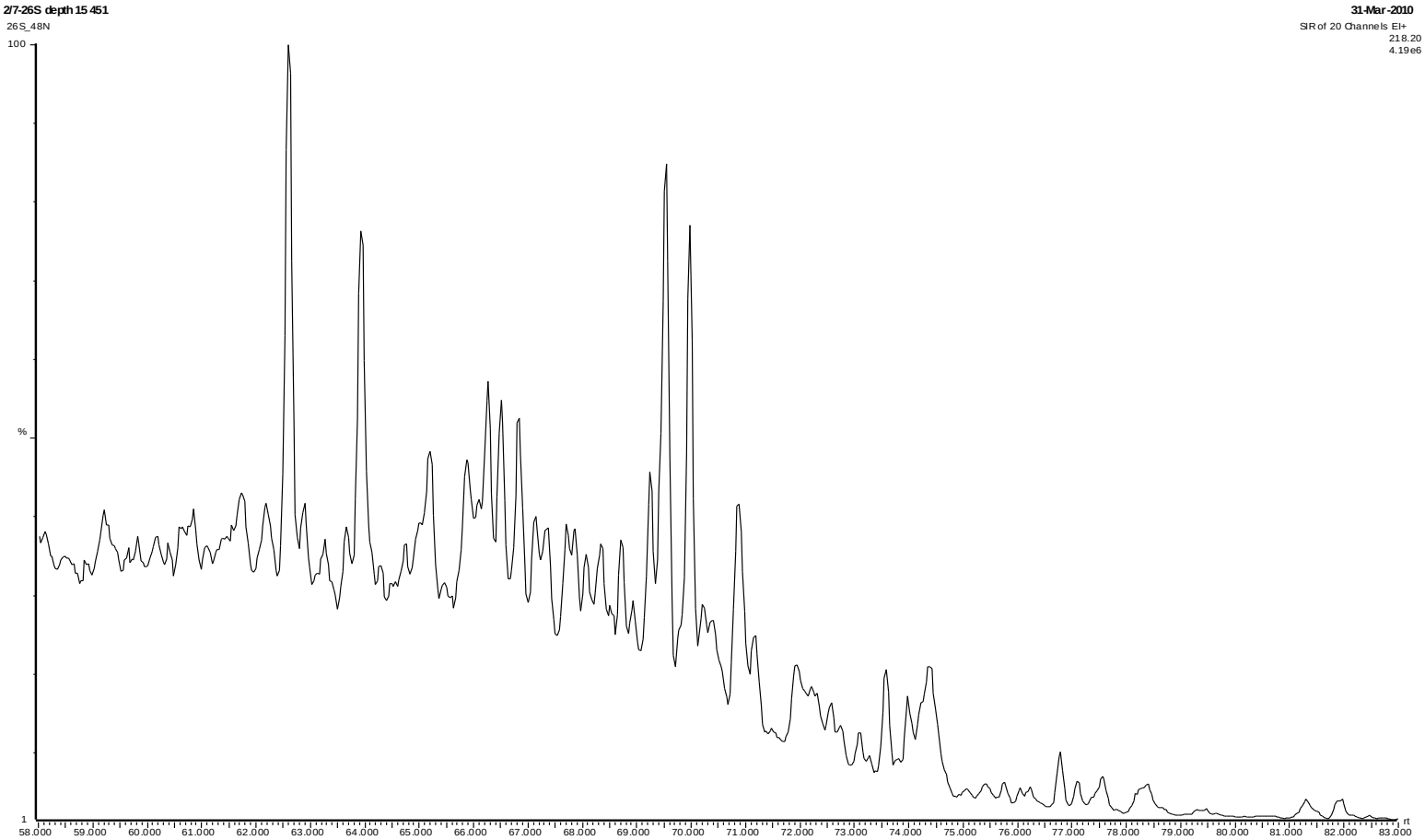
2/7-26S depth 15 451
26S_48N
31-Mar-2010
SIR of 20 Channels EI+
218.20
4.19e6
100
%
1
58.000
59.000
60.000
61.000
62.000
63.000
64.000
65.000
66.000
67.000
68.000
69.000
70.000
71.000
72.000
73.000
74.000
75.000
76.000
77.000
78.000
79.000
80.000
81.000
82.000
83.000
rt

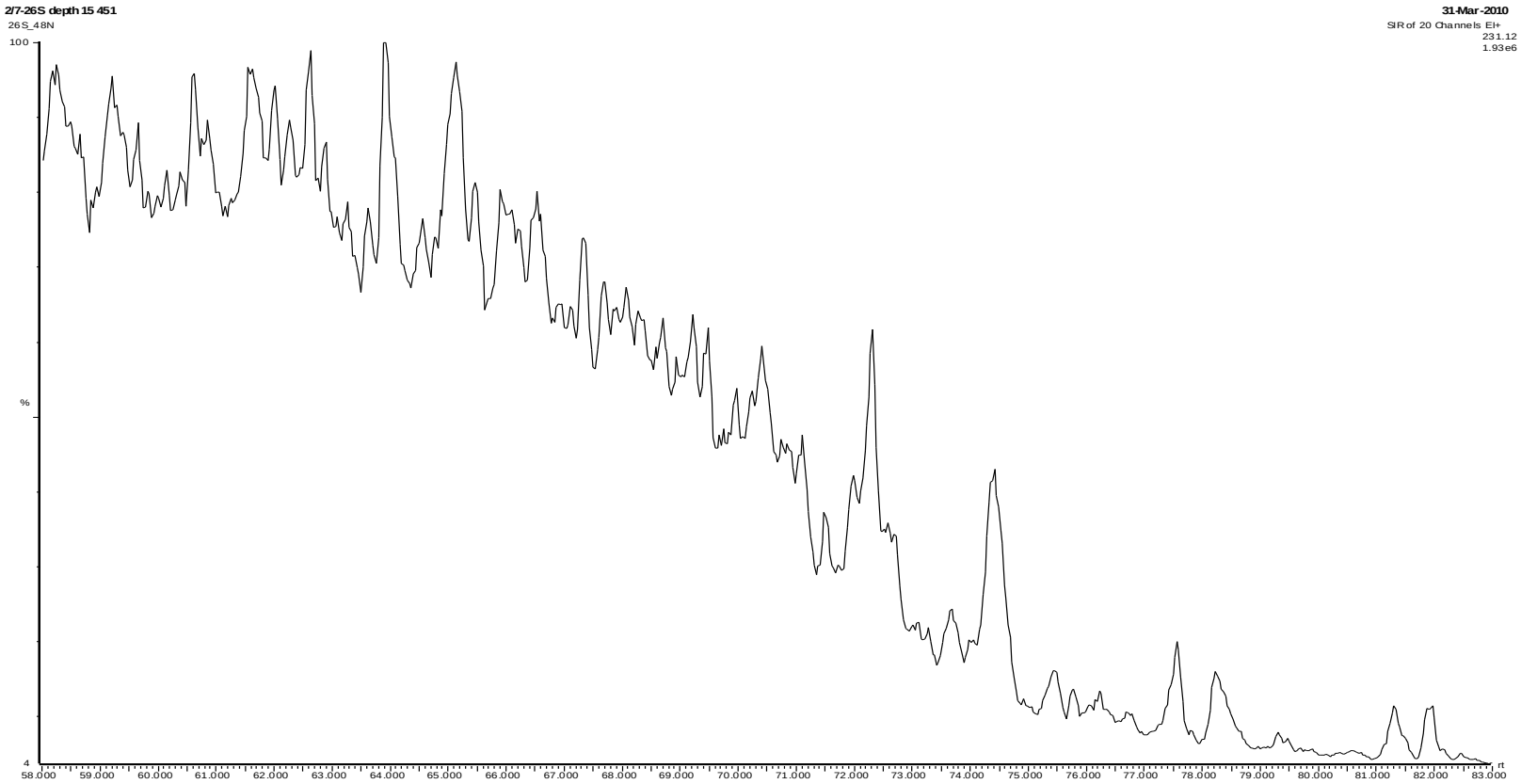
2/7-26S depth 15 451
26S_48N
31-Mar-2010
SIR of 20 Channels EI+
231.12
1.93e6
100
%
4
58.000
59.000
60.000
61.000
62.000
63.000
64.000
65.000
66.000
67.000
68.000
69.000
70.000
71.000
72.000
73.000
74.000
75.000
76.000
77.000
78.000
79.000
80.000
81.000
82.000
83.000
rt

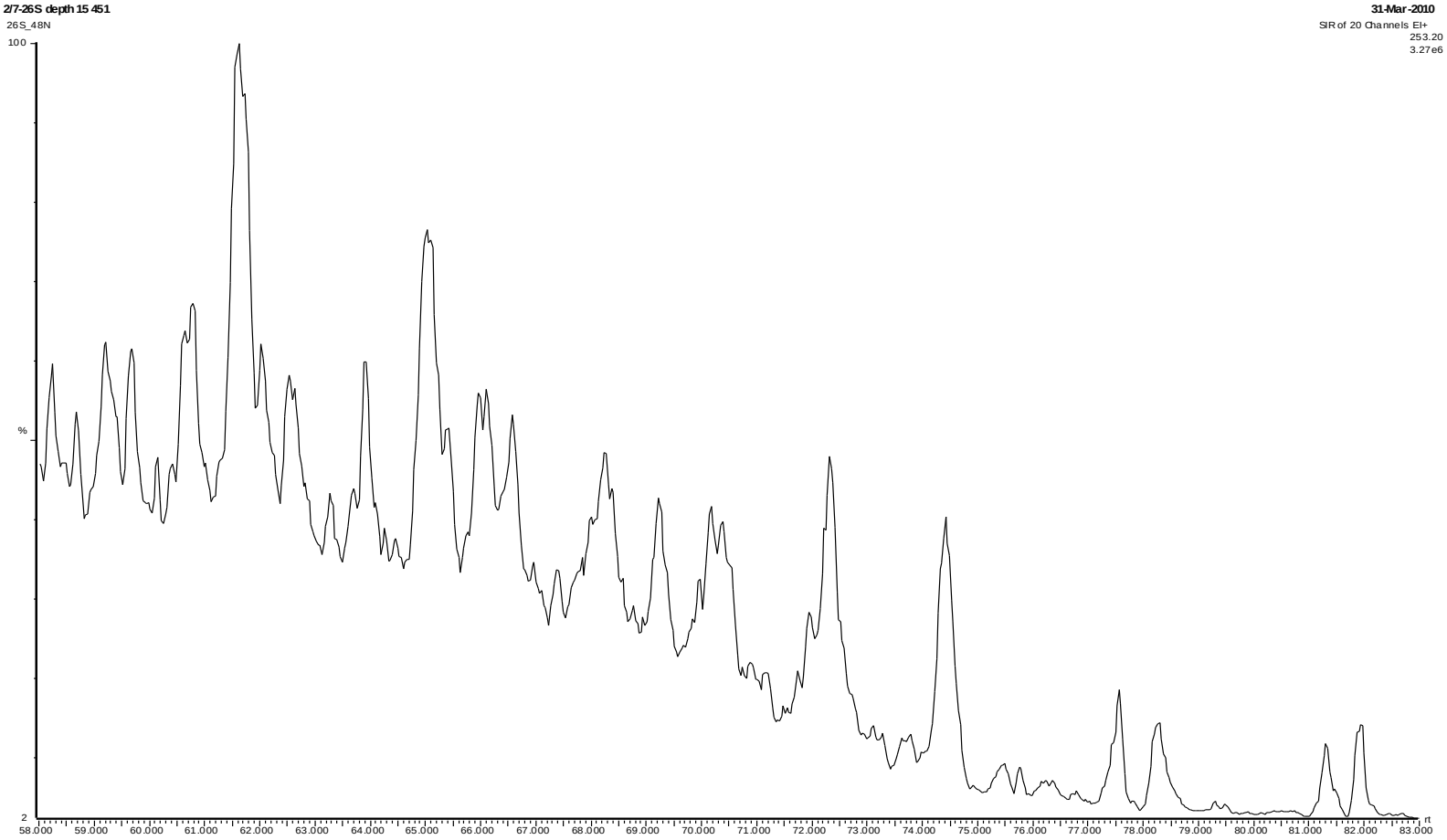
2/7-26S depth 15 451
26S_48N
31-Mar-2010
SIR of 20 Channels EI+
253.20
3.27e6
100
%
2
58.000
59.000
60.000
61.000
62.000
63.000
64.000
65.000
66.000
67.000
68.000
69.000
70.000
71.000
72.000
73.000
74.000
75.000
76.000
77.000
78.000
79.000
80.000
81.000
82.000
83.000
rt

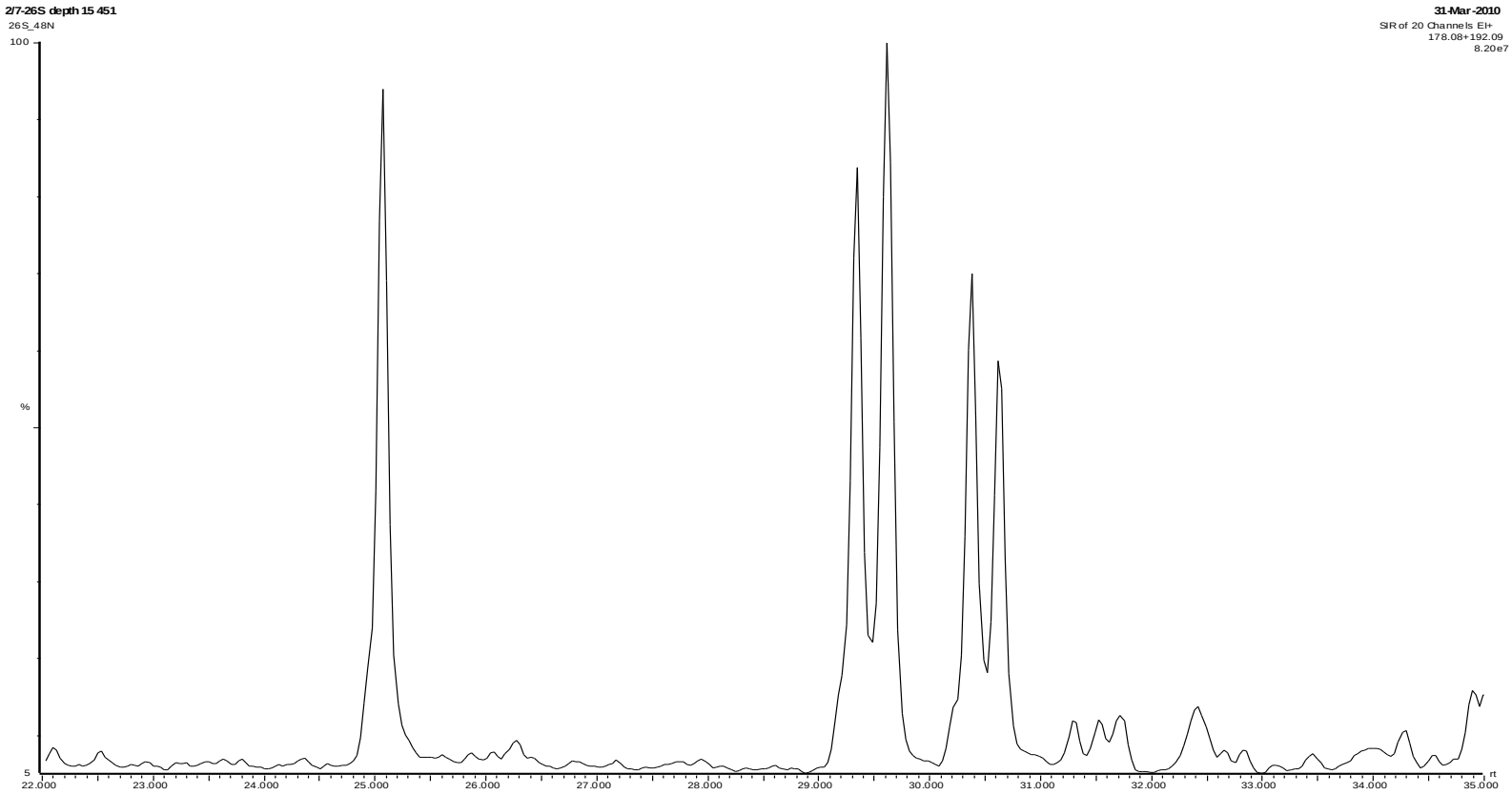
2/7-26S depth 15 451
26S_48N
31-Mar-2010
SIR of 20 Channels EI+
178.08+192.09
8.20e7
100
%
5
22.000
23.000
24.000
25.000
26.000
27.000
28.000
29.000
30.000
31.000
32.000
33.000
34.000
35.000
rt

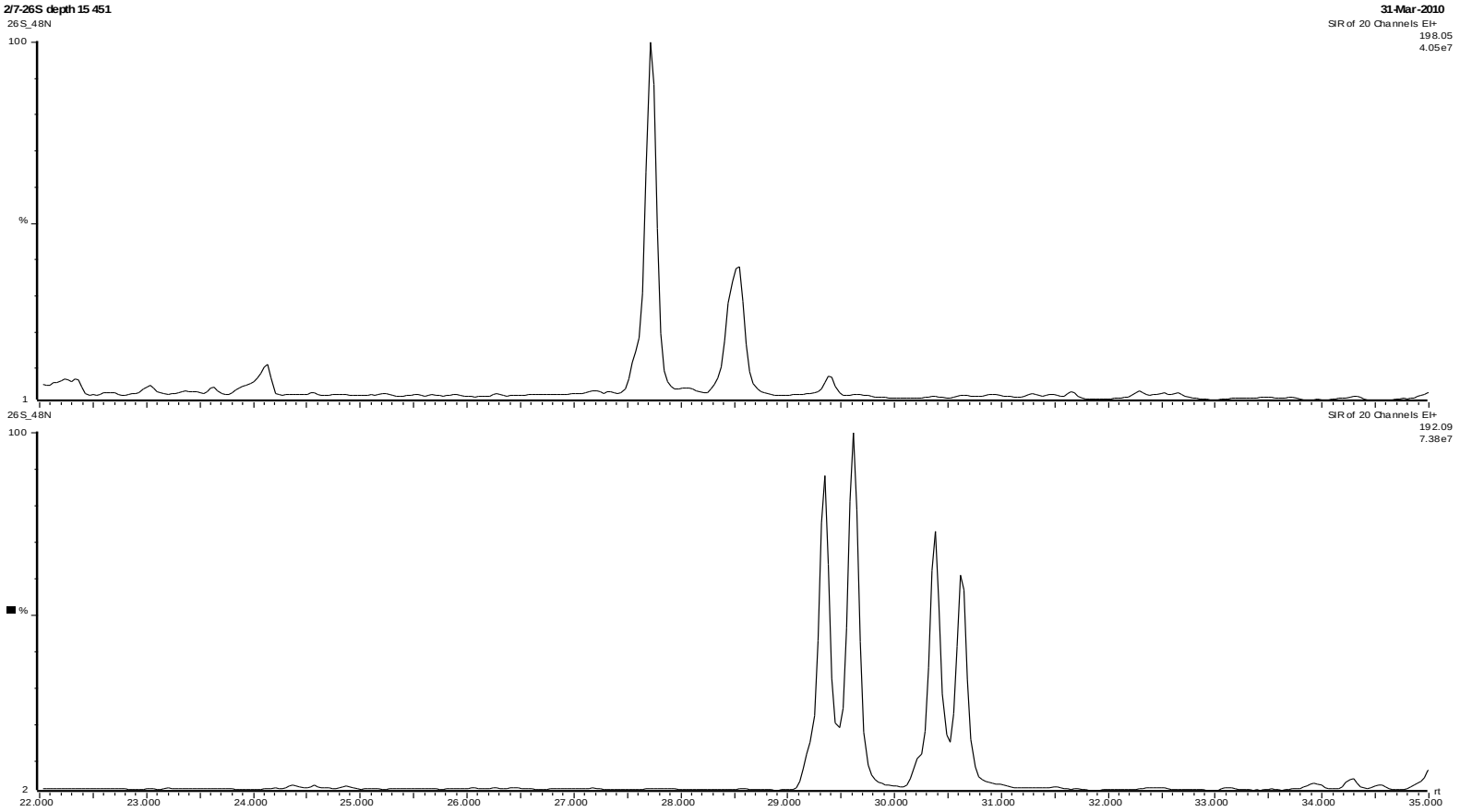
2/7-26S depth 15 451
31-Mar-2010
26S_48N
SIR of 20 Channels EI+
198.05
4.05e7
100
%
1
26S_48N
SIR of 20 Channels EI+
192.09
7.38e7
100
%
2
22.000
23.000
24.000
25.000
26.000
27.000
28.000
29.000
30.000
31.000
32.000
33.000
34.000
35.000
rt

GC-MS Chromatograms for sample E14

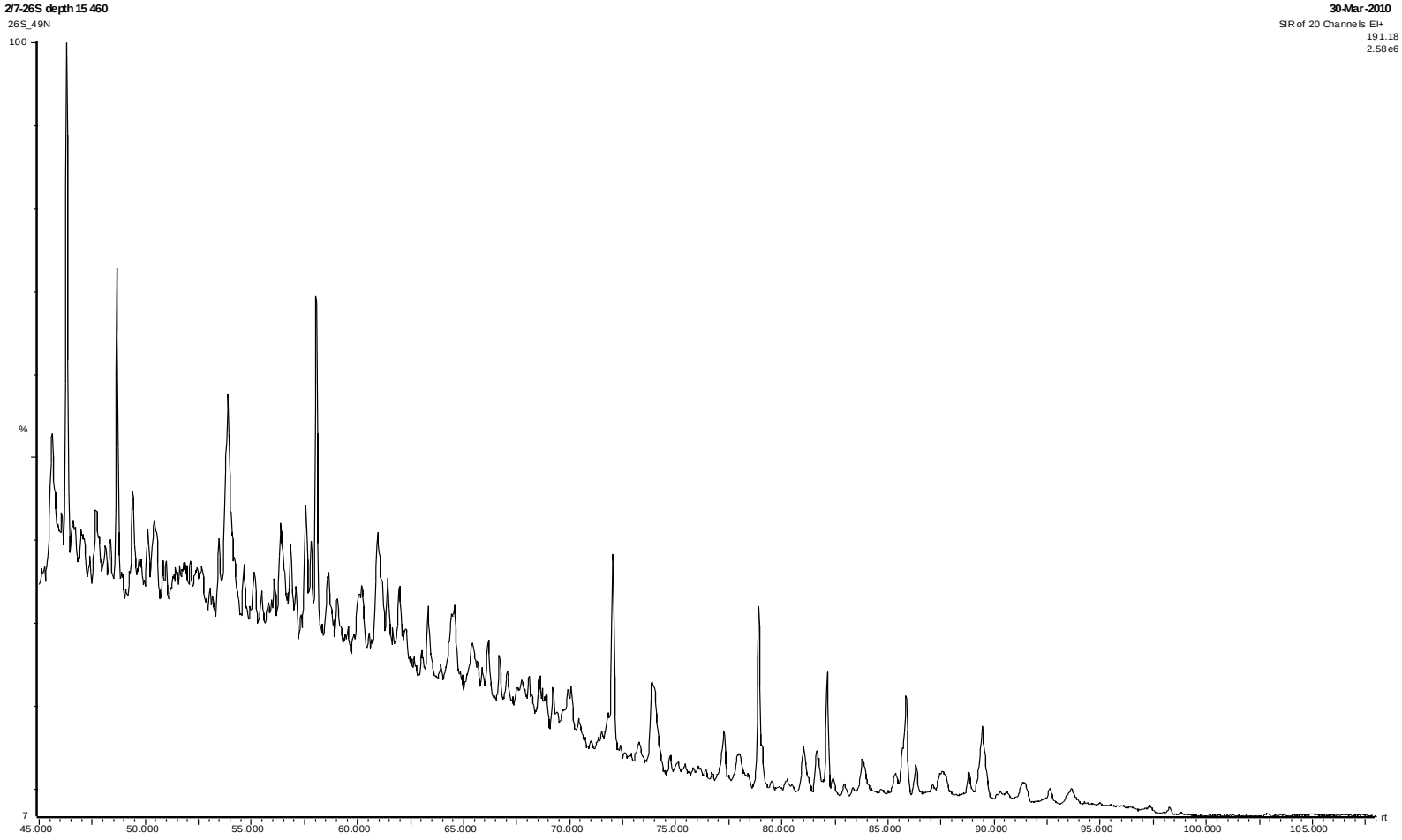
2/7-26S depth 15 460
26S_49N
30-Mar-2010
SIR of 20 Channels EI+
191.18
2.58e6
100
%
7
45.000
50.000
55.000
60.000
65.000
70.000
75.000
80.000
85.000
90.000
95.000
100.000
105.000
rt

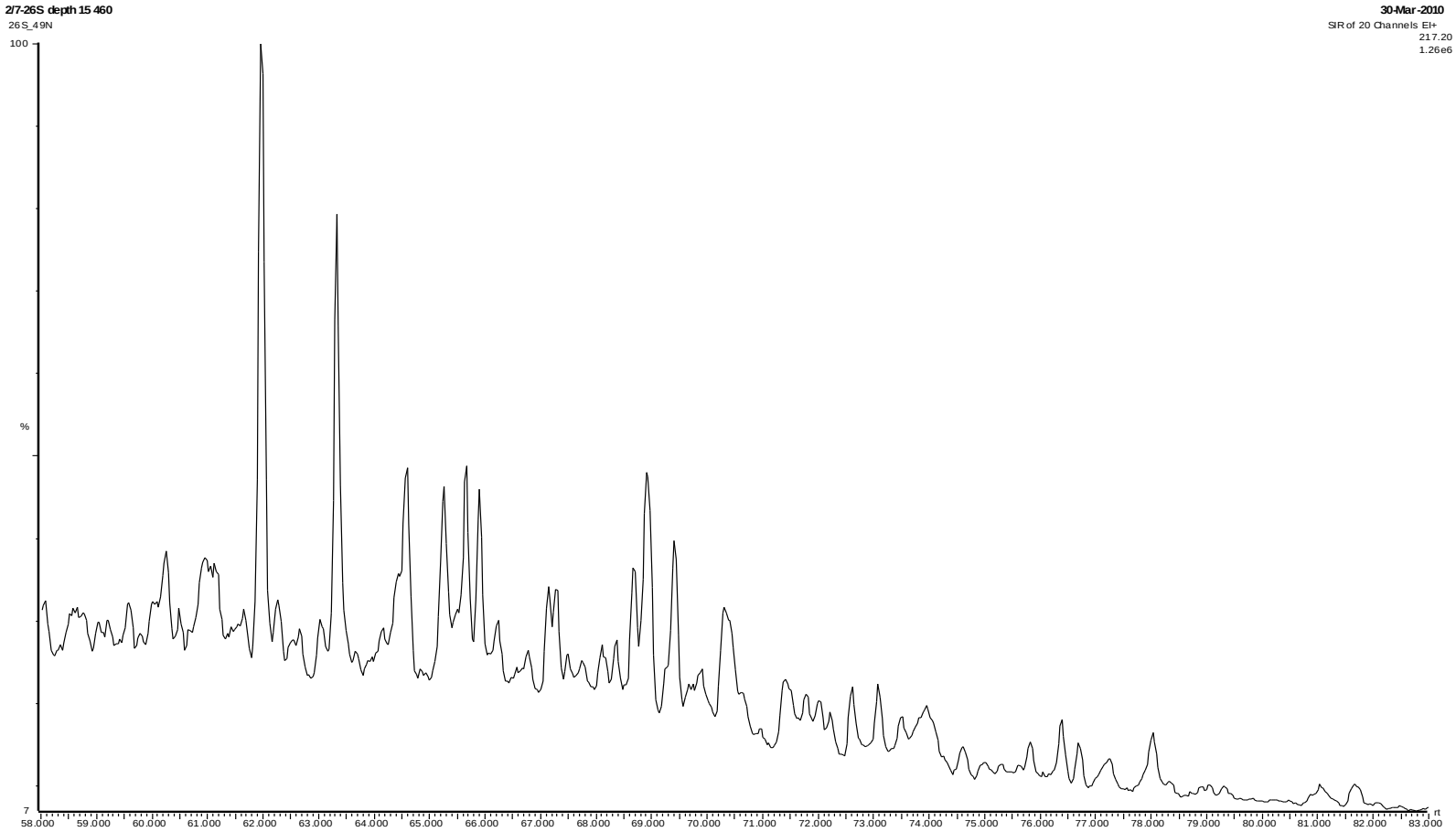
2/7-26S depth 15 460
26S_49N
30-Mar-2010
SIR of 20 Channels EI+
217.20
1.26e6
100
%
7
58.000
59.000
60.000
61.000
62.000
63.000
64.000
65.000
66.000
67.000
68.000
69.000
70.000
71.000
72.000
73.000
74.000
75.000
76.000
77.000
78.000
79.000
80.000
81.000
82.000
83.000
rt

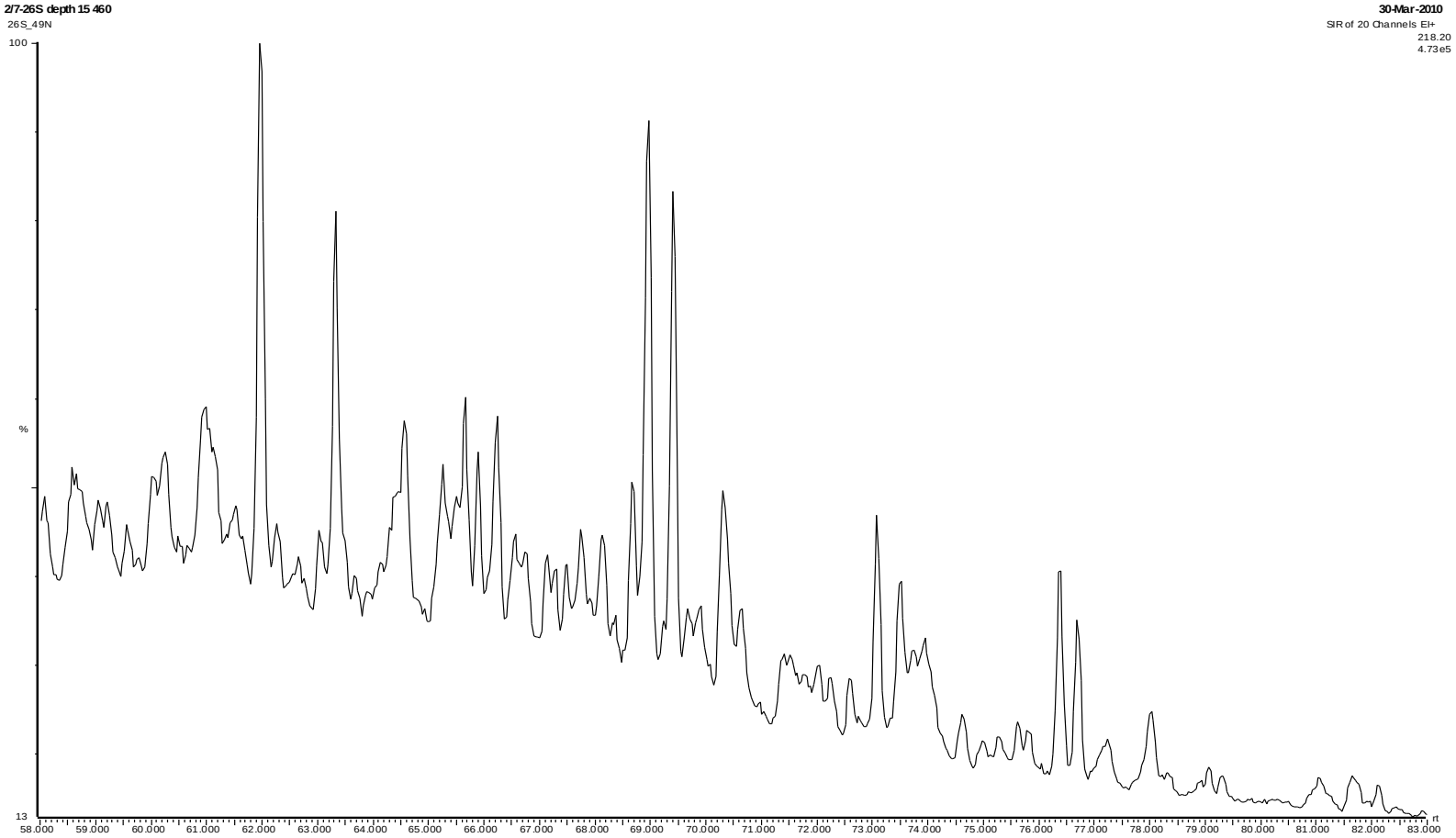
2/7-26S depth 15 460
26S_49N
30-Mar-2010
SIR of 20 Channels EI+
218.20
4.73e5
100
%
13
58.000
59.000
60.000
61.000
62.000
63.000
64.000
65.000
66.000
67.000
68.000
69.000
70.000
71.000
72.000
73.000
74.000
75.000
76.000
77.000
78.000
79.000
80.000
81.000
82.000
83.000
rt

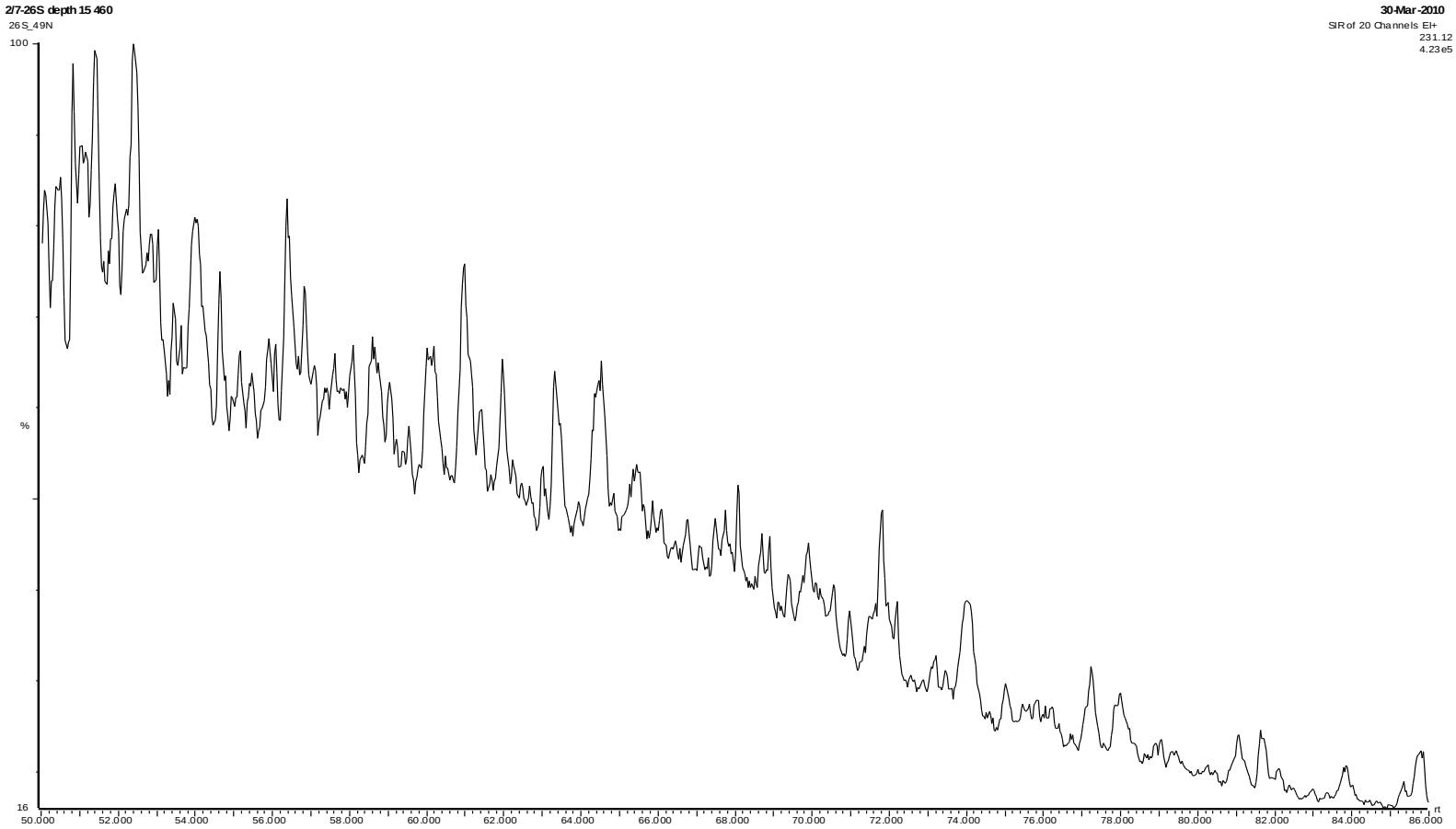
2/7-26S depth 15 460
26S_49N
30-Mar-2010
SIR of 20 Channels EI+
231.12
4.23e5
100
%
16
50.000
52.000
54.000
56.000
58.000
60.000
62.000
64.000
66.000
68.000
70.000
72.000
74.000
76.000
78.000
80.000
82.000
84.000
86.000
rt

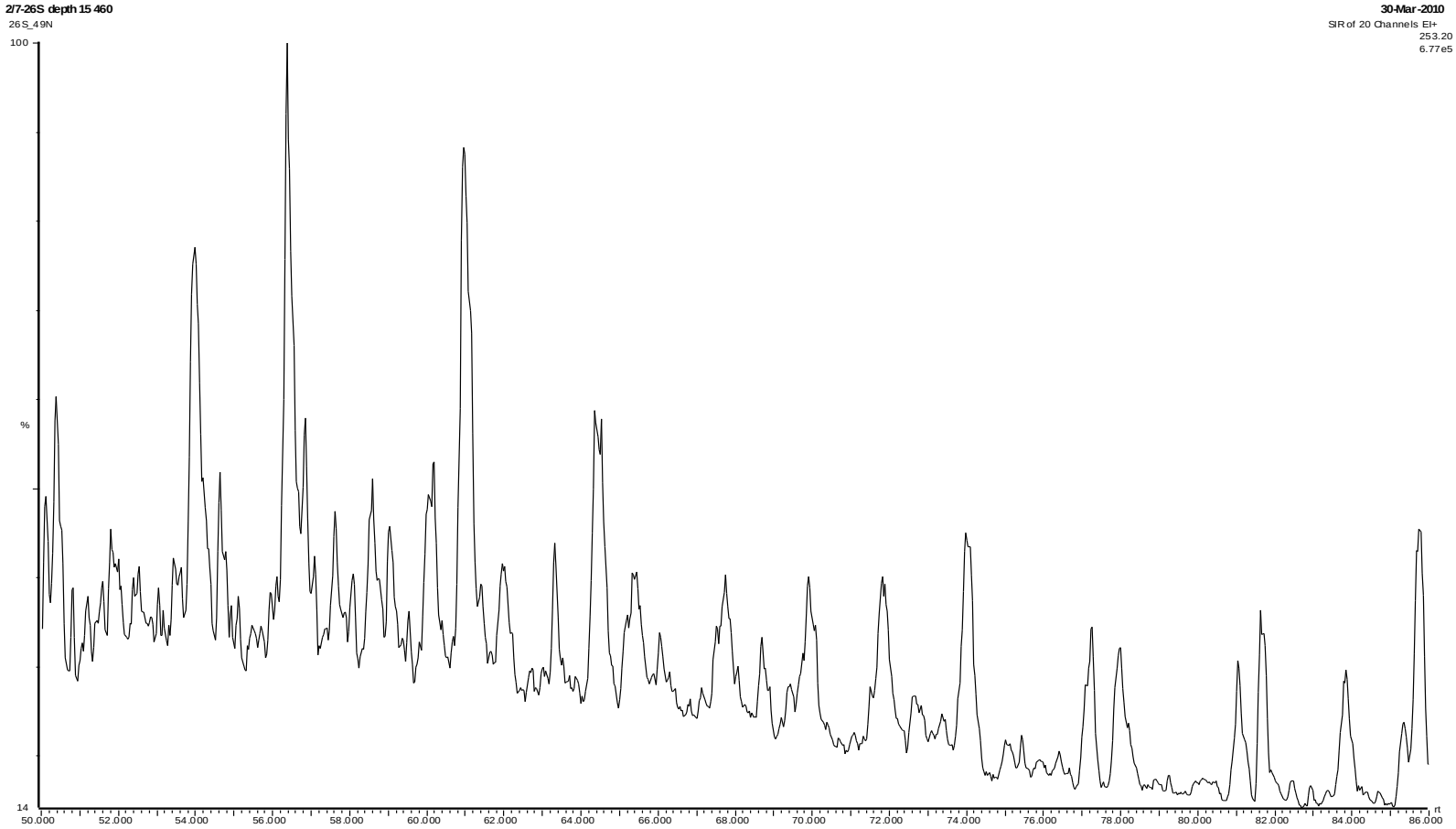
2/7-26S depth 15 460
26S_49N
30-Mar-2010
SIR of 20 Channels EI+
253.20
6.77e5
100
%
14
50.000
52.000
54.000
56.000
58.000
60.000
62.000
64.000
66.000
68.000
70.000
72.000
74.000
76.000
78.000
80.000
82.000
84.000
86.000
rt

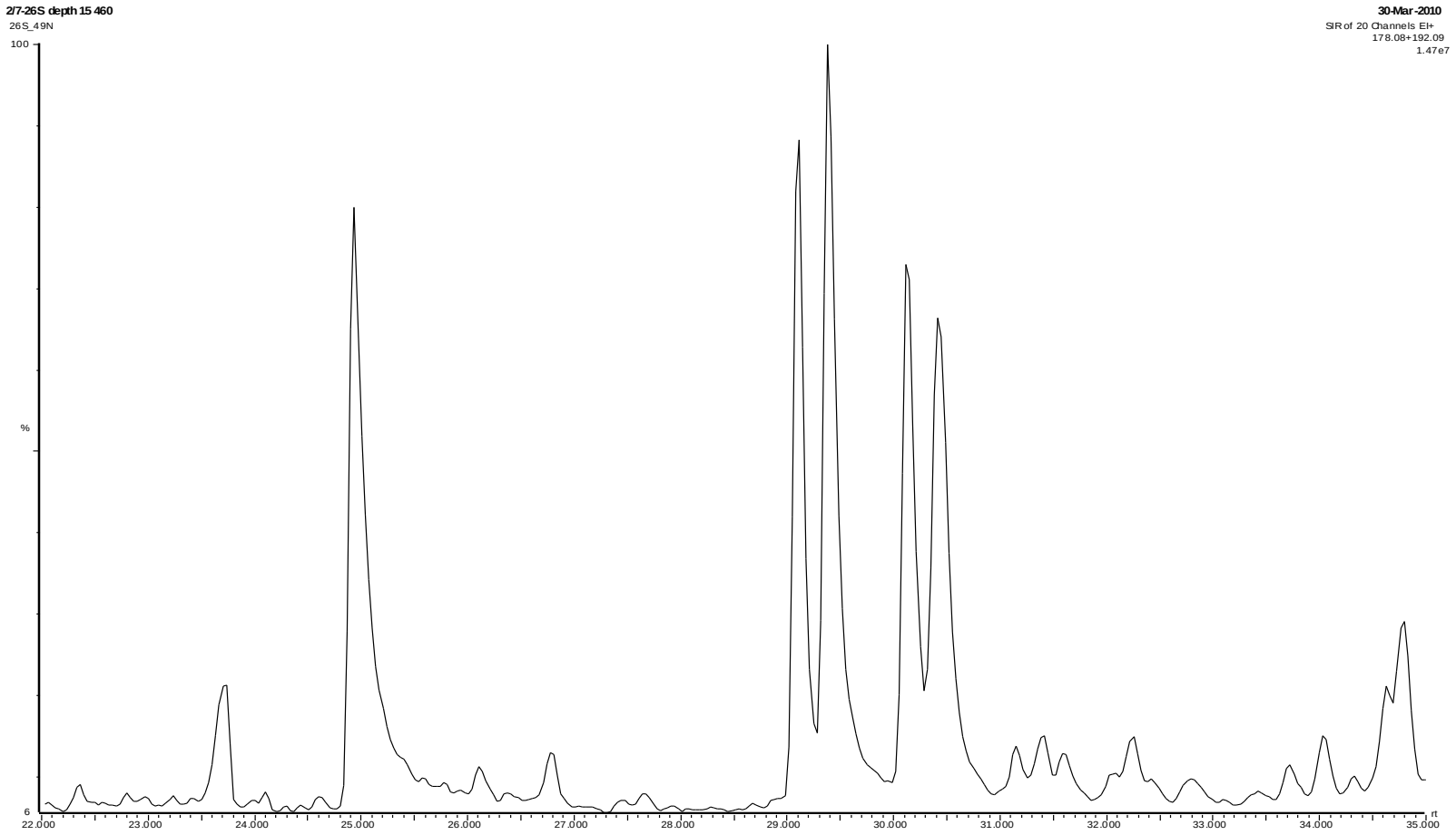
2/7-26S depth 15 460
26S_49N
30-Mar-2010
SIR of 20 Channels EI+
178.08+192.09
1.47e7
100
%
6
22.000
23.000
24.000
25.000
26.000
27.000
28.000
29.000
30.000
31.000
32.000
33.000
34.000
35.000
rt

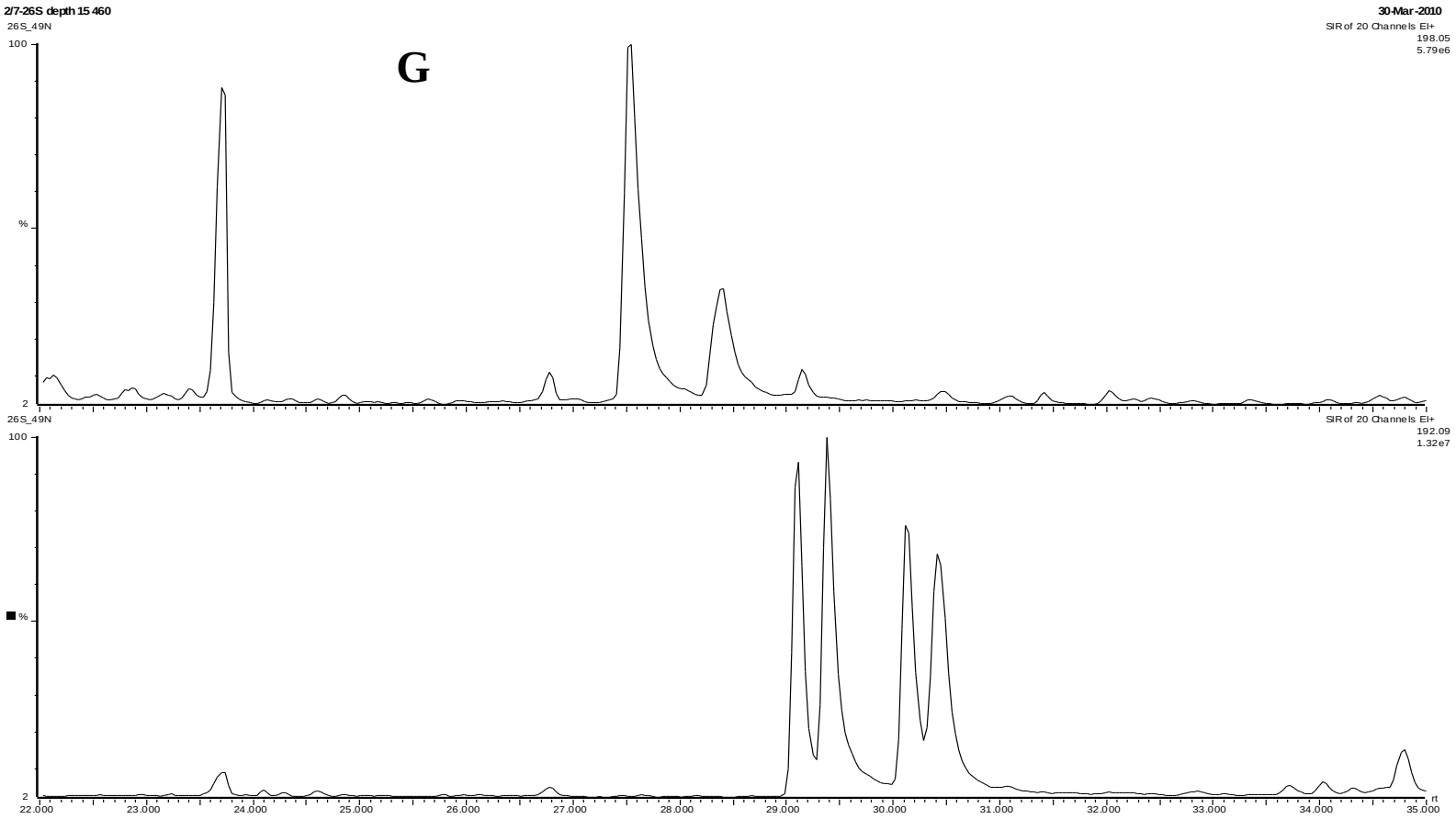
2/7-26S depth 15 460
30-Mar-2010
26S_49N
SIR of 20 Channels EI+
198.05
5.79e6
100
%
2
G
26S_49N
SIR of 20 Channels EI+
192.09
1.32e7
100
%
2
22.000
23.000
24.000
25.000
26.000
27.000
28.000
29.000
30.000
31.000
32.000
33.000
34.000
35.000
rt

GC-MS Chromatograms for sample E15

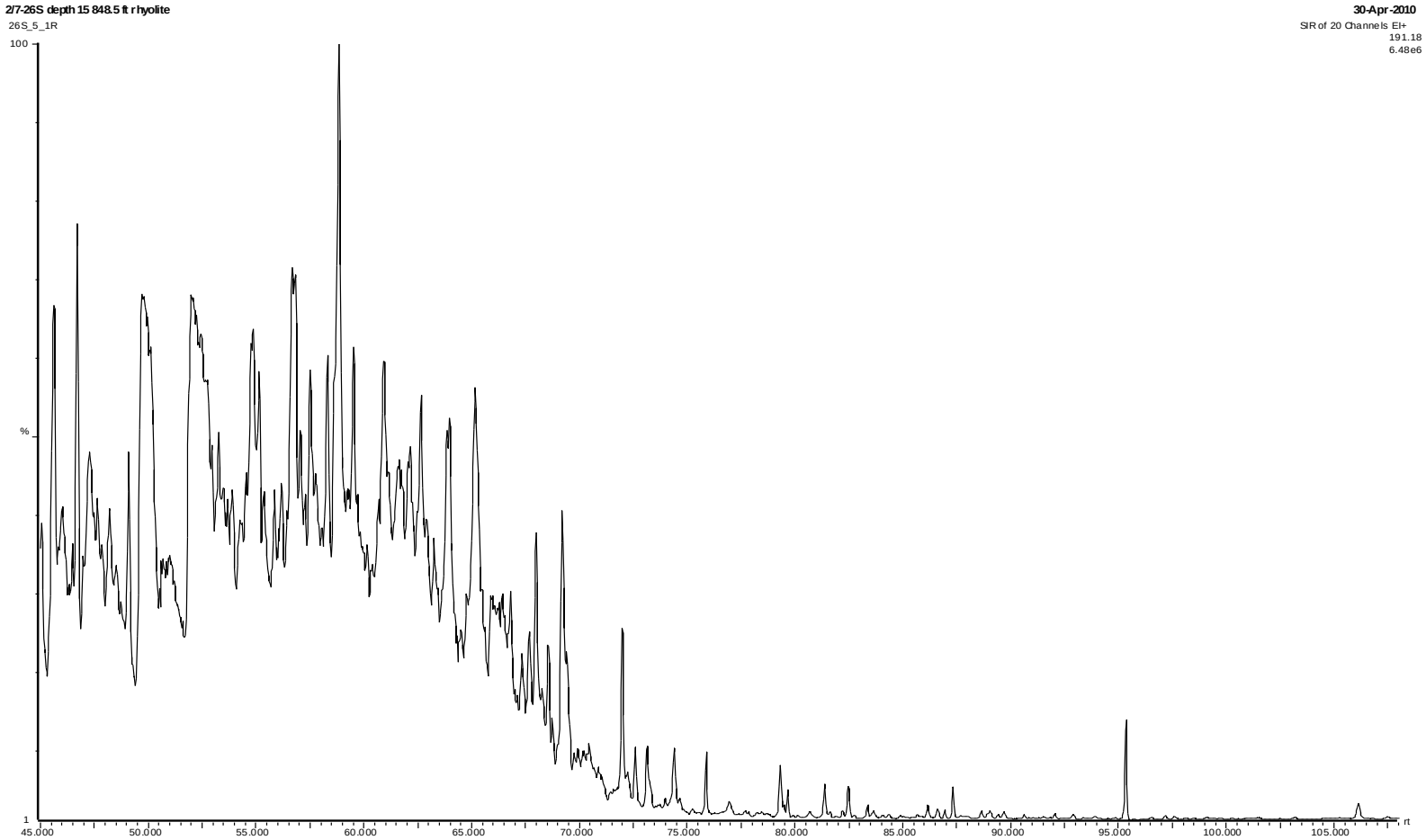
2/7-26S depth 15 848.5 ft rhyolite
26S_5_1R
30-Apr-2010
SIR of 20 Channels EI+
191.18
6.48e6
100
%
1
45.000
50.000
55.000
60.000
65.000
70.000
75.000
80.000
85.000
90.000
95.000
100.000
105.000
rt

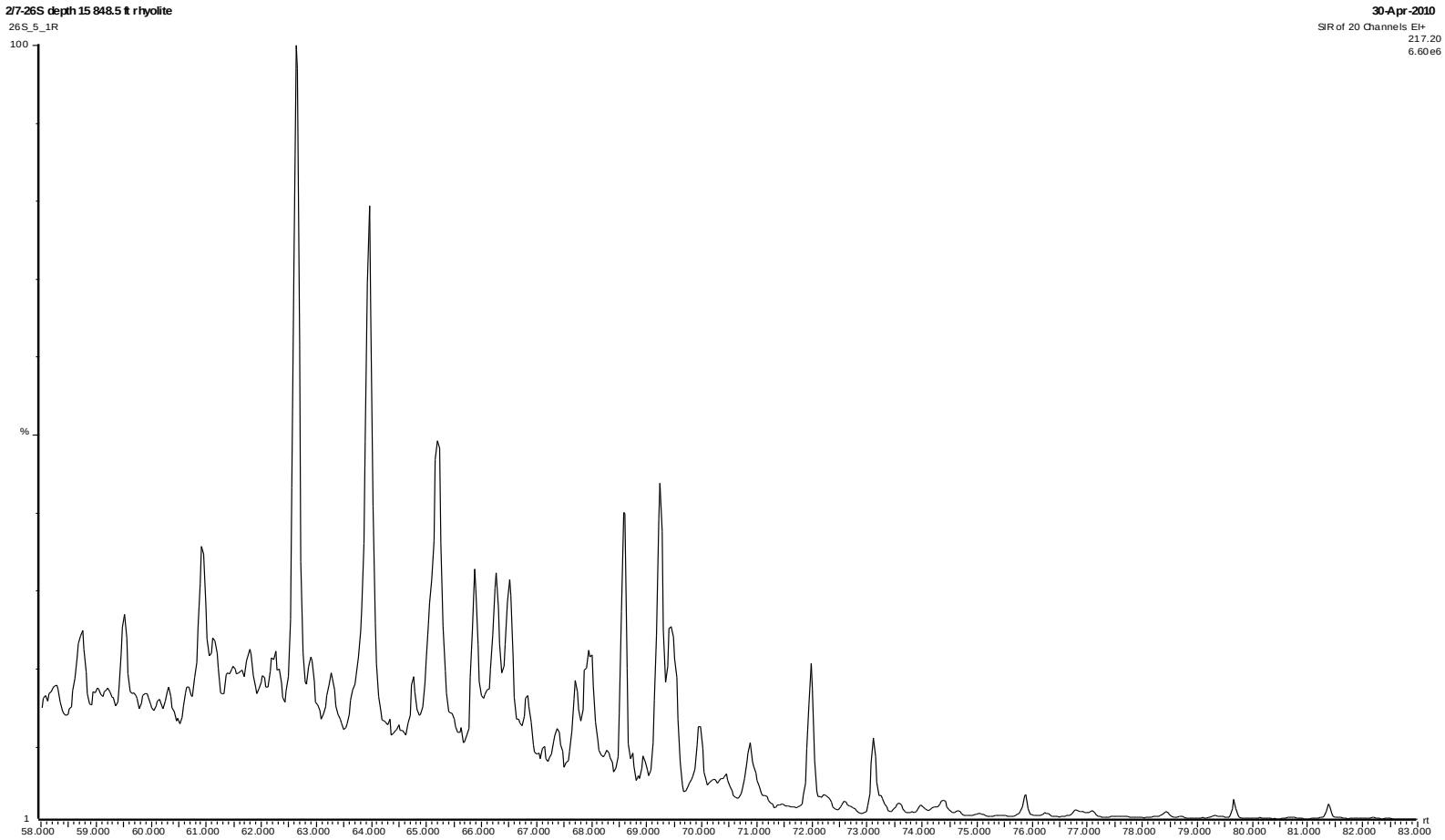
2/7-26S depth 15 848.5 ft rhyolite
26S_5_1R
30-Apr-2010
SIR of 20 Channels EI+
217.20
6.60e6
100
%
1
58.000
59.000
60.000
61.000
62.000
63.000
64.000
65.000
66.000
67.000
68.000
69.000
70.000
71.000
72.000
73.000
74.000
75.000
76.000
77.000
78.000
79.000
80.000
81.000
82.000
83.000
rt

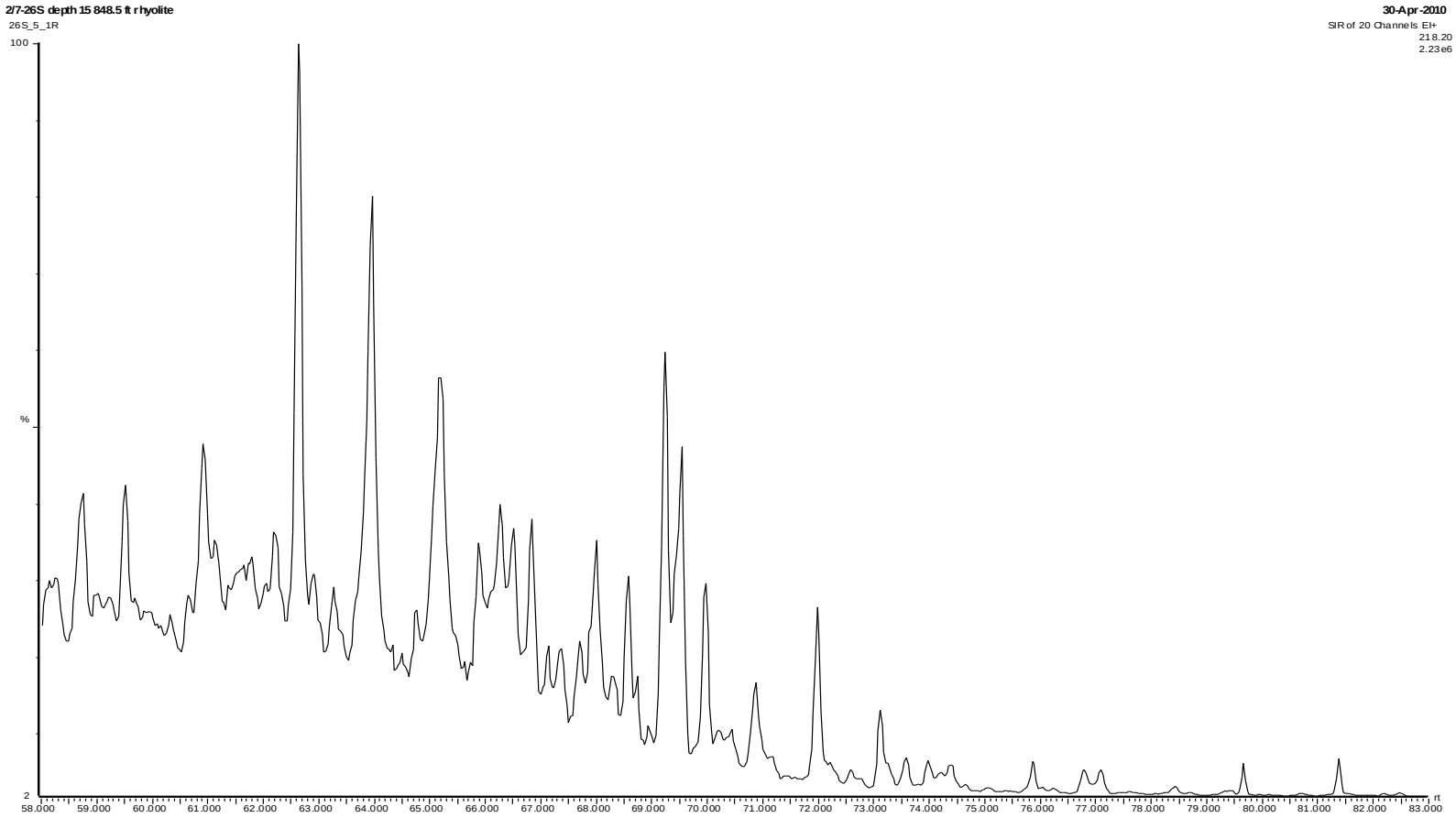
2/7-26S depth 15 848.5 ft rhyolite
26S_5_1R
30-Apr-2010
SIR of 20 Channels EI+
218.20
2.23e6
100
%
2
58.000
59.000
60.000
61.000
62.000
63.000
64.000
65.000
66.000
67.000
68.000
69.000
70.000
71.000
72.000
73.000
74.000
75.000
76.000
77.000
78.000
79.000
80.000
81.000
82.000
83.000
rt

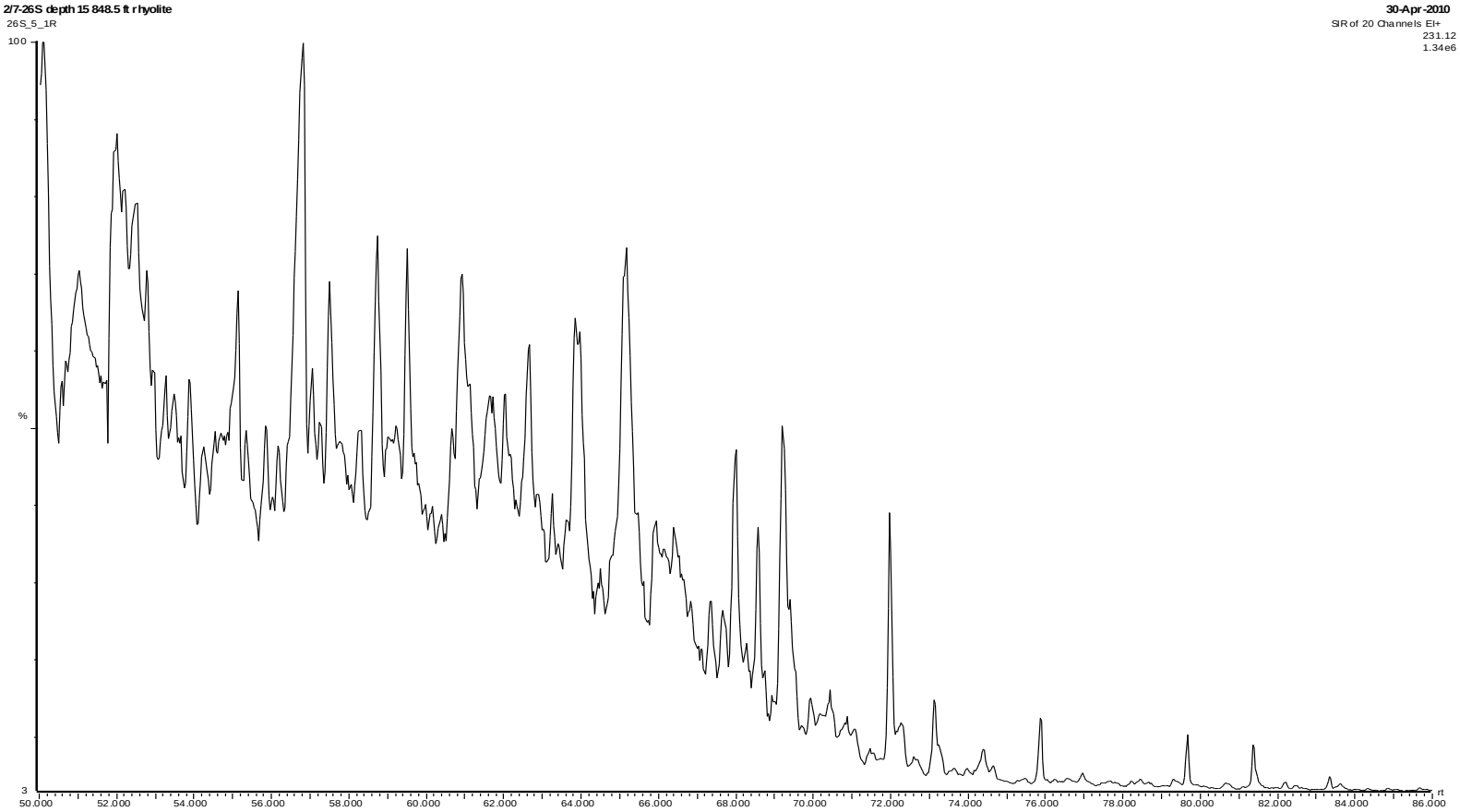
2/7-26S depth 15 848.5 ft rhyolite
26S_5_1R
30-Apr-2010
SIR of 20 Channels EI+
231.12
1.34e6
100
%
3
50.000
52.000
54.000
56.000
58.000
60.000
62.000
64.000
66.000
68.000
70.000
72.000
74.000
76.000
78.000
80.000
82.000
84.000
86.000
rt

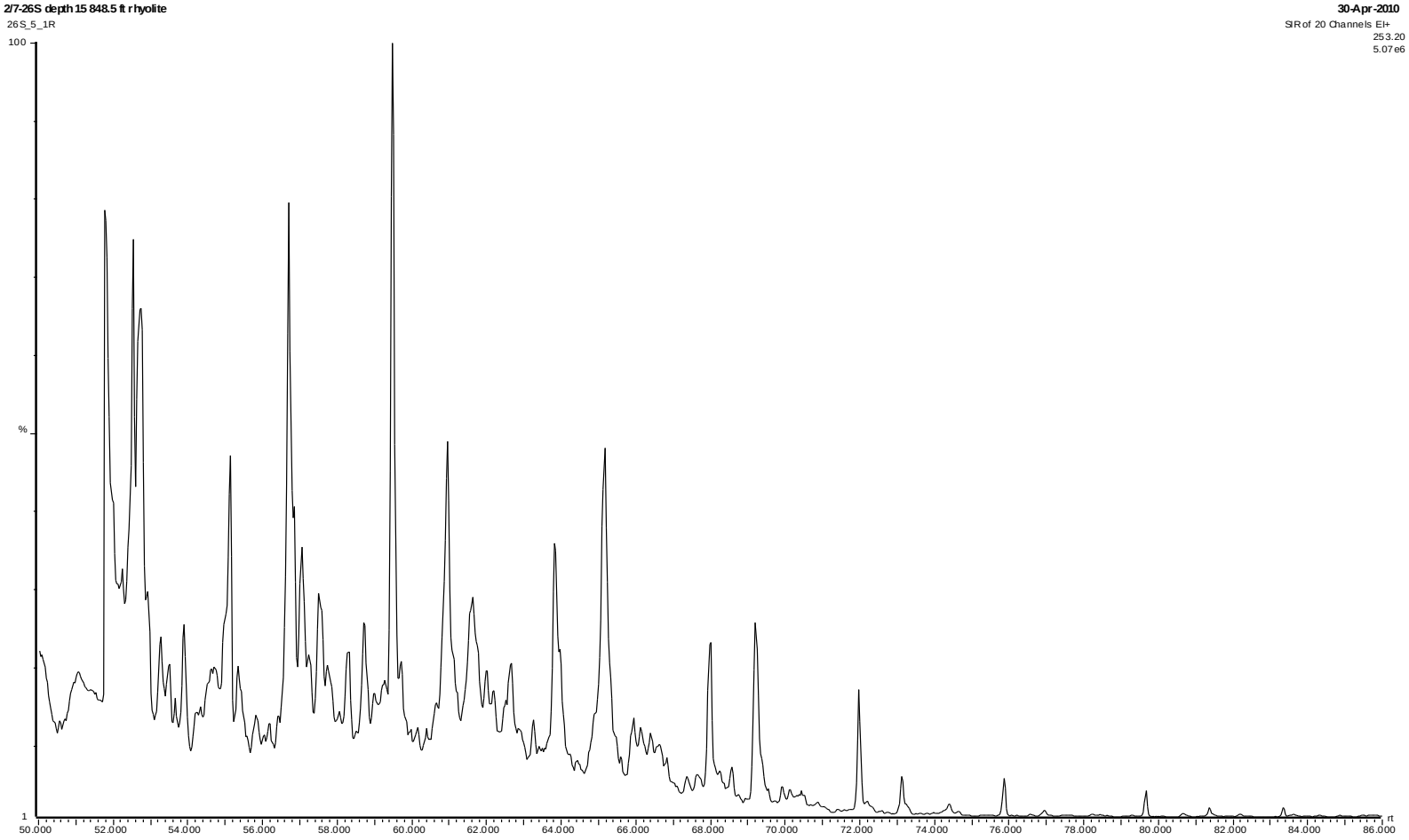
2/7-26S depth 15 848.5 ft rhyolite
26S_5_1R
30-Apr-2010
SIR of 20 Channels EI+
253.20
5.07e6
100
%
1
50.000
52.000
54.000
56.000
58.000
60.000
62.000
64.000
66.000
68.000
70.000
72.000
74.000
76.000
78.000
80.000
82.000
84.000
86.000
rt

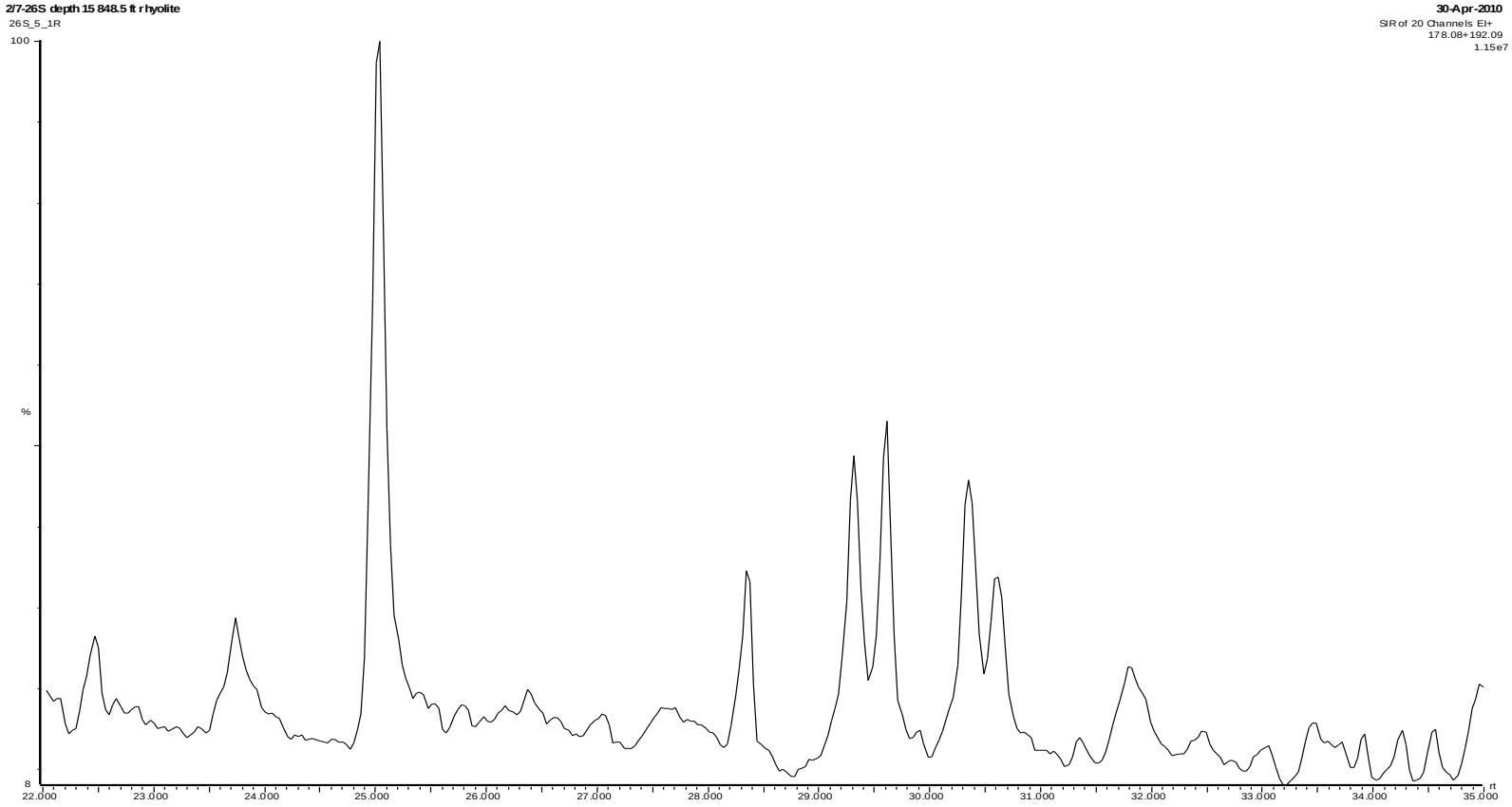
2/7-26S depth 15 848.5 ft rhyolite
26S_5_1R
30-Apr-2010
SIR of 20 Channels EI+
178.08+192.09
1.15e7
100
%
8
22.000
23.000
24.000
25.000
26.000
27.000
28.000
29.000
30.000
31.000
32.000
33.000
34.000
35.000
ft

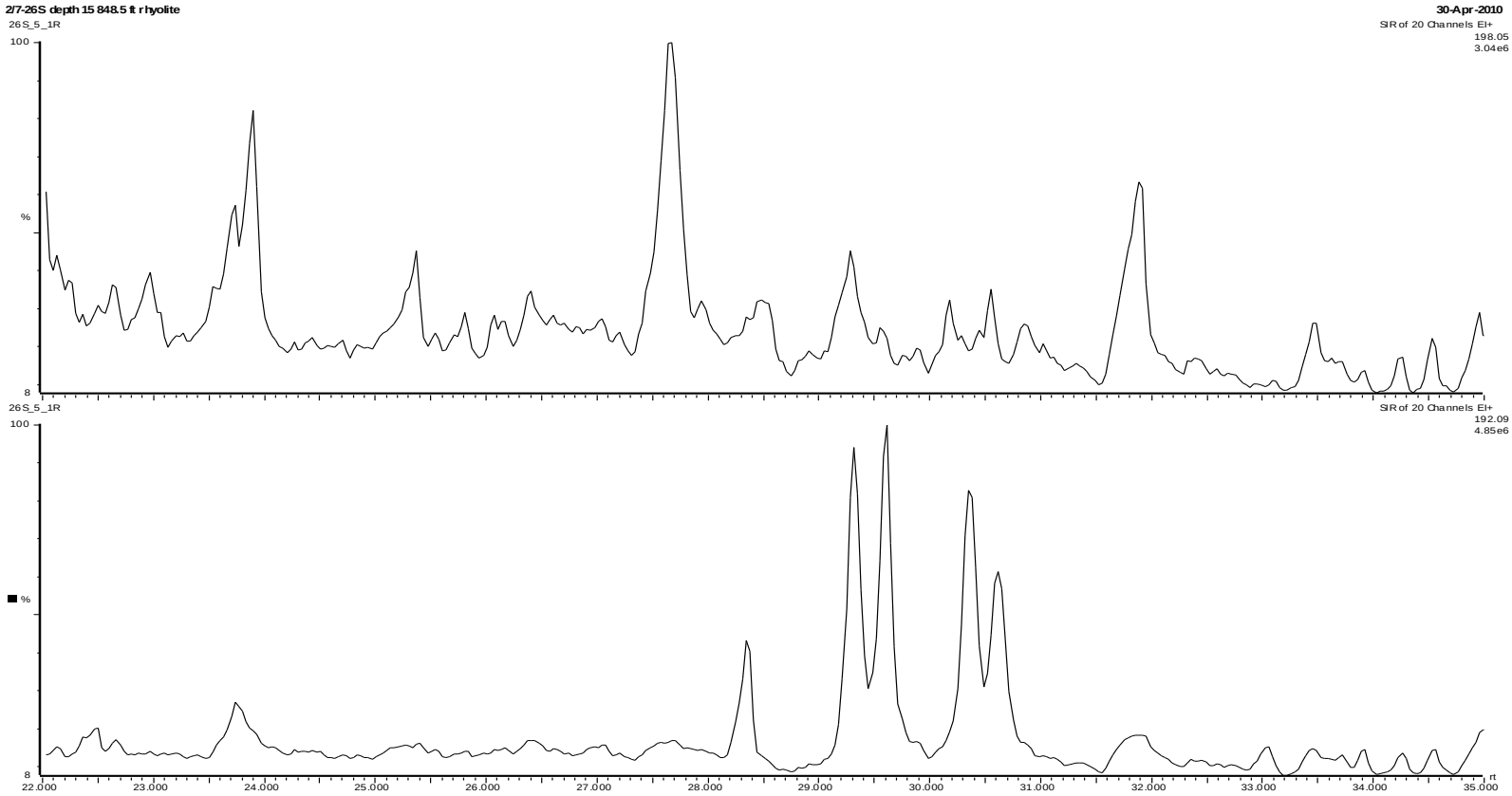
2/7-26S depth 15 848.5 ft rhyolite
30-Apr-2010
26S_5_1R
SIR of 20 Channels EI+
198.05
3.04e6
100
%
8
26S_5_1R
SIR of 20 Channels EI+
192.09
4.85e6
100
%
8
22.000
23.000
24.000
25.000
26.000
27.000
28.000
29.000
30.000
31.000
32.000
33.000
34.000
35.000
rt

GC-MS Chromatograms for sample E16

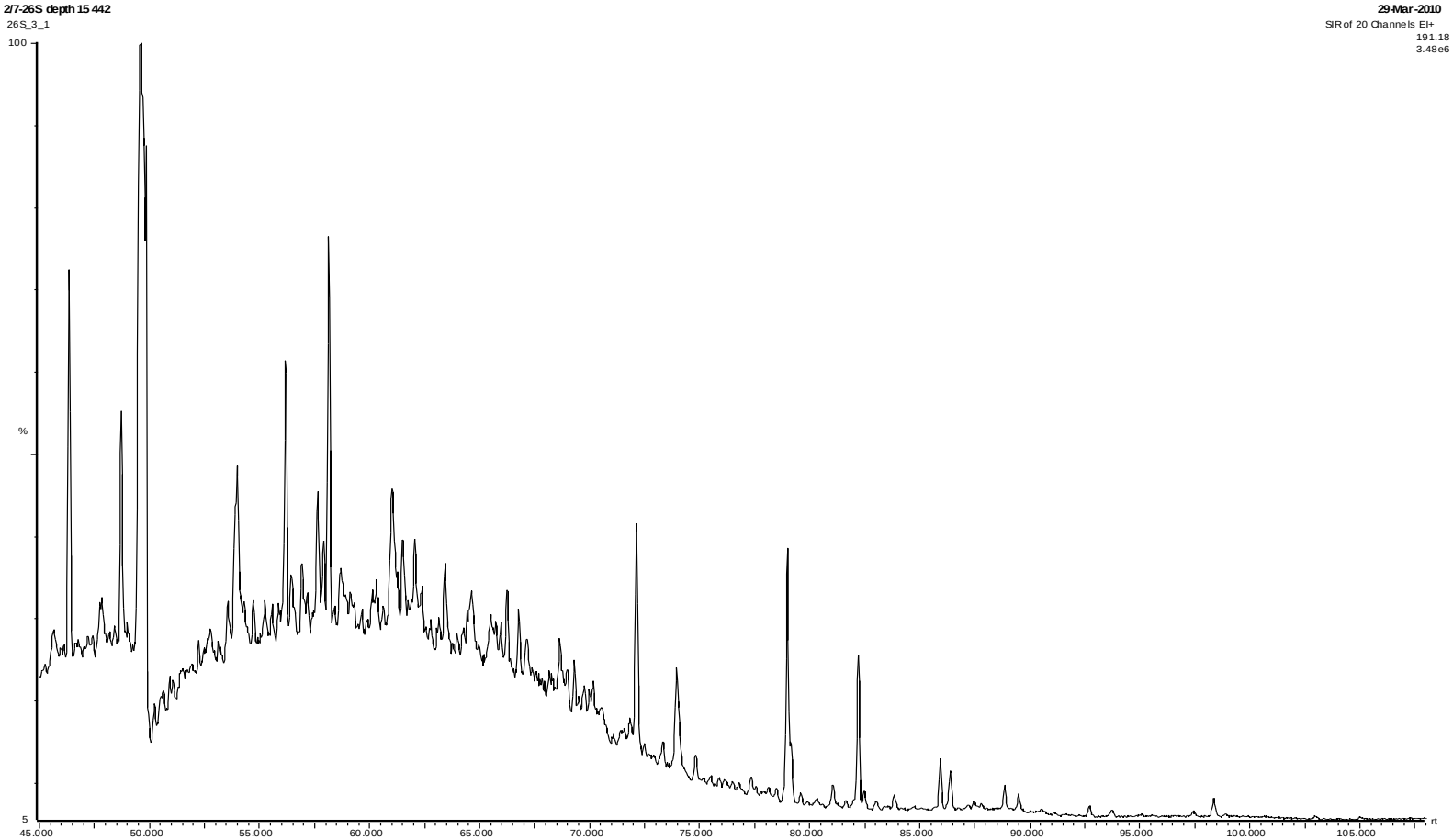
2/7-26S depth 15 442
26S_3_1
29-Mar-2010
SIR of 20 Channels EI+
191.18
3.48e6
100
%
5
45.000
50.000
55.000
60.000
65.000
70.000
75.000
80.000
85.000
90.000
95.000
100.000
105.000
rt

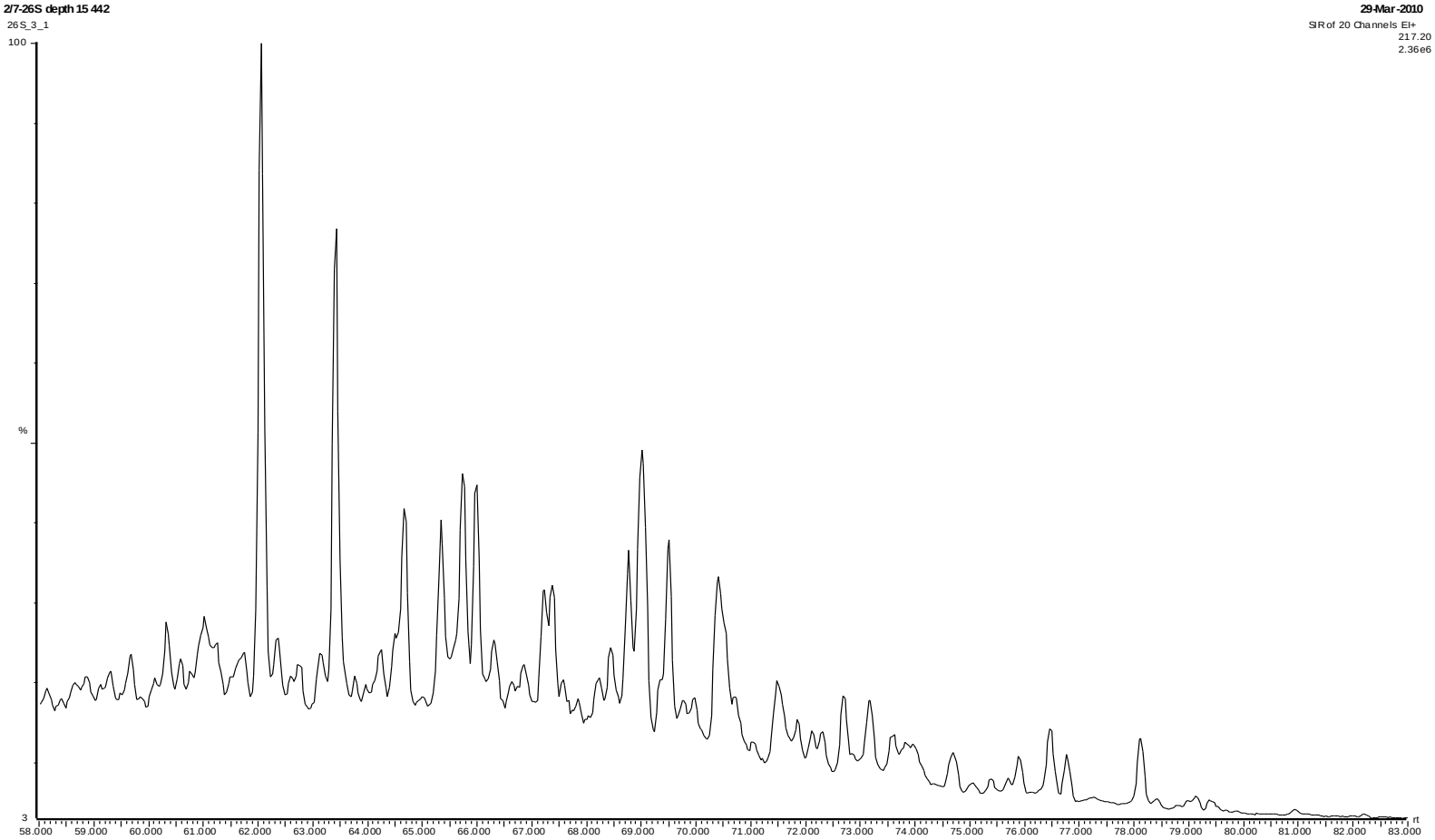
2/7-26S depth 15 442
26S_3_1
29-Mar-2010
SIR of 20 Channels EI+
217.20
2.36e6
100
%
3
58.000 59.000 60.000 61.000 62.000 63.000 64.000 65.000 66.000 67.000 68.000 69.000 70.000 71.000 72.000 73.000 74.000 75.000 76.000 77.000 78.000 79.000 80.000 81.000 82.000 83.000
rt

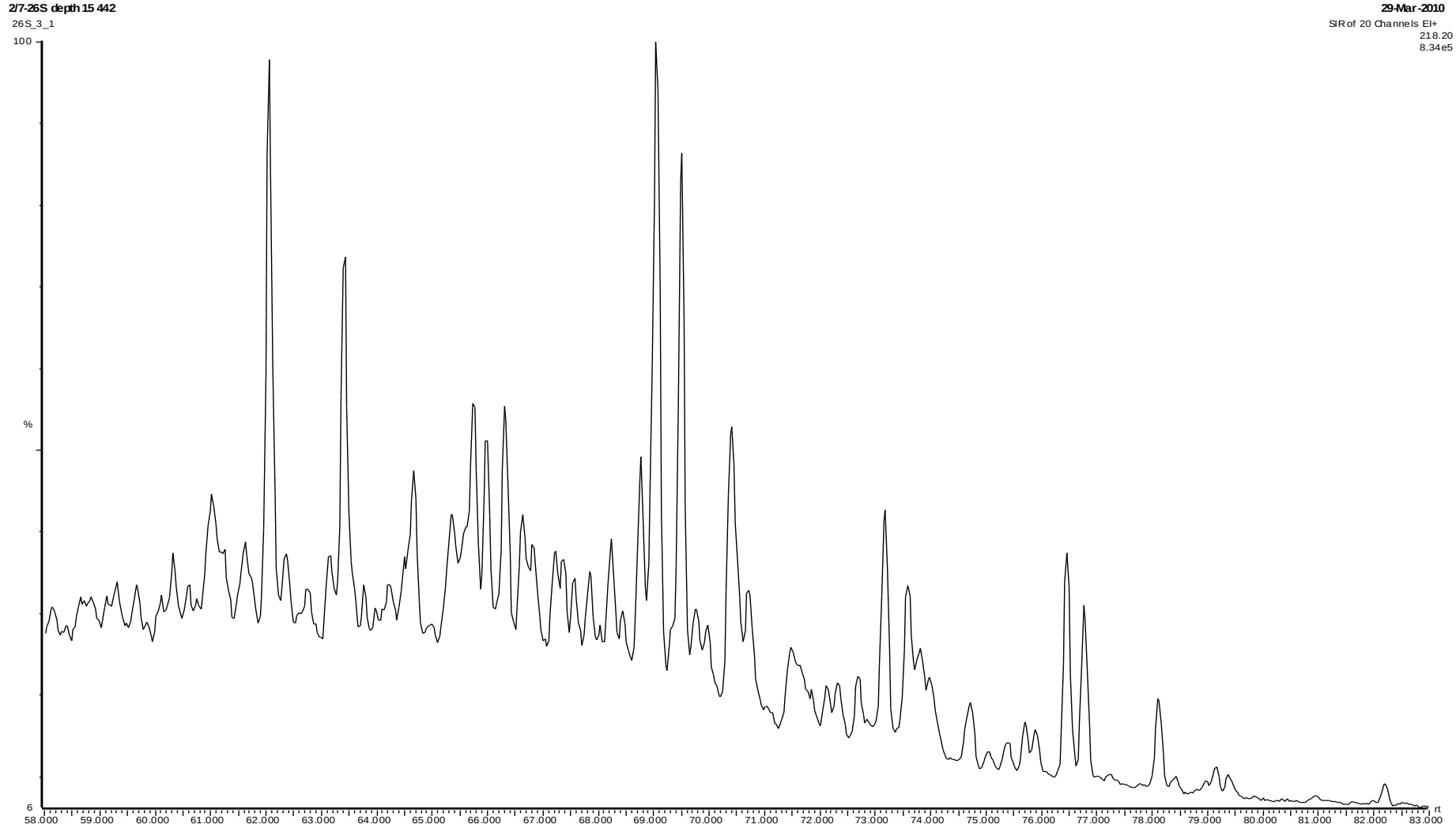
2/7-26S depth 15 442
29-Mar-2010
26S_3_1
SIR of 20 Channels EI+
218.20
8.34e5
100
%
6
58.000
59.000
60.000
61.000
62.000
63.000
64.000
65.000
66.000
67.000
68.000
69.000
70.000
71.000
72.000
73.000
74.000
75.000
76.000
77.000
78.000
79.000
80.000
81.000
82.000
83.000
rt

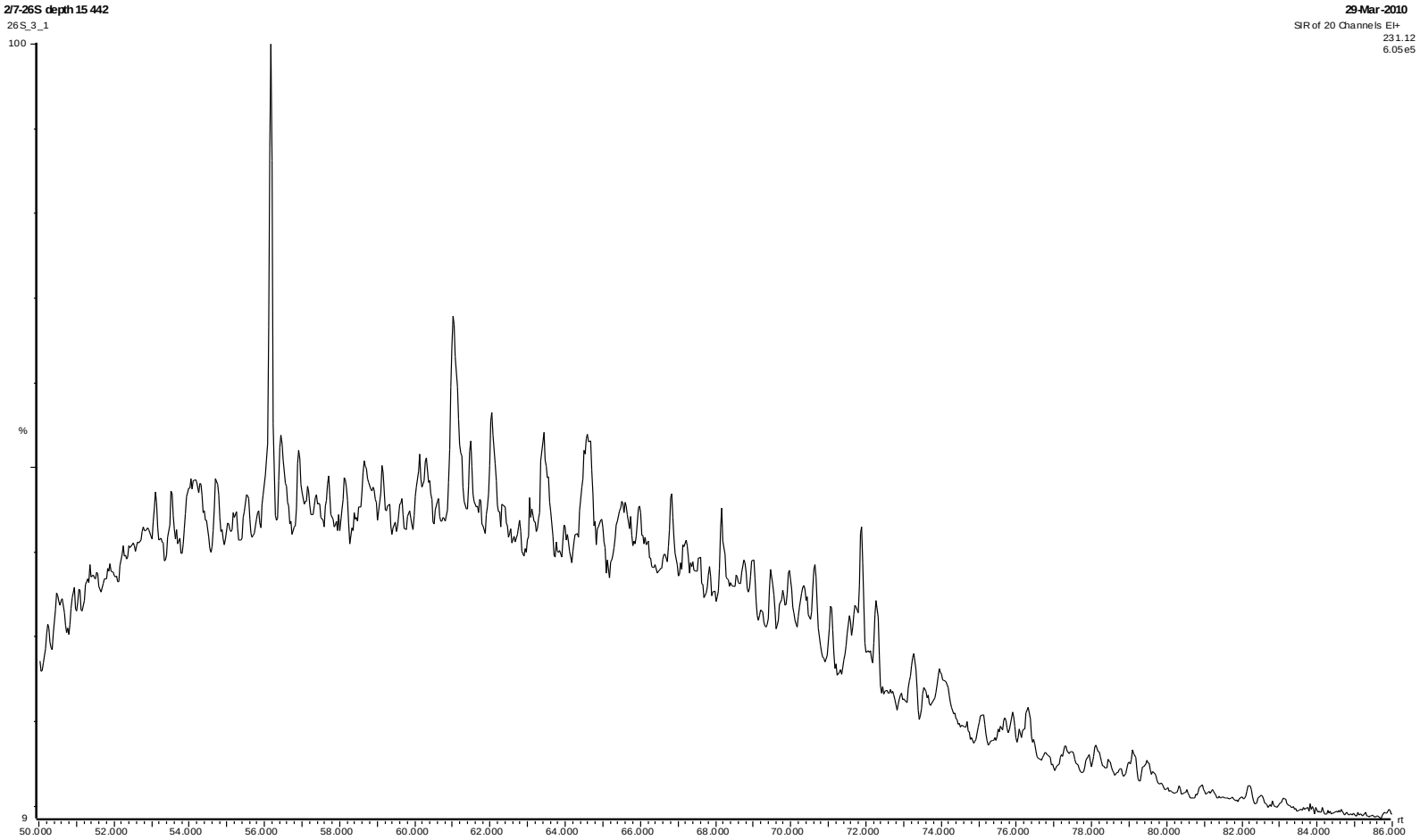
2/7-26S depth 15 442
26S_3_1
29-Mar-2010
SIR of 20 Channels EI+
231.12
6.05e5
100
%
9
50.000
52.000
54.000
56.000
58.000
60.000
62.000
64.000
66.000
68.000
70.000
72.000
74.000
76.000
78.000
80.000
82.000
84.000
86.000
rt

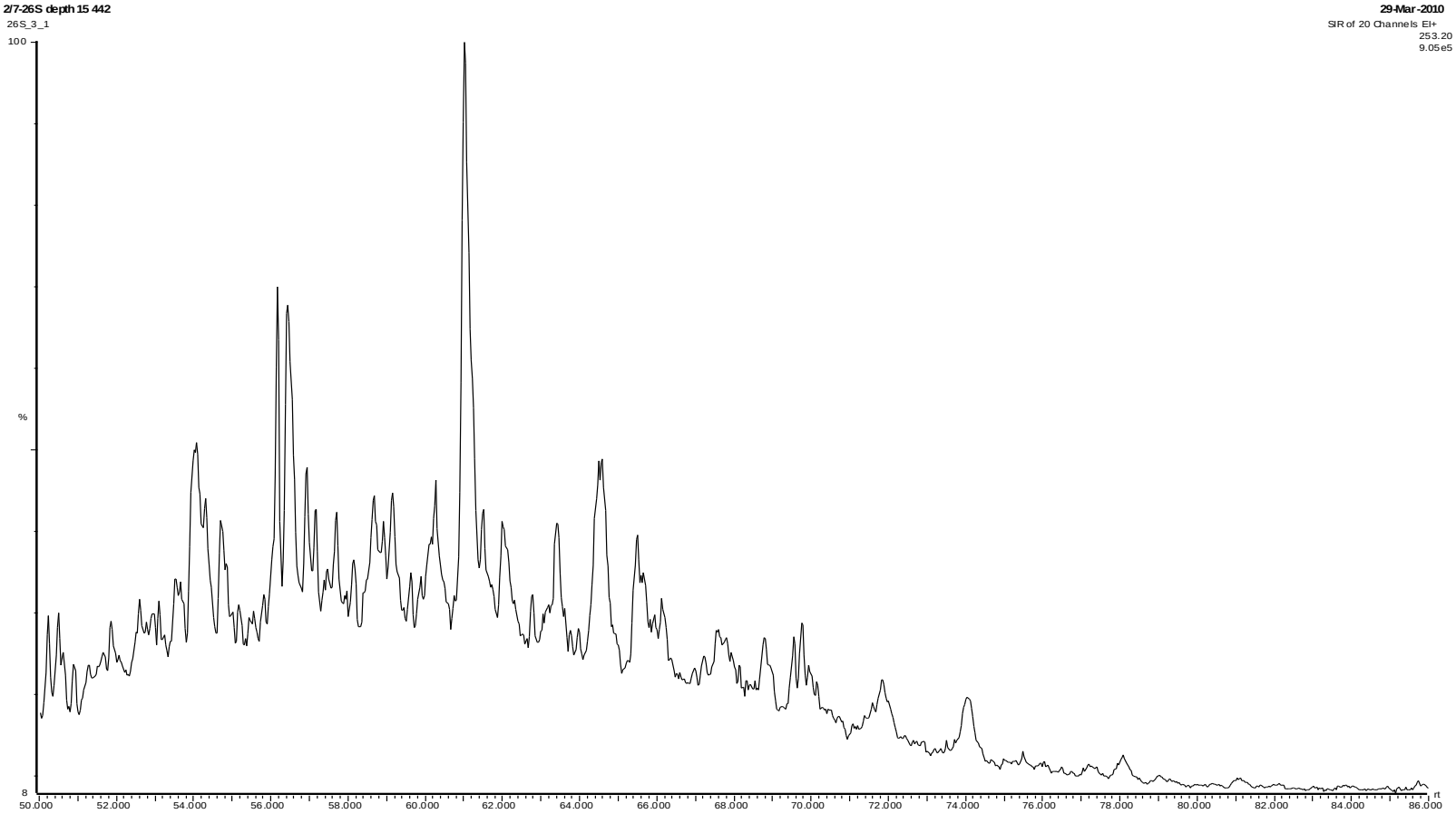
2/7-26S depth 15 442
26S_3_1
29-Mar-2010
SIR of 20 Channels EI+
253.20
9.05e5
100
%
8
50.000
52.000
54.000
56.000
58.000
60.000
62.000
64.000
66.000
68.000
70.000
72.000
74.000
76.000
78.000
80.000
82.000
84.000
86.000
rt

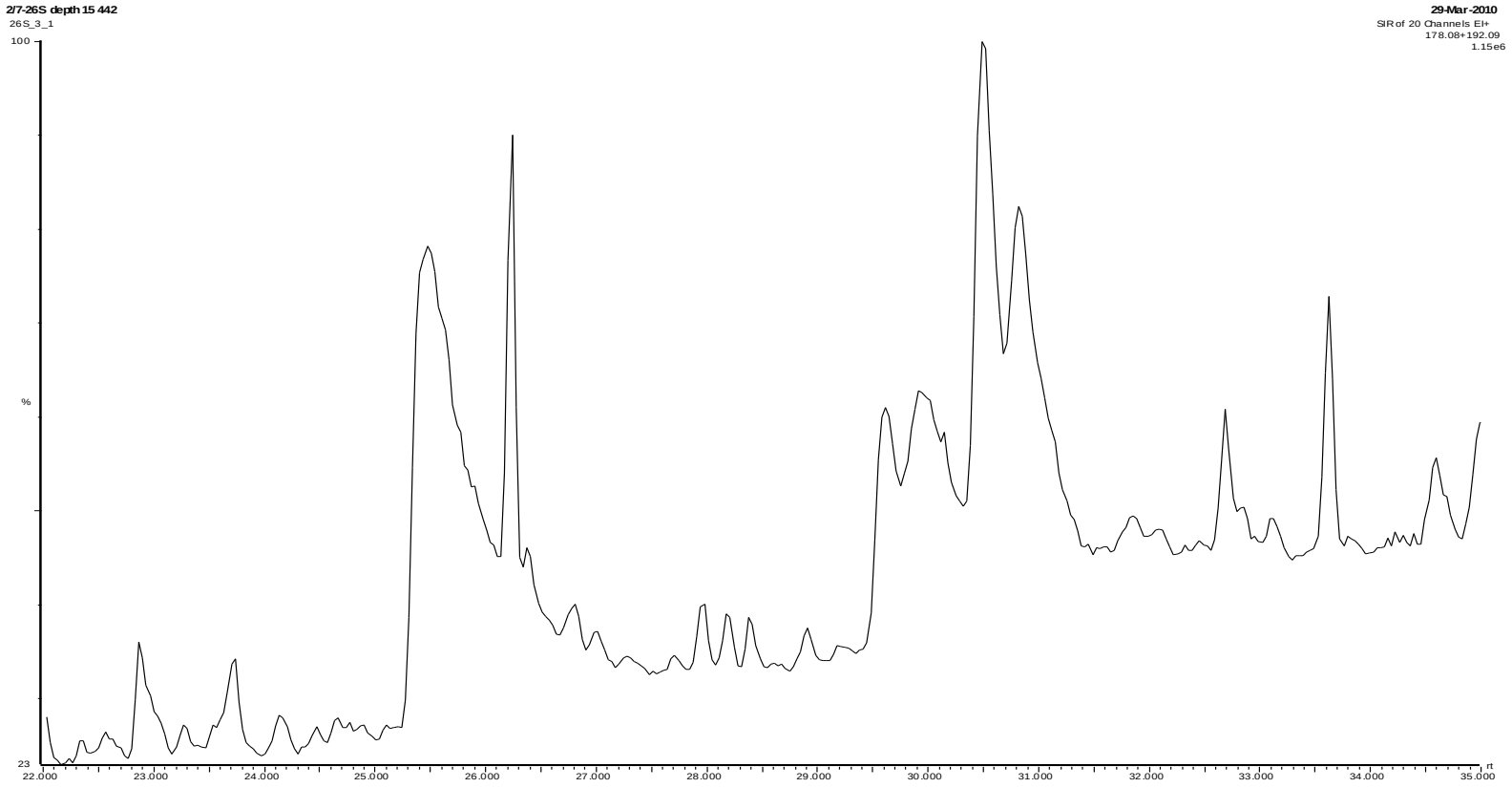
2/7-26S depth 15 442
26S_3_1
100
%
23
22.000
23.000
24.000
25.000
26.000
27.000
28.000
29.000
30.000
31.000
32.000
33.000
34.000
35.000
rt
29-Mar-2010
SIR of 20 Channels EI+
178.08+192.09
1.15e6

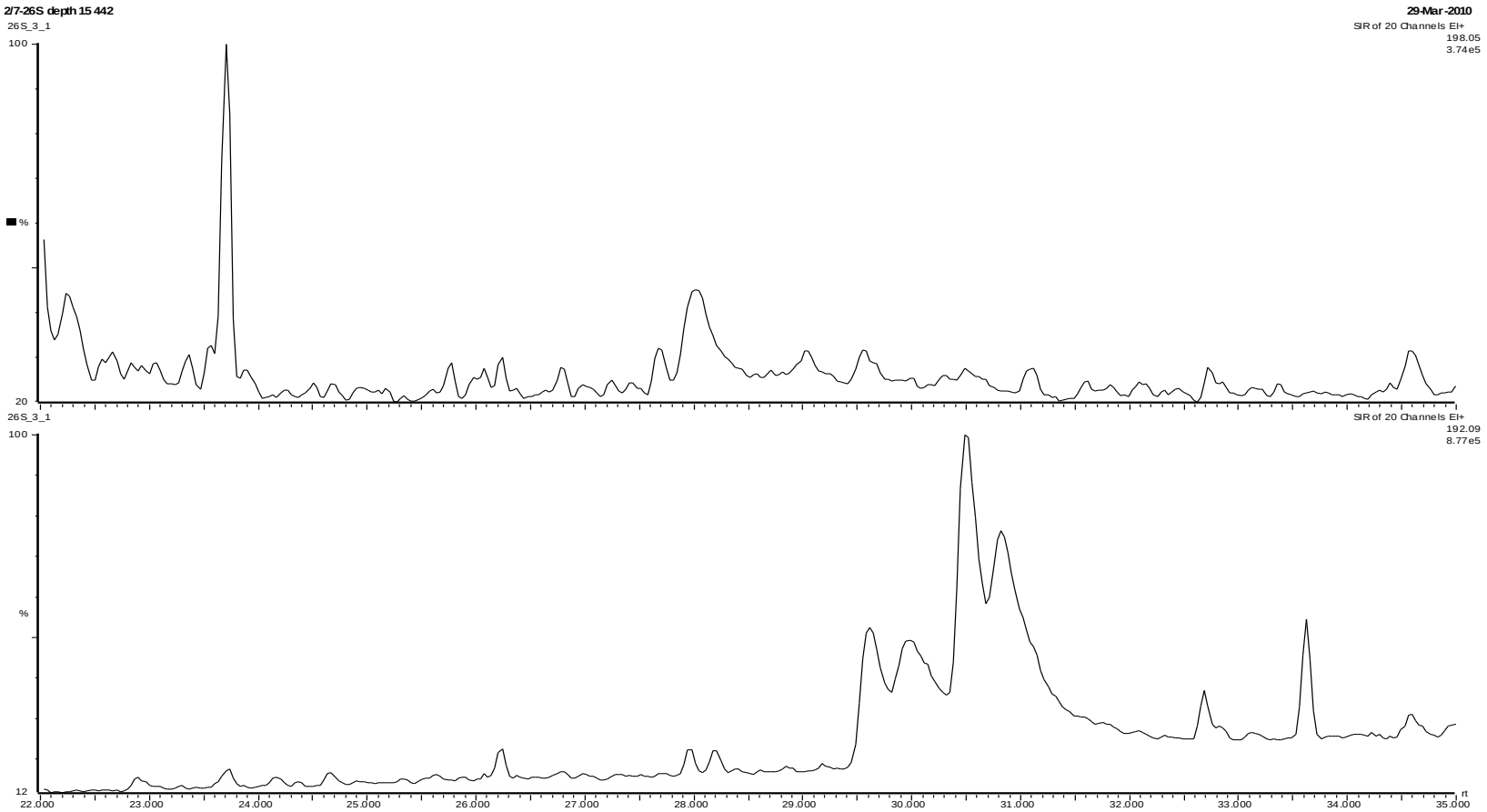
2/7-26S depth 15 442
29-Mar-2010
26S_3_1
SIR of 20 Channels EI+
198.05
3.74e5
100
%
20
26S_3_1
SIR of 20 Channels EI+
192.09
8.77e5
100
%
12
22.000
23.000
24.000
25.000
26.000
27.000
28.000
29.000
30.000
31.000
32.000
33.000
34.000
35.000
rt